

UNIVERSITÉ DU QUÉBEC À TROIS-RIVIÈRES

L'EFFECTEUR FONGIQUE MLP37347 MODIFIE LE FLUX DE PLASMODESMES  
ET AUGMENTE LA SENSIBILITÉ AUX PATHOGÈNES

THE FUNGAL EFFECTOR MLP37347 ALTERS PLASMODESMATA FLUXES  
AND ENHANCES SUSCEPTIBILITY TO PATHOGEN

THÈSE PRÉSENTÉE  
COMME EXIGENCE PARTIELLE DU  
DOCTORAT EN BIOLOGIE CELLULAIRE ET MOLÉCULAIRE

PAR  
MD SAIFUR RAHMAN

FÉVRIER 2021

Université du Québec à Trois-Rivières

Service de la bibliothèque

Avertissement

L'auteur de ce mémoire ou de cette thèse a autorisé l'Université du Québec à Trois-Rivières à diffuser, à des fins non lucratives, une copie de son mémoire ou de sa thèse.

Cette diffusion n'entraîne pas une renonciation de la part de l'auteur à ses droits de propriété intellectuelle, incluant le droit d'auteur, sur ce mémoire ou cette thèse. Notamment, la reproduction ou la publication de la totalité ou d'une partie importante de ce mémoire ou de cette thèse requiert son autorisation.

UNIVERSITÉ DU QUÉBEC À TROIS-RIVIÈRES

DOCTORAT EN BIOLOGIE CELLULAIRE ET MOLÉCULAIRE (PH. D.)

**Direction de recherche :**

---

Hugo Germain Directeur de recherche

---

Jean-François Laliberté Codirecteur de recherche

**Jury d'évaluation de la thèse :**

---

Hugo Germain Directeur de recherche

---

Jean-François Laliberté Codirecteur de recherche

---

Tagnon Missihoun Président de jury

---

Isabel Desgagné-Penix Président de jury

---

Edel Pérez-López Évaluateur interne

Thèse soutenue le 18 février 2021.

## ACKNOWLEDGEMENTS

This Ph.D. thesis is the result of the effort and support of several people to whom I am extremely grateful. First and foremost, I thank my supervisors Professor Hugo Germain and co-Supervisor Jean-François Laliberté. It has been a privilege to work with them. I hope to be able to work with you again in the near future.

Hugo, thanks for your responsiveness that brought me to Canada, as well as for inspiring and guiding my way through this unpredictable Ph.D. journey. Learned so much with you... many thanks for always being there no matter how busy life was.

Jean-Francois, I am sincerely grateful for your presence and attention during these 4 years as my co-advisor. Deeply thankful for the ideas and support for my research. Both made me go further professionally and personally.

The work presented in this thesis has been critically assessed and approved by an outstanding committee to whom I am more than grateful: Professor Hugo Germain, Professor Jean-François Laliberté, Professor Tagnon Missihoun, Professor Isabel Desgagné-Penix, and Professor Edel Pérez-López.

I am deeply indebted to Professor Yang Zhang, Department of Computational Medicine and Bioinformatics, the University of Michigan, for offering me a Visiting Scholar position and the opportunity of working together in his Lab in Ann Arbor, Michigan. I have learned a lot about computational biology during working with Prof. Yang. I also want to thank Dr. Xiaoqiang Huang for his tremendous effort to support me in the protein-protein docking analysis during the research internship.

I would also like to extend my deepest gratitude to Professor Isabel Desgagné-Penix and Céline Van Themsche (Université du Québec à Trois Rivières) for sharing instruments which helped me a lot during my experiments.



I am grateful to the Fonds de la Recherche sur la Nature et les Technologies du Québec (FRQNT) for providing me the scholarship for pursuing my Ph.D. I express my gratitude to NSERC, since our laboratory was partially funded by NSERC Discovery Grants and the Canada Research Chairs.

I am also profoundly grateful for the hard work of my labmates and their substantial contribution to uplift the studies presented in this thesis. Genevieve, Karen, Claire, Teura, Zainab, Ingrid, Joelle, Madina, Andrew, Nicolas, Tarun, Narimene, Fatma Meddeb, Annabelle, Manel, Daris, Fatima Awwad, Nikunj, Laurence, Michelle, Seydou, Serge, Manoj, Annabelle, and Dorian for their emotional support and entertainments, stimulating discussions and for all the fun we have had in the last four years. I would like to thank Mélodie B. Plourde for assisting in my research, valuable discussions, and proof-reading my manuscripts. I am delighted to have worked with you, and I look forward to working with you again.

Fortunately, I also have the privilege of having a lovely family and friends who had a fundamental role in getting me through the Ph.D. process successfully. I would like to express my deepest appreciation to my parents, Md. Motiur Rahman and Rina Begum for supporting me spiritually throughout writing this thesis and my life in general. Madina, my life partner, my love... thank you very much for being by my side for 7 years (and counting), and to my boy, Samuel, you are my inspiration to achieve greatness.

## PREFACE

The following thesis focuses on the functional studies of Mlp37347, a poplar leaf rust effector. This functional genomic study will contribute to understand how the effector localization and interaction with their targets play a role in infection. The body of the thesis consists of six chapters: introduction, materials and methods, results, discussion, conclusion, and references. The first chapter starts with the general introduction of plant immunity and poplar leaf rust *Melampsora larici-populina* effectors, and followed by its sequenced genome, preliminary studies on genomics and transcriptomics, candidate effector discovery, the importance of heterologous model systems in plant-pathogen interaction studies, and subcellular localization of effectors inside plant tissues.

Since the whole genome sequence of *M. larici populina*, and its host, *Populus trichocarpa*, is available, it offers access to further study the candidate effector proteins at the molecular level and investigate their role in pathogenesis. In this thesis, we chose an effector, Mlp37347, for the functional studies. To this end, we used *in planta* pathogen assays, genotyping, live-cell imaging, comparative transcriptomics, proteomics, and yeast two-hybrid assay to infer the functional nature of Mlp37347. The detailed materials and methods are discussed in chapter two. In the third chapter, we explained our findings and discussed those findings in chapter four. To our knowledge, this is the first attempt showing an *M. larici populina* effector is exploiting plasmodesmata.

I contributed to a review on the role of vacuolar substructure in plant immunity and pathogenesis, which I presented in Annex B. I carried out an additional research project for several months in Yang Zhang laboratory in Ann Arbor, Michigan where I studied *in-silico* analysis of Mlp124357 – *Arabidopsis*/poplar Protein disulfide-isomerase docking, which resulted in published work *Madina, Rahman et al. A poplar rust effector protein associates with protein disulfide isomerase and enhances plant susceptibility. Biology, 9, 294 2020*, which is presented in Annex C.

## RÉSUMÉ

*Melampsora larici-populina* (*Mlp*) est l'un des agents pathogènes les plus dévastateurs des peupliers - il cause la rouille foliaire du peuplier. Au cours du processus d'infection, *Mlp* sécrète un ensemble de protéines effectrices dans les cellules hôtes via son haustorium. Ces protéines effectrices ciblent les compartiments cellulaires pour modifier les processus cellulaires de l'hôte. Déterminer la fonction des effecteurs à l'intérieur des cellules est essentiel pour comprendre les mécanismes de pathogénicité et faire progresser notre capacité à protéger les cultures contre les maladies. Des études génomiques ont révélé que *Mlp* possède un répertoire d'au moins 1184 petites protéines sécrétées (SSP) et certaines d'entre elles ont été caractérisées comme des effecteurs candidats. La manière dont ces effecteurs favorisent la virulence n'est toujours pas claire.

Cette étude examine le rôle du candidat effecteur Mlp37347 au cours de l'infection. Nous avons développé une lignée transgénique stable d'*Arabidopsis* exprimant l'effecteur marqué avec la protéine fluorescente verte (GFP). Nous avons constaté que l'effecteur s'accumulait exclusivement dans les plasmodesmes (PD). Le profilage du transcriptome et une analyse de l'ontologie génique (GO) de la plante transgénique *Arabidopsis* exprimant l'effecteur et le type sauvage (WT) ont révélé que les gènes du processus catabolique du glucane sont spécifiquement régulés à la hausse dans les lignées exprimant l'effecteur, ce qui suggère que l'effecteur peut modifier l'ouverture de la PD par le métabolisme des glucanes. Par ailleurs, des tests de diffusion ont établi que l'effecteur modifie le flux de plasmodesmes. Il a été précédemment montré *in vivo* que cet effecteur interagit avec la glutamate décarboxylase 1 (GAD1). L'arrimage *in silico* de Mlp37347 à GAD1 a montré une forte affinité. L'effecteur favorise la croissance de l'oomycète *Hyaloperospora arabidopsidis* mais pas la croissance bactérienne.

Notre étude suggère que l'effecteur Mlp37347 cible le PD dans les cellules de plante pour favoriser la croissance parasitaire en régulant le flux des plasmodesmes grâce à la dérégulation du catabolisme du glucane. Par conséquent, nos résultats ont établi qu'un effecteur de *Mlp* réside au plasmodesme et module la susceptibilité des plantes.

**Mots-clés :** *Melampsora larici-populina*, effecteur, Mlp37347, plasmodesmes, glutamate décarboxylase

## SUMMARY

*Melampsora larici-populina* (*Mlp*) is one of the most devastating pathogens of poplar trees – it causes poplar leaf rust. In the process of infection, *Mlp* secretes an array of effector proteins into the host cells through its haustorium. These effector proteins target cellular compartments to alter host cellular processes. Determining the function of effectors inside of cells is key to understanding pathogenicity mechanisms and advance our ability to protect crops from disease. Genomic studies have revealed that *Mlp* possesses a repertoire of 1184 small secreted proteins (SSP), and some of them were characterized as candidate effectors. How these effectors promote virulence is still unclear.

This study investigates the candidate effector Mlp37347's role. We developed a stable transgenic *Arabidopsis* line expressing the effector tagged with the green fluorescent protein (GFP). We found that the effector accumulated exclusively in plasmodesmata (PD). Transcriptome profiling and a gene ontology (GO) analysis of transgenic *Arabidopsis* plant expressing effector compared with wild-type (WT) plant revealed that glucan catabolic process genes are specifically up-regulated in effector-expressing lines suggesting that the effector may alter PD opening through glucan metabolism. Indeed, diffusion assays established that the effector alters plasmodesmata flux. This effector has previously been shown to interact with glutamate decarboxylase 1 (GAD1). *In silico* docking of Mlp37347 to GAD1 showed strong affinity. The effector promotes *Hyaloperospora arabidopsidis* growth but not bacterial growth. Our investigation suggests that the effector Mlp37347 targets PD in host cells to promote parasitic growth by regulating plasmodesmata flux through the deregulation of glucan catabolism.

Therefore, our results established that an effector of *Mlp* resides at the plasmodesmata and modulates plant susceptibility.

**Keywords:** *Melampsora larici-populina*, effector, Mlp37347, plasmodesmata, glutamate decarboxylase

## TABLE OF CONTENTS

<b>ACKNOWLEDGEMENTS</b> .....	<b>iii</b>
<b>PREFACE</b> .....	<b>v</b>
<b>RÉSUMÉ</b> .....	<b>vi</b>
<b>SUMMARY</b> .....	<b>vii</b>
<b>LIST OF FIGURES AND TABLE</b> .....	<b>xi</b>
<b>LIST OF ABBREVIATIONS AND ACRONYMS</b> .....	<b>xiii</b>
<b>CHAPTER I</b>	
<b>GENERAL INTRODUCTION</b> .....	<b>1</b>
1.1 Plant innate immunity.....	2
1.1.1 The first layer of defense- Pattern-Triggered Immunity (PTI) .....	2
1.1.2 The second layer of defense – Effector-triggered immunity (ETI) .....	12
1.1.3 Systemic acquired resistance (SAR).....	14
1.2 Microbial effectors and their role in plant defense suppression .....	15
1.2.1 Effectors: concept and definitions .....	15
1.2.2 Diversity and structural organization of effector proteins .....	16
1.2.3 How are effector proteins introduced into host cells? .....	18
1.3 Plasmodesmata: the battlefield against intruders.....	19
1.3.1 Virus–plasmodesmata interaction.....	20
1.3.2 Fungus–plasmodesmata interaction.....	21
1.3.3 Plasmodesmata against bacterial pathogens .....	21
1.4 Role of callose in the regulation of plasmodesmal permeability.....	23
1.4.1 Specific enzymes modulate plasmodesmal callose levels .....	23
1.4.2 Plasmodesmata-located proteins regulate the plasmodesmal flux.....	24
1.5 Poplar tree.....	26
1.6 <i>Melampsora larici-populina</i> and Poplar rust.....	26
1.6.1 Pipelines of effector mining of <i>M. larici-populina</i> .....	28
1.6.2 Heterologous system to study effectors .....	30
1.7 Research objectives .....	30

<b>CHAPTER II</b>	
<b>MATERIALS AND METHODS .....</b>	<b>33</b>
2.1 Plants material and growth .....	33
2.2 Transgenic production .....	33
2.3 Crosses .....	34
2.4 Plasmid constructs and cloning procedures .....	35
2.5 Expression in <i>A. thaliana</i> and <i>N. benthamiana</i> .....	36
2.6 Pathogen infection assays .....	36
2.7 Confocal microscopy .....	36
2.8 mCherry diffusion assay .....	37
2.9 DANS assay and callose quantification .....	37
2.10 Y2H reporter assays .....	39
2.11 Western blot analysis .....	39
2.12 RNA extraction and transcriptome analysis .....	39
2.13 <i>In silico</i> protein-protein binding .....	40
<b>CHAPTER III</b>	
<b>RESULTS .....</b>	<b>43</b>
3.1 Selection and features of Mlp37347 .....	43
3.2 Plasmodesmata localization of Mlp37347 .....	44
3.3 Mlp37347 enhances plasmodesmata flux .....	45
3.4 Mlp37347 localization at plasmodesmata is required for diffusion .....	48
3.5 Mlp37347 interacts with <i>Arabidopsis</i> GAD1 and poplar GAD1 .....	50
3.6 Molecular modeling also supports the association of GAD1 and Mlp37347 .....	51
3.7 Mlp37347 decreases plasmodesmata callose deposition .....	55
3.8 Mlp37347 affects callose metabolism gene expression .....	58
3.9 Mlp37347 does not modify the morphology of <i>A. thaliana</i> leaves .....	60
3.10 Mlp37347 increases the susceptibility of <i>A. thaliana</i> to <i>H. arabidopsidis</i> .....	61
<b>CHAPTER IV</b>	
<b>DISCUSSION .....</b>	<b>63</b>
4.1 Heterologous systems .....	64
4.1.1 Advantage and disadvantages of heterologous protein expression systems .....	65

4.2	Plasmodesmata localization Mlp37347 is required for enhanced plasmodesmata flux .....	66
4.3	Mlp37347 decreases plasmodesmata callose deposition and affects callose metabolism gene expression .....	70
4.4	Mlp37347-GAD1 interaction .....	71
4.5	Mlp37347 increases the susceptibility of <i>A. thaliana</i> to <i>H. arabidopsidis</i> .....	72
4.6	DoorMan Hypothetical Model.....	73
<b>CHAPTER V</b>		
	<b>CONCLUSION</b> .....	<b>76</b>
5.1	Perspectives .....	78
	5.1.1 Short term perspectives.....	78
	5.1.2 Long term perspectives.....	79
5.2	Final conclusions .....	80
	<b>FOOTNOTES</b> .....	<b>81</b>
	<b>REFERENCES</b> .....	<b>82</b>
<b>ANNEX A</b>		
	<b>SUPPLEMENTARY TABLES AND FIGURES</b> .....	<b>103</b>
<b>ANNEX B</b>		
	<b>VACUOLAR MEMBRANE STRUCTURES AND THEIR ROLES IN PLANT-PATHOGEN INTERACTIONS</b> .....	<b>171</b>
<b>ANNEX C</b>		
	<b>A POPLAR RUST EFFECTOR PROTEIN ASSOCIATES WITH PROTEIN DISULFIDE ISOMERASE AND ENHANCES PLANT SUSCEPTIBILITY</b> .....	<b>184</b>

## LIST OF FIGURES AND TABLE

Figure		Page
1.1	Model of activation of PRR-mediated basal defenses and their suppression by type III effectors.....	3
1.2	Displays a schematic illustration of complex initiated Ca <sup>2+</sup> signaling cascades carried out by PRR that regulates the plant's defensive gene expression .....	6
1.3	A schematic illustration of steps RBOHD regulation during the rapid BIK1-mediated phosphorylation primes RBOHD activation by increasing the sensitivity to the Ca <sup>2+</sup> based regulation .....	7
1.4	Model of the FLS2 signaling pathway in <i>Arabidopsis</i> .....	11
1.5	Plant-microbe interactions and resistance in plants .....	13
1.6	Recognition of a pathogen by an NB-LRR induces a signal transduction pathway (STP) .....	15
1.7	Schematic illustration of effector proteins.....	18
1.8	Effector distribution structures of Gram-negative bacteria, oomycetes, fungi, and nematodes in plant cells.....	19
1.9	Cellular communication and plasmodesmata .....	20
1.10	Role of plasmodesmata in defense against pathogens .....	22
1.11	The callose deposit regulates the plasmodesmata opening in the cell wall surrounding the neck of the pore .....	23
1.12	Plasmodesmata-associated components and their functions.....	25
1.13	Poplar rust and <i>Melampsoralarici-populina</i> life cycle .....	27
1.14	Pipelines of effector mining of <i>M. larici-populina</i> .....	29
2.1	Overview of screening T-DNA homozygous selection .....	34
2.2	Gateway recombination reactions.....	35
2.3	Workflow of mCherry diffusion assay .....	37
2.4	Workflow of Drop-ANd-See (DANS) dye loading assay .....	38



2.5	Workflow of transcriptome analysis.....	40
2.6	I-TASSER protocol for protein structure and function prediction .....	42
3.1	Features of Mlp37347 and sequence alignment between Mlp37347 and AvrL567 .....	44
3.2	Co-localization of Mlp37347-GFP with the plasmodesmata marker PDCB1-mCherry in <i>N. benthamiana</i> .....	45
3.3	Mlp37347 enhances plasmodesmata flux .....	47
3.4	Expression of Mlp37347-GFP variants in Arabidopsis .....	48
3.5	Nuclear localization of NLS-Mlp37347-GFP in <i>N. benthamiana</i> and <i>A thaliana</i> .....	49
3.6	Plasmodesmata localization of Mlp37347 is required for enhanced plasmodesmal flux .....	50
3.7	Mlp37347 interacts with AtGAD1 and PtGAD1 .....	51
3.8	Molecular modeling of Mlp37347 .....	52
3.9	Functional approach of docking between Mlp37347 and AtGAD1 .....	53
3.10	Hydrogen bonding networks and interaction confirmation of Mlp37347-GAD1 .....	54
3.11	Sequence alignment of AtGAD1 and PtGAD1 .....	55
3.12	Callose deposition in <i>Arabidopsis</i> transgenics .....	57
3.13	Transcriptional changes induced by the expression of Mlp37347-GFP.....	59
3.14	Phenotype of Mlp37347 and gad1 knock-out in <i>A. thaliana</i> transgenic.....	60
3.15	Mlp37347 increases the susceptibility of <i>A. thaliana</i> to <i>H. arabidopsidis</i> ....	61
3.16	Mlp37347 does not promote the growth of Pst DC3000 in <i>A. thaliana</i> .....	62
4.1	A hypothetical model illustrating a potential role of Mlp37347 and plasmodesmata during infection .....	75

**Table****Page**

1.1	List of receptor-like protein (RLP)-type and receptor-like kinase (RLK)-type pattern recognition receptors (or R proteins) and their interacting proteins.....	5
-----	--	---

## LIST OF ABBREVIATIONS AND ACRONYMS

AVR	Avirulent
BAK1	BRI1-associated kinase 1
BCECF	2',7'-bis-(2-carboxyethyl)-5-(and-6)-carboxyfluorescein
BIC	Biotrophic interfacial complex
BIK1	Botrytis-induced kinase 1
BIR	BAK1-interacting RLK
CALS	Callose synthase
CaM	Calmodulin
CAMTA	Ca <sup>2+</sup> /calmodulin-binding transcription factors
CBL	Calcineurin-B-like
CDPK	Calcium-dependent protein kinase
CFDA	Carboxyfluorescein diacetate
CFU	Colony forming unit
CIPK	CBL-interacting kinase
CMU	Chorismate mutase
CNGC	Cyclic nucleotide-gated channel
CSEPs	Candidate secreted effector proteins
DAMP	Damage-associated molecular patterns
DANS	Drop-ANd-See
DDO	Double dropouts
Dpi	Days post infiltration
DTT	Dithiothreitol
eds1-1	Enhanced disease susceptibility 1-1

EHM	Extrahaustorial matrix
EM	Extrahaustorial membrane
ER	Endoplasmic reticulum
EST	Expressed sequence tag
ETI	Effector-Triggered Immunity
ETS	Effector-triggered susceptibility
FM1-43	N-(3-triethylammoniumpropyl)-4-(4-(dibutylamino)styryl) pyridinium dibromide
FM4-64	N-(3-triethylammoniumpropyl)-4-(4-diethylaminophenylhexatrienyl) pyridinium dibromide
GABA	Glutamate to gamma-aminobutyric acid
GAD	Glutamate decarboxylase
GFP	Green Fluorescent Protein
GLR	Glutamate receptor-like channel
GO	Gene Ontology
H. a	Hyaloperonospora arabidopsidis
HR	Hypersensitive response
IH	Invasive hyphae
IP	Immunoprecipitation
KO	Knock out
MAMP	Microbe-associated molecular patterns
MAMP	Microbes associated molecular pattern
MAPK	Mitogen-Activated Protein Kinases
Mlp	<i>Melampsora larici-populina</i>
MS	Mass Spectrometry
NLS	Nuclear localization signal

ORF	Open reading frame
PAMP	Pathogen associated molecular pattern
PC	Phosphatidylcholine
PCD	Programmed cell death
PD	Plasmodesmata
PDCB	Plasmodesmata Callose-Binding Protein
PDI	Protein disulfide isomerase
PDLP	Plasmodesmata-Located Protein
PE	Phosphatidylethanolamine
PR	Pathogenesis related
PRR	Pattern recognition receptor
Pst	<i>Pseudomonas syringae</i> pv. tomato strain
PTI	PAMP-Triggered Immunity
QDO	Quadruple dropouts
R	Resistance
RBOHD	Respiratory burst oxidase homologue D
RIN4	RPM1 interacting protein 4
RLK	Receptor-like kinase
RLP	Receptor-like protein
ROS	Reactive oxygen species
RT	Room temperature
SA	Salicylic acid
SAP11	Secreted AY-WB Protein 11
SD	Synthetic Defined
SDS-PAGE	Sodium dodecyl sulfate- polyacrylamide gel electrophoresis

SOBIR	Suppressor of bir
SP	Signal peptide
SSPs	Small secreted protein
T3SS	Type three-secretion system
TAL	Transcription activator-like
TEM	Transmission electron microscopy
TFs	Transcription factors
TFs	Transcription factors
TM	Template Modeling
TVS	Transvacuolar strand
VM	Vacuolar membrane
VPE	Vacuolar processing enzyme
Y2H	Yeast two-hybrid
YEP	Yeast extract pepton

## CHAPTER I

### GENERAL INTRODUCTION

Why am I in plant-microbe research today? I often asked myself this question during the first year of my doctorate. I came across how diverse, fascinating, and unforeseen this part of plant-microbe research can be. Why work on plants? There is no doubt all of us live off plant energy created from photosynthesis from the sunlight. Plants are frequently challenged by the world around them and have developed defense strategies against pathogens, including bacteria, viruses, fungi, and oomycetes. Therefore, biotic stress is a natural element in the plant lifecycle as fauna and microbes exploit nutrients from plants, and the flora in response has evolved a multilayered complex defense system to counteract biotic stresses. Plant defense from grazing often depends on mechanical approaches and the production of chemical compounds that are not desired by herbivores. The interaction between plant and microbes can have mutually beneficial results but can also be detrimental to the plant to complete its life cycle. To understand the disease development mechanism in plants, phytopathological molecular research has focused on interactions between phytopathogens and their hosts. Studies revealed that plants possess a sophisticated innate immune system capable of recognizing all pathogen classes (Chiang & Coaker, 2015, Zipfel, 2014), which consist of a large arsenal of immune receptors encoded in plant genomes. In order to penetrate the plant, colonize various tissues and cause disease, pathogens must be able to deactivate the defense responses of plants. An essential component required for pathogenesis is the secretion of pathogenic proteins, called effectors, which modulate plant immunity and facilitate infection (Hogenhout et al., 2009).

## 1.1 Plant innate immunity

Plants have mechanisms to detect various forms of environmental threat, including the attack by pathogens and damages to their own cells. The initial response in the immune system of a plant corresponds to the perception of the pathogen via the recognition of the conserved pathogen-associated molecular patterns (PAMP) by pattern recognition receptors (PRR). PAMPs are sometimes referred to as microbe-associated molecular patterns (MAMPs) due to their presence of non-pathogenic species (Ausubel, 2005). The plant induces the PAMP-triggered immunity (PTI)/MAMP-triggered immunity (MTI) as a response to the recognition of P/MAMPs. The responses constitute the plants' immunity in order to resist pathogenic attack. The plant is also able to recognize damage-associated molecular patterns (DAMPs) or endogenous peptides. DAMPs are the consequential response to invading pathogens in the plant and results in plant degradation, whereas the plant releases endogenous peptides following a pathogenic attack (Boller & Felix, 2009).

### 1.1.1 The first layer of defense- Pattern-Triggered Immunity (PTI)

The "watchtowers" of the plant are found at the cell surface as pattern-recognition receptors (PRR). They are the first layer of defense and activate PAMP-Triggered immunity. One of these PAMP is a 22 amino acid section of the C-terminal end of flagellin, the main subunit of bacterial flagella (Gómez-Gómez & Boller, 2000). The flg22 peptide binds to the flagellin receptor FLS2 in *A. thaliana*, which is similar to the human toll-like receptor 5 (TLR5) (Hayashi et al., 2001). Since FLS2 was identified, other MAMPs and their receptors have been found, including the chitin receptor in *Oryza sativa* and *A. thaliana*, and the Elongation Factor-Tu receptor (EFR) in *A. thaliana* (Zipfel et al., 2006, Miya et al., 2007, Kaku et al., 2006) (Figure 1.1). Chitin is a  $\beta$ -1,4-linked N-acetyl-glucosamine oligomer (GlcNAc) that is found as a building block in fungal cell walls, and EF-Tu is a protein responsible for supplying aminoacyl-tRNA to the ribosome during bacterial translation. The recognition of MAMP/PAMP initiates an innate immune response and some of the common responses are discussed in the following paragraphs.

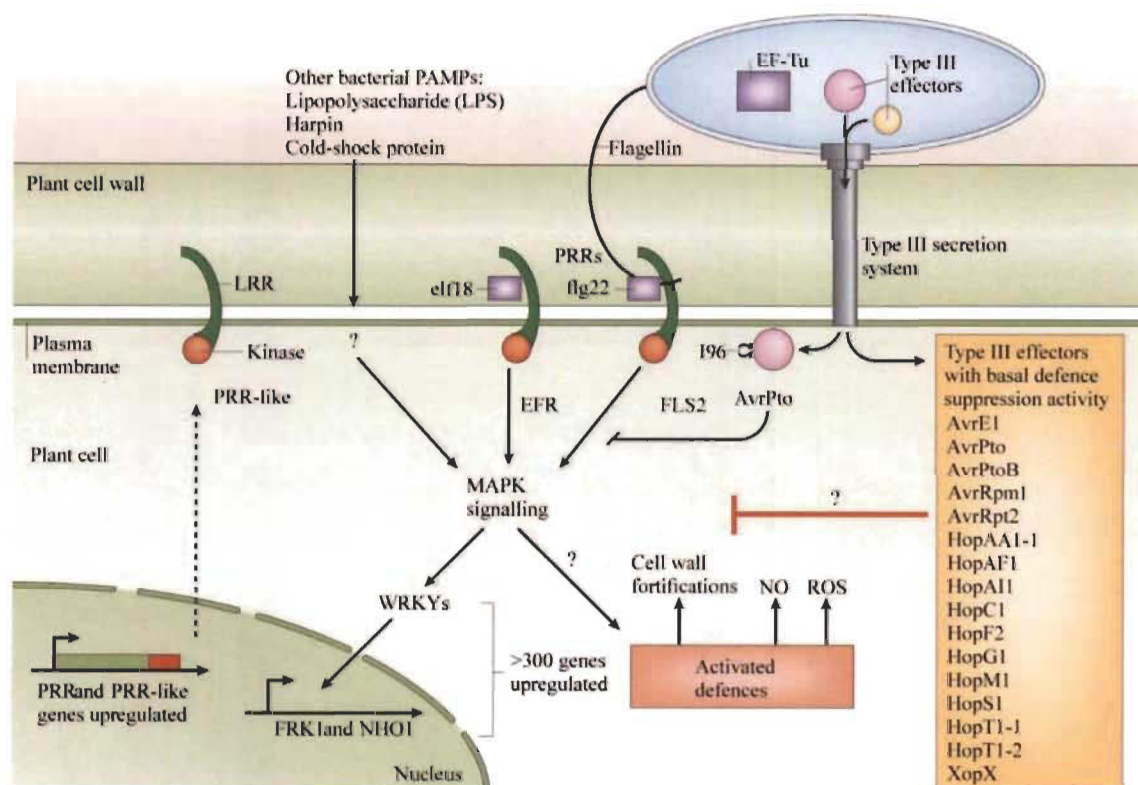


**Figure 1.1. Model of activation of PRR-mediated basal defenses and their suppression by type III effectors.**

Plasma-membrane-localized PRRs, which in many cases consist of a leucine-rich repeat (LRR) extracellular domain and a serine/threonine-protein kinase (PK) cytoplasmic domain. In *A. thaliana*, FLS2 and EFR are two examples of PRRs that recognize flagellin flg22 or EF-Tu elf18 peptide, respectively. The activation of PRR triggers signaling events that lead to the upregulation of more than 300 plant genes. A complete pathway of the mitogen-activated protein kinase (MAPK) and various WRKY transcription factors have been identified that function downstream of FLS2. Subsequent effectors are responsible for the buildup of cellular response, as well as initiating signaling in the SAR program. Delivery of effector proteins through the type III secretion system (T3SS) to plant cells is a strategy used by bacteria to suppress PRR-mediated defenses. Some bacterial proteins have been identified as effectors that suppress basal defenses. The figure highlights the effector AvrPto required to suppress the recognition of flg22 and other PAMPs. (Image from Abramovitch et al., 2006)

### 1.1.1.1 Ion fluxes and oxidative burst

The perception of MAMP/DAMP by their cognate receptors triggers ionic fluxes (including  $\text{Ca}^{2+}$ ) at the plasma membrane, rapid production of reactive oxygen species (ROS) and nitric oxide (NO), phosphorylation events (e.g., by mitogen-activated protein kinases (MAPK)) or  $\text{Ca}^{2+}$ -dependent protein kinases (CDPK). Depending on the elicitor's perception, within 1-2 minutes the channels of the plasma membrane are open and



increase the level of intracellular  $\text{Ca}^{2+}$  and  $\text{H}^+$  (Lecourieux et al., 2002).  $\text{Ca}^{2+}$  is known as the secondary messenger in various cellular processes (Lecourieux et al., 2006). In this regard, innate immunity is regulated by calcium-dependent protein kinases (CDPK), where  $\text{Ca}^{2+}$  acts as a sensor to initiate CDPK (Boudsocq et al., 2010).

In table 1.1 and figure 1.2, the regulation of defensive genes of a plant is initiated by a set of pathogen recognition receptors (PRR) that initiates  $\text{Ca}^{2+}$  signaling cascades. The negative regulator, RASSINOSTEROID INSENSITIVE 1-associated receptor kinase 1 (BAK1)-interacting RLK (BIR), which is found in resting cells, interacts with SOBIR or BAK1 to, seemingly, prevent interactions with the pathogen recognition receptors. When DAMP/MAMP is recognized in the plant, SOBIR and BAK1 are recruited by the RLP-type and RLK-type PRRs, respectively. It is important to note that RLK signaling has not been shown as necessary for the function of SOBIR; however, BAK1 is further utilized for the function of RLP. The intracellular kinase domains of the RLK-types and/or other related cytoplasmic kinases (e.g., BIK1) trigger phosphorylation events that are needed for the signaling to the  $\text{Ca}^{2+}$  channels. There is uncertainty related to some possible plasma membrane-localized proteins that are representative of  $\text{Ca}^{2+}$  channels as the identity designation of many DAMP/MAMP activated channels have not been thoroughly identified. The  $\text{Ca}^{2+}$  sensors and/or decoders, such as CDPKs, CaM, and CBL-CIPK, pairs sense alterations of cellular  $\text{Ca}^{2+}$  concentration and work with MAPK activation to coordinate the transcriptional control of the plant's defensive gene expression. The coordination between  $\text{Ca}^{2+}$  and Respiratory burst oxidase homolog protein D (RBOHD), the NADPH oxidase, is accentuated by the orange arrows in figure 1.2. Furthermore,  $\text{Ca}^{2+}$  can be sensed by the EF-hands in the NADPH oxidase. The activities of the RBOHD are regulated by differential phosphorylation, done by the kinases. This phosphorylation takes place upstream of  $\text{Ca}^{2+}$  (i.e., directly from BIK1, the receptor-complex component) and downstream of  $\text{Ca}^{2+}$  (i.e., CDPKs). The process of dismutation causes the superoxide to turn into  $\text{H}_2\text{O}_2$ . This triggers the induction of  $\text{Ca}^{2+}$  fluxes as the  $\text{H}_2\text{O}_2$  loops back. The propagation of ROS/Ca in systemic (cell-to-cell) and local (intracellular) waves results from an amplificatory feedback circuit.

**Table 1.1. List of receptor-like protein (RLP)-type and receptor-like kinase (RLK)-type pattern recognition receptors (or R proteins) and their interacting proteins**

MAMP/DAMP/effector	Receptor/R protein	Receptor type	Partner proteins	Reference <sup>a</sup>
Flg22	FLS2	RLK	BIK1/PBLs; BAK1; SERK4/SERKs; SCD1	1,2
Elf18	EFR	RLK	BIK1/PBLs; BAK1 SERK4/SERKs; SCD1	2,3
AtPep(s)	PEPR1/2	RLK	BIK1/PBLs; BAK1 SERK4/SERKs	4
Chitin	CERK1/LYMs/CEBiP	RLK	BIK1	5,6,7,8
Peptidoglycan	CERK1/LYMs	RLK	LYM1/LYM3	9
Oligogalacturonides	WAK1	RLK	?	10
Xylanase	Eix2	RLP	BAK1; SOBIR	11
Verticillium dahliae Ave1	Ve1	RLP	BAK1; SOBIR	12,13
Avr2/9	Cf2/9	RLP	BAK1; SOBIR	14
Xanthomonas eMax	ReMAX	RLP	?	15
Sclerotinia sclerotiorum effector (SsE1)	RLP30	RLP	BAK1; SOBIR	16
Extracellular ATP	DORN1	LecRK	?	17
RALF	FERONIA	RLK	?	18

<sup>a</sup>. Selected references

1, (Chinchilla et al., 2007); 2, (Roux et al., 2011); 3, (Zipfel et al., 2006); 4, (Krol et al., 2010); 5, (Kaku et al., 2006); 6, (Miya et al., 2007); 7, (Shimizu et al., 2010); 8, (Petutschnig et al., 2010); 9, (Willmann et al., 2011); 10, (Brutus et al., 2010); 11, (Ron & Avni, 2004); 12, (Fradin et al., 2011); 13, (de Jonge et al., 2012); 14, (Stergiopoulos et al., 2010); 15, (Jehle et al., 2013); 16, (Zhang et al., 2013); 17, (Choi et al., 2014); 18, (Haruta et al., 2014).

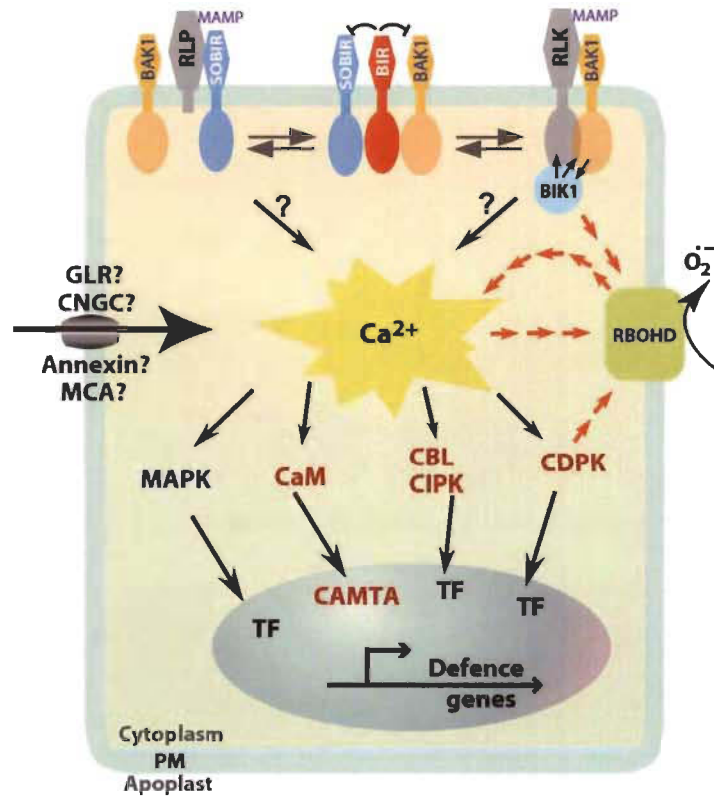


**Figure 1.2.** Displays a schematic illustration of complex initiated  $\text{Ca}^{2+}$  signaling cascades carried out by PRR that regulates the plant's defensive gene expression. (Adapted from Seybold et al., 2014.)

The NADPH oxidases found in both plants and animals produce reactive oxygen species (ROS) as a result of pathogen recognition (Canton & Grinstein, 2014). ROS are signaling molecules that initiate immune outputs and have distinct antimicrobial properties. The respiratory burst oxidase homolog D (RBOHD) contains NADPH oxidases that are found in both plants and animals hold ten members in the model plant *Arabidopsis thaliana* (Kadota et al., 2015). During an immune response, the RBOHD will be released in a two-step activation process. Upon PAMP recognition, FLS2 and EFR- which are PRRs, will activate and phosphorylate BIK1 with the co-receptor BAK1. A higher binding affinity of RBOHD to the phosphorylated BIK1 allows for the phosphorylation on fixed binding sites (Figure 1.3). A priming process is induced for the  $\text{Ca}^{2+}$  based regulation of RBOHD by the BIK1-mediated phosphorylation to generate conformational changes. These conformational changes could potentially increase the  $\text{Ca}^{2+}$  binding affinity for greater availability for CPK-mediated phosphorylation and/or for EF-hand motifs. At the same time, the indirect and direct activation of  $\text{Ca}^{2+}$  channel(s)

and induction of  $\text{Ca}^{2+}$  influx is produced through the cooperative work of BIK1 and PRRs. The result of the process is the binding of an EF-hand motif to  $\text{Ca}^{2+}$  in RBOHD and the phosphorylation of RBOHD that is completed through the activation of CPKs. The activation process of  $\text{Ca}^{2+}$  channel(s) is triggered by the production of  $\text{H}_2\text{O}_2$ , which leads to the full activation of  $\text{Ca}^{2+}$ -based regulation and  $\text{Ca}^{2+}$  signaling of RBOHD.

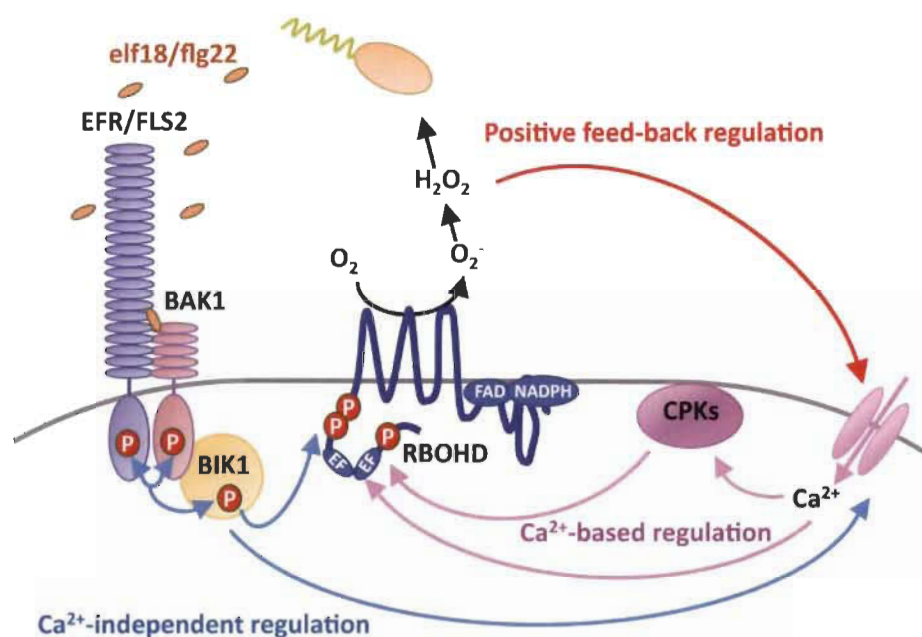
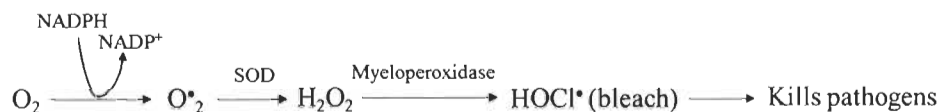


**Figure 1.3.** A schematic illustration of steps RBOHD regulation during the rapid BIK1-mediated phosphorylation primes RBOHD activation by increasing the sensitivity to the  $\text{Ca}^{2+}$  based regulation. (Adapted from Seybold et al., 2014.)

The production of reactive oxygen species (ROS) is regulated by the phosphorylation of the ROS-producing enzyme NADPH oxidase located in the plasma membrane. This enzyme produces superoxide anion ( $\text{O}_2^-$ ) from oxygen ( $\text{O}_2$ ). Afterward, with the help of superoxide dismutase (SOD),  $\text{O}_2^-$  converts to hydrogen peroxide ( $\text{H}_2\text{O}_2$ ). This  $\text{H}_2\text{O}_2$  is further converted to hypochlorite ( $\text{HOCl}^\bullet$ ) by myeloperoxidase. The hypochlorite ( $\text{HOCl}^\bullet$ ) is known as bleach, act as broad-spectrum bactericidal.



### ***1.1.1.2 Mitogen-activated Protein Kinases (MAPK) activation***

MAPK plays an essential role in transducing environmental and development signals by phosphorylation of downstream signaling. Upon PAMP perception, the activation of MAPK cascades transpires within five to ten minutes (Boller & Felix, 2009). MAPK signaling depends on sequential phosphorylation events between three protein forms- a MAP kinase (MPK), a MAP kinase kinase (MAPKK or MKK), and a MAP kinase kinase kinase (MAPKKK or MEKK) (Pedley & Martin, 2005). The initial proposal of the MAPK cascade that involved MAPKK1-MAPKK4/5-MPK3/6 was thought to be involved in flg22-triggered signaling in the *Arabidopsis thaliana* (Asai et al., 2002). Nevertheless, further studies proved that MAPKKK1 was involved in the activation of MPK4, and not in the activation of MPK3/6 (Gao et al., 2008, Suarez-Rodriguez et al., 2007, Nakagami et al., 2006, Ichimura et al., 2006). This revelation denotes that the MAPKKK upstream of MPK3/6 is not yet identified. MAPKK1 and MAPKK2 are key proteins in flg22-induced activation of MPK4 (Figure 1.4) (Qiu et al., 2008, Mészáros et al., 2006, Gao et al., 2008). Additionally, MPK11, which is homologous with MPK4, was recently discovered to be an ancillary component of FLS2 signaling (Figure 1.4) (Bethke et al., 2012). The original description of MPK4 characterized it as a positive regulator of ethylene/jasmonic acid (JA)-dependent defense responses but as a negative regulator of salicylic acid (SA)-mediated resistance (Brodersen et al., 2006, Petersen et al., 2000). This statement was disputed when it was shown that the MPK4 pathway is guarded by the R protein, SUMM2 (Zhang et al., 2012). This explains why *mekk1* and *mpk4* mutation leads to constitutive defense activation and why MEKK1 and MPK4 were proposed as negative regulators. It was proven that the MAPKKK1-MAPKK1/2-MPK4 pathway positively regulates PTI when a genetic analysis of double mutants with *summ2* was conducted (Kong et al., 2012). The phosphorylation and subsequent deactivation of the ethylene biosynthesis enzyme, 1-amino-cyclopropane-1-carboxylic acid (ACS), is occurred by the MPK3 and MPK6 (Li et al., 2012, Bethke et al., 2009, Yoo et al., 2008, Liu & Zhang, 2004). The induction of ethylene accumulation through PAMP perception could be explained through this observation (Felix et al., 1999). MPK phosphatases can be negative regulators of MAPK cascades (Bartels et al., 2010). The interaction between MPK2 with MPK6 and MPK3

controls the pathogenic defense responses and the oxidative stress in *Arabidopsis* (Lumbreras et al., 2010). The infection of the biotrophic pathogen, *Ralstonia solanacearum*, in *mkp2* mutant plants was found to decrease disease symptoms, although the susceptibility to the necrotrophic fungus *B. cinerea* is increased (Lumbreras et al., 2010). This is indicative of the fact that necrotrophic and biotrophic pathogens are regulated differently according to the functions of MPK2 (Lumbreras et al., 2010). Moreover, MKP1 and PTP1 (protein tyrosine phosphatase 1) act as repressors of MPK3/MPK6-dependent stress signaling (González Besteiro et al., 2011, Anderson et al., 2011, Bartels et al., 2009). The doubles mutants, *mkp1 ptp1*, showed increased greater resistance to *Pto* DC3000 (Bartels et al., 2009). The enhancement of PAMP-induced responses was also demonstrated in *mkp1* mutant plants recently (Anderson et al., 2011). In addition, the deactivation of MAPK cascades was shown to originate from multiple PP2Cs. The interaction of MPK3, MPK4, and MPK6 with AP2C3/PP2C5 and AP2C1 (*Arabidopsis* phosphatase 2C) regulate many processes, such as plant defense responses (Brock et al., 2010, Schweighofer et al., 2007). Remarkably, the susceptibility to *Botrytis cinerea*, the necrotrophic fungus, is enhanced by the overexpression of AP2C1 (Schweighofer et al., 2007).

### ***1.1.1.3 Callose deposition***

Callose, a plant polysaccharide, is mainly found in the cell wall. The plant cell wall is mostly made of complex carbohydrates. Many changes are triggered in the cell walls in response to biotic and abiotic stress. In *Arabidopsis*, callose deposition was detected from 16 hours after the MAMP treatment following fixation and staining with aniline blue (Gómez-Gómez et al., 1999). The callose deposit becomes rigid at the plant cell wall, making it difficult for pathogens to propagate.

We discuss the specific role of callose in section 1.4.

#### ***1.1.1.4 Hormonal integration***

Among the classic plant hormones (such as ethylene, abscissic acid, auxin, gibberellins, jasmonic acid, cytokinins, salicylic acid, and brassinosteroids) several are involved in defense responses (Shigenaga & Argueso, 2016). Amongst them, jasmonic acid (JA) and salicylic acid (SA) are the main phytohormones linked to plant defense. JA and SA are positive regulators of plant defense. SA regulates immunity against biotrophic pathogens while JA regulates immunity against necrotrophic pathogens (Berens et al., 2017, Pieterse et al., 2009).

#### Hormonal crosstalk in defense responses

The resistance to necrotrophic pathogens is usually associated with JA and ET signaling, whereas the resistance to biotrophic and hemibiotrophic pathogens comes from SA-dependent defense (Glazebrook, 2005). The involvement of SA in the formation of systemic acquired resistance (SAR) is triggered by local infection to induce a broad-spectrum resistance (Grant & Lamb, 2006). Although SA and ET/JA defense response pathways act mostly antagonistically, as the activation of one often suppresses the activation of the other, synergistic interactions have also been reported (Beckers & Spoel, 2006, Kunkel & Brooks, 2002, Schenk et al., 2000). An essential regulator of the cross-talk between the two pathways is MPK4 (Brodersen et al., 2006, Petersen et al., 2000). mpk4 mutant plants display elevated SA levels and constitutive expression of SA-induced genes, whereas the expression of JA responsive genes is impaired (Brodersen et al., 2006, Petersen et al., 2000). This indicates that MPK4 positively regulates JA-mediated responses but acts as a negative regulator of SA signaling or that in the mpk4 mutants, SUMM2 activation promotes SA accumulation and, thus, downregulation of JA-signaling.

*Salicylic acid:* Primary regulation of the SA signaling pathway is made by NPR1 as it conveys the induction of PR-1 and other SA-responsive genes (Dong, 2004). Notably, it was reported recently that NPR1 directly binds SA and was therefore implied to function as a SA receptor (Wu et al., 2012). However, another study demonstrated that the closely

related NPR3 and NPR4 but not NPR1 exhibit SA binding affinity (Fu et al., 2012). Furthermore, NPR3 and NPR4 were shown to function as adaptors for an E3 ubiquitin ligase to mediate SA-dependent degradation of NPR1 (Fu et al., 2012). Thus, further investigation must be undertaken to explain these apparently contradictory results.

*Jasmonic acid*: JA mediates defense against necrotrophic pathogens; however, JA was also recently implied to play a role in SAR (Robert-Seilaniantz et al., 2011). Most JA responses are mediated through the F-box protein CORONATINE INSENSITIVE1 (COI1) (Sheard et al., 2010, Fonseca et al., 2009, Browse, 2009, Xie et al., 1998). *coil* mutant plants display elevated SA levels and exhibit enhanced susceptibility to necrotrophic pathogens such as *Alternaria brassicicola* and *B. cinerea* (Kloek et al., 2001, Thomma et al., 1998). Using mutational and transcriptional approaches, a family of JASMONATE ZIM domain-containing (JAZ) proteins was identified that represses JA signaling (Chini et al., 2009, Yan et al., 2007, Thines et al., 2007). JAZ proteins interact with COI1 and the basic helix-loop-helix (bHLH) transcription factor MYC2, a key regulator of JA-induced plant defense responses (Katsir et al., 2008, Melotto et al., 2006). Perception of JA leads to COI1-mediated degradation of JAZs and relieves repression on MYC2 to facilitate activation of JA-responsive genes (Robert-Seilaniantz et al., 2011).

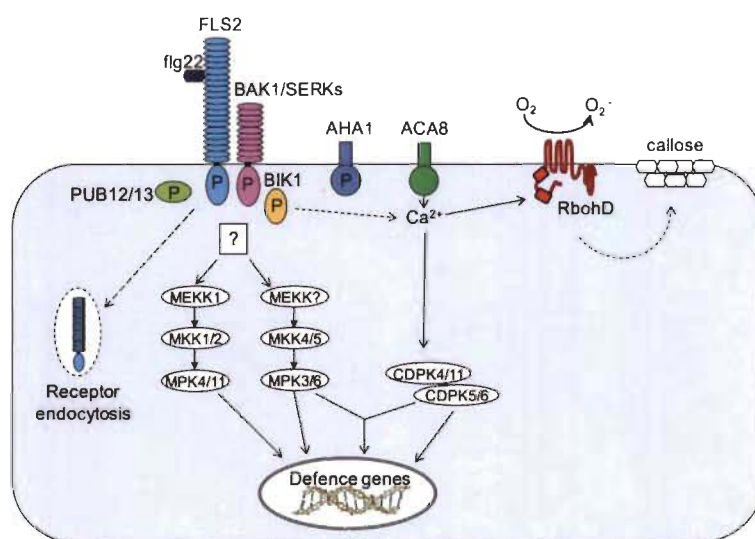


**Figure 1.4. Model of the FLS2 signaling pathway in *Arabidopsis*.**  
Continued on next page.



(continued) Flg22 perception leads to rapid phosphorylation of AHA1, which was implied to facilitate PAMP-induced stomatal closure. Ca<sup>2+</sup> influx, which is partially mediated by the ATPase ACA8, induces the activation of Ca<sup>2+</sup>-dependent protein kinases and RbohD, which is required for PAMP-triggered ROS burst. Flg22 perception also leads to the activation of at least two MAPK cascades. Both cascades regulate synergistically and independently of CDPK4/5/6 and 11 the expression of defense-related genes. Flg22 perception also induced FLS2 endocytosis and potentially attenuates the FLS2 signaling pathway. Phosphorylated proteins are marked with a P. (Adapted from Taj et al., 2010.)

### 1.1.2 The second layer of defense – Effector-triggered immunity (ETI)

Some pathogens have developed strategies to deceive PTI even though PTI inhibits infection. Successful pathogens defeat PTI by secreting virulence factors known as effectors that lead to effector-triggered susceptibility (ETS) (Kawamura et al., Kawamura et al., 2009b) (more on effectors in section 1.3). However, plants have a second layer of defense named effector-triggered immunity (ETI) and also known as gene-for-gene resistance (Flor, 1971b, Flor, 1971a).

The gene-for-gene hypothesis was initially defined by Harold Flor about 60 years ago. He defined this hypothesis based on his observation of the interaction between flax and flax rust fungus. According to this hypothesis, two components are needed during disease resistance in plants. The first is an avirulence (Avr) gene that comes from the pathogen, and the second is found in the host, a matching resistance (R) gene (Flor, 1971a). An HR-like necrotic response was observed when L6, a flax R protein in the plant, interacted with AvrL567, an avirulence factor from flax rust (Dodds et al., 2006). The recognition of effectors has been seen through indirect interactions and has only been observed a handful of times when direct interaction ensued between the R proteins and the effector. A different guard hypothesis was made that described that the target (guardee) of a pathogen effector is monitored by R proteins. This implies that the detection of effectors on host molecules is produced through their effect (Dangl & Jones, 2001).

A classic example of an indirect interaction is RIN4 that is guarded by the R proteins RPM1 (Resistance to *P. syringae* Pv maculicola 1) and RPS2 (Resistant to *P. syringae* 2) (Mackey et al., 2003, Axtell & Staskawicz, 2003, Mackey et al., 2002). RIN4 is a target of the *P. syringae* effectors AvrRpt2, AvrRpmI, and AvrB. AvrRpt2, a cysteine protease,

can degrade RIN4, while AvrRpm1 and AvrB can induce phosphorylation of RIN4. RIN4 cleavage and phosphorylation activate RPM1 and RPS2, which leads to ETI and restriction of bacterial growth (Mackey et al., 2003, Axtell & Staskawicz, 2003, Mackey et al., 2002).

The decoy model is a continuation of the guard hypothesis, which implies that a guardee can evolve into a decoy. The effector is attracted to the decoy through the mimicking of the effector target, and a decoy-associated R protein prompts its perception (van der Hoorn & Kamoun, 2008). Despite this, the decoy does not have a role in defense signaling, unlike the guardee. To exemplify this process, the *Pseudomonas syringae* effector, AvrPto, targets the serine/threonine kinase, Pto, that acts as a decoy (Zipfel & Rathjen, 2008). AvrPto is a type of kinase inhibitor that was observed to function as a binder and blocker of several different PRRs (Shan et al., 2008). ETI is based on the recognition of effectors by resistance (R) proteins. R genes mainly code for the intracellular proteins NB-LRR (Nucleotide Binding Proteins with Leucine-Rich Repeat domains) (Jones & Dangl, 2006) (Figure 1.5).

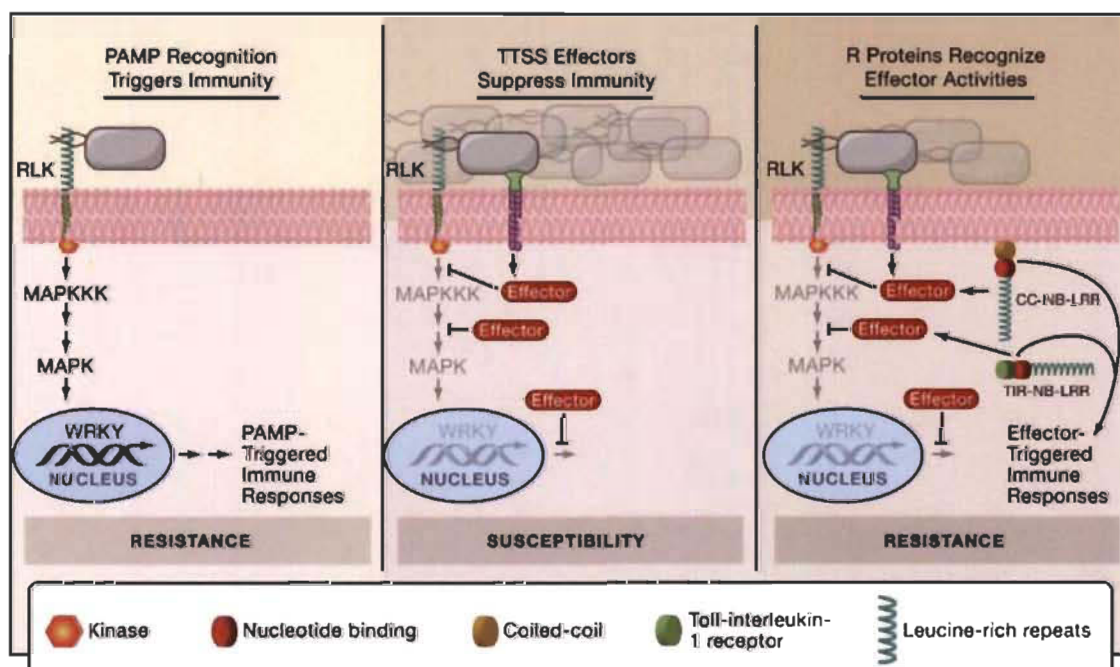


Figure 1.5. Plant-microbe interactions and resistance in plants.

Continued on next page.

(continued) From left to right, recognition of PAMP by extracellular RLKs instantly triggers PAMP triggered immunity, to exercise defensive action, MAP kinase cascades and transcription mediated by WRKY transcription factors are required. Pathogens use the secretion system to deliver effectors that target various host proteins to inactivate PAMP-triggered immunity (PTI). Plant resistance proteins, CC-NB-LRR or TIR-NB-LRR, recognize effector activity and restore resistance by effector-triggered immune responses (ETI). (Adapted from Chisholm et al., 2006.)

### 1.1.3 Systemic acquired resistance (SAR)

Systemic acquired resistance (SAR) was first proposed by Ross and his group. When they observed the lower three leaves of a tobacco plant were infected with tobacco mosaic virus (TMV), the upper leaves developed much weaker symptoms of infection after a second infection 7 days after the first infection (Ross, 1961). SAR is a complex systemic defense mechanism in plants that is triggered by exposure to certain avirulent and non-pathogenic microbes (Vallad & Goodman, 2004). From a local infection, defense transport signals are generated (Figure 1.6), and these signals are transported through the phloem via the apoplast to the uninfected distal tissue and provide them immunity (Singh et al., 2017, Gao et al., 2015, Tuzun & Kuć, 1985). The nature of these systemic signals is unclear. But in recent years, around 13 different possible signals have been proposed (Gao et al., 2015). One of the main signals proposed is SA or its derivative, methyl salicylate, and the accumulation of PR transcripts is required for SAR (Mishina & Zeier, 2007). *Arabidopsis* expressing SA hydroxylase did not show acquire systemic resistance and are unable to accumulate SA upon infection with necrotizing pathogens (Gaffney et al., 1993), presumably due to the destruction of the SA signal. On the other hand, when *Arabidopsis* plants overexpressed SA, they showed enhanced defense to pathogens (Conrath et al., 2006). Along with this, pathogenesis related genes accumulation is often seen as the molecular basis of SAR.

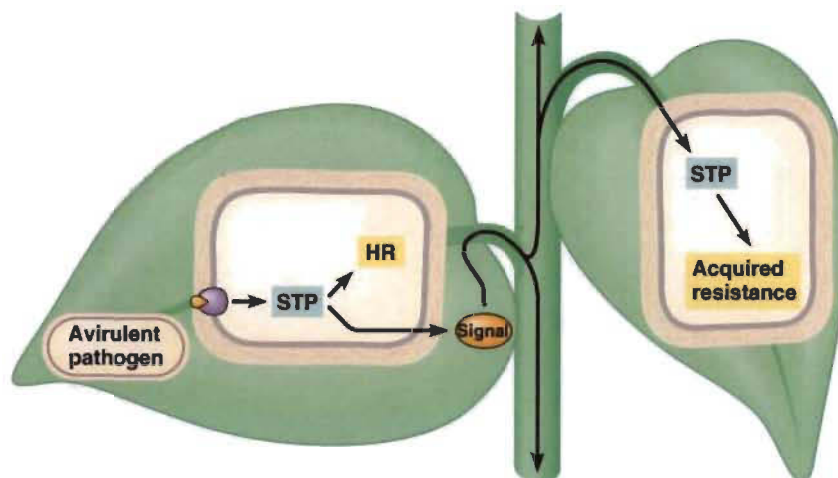


**Figure 1.6. Recognition of a pathogen by an NB-LRR induces a signal transduction pathway (STP).**

STP causes a hypersensitive response (HR), which kills infected plant cells. Before they die, they release antimicrobial molecules. Infected cells release salicylic acid, which is transported throughout the plant. In healthy plant cells, salicylic acid induces STP, which produces antimicrobial molecules, thereby preventing infection. This response is known as Acquired Systemic Resistance (SAR). (Adapted from Dempsey & Klessig, 2012.)

## 1.2 Microbial effectors and their role in plant defense suppression

### 1.2.1 Effectors: concept and definitions

During the arms race between a pathogen and its host, the host produces its defense response against the attacking pathogen; to counteract this defense responses, many pathogens utilize a wide array of strategies, including secreted proteins, called effectors. Effectors are secreted proteins with diverse structural and functional characteristics unique to the pathogen and promote pathogenicity (Hogenhout et al., 2009, Win et al., 2012). They are known to change the physiology of their hosts to support pathogen growth. Although the term "effector" is broadly used in the studies of plant-microbe interaction, its definition is constantly evolving with the increased understanding of the molecular mechanisms involved in pathogenicity. Kamoun (2003) and Huitema et al. (2004) defined effectors as "all molecules (proteins, carbohydrates, and secondary metabolites) that alter the structure and function of host cells, thereby facilitating infection (virulence factors or toxins) and triggering defense response (avirulence factors or elicitors) (Kamoun, 2003, Huitema et al., 2004). The notion of

effector was used in the field of plant-microbe interactions with protein discovery secreted by Gram-negative bacteria in host cells (McCann & Guttman, 2008, Abramovitch et al., 2006). In another definition, Pritchard and colleagues (2014) referred to effectors in plant-pathogen interactions as "any protein synthesized by a pathogen that is exported to a potential host, which has the effect of making the host environment beneficial to the pathogen (Pritchard & Birch, 2014)." However, the widely accepted hallmarks of effectors include; small secreted proteins (SSPs) having an N-terminal signal peptide with low sequence homology across species, no conserved host-targeting signal capable of manipulating and re-programming host metabolism or immunity (Hogenhout et al., 2009). Although many bacterial effectors and filamentous pathogens are indeed involved in the suppression of immune responses, many effectors have shown far more diverse functions such as enzymatic functions (for example, AvrPphB and AvrRpt2 of *Pseudomonas syringae* have cysteine proteases activity), HopZ1a which has acetyltransferase activity, which activates transcription in *Xanthomonas campestris* (Deslandes & Rivas, 2012). Most of the described effectors are proteins; however, non-protein effectors have also been described such as metabolites, toxins, and small interfering RNAs (Cuomo et al., 2011, Arias et al., 2012, Collemare & Lebrun, 2011, De Wit, 2016, Weiberg et al., 2013).

### **1.2.2 Diversity and structural organization of effector proteins**

Plant-associated microbe, bacteria, fungi, oomycetes secrete effectors in the host, which can be either apoplastic or cytoplasmic. The apoplastic effectors are secreted and function extracellularly at the microbe-plant interface (apoplast), and many have been described as inhibitors of host proteases (De Wit, 2016, Song et al., 2009) (Figure 1.7A). These apoplastic effectors interact with host extracellular proteins and can also be recognized by some R proteins that are similar to PRR (Effector-triggered defense against apoplastic fungal pathogens). For example, the apoplastic effectors Avr2, Avr4, and ECP6 of the fungus *Cladosporium fulvum*, which causes tomato leaf mold, target various extracellular processes in the host tomato plant (Bolton et al., 2008, Song et al., 2009, van den Burg et al., 2006). Avr2 is an inhibitor of tomato apoplastic cysteine proteases, Avr4 interact with Cf4 and protects against chitinases. ECP6 interferes with the perception

of *C. fulvum* cell wall chitin by the extracellular immune receptors of the tomato plant (De Jonge et al., 2010).

Cytoplasmic effectors are translocated intracellularly and target subcellular compartments, where they modulate plant immunity, physiology, and metabolism to support pathogen growth and development (Bos et al., 2006, Rafiqi et al., 2012). *Magnaporthe oryzae* fungus effectors are accumulated into host cells at a membranous cap known as the biotrophic interfacial complex (BIC) (Valent & Khang, 2010). Cytoplasmic effectors of *Melampsora larici-populina* (*Mlp*) showed accumulation in plant cells in chloroplasts, nucleus, plasmodesmata, and cytoplasmic bodies (Germain et al., 2018).

The typical organization of the effector proteins of the fungal pathogen contains a signal peptide in the initial 60 amino acids (AA) at the N-terminal end, followed by several domains towards the C-terminal end (Figure 1.7B). These types of effectors are comparatively small and rich in cysteine residues like most serine or cysteine protease inhibitory proteins. For example, known effectors (Avr2, Avr4, Avr9, and ECP2) of *Cladosporium fulvum*, a tomato fungal pathogen, are small cysteine-rich proteins that are believed to function exclusively in the apoplast (Thomma et al., 2005). The apoplastic effectors of *C. fulvum* and other fungal pathogens can inhibit and protect against plant hydrolytic enzymes, for example, glucanases, proteases, and chitinases (reviewed by (Misas-Villamil & Van der Hoorn, 2008). RXLR (arginine, any AA, leucine, arginine) is the most common motif found in over 700 CSEP predicted in two *Phytophthora* species, *P. sojae* and *P. ramorum* (Jiang et al., 2008). RXLR mediates the effector entry into host cells by binding to Plasma membrane intrinsic proteins (PIPs) exposed on the plasma membrane, which induces endocytosis of the effectors in plant cells (Kale et al., 2010). Most effectors carrying RxLR also have a second conserved motif called DEER (aspartate, glutamate, glutamate, arginine) towards the C-terminus.

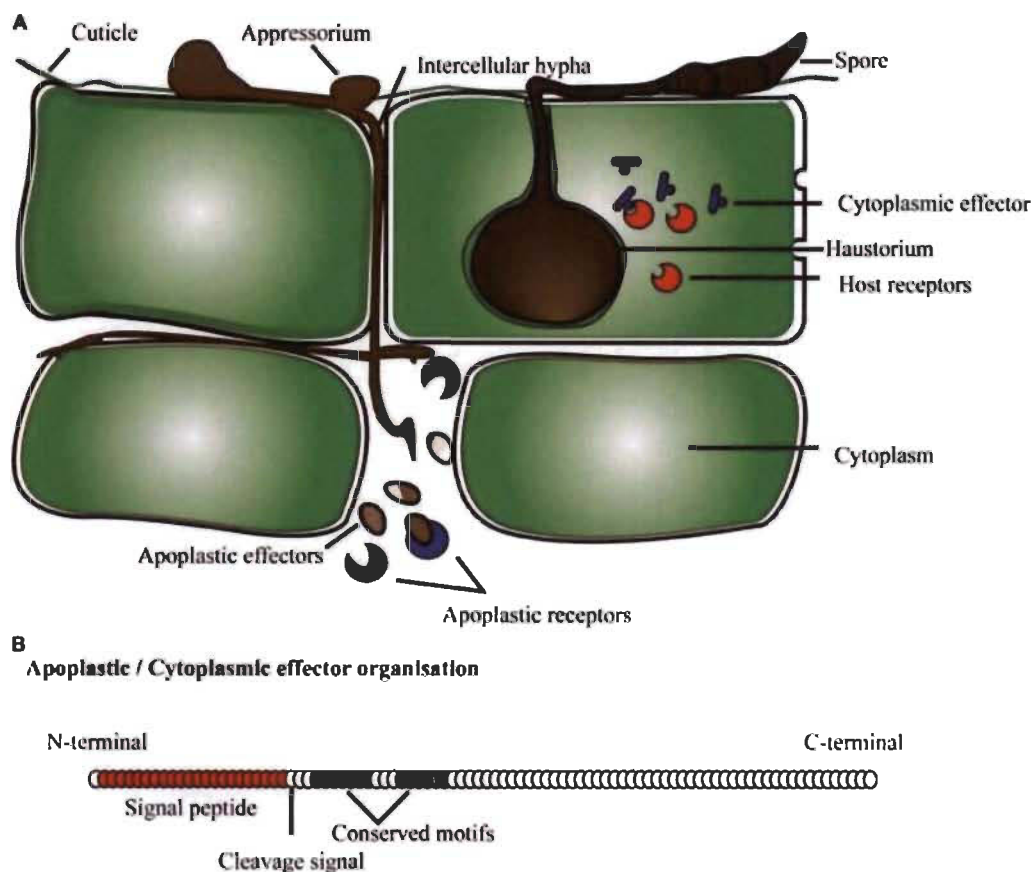


**Figure 1.7. Schematic illustration of effector proteins.**

(A) secreted by fungi/oomycetes in the apoplastic and cytoplasmic region of the plant cell; (B) typical organization of effector proteins. (Image from Sonah et al., 2016.)

### 1.2.3 How are effector proteins introduced into host cells?

One of the critical functions of effector proteins is their successful entry to the site of action in the host cell. The plant pathogens have evolved different strategies to deliver effectors inside the host cells. For example, in the bacterial pathogen, the effectors are usually secreted into the cells using a type III secretion system, a type IV secretion system, or a type VI secretion system (Depluvere et al., 2016) (Figure 1.8A). Many biotrophic fungi and oomycetes pathogens use haustoria, a specialized structure for feeding and effector delivery into host cells (Chibucos & Tyler, 2009). Effector proteins of fungi or oomycetes are often secreted via the conventional endoplasmic reticulum-Golgi apparatus route with their N-terminal secretion signal. They are commonly expressed after contact with their host as their expression is tightly correlated with the different infection stages. Hemibiotrophic and necrotrophic fungi use specialized invasive hyphae (IH) for effector



delivery inside host cells. For example, the hemibiotrophic rice pathogen *M. oryzae* accumulate effectors in a lobed structure at the hyphal tip called the biotrophic interfacial complex (BIC) before subsequent delivery into the host cytosol (Khang et al., 2010) (Figure 1.8B). Other large obligate biotrophic plant-parasitic classes are *Chromadorea* and *Insecta*; they secrete effectors from the secretory gland into the plant cell using the nematode stylet (Figure 1.8C).

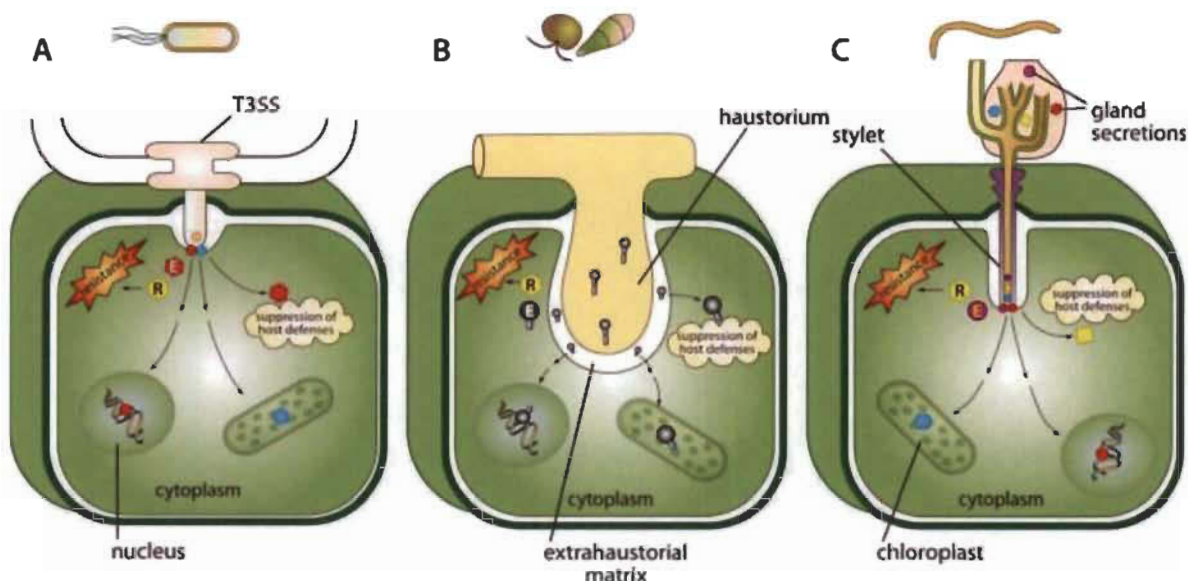


**Figure 1.8. Effector distribution structures of Gram-negative bacteria, oomycetes, fungi, and nematodes in plant cells.**

(A) The type III secretion system in Gram-negative bacteria injects effectors into the host cell. (B) Biotrophic and hemibiotrophic filamentous pathogens are believed to form the haustorium at the site of effector release into the host cell. (C) Effectors from the secretory gland are injected into the plant cell via the nematode stylet. (Adapted from Torto-Alalibo et al., 2009.)

### 1.3 Plasmodesmata: the battlefield against intruders

Plasmodesmata (singular plasmodesma) are channels that connect the cytoplasm of neighboring plant cells, allowing the passage of small molecules such as ions, sugars, essential nutrients, and RNAs (Lucas & Lee, 2004) (Figure 1.9A-B). Decades of research have demonstrated that plasmodesmata regulate cell-to-cell communication during the plant developmental stage and in response to abiotic and biotic stress. Because of this role, opportunistic pathogens have evolved to exploit plasmodesmata as gateways to spread infection from one cell to another. Although these pathogens have acquired the ability to



disrupt plasmodesmal traffic, it is unlikely that plants will give up control so easily over the structure essential to their survival. In the following paragraphs, I will be discussed how pathogens exploit plasmodesma to spread infection.

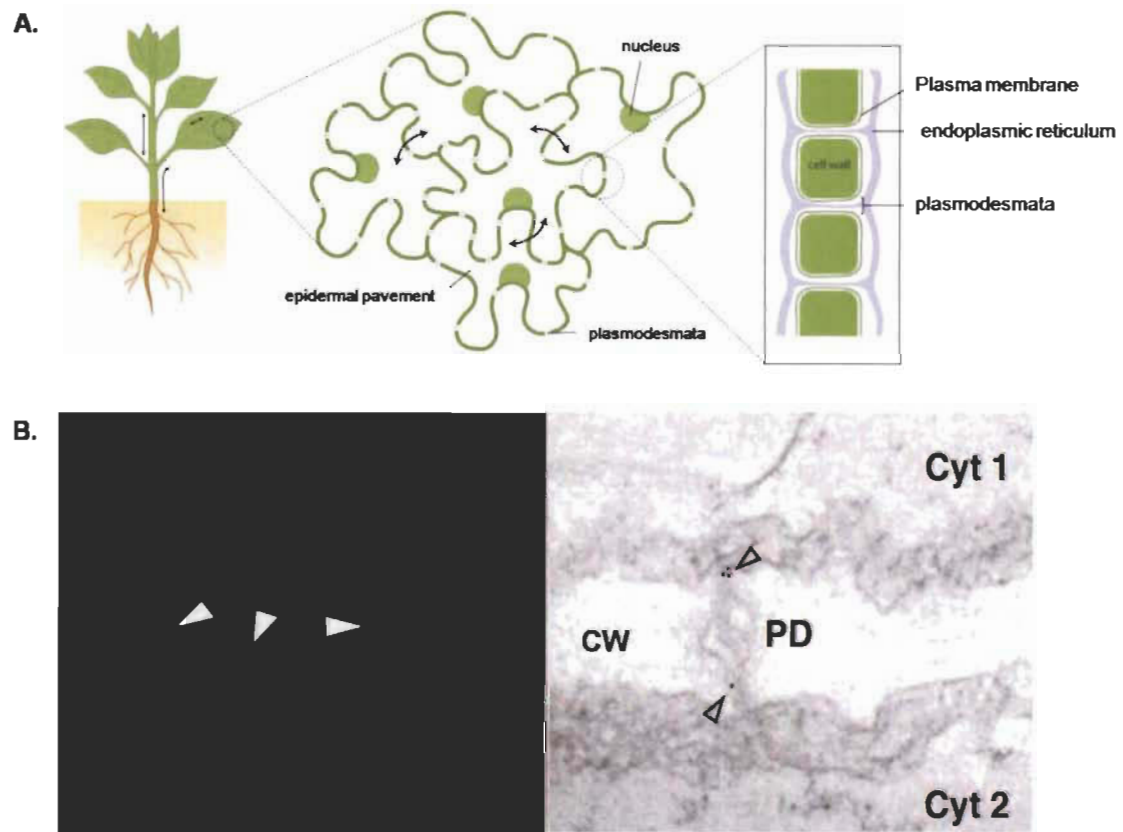


**Figure 1.9. Cellular communication and plasmodesmata.**

A diagram illustrating the cell-to-cell communication via plasmodesmata (A). Confocal image of plasmodesmata as punctate green signals (B, arrowheads left side) in the *Arabidopsis* epidermal cell. Immunogold staining (IGS) of callose (arrowheads) at a plasmodesma (PD) (B, right-sided). (Adapted from Maule et al., 2012.)

### 1.3.1 Virus–plasmodesmata interaction

Plant viruses are obligate pathogens well known to exploit the plasmodesmal trafficking machinery. Viruses use a non-structural specialized component called "movement protein" (MP) to transfer viral genomes from one infected cell to a healthy cell via plasmodesmata. To transfer viral genome, MPs encodes as non-tubule or tubule, which implies specific molecular interactions between cargoes and transporters, as well as the gating of nuclear pore and plasmodesmata channels (Lee et al., 2000). Studies on

cucumber mosaic virus (CMV), tobacco mosaic virus (TMV), and potato virus X (PVX) have shown that viral MP is associated either by direct targeting or indirect interactions with plasmodesmata (Figure 1.10A) using the elements of the cytoskeleton or secretory pathways. (Su et al., 2010, Haupt et al., 2005, Ju et al., 2005, Brandner et al., 2008, Sasaki et al., 2006). In addition, an association of MPs with the ER acts for delivering the MPs in adjacent cells along with the appressed ER; an ER passes through plasmodesmata (Harries et al., 2010, Epel, 2009).

### 1.3.2 Fungus–plasmodesmata interaction

Interestingly, the fungi appear to have a different strategy for exploiting plasmodesmata to spread infection. During a cell-to-cell infection, the rice blast fungus *Magnaporthe oryzae* initially creates a structure called invasive hyphae (IH), which is several microns in diameter (Kankanala et al., 2007). Live imaging suggested that within two hours, IH searched the cell periphery to find suitable intercellular pores and grew into the neighboring cell through the wall at the plasmodesmata (Figure 1.10B). Once the IH is in the intracellular space, it delivers effectors following haustorium formation. The diameter of the IH is highly variable, ranging from  $> 1.5$  nm (when exploiting the PD channel) to up to 30 nm in diameter. This observation suggests that it is not possible to pass the IH through a single intact plasmodesma unless the IH becomes less constricted or a significant reshaping of the size of the plasmodesma channel.

### 1.3.3 Plasmodesmata against bacterial pathogens

Unlike viral and fungal pathogens, bacterial pathogens do not need to interact directly with plasmodesmata to spread the infection. Bacteria use the specialized type III secretion system (T3SS) to secrete effector proteins in the intracellular host space (Zhou & Chai, 2008, Hauck et al., 2003, Xiang et al., 2008). These effectors target different host compartments; some of them target plasmodesmata channels to modulate plasmodesmal function by acting on callose production mainly or other unknown means. *Pseudomonas syringae*, a bacterial pathogen, deploys an effector HopO1-1 that interacts with *Arabidopsis* Plasmodesmata-located protein 7 (PDLP7) and increases the PD-

dependent molecular flux between neighboring plant cells and maximizing the spread of bacterial infection (Aung et al., 2020).

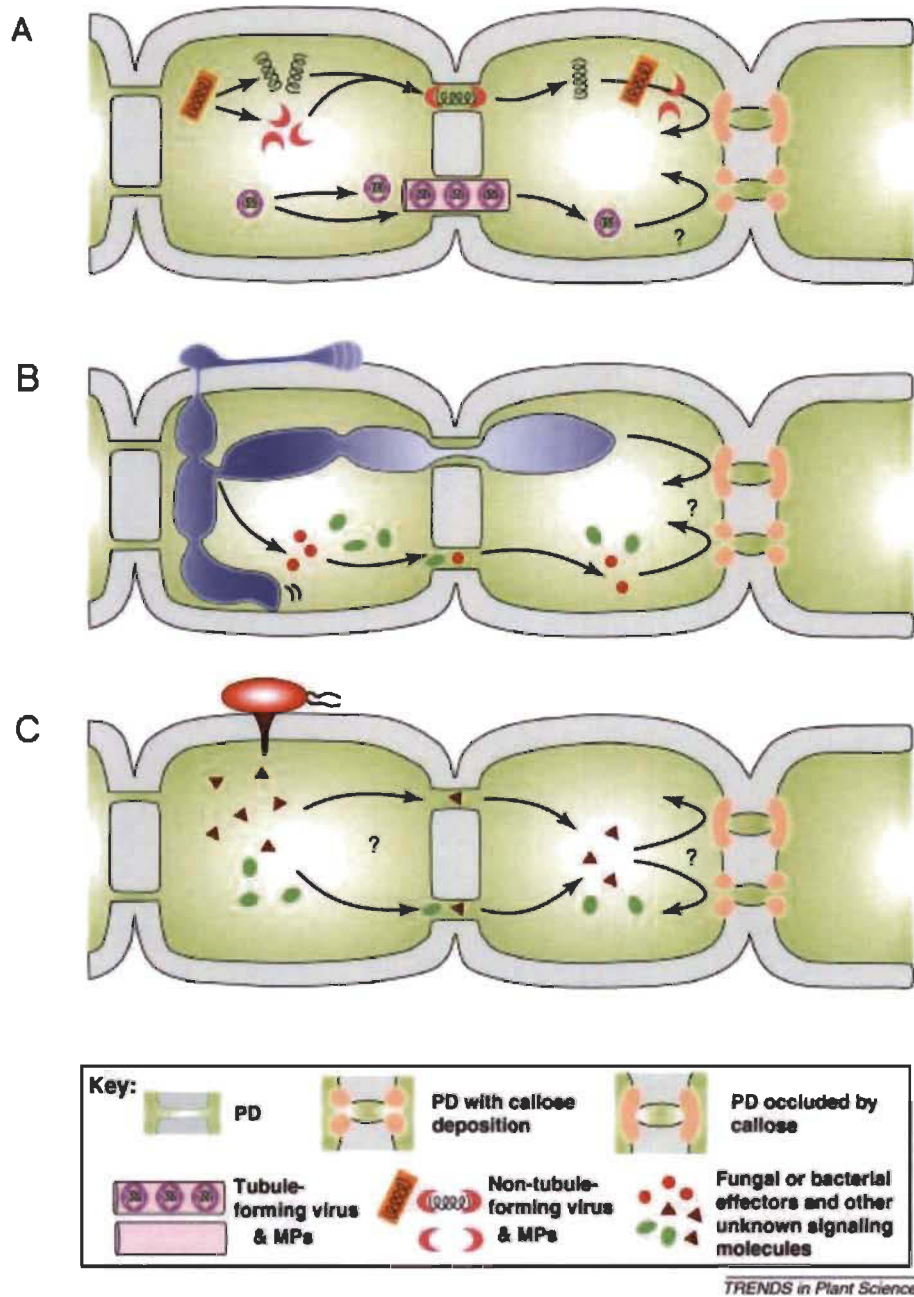


**Figure 1.10. Role of plasmodesmata in defense against pathogens.**

Models are demonstrating the role of plasmodesmata (PD) in interactions with pathogens. (A) Non-tubule viruses encode MP, which modulates the plasmodesmata size exclusion limit (SEL) to allow transport of infectious material. In contrast, tubule-forming viruses encode MP, which reshapes plasmodesma by forming self-assembled tubules, through which the virions pass. In response to virus by plant cell wall induces a callose deposit in the plasmodesma, which can discourage viral spread and could help control cell death by symplastic isolation of infected cells

during HR. (B) IH and effector hemibiotrophic fungal molecules use plasmodesmata during intercellular infection. The promising defense mechanism against fungal involves the plasmodesmata permeability by the deposition of callose. (C) Though bacterial pathogens do not directly meet plasmodesmata because since their T3SS is mainly limited to release effectors in the plant intracellular spaces. Still, to counter the plant defense responses, bacterial could use plasmodesmata channels to transport their specific effector molecules. Likewise, to prevent this from happening, the plant could close the plasmodesmata with callose or other yet unknown means. (Adapted from Lee & Lu, 2011.)

#### 1.4 Role of callose in the regulation of plasmodesmal permeability

Callose, a  $\beta$ -1,3-glucan polysaccharide, is a plasmodesmata marker molecule. The production and degradation of calloses are due to the glucan synthase-like (GSL) and  $\beta$ -1,3-glucanases (BG) gene, respectively, in various locations in the plant. The high level of callose deposition at the cell walls near the neck area of the plasmodesmata narrows the opening of the plasmodesmata channel and *vice versa* (De Storme & Geelen, 2014) (Figure 1.11).

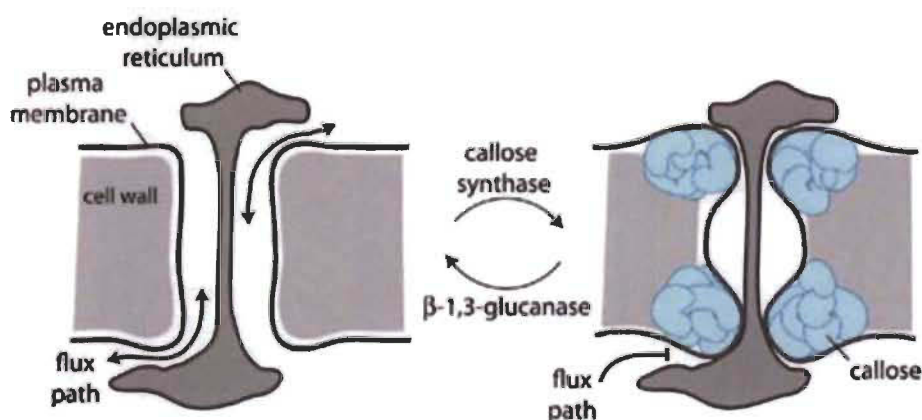


**Figure 1.11. The callose deposit regulates the plasmodesmata opening in the cell wall surrounding the neck of the pore.**

Callose synthases and  $\beta$ -1,3-glucanases located in the plasmodesmata control the regeneration of callose, which determines whether a plasmodesmal is open (left) or closed (right) and if the movement can occur freely between cells (left) or if it is obstructed (right). (Adapted from Maule et al., 2012.)

##### 1.4.1 Specific enzymes modulate plasmodesmal callose levels

The major genes that regulate callose levels at plasmodesmata include members of *A. thaliana*  $\beta$ -1,3-glucanase. AtBG\_ppap (Levy et al., 2007) as well as the family of

*A. thaliana* callose synthase (CalS), coded by *CalS10*, *CalS3*, *CalS1*, *CalS8*. Mutations in plasmodesmal-localized  $\beta$ -1,3 glucanases 1 (PDBG1) or PDBG2, genes increase the accumulation of callose (Benitez-Alfonso et al., 2013). In the *cals10* mutant plant, the lethality of the seedlings and pleiotropic phenotypes were observed due to lack of callose deposit on the cell plate (Guseman et al., 2010, Han et al., 2014). *cals1* mutations decrease the callose hyperaccumulation induced by a pathogenic bacterial infection or salicylic acid. In addition, the *cals8* mutants show an increase in basal plasmodesmal permeability compared to wild type plants (Cui & Lee, 2016). These observations suggest that a network of factors regulating callose controls the permeability of the plasmodesmal channels.

#### 1.4.2 Plasmodesmata-located proteins regulate the plasmodesmal flux

Numerous plasmodesmata-associated proteins, not related to the callose synthase/hydrolase family, control plasmodesmal permeability in a callose-dependent or independent manner (Fig 1.12). *Arabidopsis* Plasmodesmata Callose-Binding Protein 1 (PDCB1) encodes for an extracellular protein, PDCB1, which binds to callose *in vitro*, and its ectopic overexpression increases the deposition of callose at plasmodesmata. LYSIN Motif Domain Containing Gpi-Anchored Protein 2 (LYM2), a chitin-binding receptor-like protein, is a plasma membrane protein that also accumulates in plasmodesmata (Faulkner et al., 2013). In *Arabidopsis lym2* mutants, reduced cell-to-cell movement induced by chitin is abolished, and the chitin-triggered defenses are also compromised. It is not clear if LYM2 regulates plasmodesmata permeability by a callose-dependent mechanism. The Plasmodesmata-Located Protein (PDLP) family encodes eight receptor-like integral membrane proteins in *Arabidopsis*; they consist of a short cytoplasmic tail across a transmembrane helix (Thomas et al., 2008) (Figure 1.12). The double mutants of *pdlp1 pdlp3* and *pdlp2 pdlp3* exhibit increased GFP movement between cells; on the other hand, overexpressed PDLP1 decreases GFP trafficking (Thomas et al., 2008). A summary of plasmodesmata-associated components and their functions is presented in figure 1.12.



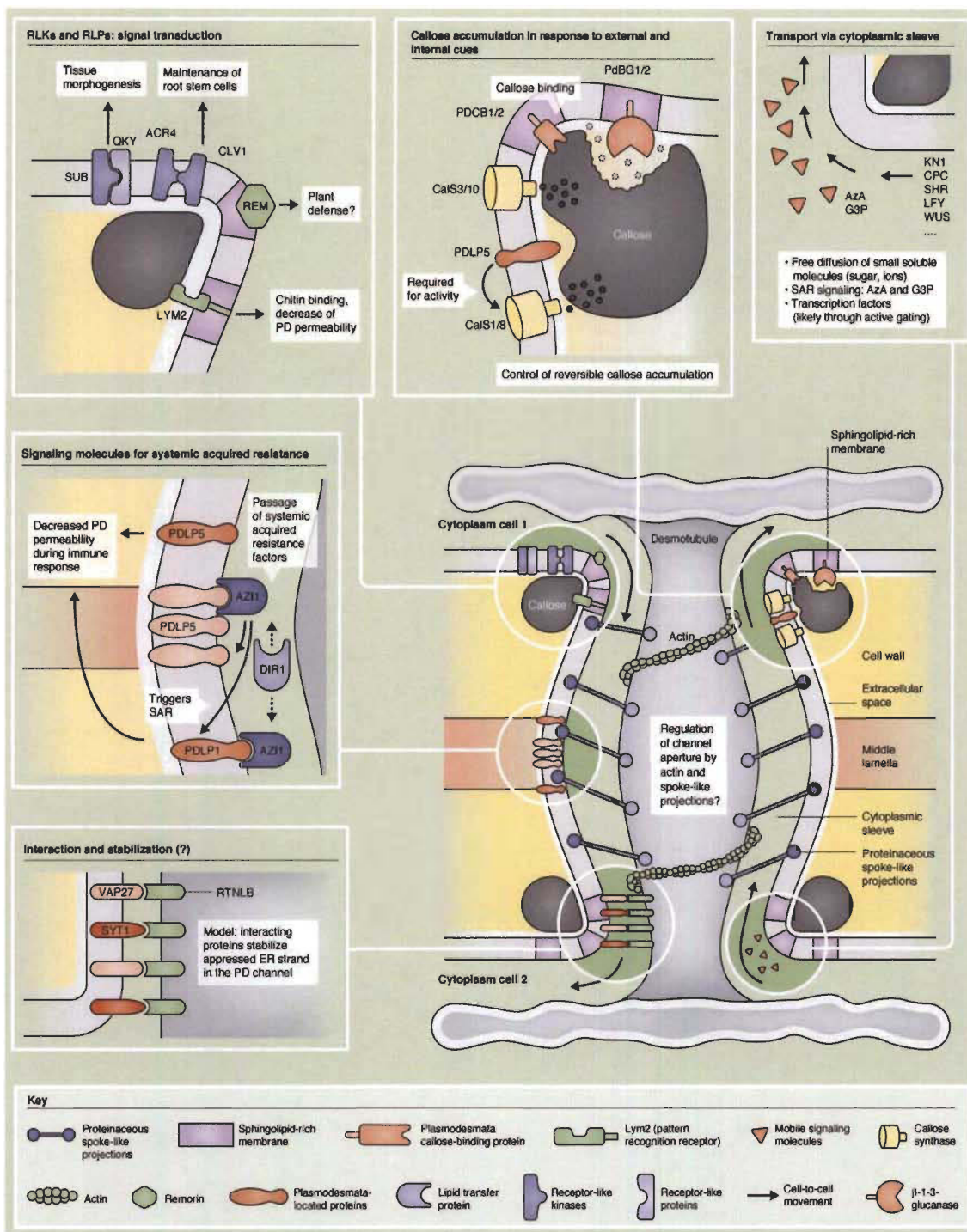


Figure 1.12. Plasmodesmata-associated components and their functions. (Adapted from Sager & Lee, 2018.)

## 1.5 Poplar tree

Poplar (genus *Populus*), a genus of some 35 species of trees in the willow family (*Salicaceae*), is native to the Northern Hemisphere. The native species of poplars from North America are divided into three major groups: 1) the cottonwoods, 2) the aspens, and 3) the balsam poplars. Poplar is mainly cultivated for the production of wood and biomass. Poplar wood is relatively soft and therefore is mostly used to make cardboard boxes, crates, paper, and veneer. Poplar was the first tree whose genome was sequenced, making it a reference model species in tree biology (Tuskan et al., 2006, Meikle, 1984). We have developed an interest in a particular species *Populus trichocarpa*, the black cottonwood poplar, which is a deciduous tree native to North America and abundant in Canada. *P. trichocarpa* has several qualities that make it a suitable model species for trees, such as - the size of the genome (although larger than other model plants such as *Arabidopsis thaliana*), rapid growth, it reaches reproductive maturity in 4-6 years, economically important, represents a phenotypically diverse genus, etc. In Canada, the main limitation of poplar culture comes from epidemics of poplar leaf rust caused by fungi of the genus *Melampsora* (Figure 1.13A).

## 1.6 *Melampsora larici-populina* and Poplar rust

*Melampsora larici-populina* (*Mlp*) is an obligate biotrophic fungal pathogen that causes poplar rust. *Melampsora* alone has more than 50 species, 17 of which are pathogenic to the genus *Populus* (Vialle et al., 2011). Heteroecism is one of the remarkable features of *Mlp*; they infect two completely independent host plants to complete their life cycle; poplar (*Populus* sp., a dicot, telial host) for asexual reproduction and larch (*Larix* sp., conifer, aecial host) for sexual reproduction. To do this, they present a macrocyclic way of life, which involves the production of five different forms of spores; teliospores, basidiospores, pycniospores, ecidiospores, and urediniospores (Figure 1.13B).

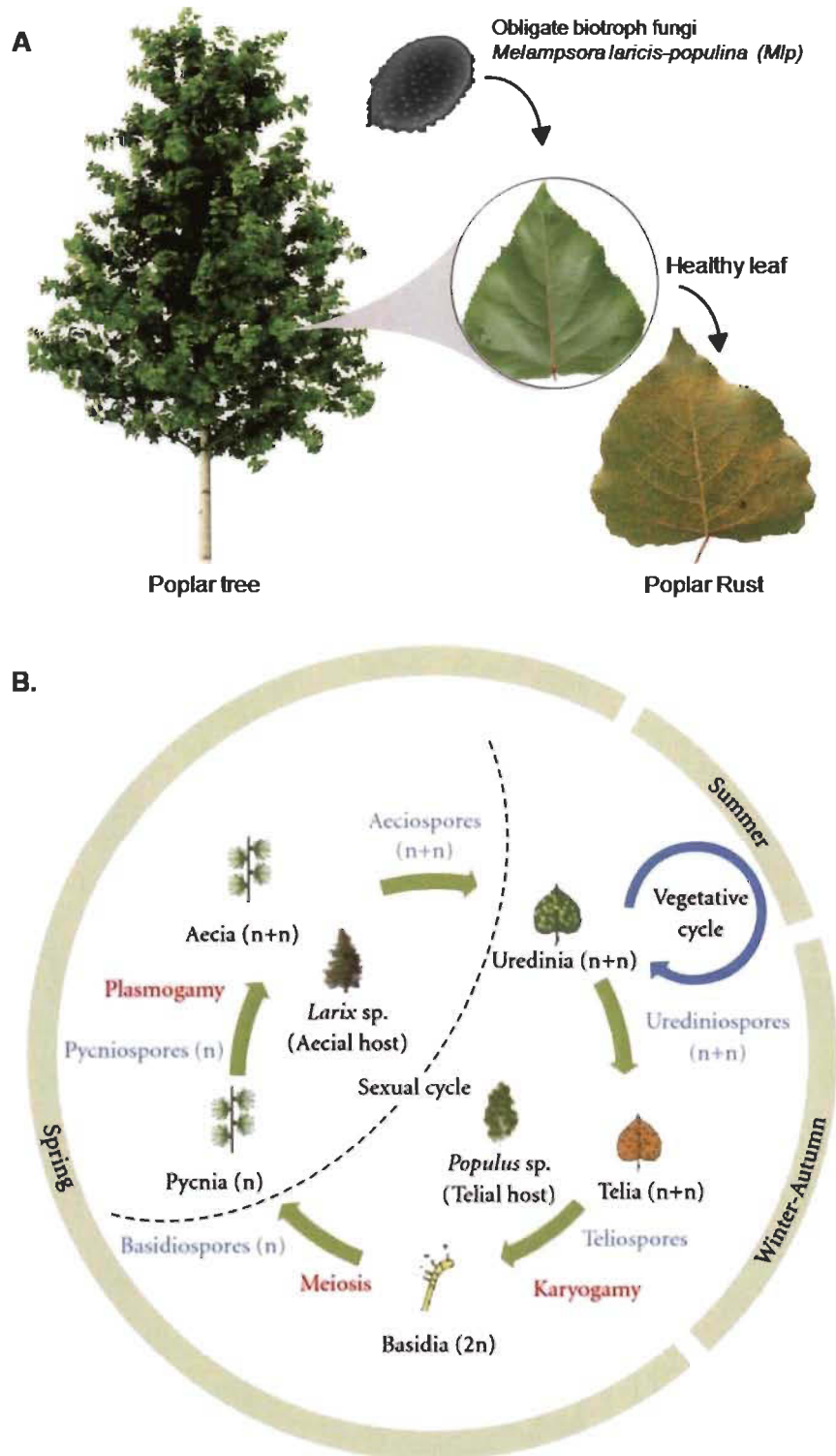


**Figure 1.13. Poplar rust and *Melampsora larici-populina* life cycle.**

(A) Poplar leaf rust caused by *M. larici-populina*. (B) The biological macrocyclic heteroecious cycle of *M. larici-populina*. (Adapted from Hacquard et al., 2011.)



The majority of *Mlp* pathogenic invasion is observed during the asexual developmental phase of the vegetative cycle (urediniospores formation and spreading) (Figure 1.13B). Though *Mlp* infects both larch and poplar, infected larch needles are marked by limited symptoms over time without impacting the growth and development of the host and usually leads to minor damage. The infection of poplar has extensive consequences and causes epidemics in the poplar population for many years. Infected poplars become weak, suffer from a decrease of photosynthesis efficiency, early defoliation, and reduce their viability (Pinon & Frey, 2005). Repeated attacks cause growth loss of up to 60% every year. Poplar-poplar rust is considered a model pathosystem to study not only poplar rust but also other rust diseases due to the genomic information available on poplar and *Mlp* (Duplessis et al., 2011a, Duplessis et al., 2011b, Hacquard et al., 2013, Hacquard et al., 2010, Hacquard et al., 2012, Joly et al., 2010, Pernaci et al., 2014, Persoons et al., 2017, Petre & Kamoun, 2014, Tuskan et al., 2006).

### **1.6.1 Pipelines of effector mining of *M. larici-populina***

The combination of transcriptomic and genomic studies revealed that *Mlp* contains an estimated 1184 small secreted proteins (SSP), candidate-secreted effector proteins (CSEP) (Duplessis et al., 2011a). Based on the results of two independent groups (Figure 1.14), a distinctive pipeline for prioritizing *Mlp* CSEP has been described (Hacquard et al., 2012, Saunders et al., 2012). These effectors are expressed *in planta* and haustoria and, for most, not in spores. No specific domain and function were recognizable or predicted, and in most cases, their sequences were specific to *Pucciniales* (Hacquard et al., 2010, Hacquard et al., 2012, Joly et al., 2010) (Figure 1.14). The study showed the accumulation at various cellular compartments in leaf tissue such as the nucleus, chloroplast, mitochondria, cytosolic bodies, and the nucleolus and protein interaction of *Mlp* CSEPs (Germain et al., 2018, Petre et al., 2015).

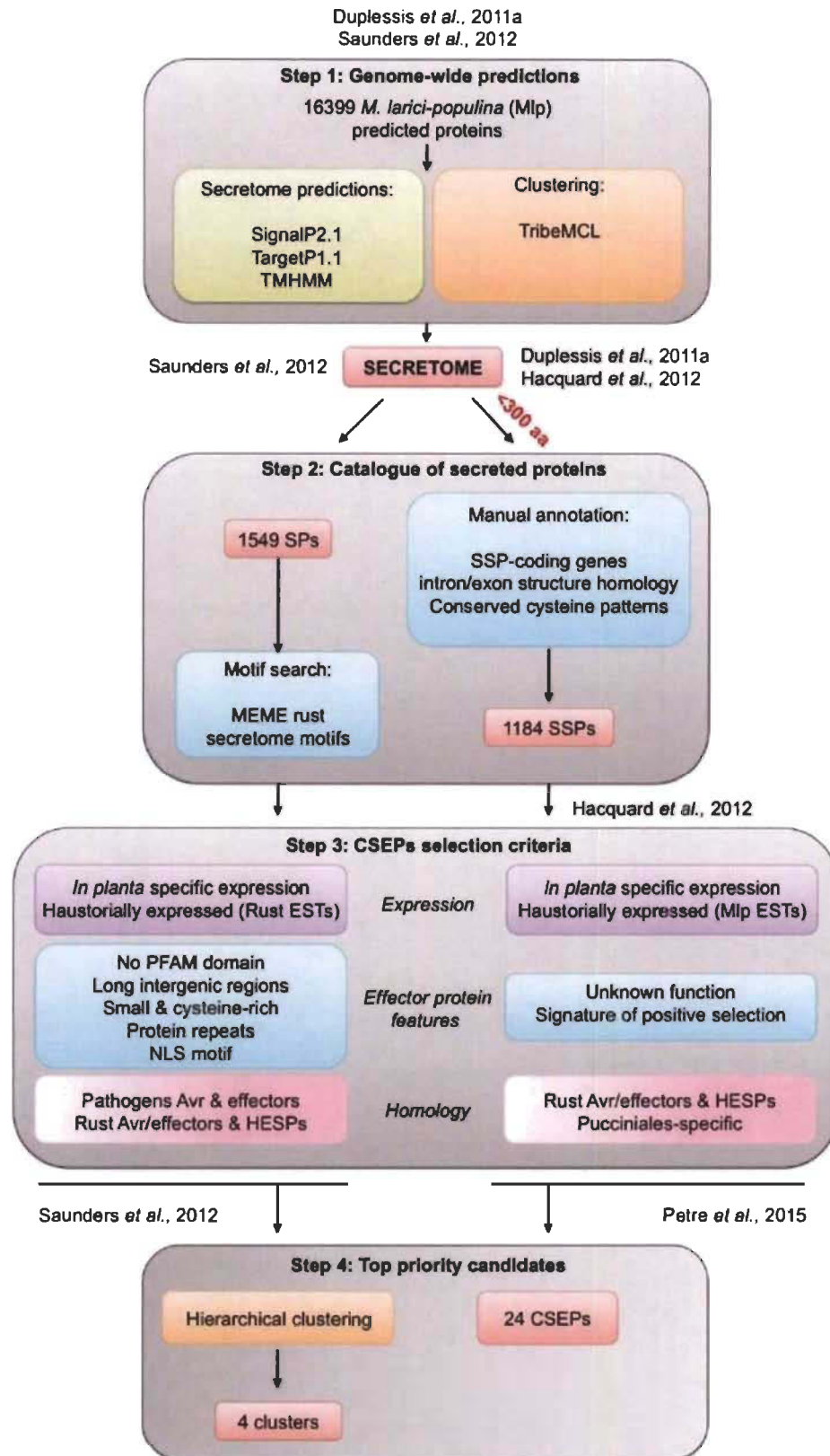


**Figure 1.14. Pipelines of effector mining of *M. larici-populina*.**  
Continued on next page.

(continued) The *M. larici-populina* effector mining pipeline consists of four main stages: stage 1: genome-wide predictions identify the *M. larici-populina* secretome using prediction tools (green) and grouping of families of genes with Tribe<sup>TM</sup> (orange); step 2: the catalog of secreted proteins identifies a set of secreted proteins; step 3: the CSEP selection criteria identify the CSEP by different characteristics; and step 4: high priority candidates give priority to CSEP for further functional studies. Avr = avirulence protein; EST = expressed sequence tag; SP = secreted protein; SSP = small secreted protein; HESP = secreted haustorial expressed secreted protein. (Adapted from Lorrain et al., 2015.)

## 1.6.2 Heterologous system to study effectors

In this study, we used *A. thaliana* and *N. benthamiana* as systems to perform the functional analysis of an *Mlp* candidate effector. *A. thaliana* appeared as a model organism more than three decades ago (Meyerowitz, 1989, Meyerowitz, 2001, Ossowski et al., 2008, Rédei, 1975) and has become a powerful model system in molecular biology and genetics and plant-microbe interactions (Koornneef & Meinke, 2010, Bulbul 2019; Madina 2020). Investigating the molecular basis of rust fungi pathogenicity is hampered by the fact that rust fungi cannot be cultured *in vitro* and genetically modified. Moreover, in the case of poplar leaf rust, the genetic transformation of poplar is only possible with poplar cultivars that are not susceptible to rust, limiting our capacity to manipulate either the pathogen or susceptible host genetically. To circumvent this hurdle, many groups have resorted to using heterologous systems that still allow the study of effectors *in planta* (Sohn et al., 2007, Rafiqi et al., 2012, Fabro et al., 2011). Recently, heterologous systems are commonly used to investigate effector, from biotrophic pathogens, functionality (Caillaud et al., 2012b, Caillaud et al., 2012a, Du et al., 2015, Gaouar et al., 2016, Germain et al., 2018, Kunjeti et al., 2016, Petre et al., 2016a, Petre et al., 2015).

## 1.7 Research objectives

The continuous evolution of new plant varieties and resistance development is crucial to minimizing the damage of crops by rust pathogen. It is crucial to understand better the mechanisms of plant-microbe interaction in disease development in plants. Molecular research in phytopathology has studied the direct interactions between phytopathogens and their hosts to develop effective defense strategies and produce more

resistant crops. Several factors are involved in developing plant disease; among them, effectors are an essential component required for pathogenesis, which modulates plant immunity and facilitates infection. It is not yet clear how these effectors promote virulence in plant rust interaction.

For this thesis research, we selected a plasmodesmata-localized effector protein Mlp37347 from *Mlp* pathogen. More specifically, the localization of Mlp37347 was previously described as cytosolic bodies (further demonstrated as plasmodesmata (Germain et al., 2018), and glutamate decarboxylase 1 (GAD1) was identified as an interaction partner of effector Mlp37347 (Petre et al., 2015). Glutamate decarboxylase (GAD1) is an enzyme that catalyzes the conversion of glutamate to gamma-aminobutyric acid (GABA).

Thus, we wanted to answer the following questions:

- a) Does the Mlp37347 candidate effector manipulate the plasmodesmata size?
- b) If so, how does it control it?
- c) Does Mlp37347 alter plant susceptibility?

To address the questions stated above, we have combined all of our works to tell one complete story. We simply separated this thesis into the following sections- a general introduction, materials and methods, results, and discussion.

The project was started a little before I joined the lab. However, Petre et al. (2015) studied 24 *Mlp* CSEPs and found their localization using *Nicotiana benthamiana* in various cellular compartments in leaf tissue. More specifically, the localization of Mlp37347 was described as cytosolic bodies. Our lab further refined this localization and demonstrated that these cytosolic bodies were, in fact, plasmodesmata (Germain et al., 2018). Moreover, a single interaction protein, glutamate decarboxylase 1 (GAD1), was identified through mass spectrometry (Petre et al., 2015). This unique localization of Mlp37347, PD localization, made us curious to study further the impact of the effector on

the plasmodesmata. Since pathogen proteins, mainly from viruses and bacteria, are associated with plasmodesmata to control intercellular communication (Han et al., 2019). However, reports of fungal proteins interfering with the plasmodesmata flux are limited.

In order to know the impacts of Mlp37347 on plasmodesmata, we have developed several constructs and transgenics to perform an intercellular flux test by measuring the diffusion of mCherry in the presence or absence of Mlp37347 as well as Drop-ANd-See (DANS) assay by measuring the distribution of the carboxyfluorescein diacetate (CFDA) dye. Once we understood the impacts of the effector on plasmodesmata, we followed our interest to identify the components involved in the plasmodesmata flux mediated by the effector. To do that, we investigated the callose level and performed a full transcriptome analysis in an effector overexpressing line.

Finally, we looked at whether the effector makes the plant more susceptible to the pathogen, and if so, how does this virulence achieve. In order to address these, we performed a pathogenicity assay, validated the interaction using yeast two-hybrid, used *in-silico* three-dimensional model analysis, and protein-protein docking.

We conclude that Mlp37347 may take place to cause effector-triggered susceptibility (ETS).

## CHAPTER II

### MATERIALS AND METHODS

#### 2.1 Plants material and growth

Seeds of *Arabidopsis thaliana* and *Nicotiana benthamiana* were vernalized in dH<sub>2</sub>O at 4 °C for 48 h. Plants were grown in soil (PV20 Agromix, Fafard), at 22 °C, 60% relative humidity with a 14h/10h light/dark cycle in a growth chamber. We used *A. thaliana* accession *Columbia-0* as a wild type (control), and a previously described line expressing the Green Fluorescent Protein (GFP) as a control in the infection as well as subcellular localization assay (Ahmed et al., 2018).

#### 2.2 Transgenic production

*Arabidopsis* Col-0 plants were transformed using *Agrobacterium tumefaciens* strain C58C1 to develop transgenic using the modified floral dip method (Mireault et al., 2014). *Arabidopsis* flowers (4-weeks-old) were dipped for 30 seconds into an *Agrobacterium* (OD<sub>600</sub>= 0,6) solution carrying the plasmid of interest and 0.05% OFX as a surfactant. In pre-culture, we inoculated *Agrobacterium tumefaciens* strain C58C1 colony in 4 mL of yeast extract peptone (YEP) media containing spectinomycin (50 mg/L) overnight at 28 °C and using 1 mL of pre-culture to start the main 300 mL culture with the same condition until OD<sub>600</sub>= 1.0. The cells were precipitated by centrifugation at 5000 rpm for 10 min and resuspended in 300 mL 5% sucrose, 0.05% OFX-309 in dH<sub>2</sub>O, and adjusted to OD<sub>600</sub> of 1.5. The dipped flowers were covered with a dome for 48h, and seeds were harvested 3-weeks later. To select the single insertion homozygous transgenic plants, mendelian segregation of the Basta resistance (15 mg/mL) was followed in T1, T2, and T3 generations (Figure 2.1). T3 generations were used for further experiments.

The Salk T-DNA mutant line, Salk\_022227 (*gad1-6*) was obtained from *Arabidopsis* Biological Resource Center (ABRC), Columbus OH, USA. The mRNA of the *gad1* mutant was verified previously by RT-PCR for aberrant transcript (Miyashita & Good, 2008).

### 2.3 Crosses

The Mlp37347-GFP line (Basta resistant) was used as the male parent and the *gad1*-knockout line as the female parent. The F1 seeds were harvested, sown, and screened for resistance to phosphinothricin (Basta). The F1 Basta resistant seedlings were transplanted, further grown on the soil, and observed under a confocal laser scanning microscope (GFP), and F2 was screened for homozygous selection by PCR using specific primers pair (Supplementary Table 1).

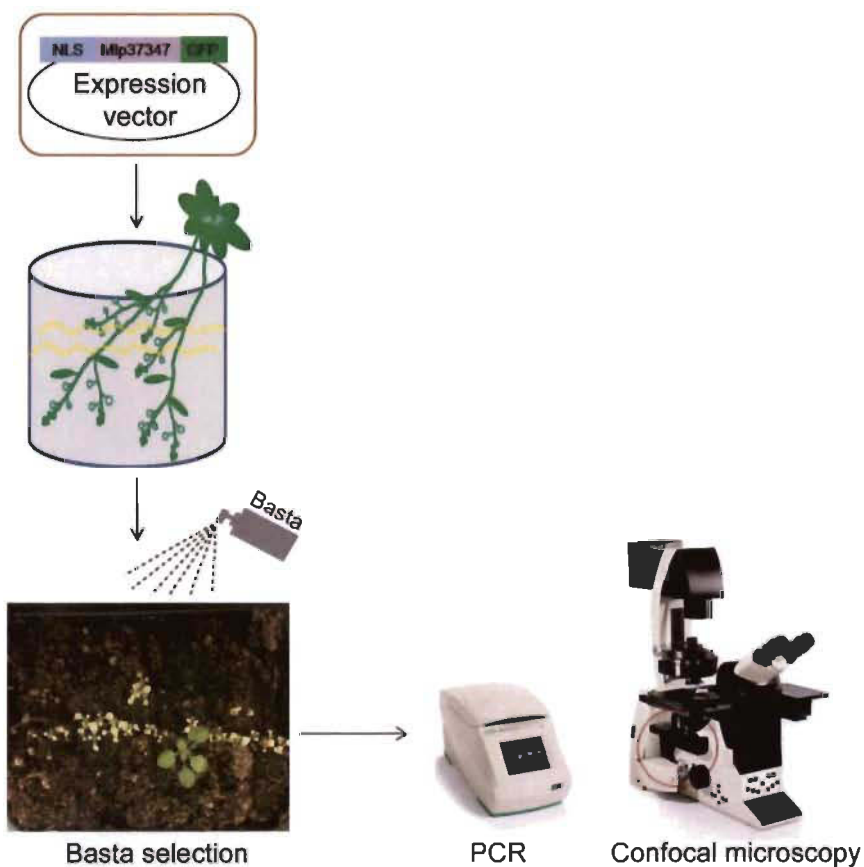
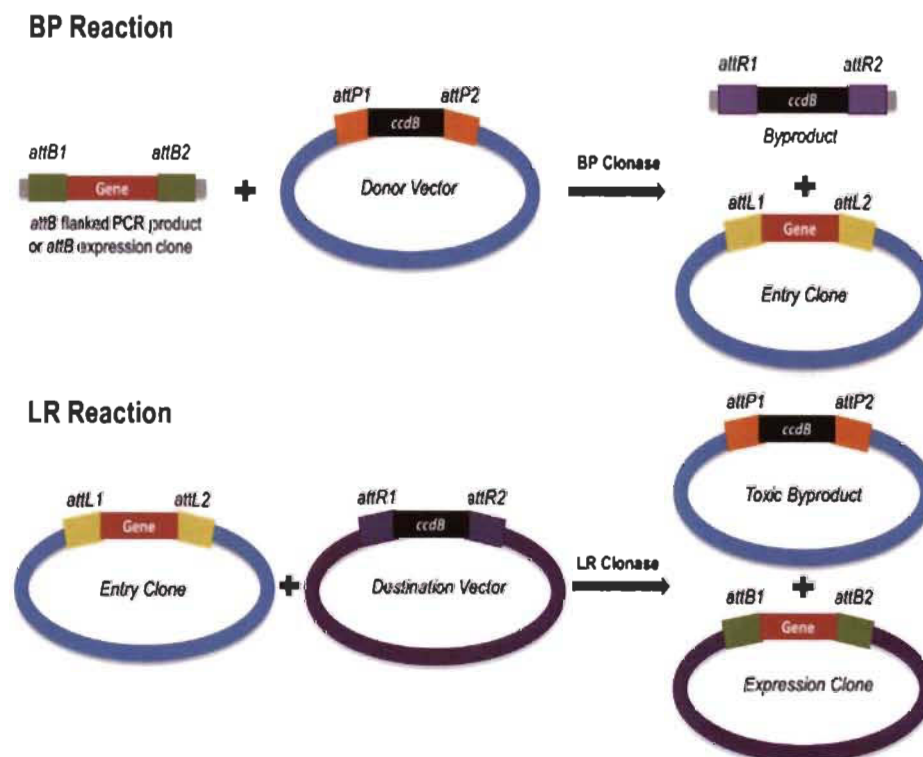


Figure 2.1. Overview of screening T-DNA homozygous selection.

## 2.4 Plasmid constructs and cloning procedures

The GFP-tagged Mlp37347 construct and the transgenic line were previously reported (Germain et al., 2018). To obtain the NLS-tagged construct, the Mlp37347 ORF was PCR amplified with a sens PCR primer encoding the NLS and overlapping with the 5' end of the ORF and recombined in the entry vector pDONR221 by BP reaction and then into vector pB7FWG2 by LR recombination reactions using Gateway technology (Karimi et al., 2002). The sequencing of all the constructs was performed before transformation in *Agrobacterium*. To generate 2XmCherry, two tandem copies of mCherry of gBlocks double-stranded DNA fragments were obtained from Integrated DNA Technologies, Inc. (Iowa, USA). The 2XmCherry fragment was amplified by PCR and cloned into the pDONR221 entry vector, followed by LR reaction into the pK7WG2 vector using the Gateway protocol. Gateway cloning is completed in two recombination reactions: (I) BP recombination and (II) LR recombination (Figure 2.2).



**Figure 2.2. Gateway recombination reactions.**

The Gateway system adopts phage integration into the BP and LR reactions. The BP reaction creates an *attL*-flanked entry clone. The LR reaction creates an expression clone with all the components necessary for gene expression. (Image from Soriano, 2017.)



## 2.5 Expression in *A. thaliana* and *N. benthamiana*

Transient agro-mediated transformation, a technique to introduce transient and high-level expression of genes of interest of *N. benthamiana* leaves, was performed according to the protocol of Krenek et al. (2015). The recombinant bacterial strains were grown overnight in peptone yeast extract (YEP) with appropriate antibiotics, then harvested and resuspended in infiltration buffer (10 mM MgCl<sub>2</sub> and acetosyringone 150 μM). The construct's bacterial suspensions were infiltrated at an OD<sub>600</sub> of 0.5, but the 1XmCherry and 2XmCherry were at an OD<sub>600</sub> of 0.1. Since we aimed to obtain a single or a minimum number of cells express mCherry to investigate PD-dependent flux. We found an OD<sub>600</sub> of 0.5 for mCherry causes an excessive expression, making it challenging to select a single positive cell.

## 2.6 Pathogen infection assays

For the infection assay, we followed the method previously described (Ahmed et al., 2018). *Pseudomonas syringae* pv. *tomato* (Pst) DC3000 cultured overnight at 28 °C and infiltrated using a needleless syringe on the abaxial side of the leaves at an OD<sub>600</sub> of 0.001.

*Hyaloperonospora arabidopsidis* (Hpa) Noco2 infections were performed with 3-weeks-old *Arabidopsis* plants using spray inoculation method at 20 000 spores/mL. Spores were counted at 7 days post-inoculation (dpi) in triplicates [spores/gFW (x 10<sup>4</sup>)] using a hemacytometer.

## 2.7 Confocal microscopy

Live-cell imaging was performed with the Leica TCS SP8 confocal laser scanning microscope (Leica Microsystems) with a 40x/1.40 oil immersion objective. Small excised young leaves from *Arabidopsis* or *N. benthamiana* were mounted in water and were immediately observed. The GFP was excited at 488nm, and emission was recorded at 505–530 nm. Excitation of mCherry was carried out at 552 nm, and emission was captured

between 597–627nm. Images were taken at 512x512 resolution using line-by-line scanning and using sequential scanning (when appropriate). The LAS AF Lite software (Version 3.3), Adobe Photoshop CS6, ImageJ, and Illustrator were used for the post-acquisition image processing.

## 2.8 mCherry diffusion assay

The mCherry diffusion assay was performed in the leaves of *N. benthamiana* in a time-dependent manner (Cao et al., 2018). Briefly, suspensions of *Agrobacterium* cells containing a construct for 1X or 2XmCherry at an OD<sub>600</sub> of 0.1 were infiltrated into the abaxial side of the leaves, containing the effector or not. Thirty-six hours later, the samples were examined by confocal laser scanning microscopy and microscope fields where single cells expressing mCherry (and also expressing or not the effector) were identified and marked. Four hours later, the same cells were imaged again, and the number of surrounding cells now positive for the mCherry was counted; these experiments were repeated three times (Figure 2.3). Statistical significance was calculated using the Student's t-test.

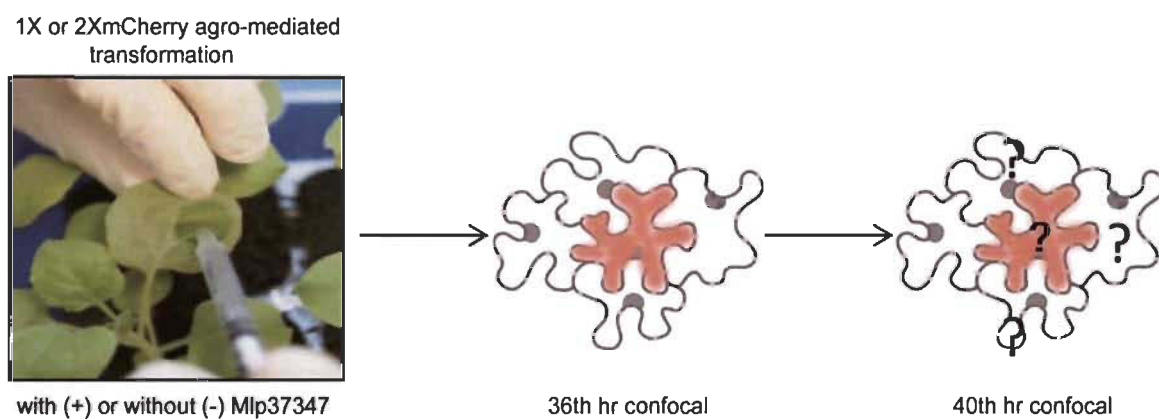


**Figure 2.3.** The workflow of mCherry diffusion assay.

## 2.9 DANS assay and callose quantification

Drop-ANd-See (DANS) dye loading assay was performed on fourth and fifth intact rosette leaves of 3.5-weeks-old *Arabidopsis* plants, as previously described by Cui et al.

(2015). Briefly, the leaves were sprayed with  $\text{H}_2\text{O}_2$  and incubated at room temperature for 2 hours. Subsequently, a  $1\ \mu\text{l}$  droplet of  $1\ \text{mM}$  carboxyfluorescein diacetate (CFDA) was loaded on the center of the upper surface of an intact leaf, followed by confocal imaging of the abaxial surface of the washed leaf 5 minutes after loading CFDA dye. Confocal imaging was performed under a  $40\times/1.40$  objective lens, using laser excitation of  $488\ \text{nm}$  with an emission of  $505$  to  $525\ \text{nm}$  (Figure 2.4).

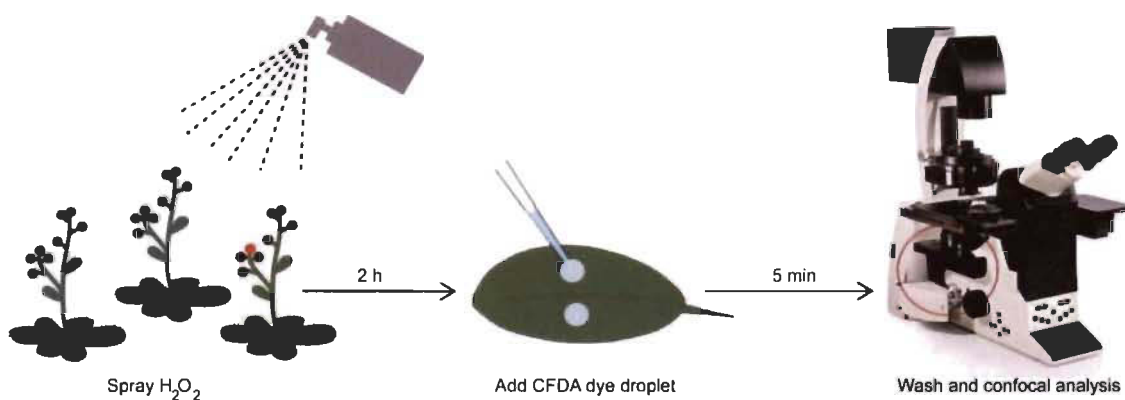


**Figure 2.4. The workflow of Drop-AND-See (DANS) dye loading assay.**

Image of callose deposition at plasmodesmata using aniline blue was carried out according to the protocol described by Zavaliev & Epel (2015) with minor modifications. Entire leaf of 2-weeks old *Arabidopsis* transgenic was submerged in 96% ethanol and incubated at room temperature (RT) on a slow shaker (30 rpm) until complete bleaching. The bleached leaf was removed from the ethanol and gently placed on a flat surface, and strips of 1 mm wide were cut. Leaf strips were rehydrated by placing in  $\text{dH}_2\text{O}$  with 0.01% Tween-20 at room temperature for 1 h and then transferred in 0.01 % (w/v) aniline blue in 0.01 M  $\text{K}_3\text{PO}_4$  (pH = 12). The tubes were placed in a vacuum desiccator at RT for 10 min, and tubes were then wrapped with aluminum foil for 2h on a 100 rpm agitator. Confocal microscope observation was performed at  $405\ \text{nm}$  for excitation and  $475$  to  $525\ \text{nm}$  detection at  $40\times$ . The images were analyzed by ImageJ software using the Analyze Particle tool to quantify the amount of callose.

## 2.10 Y2H reporter assays

The coding sequences of *Mlp37347* (without signal peptide) and *GAD1* were cloned into pGBKT7 (binding domain) and pGADT7 (activation domain), respectively, by homologous recombination in the yeast strain Y2H gold. Both plasmids were extracted and co-transformed in strain Y2H gold. The co-transformants were plated on the medium of double drop out (DDO) without Leu and Trp and a selective quadruple drop out (QDO) without Trp, Leu, His, and Ade (Sigma-Aldrich) and incubated at 30 °C for 3 to 4 days. For photography, dilution series of ( $10^0$ ,  $10^{-1}$ ,  $10^{-2}$ ) were prepared for each transformant, and 10  $\mu$ l were plated on DDO and QDO medium.

## 2.11 Western blot analysis

To verify the protein expression, western blotting was carried out as described by (Germain et al., 2008) with minor modification. 3-weeks-old plant leaves were collected for protein extracts, and leaves were ground to a fine powder with liquid nitrogen and immediately transferred to 1.5 ml Eppendorf tube with extraction buffer 100 mM (Tris-HCl pH8 0.1% SDS, 2% beta-mercaptoethanol and protease cocktail inhibitor 1X). Eppendorf tubes were kept on ice for 5 minutes and centrifuged at 13000 rpm for 10 minutes. The supernatant was transferred to a clean tube. Samples were mixed with loading buffer and boiled for 5 minutes before loading.

The presence of Mlp37347-GFP, NLS-Mlp37347-GFP, and GFP was determined by western blotting. The blot was probed with an  $\alpha$ -GFP-HRP antibody (1:500 dilution, Molecular Probes, Santa Cruz Biotechnology, USA). The bands were revealed with the Clarity<sup>TM</sup> western ECL substrate (Bio-Rad) according to the manufacturer's instruction.

## 2.12 RNA extraction and transcriptome analysis

Total RNA was extracted from 4-days-old *A. thaliana* Col-0 and transgenic plants expressing GFP alone (control) or effector Mlp37347-GFP using Total RNA Mini Kit

(Geneaid). The samples were treated with DNase, and the RNA quality was evaluated by agarose gel electrophoresis. Using 100ng of total RNA and TruSeq strand mRNA library preparation kit (Illumina), the libraries (triplicates for each) were generated with the NeoPrep library preparation system (Illumina). The libraries were then sequenced with Illumina HiSeq 4000 sequencer. The gene ontological (GO) enrichment of up and down-regulated genes (having a Q value  $\leq 0.05$  and a fold change  $\geq 2$ ) was studied using Cytoscape software (version 3.1.1) with the ClueGO and CluePedia plug-in (Bindea et al., 2013) (Figure 2.5).

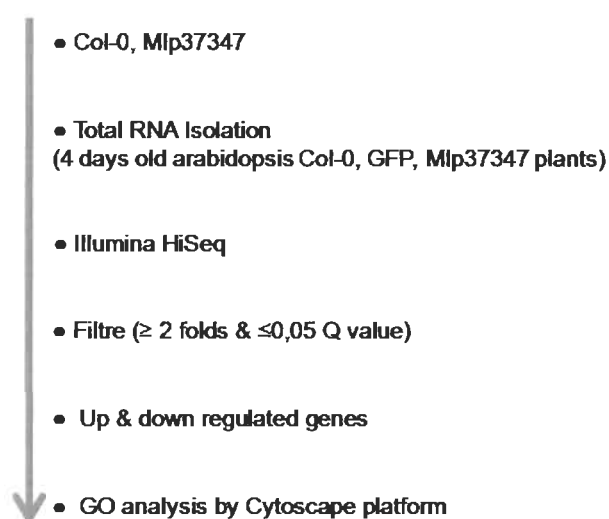


Figure 2.5. Workflow of transcriptome analysis.

### 2.13 *In silico* protein-protein binding

The three-dimensional (3D) structures of Mlp37347 were produced by homology modeling using the I-TASSER server (Yang et al., 2015). This server works in three basic steps.

- Once an amino acid sequence is submitted to the server, the server tries to retrieve model proteins of similar folds or super-secondary structures from the PDB library by LOMETS, a meta-threading approach installed locally.
- In the second step, the continuous fragments extracted from the PDB templates are reassembled into complete models by *Monte Carlo* simulations of replica

exchange with the non-aligned threading regions (mainly loops). When no suitable template is identified by LOMETS, I-TASSER builds the structures by *ab initio* modeling.

- c) In this step, the fragment assembly simulation is performed using SPICKER, a clustering algorithm to identify the close by native models, where the spatial restrictions are collected from both LOMETS and PDB by template modeling (TM)-alignment (Figure 2.6). The value of the TM score scales the structural similarity; TM-score has the value from 0 to 1, where 1 indicates a perfect match between two structures.

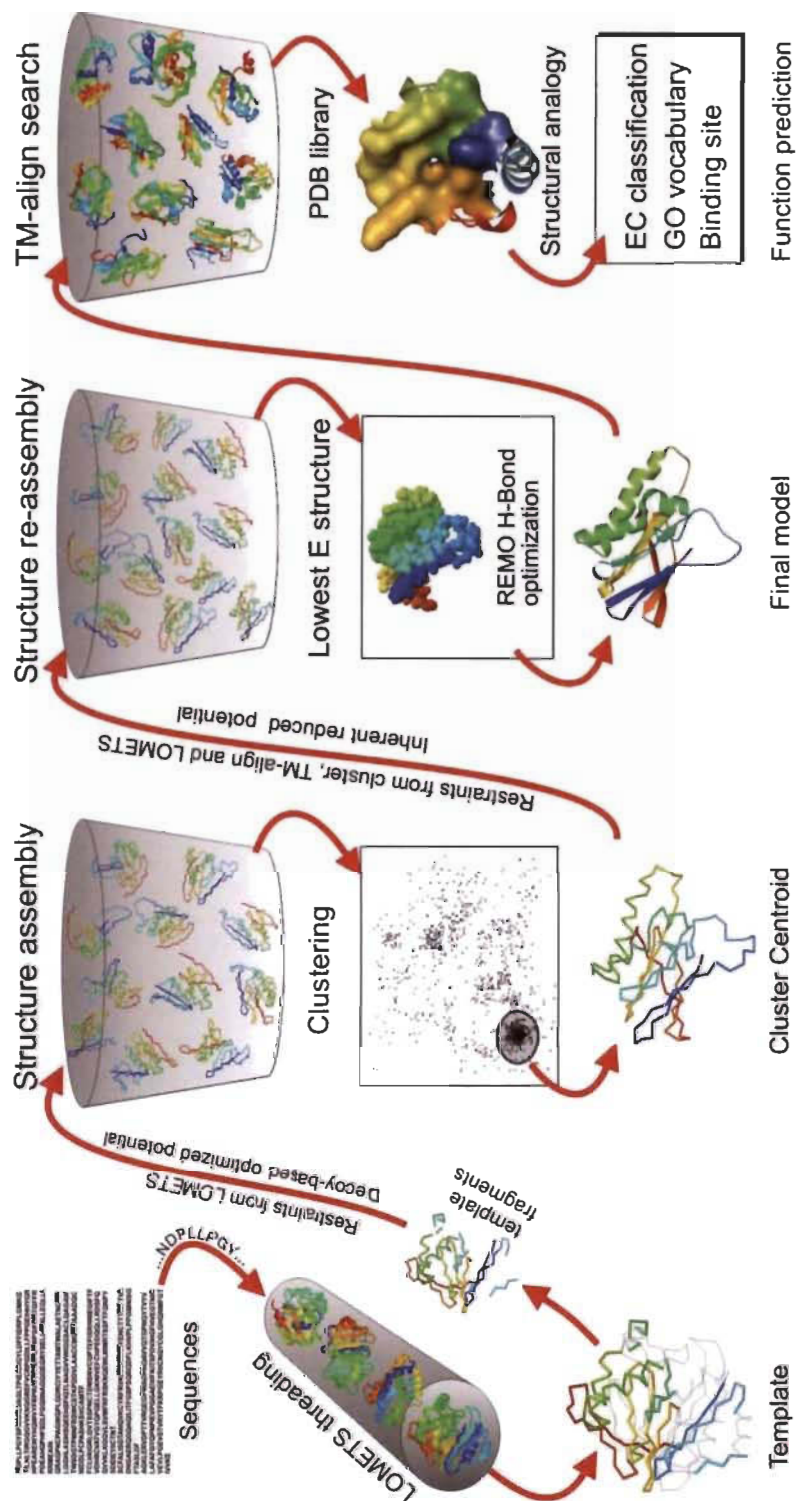


**Figure 2.6. I-TASSER protocol for protein structure and function prediction.**

The *Arabidopsis* GAD1 structure (PDB ID: 3HBX) was obtained from the Protein Data Bank database (<https://www.rcsb.org/>). The binding efficiency of Mlp37347 to GAD1 was determined using four different protein-protein docking host servers Cluspro, Grammx, Patchdock, and ZDock (Kozakov et al., 2017, Pierce et al., 2011, Schneidman-Duhovny et al., 2005, Tovchigrechko & Vakser, 2006).

## CHAPTER III

### RESULTS

#### 3.1 Selection and features of Mlp37347

*M. larici-populina* secretes  $\approx 1184$  potential small secreted proteins (SSP) as revealed by genomic study (Duplessis et al., 2011). Three main selection criteria were considered to identify candidate effectors: i) the effector is expressed during infection (*in planta* and haustoria) but not in spores, ii) no specific domain and function was recognizable or predicted iii) the sequence is specific to *Pucciniales*. Among them, the effectors Mlp37347 encodes for the putative homolog of the avirulence protein AvrL567 protein of *Melampsora lini* (Wang et al., 2007). *Melampsora lini* is a phytopathogenic fungus responsible for a rust disease in cultivated flax (*Linum usitatissimum*).

Mlp37347 displays a plasmodesmata localization (Germain et al., 2018). For the above-mentioned reasons, the mature peptide (corresponding to 128 amino acids, molecular weight 15-17kDa) was investigated for functional studies (Figure 3.1).



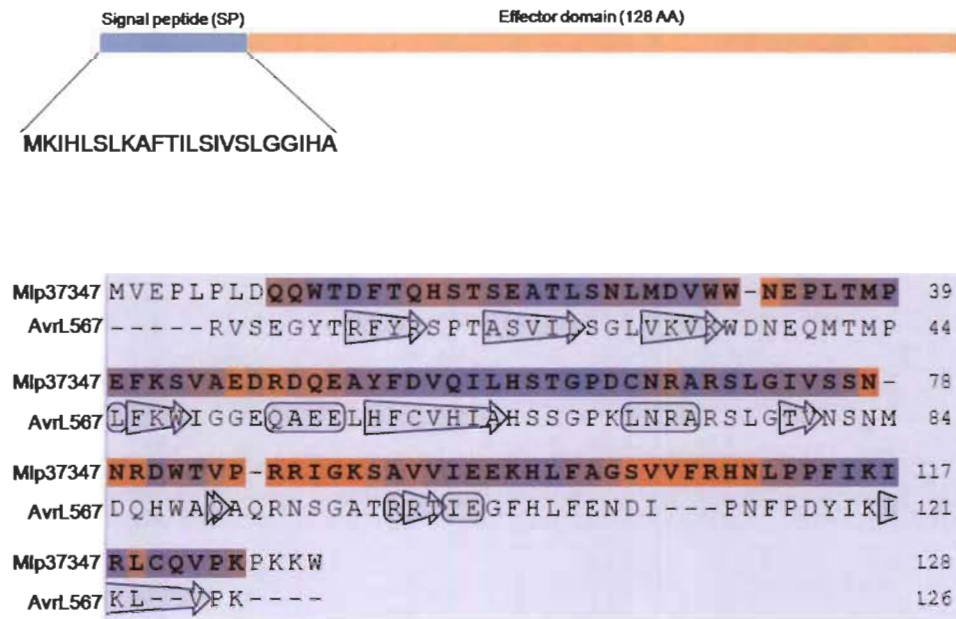


**Figure 3.1. Features of Mlp37347 and sequence alignment between Mlp37347 and AvrL567.** (A) Signal peptide residues in the N-terminus region and is followed by the effector domain of 128 amino acids. (B) Secondary structure prediction based on sequence homology. Arrows and boxes denote template homology among Mlp37347 and AvrL567.

### 3.2 Plasmodesmata localization of Mlp37347

To set up the diffusion assay in *N. benthamiana*, we first assessed if Mlp37347-GFP localization correlated to the plasmodesmata localization previously observed in *A. thaliana* (Germain et al., 2018). To this end, we expressed Mlp37347-GFP by agro-infiltration, and its subcellular localization was determined by confocal microscopy; most importantly, we evaluated its co-localization with the plasmodesmata marker PDCB1-mCherry. Both fluorescent proteins overlapped in punctate structures (Figure 3.2), confirming that Mlp37347-GFP accumulates at the plasmodesmata in *N. benthamiana* as it did in *A. thaliana*.

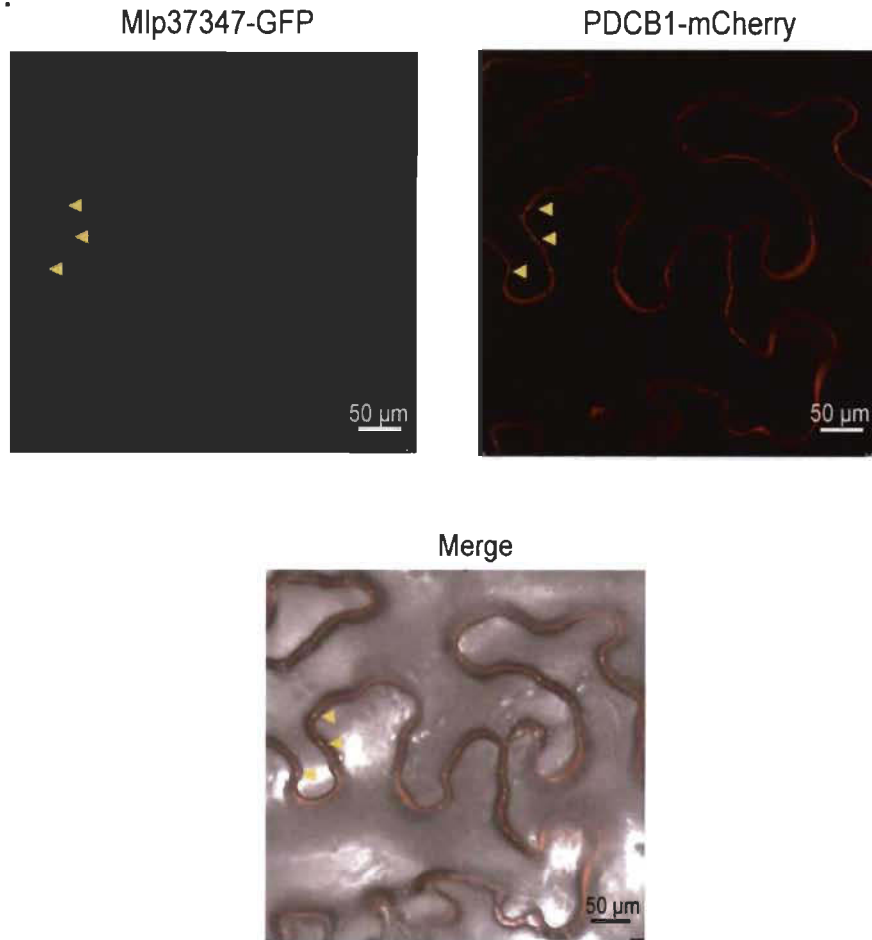


**Figure 3.2. Co-localization of Mlp37347-GFP with the plasmodesmata marker PDCB1-mCherry in *N. benthamiana*.**

Co-localization between Mlp37347-GFP and PDCB1-mCherry, a plasmodesmata marker to confirm Mlp37347-GFP localization. Upper left panel, green channel; upper right panel, red channel; lower panel, overlay with differential interference contrast (DIC).

### 3.3 Mlp37347 enhances plasmodesmata flux

In order to assess if Mlp37347 could be involved in the manipulation of the plasmodesmata flux, we performed an intercellular flux assay by measuring the diffusion of mCherry in the presence or absence of Mlp37347.

It was previously shown that fluorescent proteins could diffuse across the plasmodesmata, whereas tandem fluorescent proteins exceed the size exclusion limit (SEL) of plasmodesmata, i.e., its size would prevent the diffusion of the protein to the neighboring cells unless the plasmodesmata in enlarged (Zambryski & Crawford, 2000).

For this assay, we use a single and a tandem mCherry (thereafter 1XmCherry and 2XmCherry). Thirty-six hours after co-agroinfiltration, mCherry positive cells were identified and marked. Four hours later, the same fields were re-imaged, and the positive cells neighboring the initial positive cells were counted (Figure 3.3). As expected, the 1XmCherry could diffuse to neighboring cells, and its diffusion was accelerated in the presence of Mlp37347 (Figure 3.3).

However, the 2XmCherry did not diffuse to neighboring cells when Mlp37347 was not present, but diffusion was observed when co-expressed with Mlp37347 (Figure 3.3). These observations suggest that 2XmCherry through the plasmodesmata is facilitated in the presence of Mlp37347.

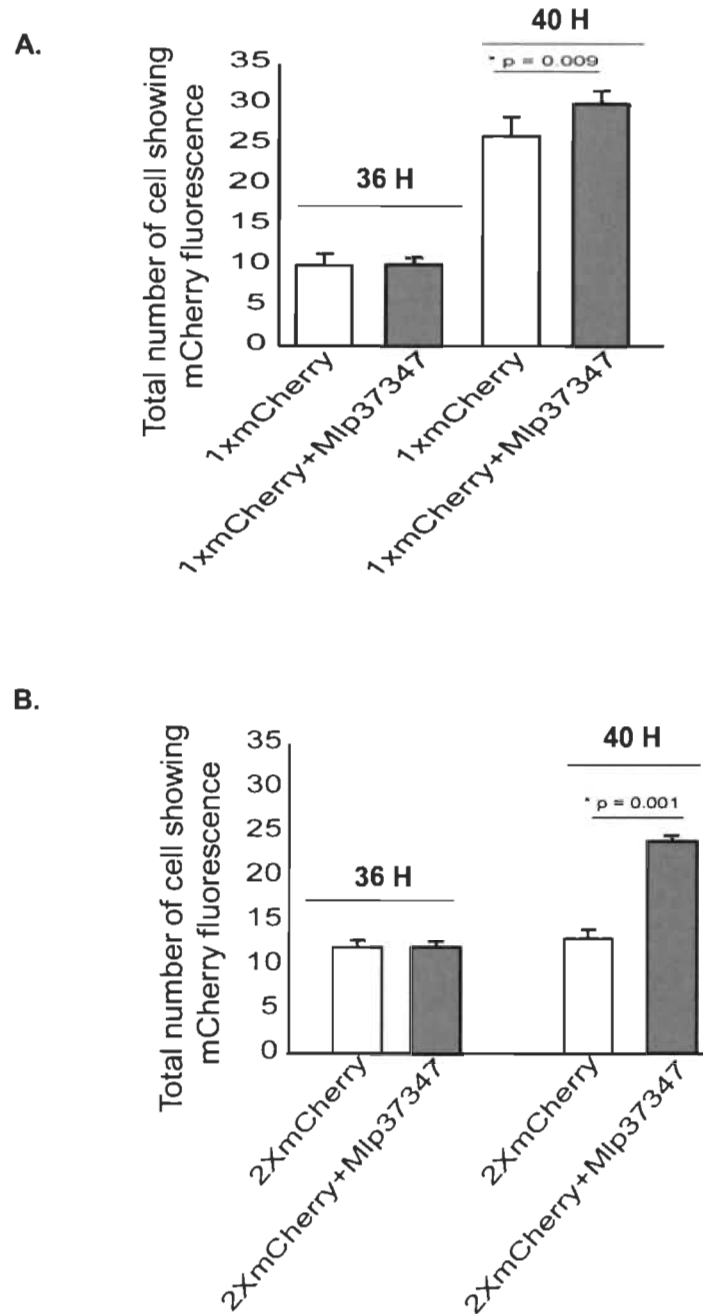


**Figure 3.3. Mlp37347 enhances plasmodesmata flux.**

(A) 1XmCherry expressing cells at 36-hour and 40-hours when infiltrated with the 1XmCherry without Mlp37347-GFP. (B) 2XmCherry expressing cells at 36-hour and 40-hours when infiltrated with the 2XmCherry without Mlp37347-GFP and with Mlp37347-GFP. Quantification of diffusion of mCherry to surrounding cells provided a measure of molecular flux through plasmodesmata. Data represent mean  $\pm$  SD,  $n = 8$  observations. Student's t-test determined the statistical difference from the control leaves without Mlp37347-GFP; asterisks indicate statistical significance. Experiments were repeated three times ( $N = 3$ ).

### 3.4 Mlp37347 localization at plasmodesmata is required for diffusion

To determine if the localization of Mlp37347 at the plasmodesmata is important for the increased flux observed using the mCherry diffusion assay, we developed an *Arabidopsis* stable transgenic line in which a nuclear localization signal was added to the N-terminal of the effector (NLS-Mlp37347-GFP). We also verified the integrity of the GFP recombinant proteins by Western Blotting and concluded that all constructs were at the expected molecular weight (Figure 3.4).

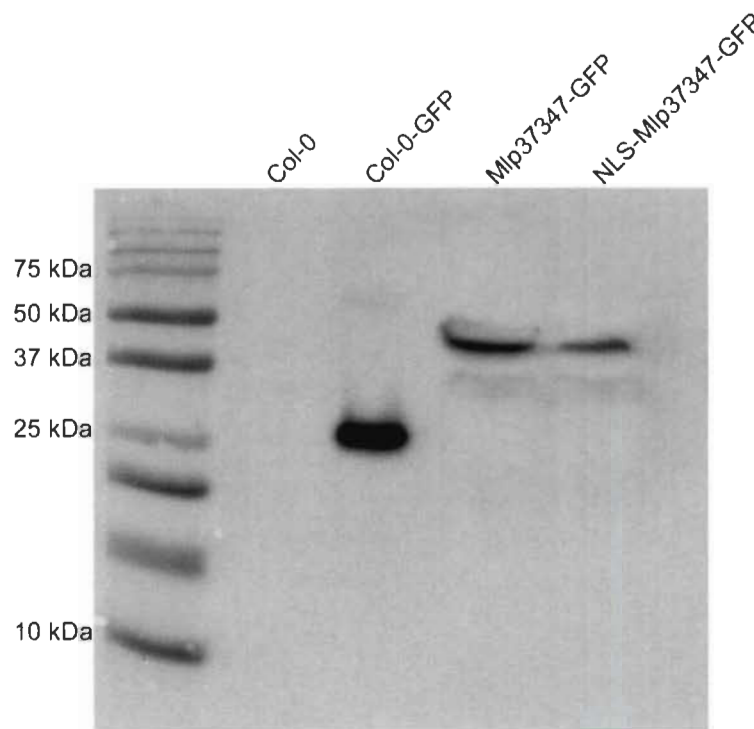


**Figure 3.4. Expression of Mlp37347-GFP variants in *Arabidopsis*.** Immunodetection of GFP protein in wild-type (Col-0) and stable transgenic seedlings expressing Mlp37347 from 14 days old plantlets.

Because DAPI staining is more easily performed in *N. benthamiana*, we verified that the new construct co-localized with DAPI in *Nicotiana*. The NLS-tagged effector Mlp37347-GFP now segregates in the nucleus and no longer accumulated at the plasmodesmata (Figure 3.5A-B).

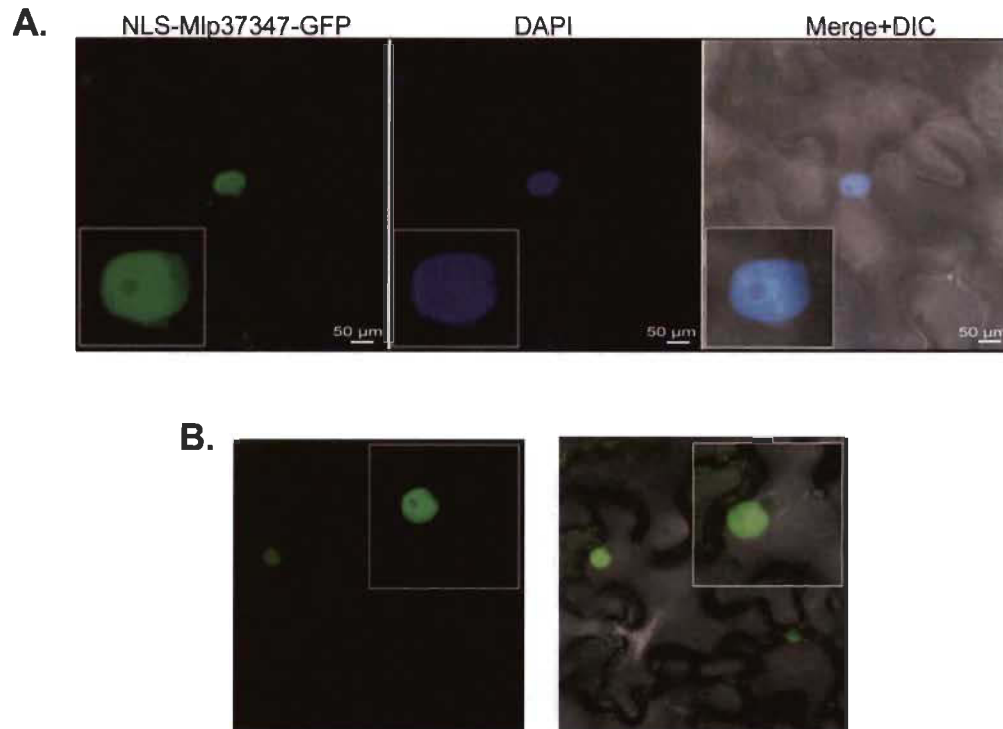


**Figure 3.5. Nuclear localization of NLS-Mlp37347-GFP in *N. benthamiana* and *A. thaliana*.** Subcellular accumulation of NLS-Mlp37347-GFP in *N. benthamiana* epidermal cells at 3-days post-infiltration, the nucleus was stained by DAPI, and epidermal cells were observed under the green channel (left panel), blue channel (middle panel), and merge of the two channels +DIC (right panel). (B) Subcellular localization of NLS-Mlp37347-GFP in *A. thaliana* cells at 3-days post-infiltration.

To test plasmodesmata permeability in plants expressing this new construct, we then performed a dye diffusion assay called Drop-ANd-See (DANS) (as described by Sun et al. (2019) in wild type (Col-0), Mlp37347-GFP and NLS-Mlp37347-GFP plants. We measured the diffusion area of CF dye. This assay showed a significant flux increase, revealed by the larger area stained by the CF dye, in the presence of Mlp37347-GFP (Figure 3.6); however, this increase not observed when the effector is restricted to the nucleus. This result demonstrates that the localization of Mlp37347 at the plasmodesmata is indeed required to increase the intercellular flux.

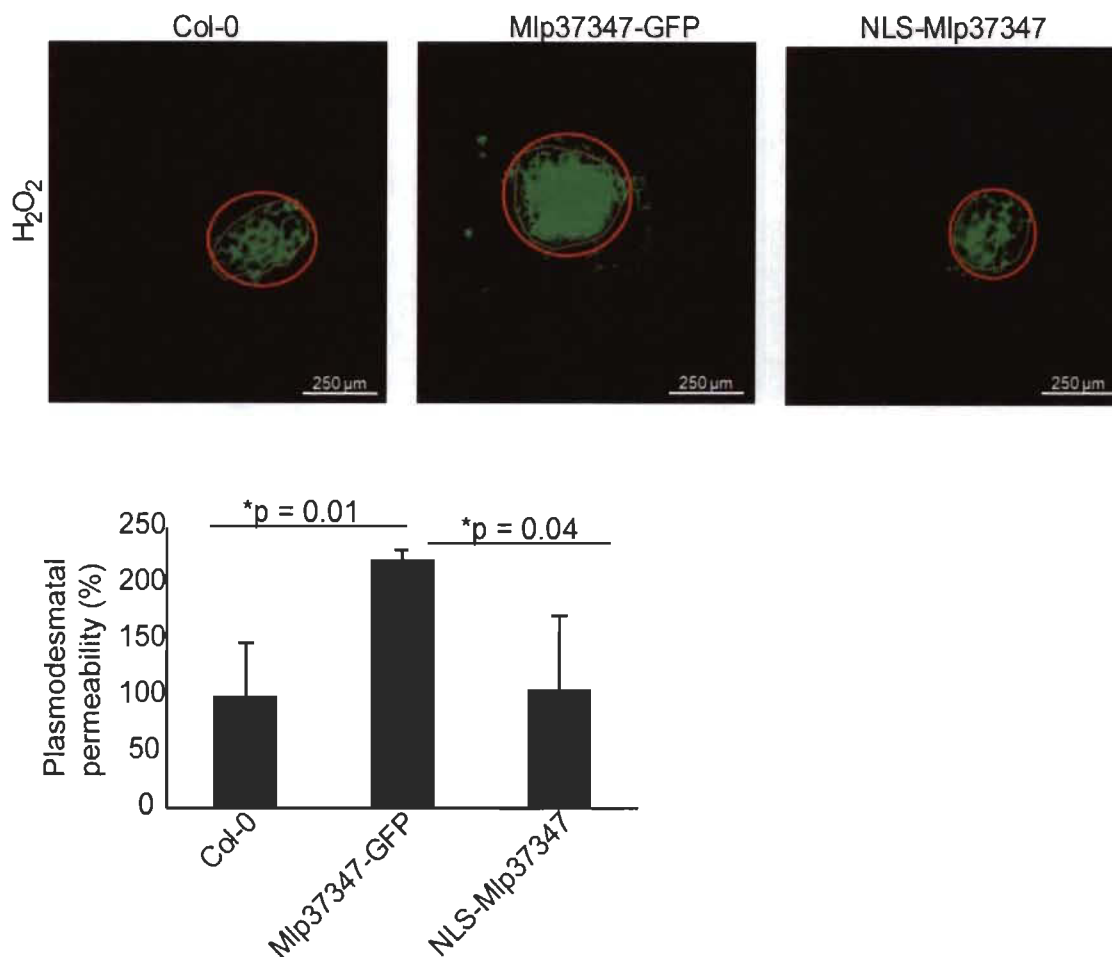


**Figure 3.6. Plasmodesmata localization of Mlp37347 is required for enhanced plasmodesmal flux.**

DANS experiments were performed on the fifth and sixth leaves of 3.5-week-old *A. thaliana* plants. After mock or chemical treatment, DANS assays were performed by loading a 1  $\mu$ l droplet of the probe on each side of the leaf surface in the central region. For the ROS treatment, plants were sprayed with either water (for mock treatment) or 10 mM H<sub>2</sub>O<sub>2</sub> and incubated for 2 h before measurement. Permeabilities were measured in percentage compared to control. Data represent mean  $\pm$  percent of SD error. The statistical difference from the control Col-0 leaves was determined by Student's t-test, asterisks indicate statistical significance, P-values as indicated. Experiments were repeated at least three times (N=3), and representative data are shown.

### 3.5 Mlp37347 interacts with *Arabidopsis* GAD1 and *Populus* GAD1

In an effort to dissect the molecular mechanisms responsible for the effect of Mlp37347-GFP *in planta*, we focused our attention on its only known interactant, GAD1. First, we used the yeast-two hybrid (Y2H) method to support the interaction between GAD1 and Mlp37347 previously identified by immunoprecipitation and mass spectrometry (Petre et al., 2015). Independent co-transformation experiments showed that

yeast co-expressing a bait-Mlp37347 construct with a prey- *Arabidopsis thaliana* (AtGAD1) or *Populus trichocarpa* (PtGAD1) construct was able to grow on quadruple dropout (QDO) medium (Figure 3.7), confirming their ability to establish contact.

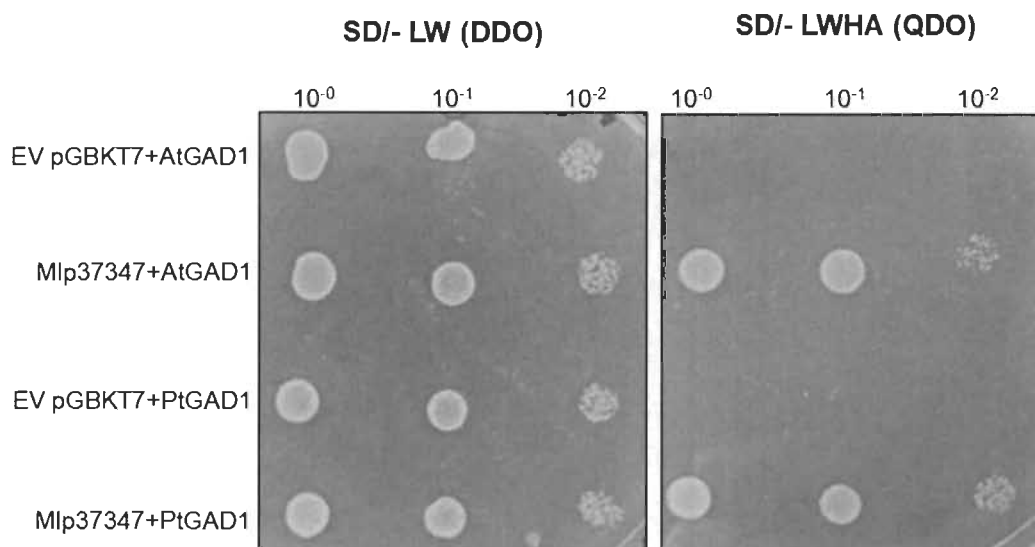


**Figure 3.7. Mlp37347 interacts with AtGAD1 and PtGAD1.**

Co-expression of AtGAD1/PtGAD1 with Mlp37347 in yeast shows interaction assay between GAD1 and Mlp37347. Yeast co-expressing the indicated combination of bait and prey were spotted on the synthetic double dropout medium lacking leucine and tryptophan (SD/-LW (DDO)) and quadruple dropout medium lacking leucine, tryptophan, histidine, and adenine (SD/-LWHA (QDO)). The plates were photographed 3-4 days after inoculation.

### 3.6 Molecular modeling also supports the association of GAD1 and Mlp37347

*In silico* approaches have been of crucial importance in the evaluation of protein-protein interactions (Rao & Srinivas, 2011). To further characterize this interaction, a 3D structure model of Mlp37347 was constructed by iterative template-based fragment assembly simulations using I-TASSER (Zhang, 2008). This model (Figure 3.8) estimated a template modeling score (TM-score) of 0.85 and showed a structural homology with the avirulence protein from *Melampsora lini*, AvrL567-A (PDB ID: 2OPC), and their known sequence identity was calculated which is 40%.



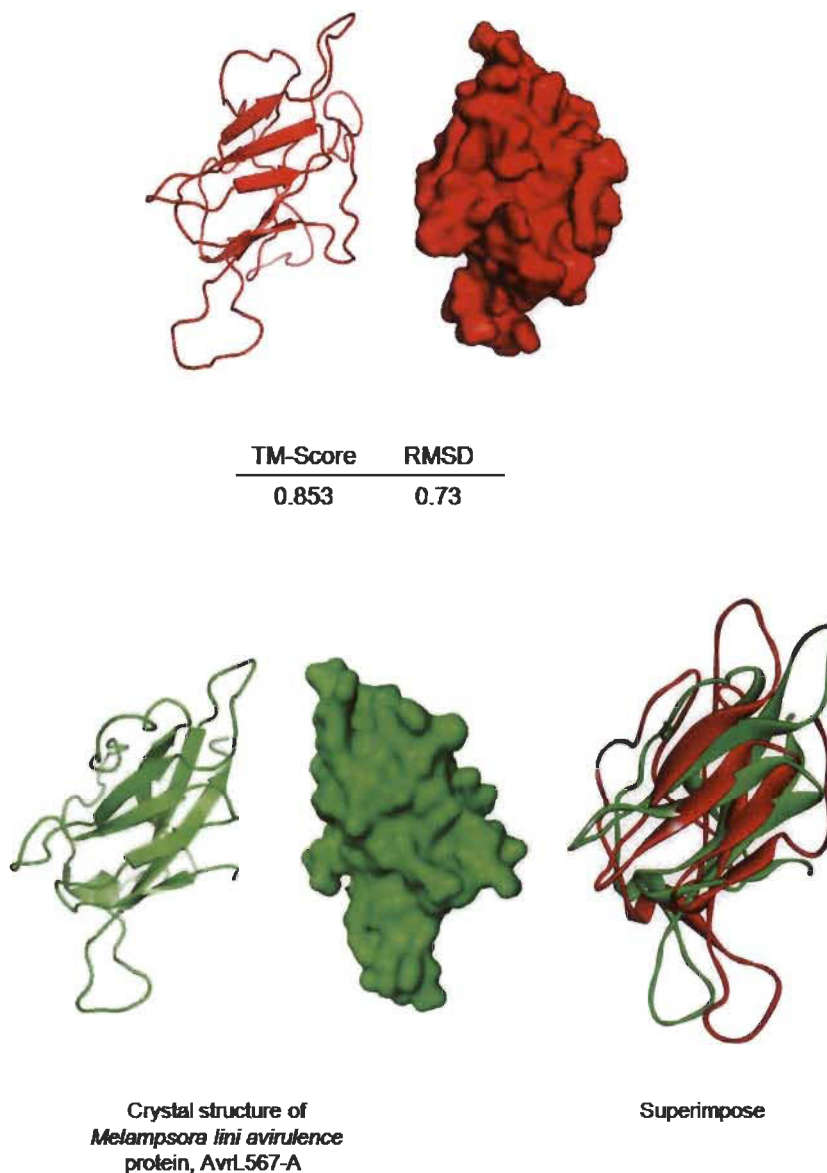


**Figure 3.8. Molecular modeling of Mlp37347.**

Predicated structure of Mlp37347 (red ribbon). TM-score value is 0.85, where 1 indicates a perfect match between two structures. On the right, superimposition between Mlp37347 and AvrL567 (green ribbon).

This simulation result gave us the confidence to perform a molecular docking with the plant GAD1. We used *A. thaliana* (At) GAD1 (PDB ID: 3HBX) and prepared the monomer AtGAD1 (chain B) by removing the polymer chain and the endogenous ligand (2S)-2-amino-6-[[3-hydroxy-2-methyl-5-(phosphonooxymethyl) pyridin-4-yl] methylideneamino] hexanoic acid (LLP). Both Mlp37347 and AtGAD1

structures were then executed an energy minimization (MMFF94), and obtained conformations were subjected as preliminary structures to carry out docking analysis (Figure 3.9).

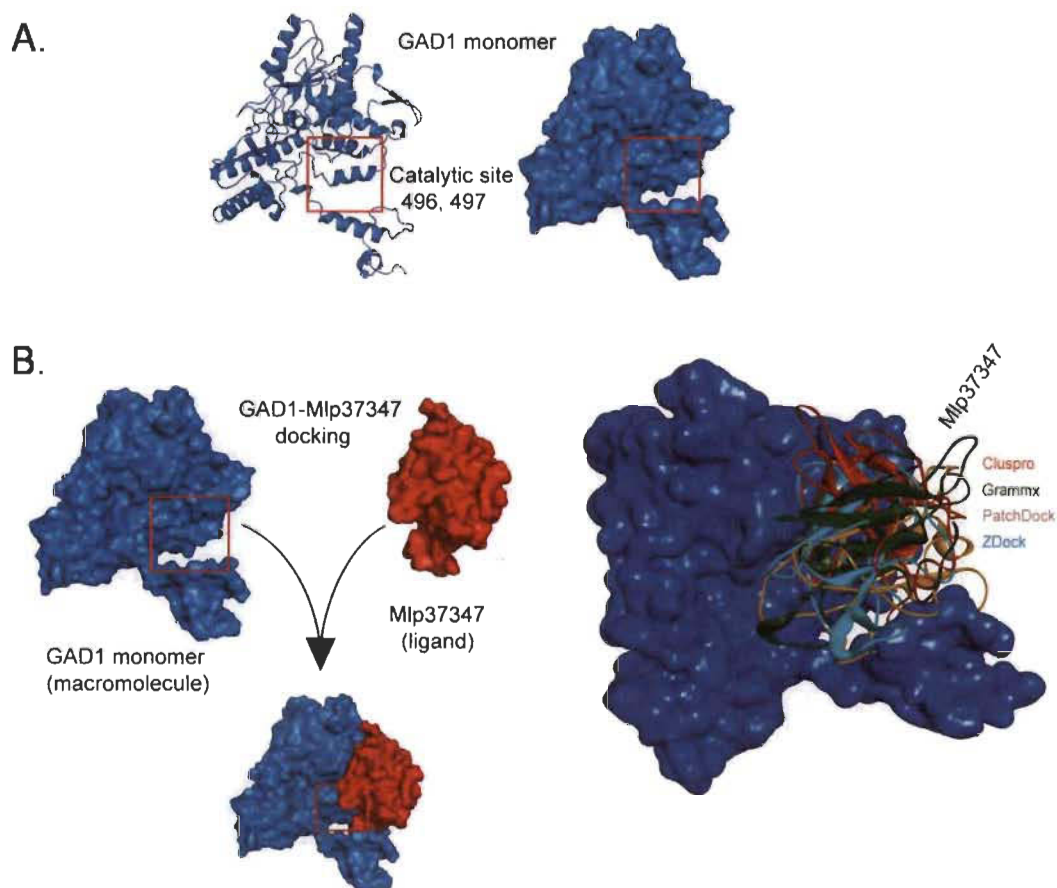


**Figure 3.9. Functional approach of docking between Mlp37347 and AtGAD1.**

(A) Structure of AtGAD1 from *A. thaliana*, PDB ID: 3HBX. AtGAD1 monomer with B- chain is prepared for docking. The red square box indicates the binding pocket of GAD1. (B) The general scheme of docking between AtGAD1 (blue) and Mlp37347 (red) using different servers. Mlp37347 in different colored ribbons represent binding results from different servers.

The docking between Mlp37347 and AtGAD1 was performed with different methods (Z-DOCK, ClusPro, PatchDock) (Duhovny et al., 2002, Pierce et al., 2014, Kozakov et al., 2017). The highest-ranked docking results from these different servers showed similar binding of Mlp37347 linked to AtGAD1 (Figure 3.10; a representative image from Z-DOCK). In figure 3.10, hydrogen bonding networks show Glu46, Asn79, Arg80, and Se104 of Mlp37347 binding to Arg139, Phe302, His303-Asn305, and Arg29 of AtGAD1, respectively.

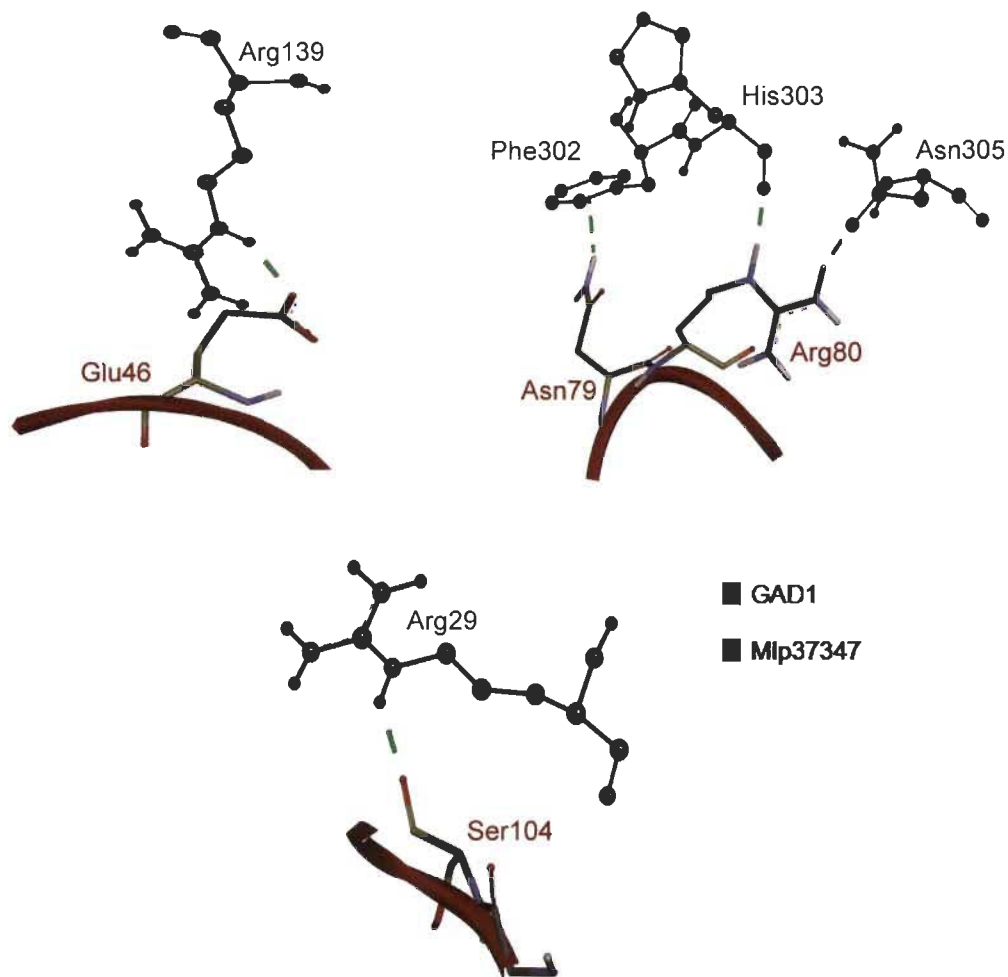


**Figure 3.10. Hydrogen bonding networks and interaction confirmation of Mlp37347-GAD1.** Close-up views of the hydrogen bonding network orientation of the GAD1-Mlp37347 complex. The GAD1 and Mlp37347 are shown as blue and red colors, respectively.

An alignment of the GAD1 protein sequences from *Arabidopsis* and *Populus trichocarpa* showed 84.26% identity, and importantly same hydrogen bonding network residues are present in PtGAD1 (Figure 3.11, marked in the blue box); this indicates that PtGAD1 also shared a similar protein binding fold as AtGAD1. Taken together, our yeast two-hybrid result, the molecular modeling approach, the previous immunoprecipitation results, and the amino acid sequence homology with poplar GAD1 strongly suggest that Mlp37347 could interact either with GAD1 of its host (poplar) or *Arabidopsis* GAD1.

```

AtGAD1 MVL SHAV SESD VSVHSTFASRYVRTSLPRFKMPENSIPKEAAYQII NDELMLDGNPRLNLA 61
PtGAD1 MVL SKT S SESD DSVHSTFASRYVRASLPRFKMPENSIPKEAAFQII NDELMLDGNPRLNLA 61
AtGAD1 SFVTTWMEPECDKLIMSSINKNYVDMDEYPVTTTELQNRVNMIAHLFNAPLEEAETA VGVG 122
PtGAD1 SFVTTWMEPECDKLIMASINKNYVDMDEYPVTTTELQNRVNI I AHLFNAPLGDSETA I GVG 122
AtGAD1 TVGSSEA IMLAGLAFKRRKWKONKRKAEGKPVDPKNI VITGANVQVCWEKFARYFEVELKEVKL 183
PtGAD1 TVGSSEA IMLAGLAFKRRWKONKMKAEKPYDPKNI VITGANVQVCWEKFARYFEVELKEVKL 183
AtGAD1 SEGYYVMDPQQAVDMVDENTICVAAI LGSTLNGEFEDVKLLNDLLVEKNKETGWDTP IHVD 244
PtGAD1 RDGYYVMDPEKAVKMDVENTICVAAI LGSTLNGEFEDVKLLNDLLVEKNKETGWDTP IHVD 244
AtGAD1 AASGGFIAPFLYPELEWDFRLPLVKSINVS GHKYGLVYAGIGWV IWRNKEDLPEELIFHIN 305
PtGAD1 AASGGFIAPFIYPELEWDFRLPLVKSINVS GHKYGLVYAGIGWV VWRNKEDLPEELIFHIN 305
AtGAD1 YLGADQPTFTLNFSKGSSQVIAQYYQLIRLGHEGYRNV MENCRENM I VLREGLEKTERFNI 366
PtGAD1 YLGADQPTFTLNFSKGSSQVIAQYYQLIRLGYEGYKNV MENCRDNMVLKQGLENTGKFN I 366
AtGAD1 VSKDEGVPLVAFSLKDNSSCHTEFEISDMLRRYGWIVPAYTMPPNAQH I TVLRVVIREDFSR 427
PtGAD1 VSKDNGVPLVAFSLKDNSSHKEFEVSEMLRRFGWIVPAYTMPPDAQH V TVLRVVIREDFSR 427
AtGAD1 TLAERLV I D I EKVMRELD ELP SRV I HK I S LGQEKSESNSDNLMVTVK KSD I DKQRDI I TGW 488
PtGAD1 TLAERLVLD I EKVLHELET LPCR I STK I A L ANEEKEAAAANK - - - - EKRDLEKTR E I TT V W 483
AtGAD1 KKFVADRKKTS G I C 502
PtGAD1 RKFVMDRKKM - NGVC 496

```

**Figure 3.11. Sequence alignment of AtGAD1 and PtGAD1.**

An amino acid sequence alignment between *A. thaliana* GAD1 (AtGAD) and *Populus trichocarpa* GAD1 (PtGAD). Identical hydrogen-bonding network residues in PtGAD1 (marked in the blue box).

We have constructed an Mlp37347 homology model based on sequence and structure alignments with the bacterial AvrL567 protein, whose crystal structure has been defined. Mlp37347 model contributes to the formation of a resonant network near the catalytic site of AtGAD1. This binding network provides significant information on the positioning of Mlp37347 within this catalytic pocket. These critical amino acids may cause the active site to undergo a change in its conformation, which ultimately interferes with a better fit between the active site and the GAD1 substrate CaM. According to the induced fit theory of the mechanism of enzyme catalysis, loss of substrate binding site may lead to loss of catalytic activity to a maximum extent because precise catalytic site forms only after substrate binding.

### 3.7 Mlp37347 decreases plasmodesmata callose deposition

As the primary known regulatory mechanism of plasmodesmal flux during a pathogen attack is callose deposition, we compared the callose levels in *A. thaliana* transgenic lines expressing Mlp37347-GFP and NLS-Mlp37347-GFP (and in Col-0 as a control). We also looked at a *gad1* knock-out line and a cross between this *gad1* knock-out line and expressing Mlp37347-GFP. To quantify callose deposition, we used the ImageJ software to quantify the fluorescence of aniline blue staining of callose. Callose was

significantly reduced in the stable Mlp37347-GFP line (Figure 3.12) compared to Col-0. By contrast, in the stable *gad1* knock-out line, the cross between *gad1* and Mlp37347-GFP, and the transgenic expressing NLS-Mlp37347-GFP, the amount of callose deposition did not vary significantly. These data confirm our previous observation that Mlp37347-GFP localization to the plasmodesmata is important for its action on plasmodesmata opening and points to the physiologically relevant target of this *Melampsora* effector.

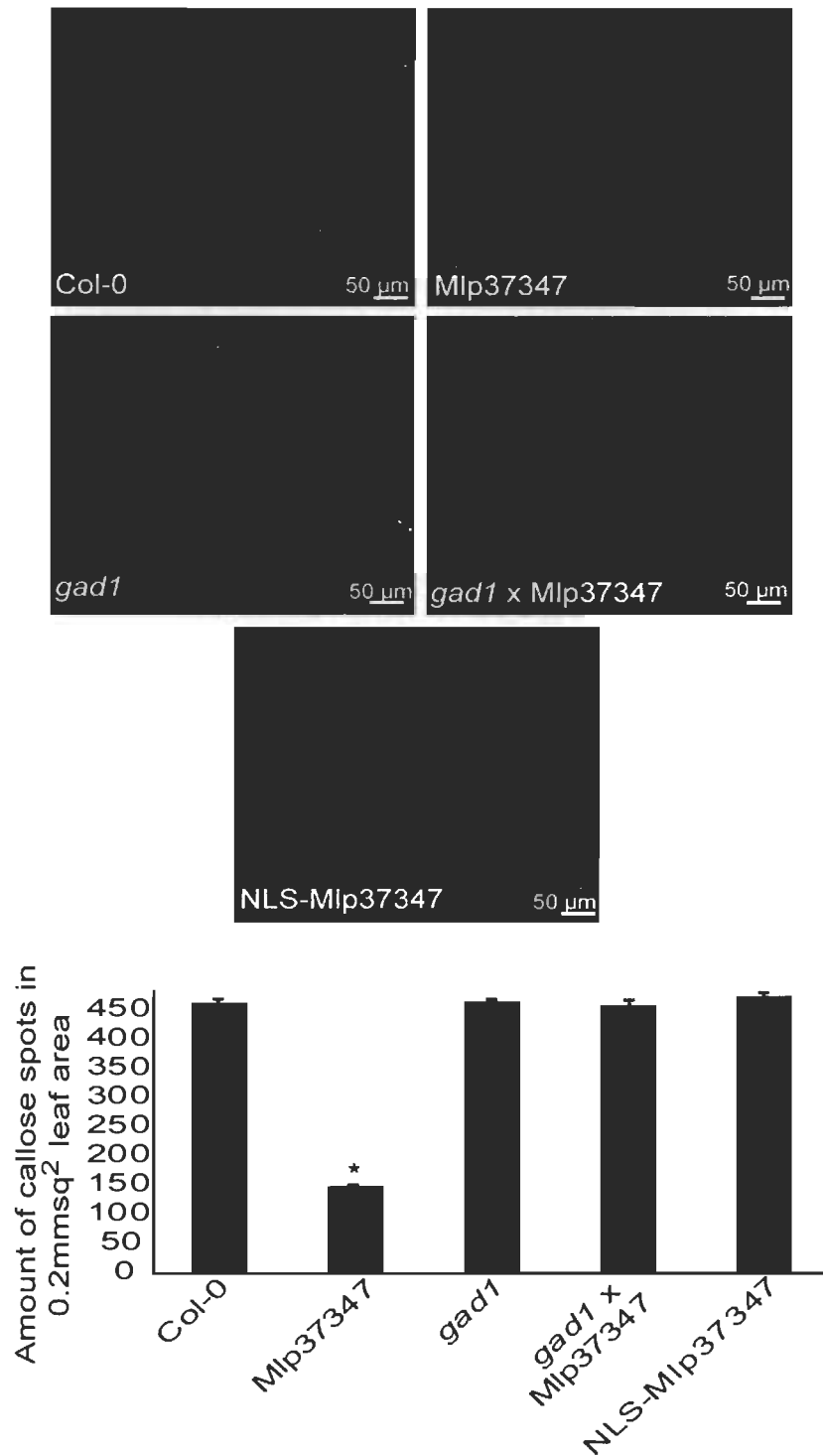


**Figure 3.12. Callose deposition in *Arabidopsis* transgenics.**

Aniline blue staining to visualize the callose levels in *A. thaliana* transgenic lines expressing Mlp37347-GFP, NLS-Mlp37347-GFP (and in Col-0 as a control), *gad1*, and *gad1* x Mlp37347-GFP. Images of callose deposition taken at 40 x/1.40 magnification and excitation of 488 nm with an emission of 505 to 550 nm using a Leica SP8 confocal microscope. Absolute quantification of callose deposition in different lines. Data represent mean  $\pm$  SD. The statistical difference from the control Col-0 leaves was determined by Student's t-test, asterisks indicate statistical significance.

### 3.8 Mlp37347 affects callose metabolism gene expression

To further investigate the mechanism by which Mlp37347 influences callose deposition, we performed transcriptomic profiling of 4-days-old *A. thaliana* stable transgenic seedlings expressing Mlp37347-GFP and control plant expressing only GFP. To determine the relevant biological processes affected by Mlp37347-GFP overexpression, a gene ontology (GO) terms enrichment analysis was carried out on the deregulated genes (filtered by a Q-value  $\leq 0.05$  and a fold change  $\geq 2$ ) using the Cytoscape software (version 3.1.1). In the Mlp37347 transgenic line, 84 and 395 genes were up and down-regulated by 2-fold or greater, respectively (ANNEX A, Supplementary Table 2), in comparison with control plants (ANNEX A, Supplementary Table 2). This analysis revealed that many genes for the catabolic process of glucan (ISA3, DPE1, PHS1, PHS2) are significantly up-regulated while some genes linked to the synthesis of glucan (GSL04, XTH19) and plant defense-related genes are down-regulated in the line expressing Mlp37347-GFP (Figure 3.13), reinforcing the link between Mlp37347 and the control of plasmodesmata by the control of callose deposition.



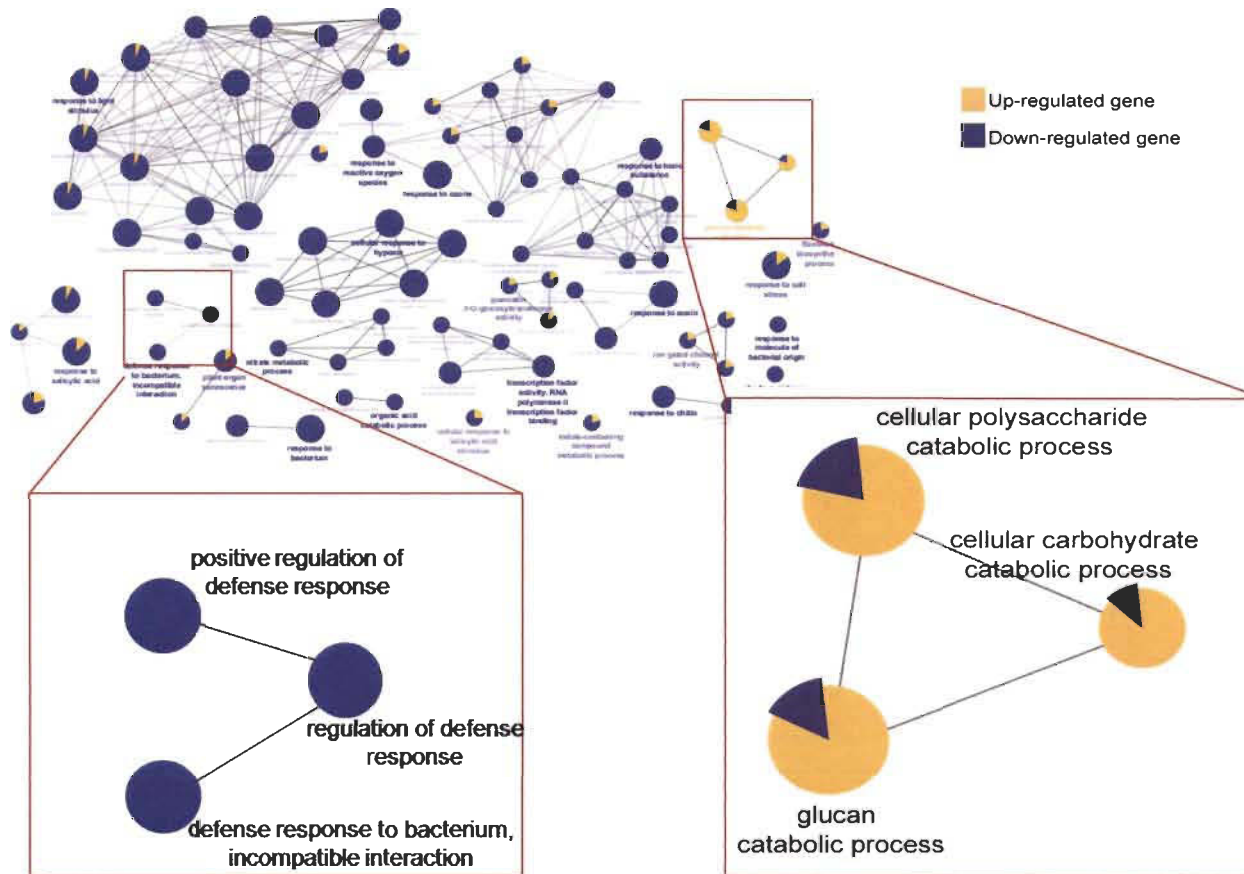


**Figure 3.13. Transcriptional changes induced by the expression of Mlp37347-GFP.**

Term enrichment analysis was performed with deregulated genes filtered with  $Q\text{-value} \leq 0.05$  and  $\text{fold-change} \geq 2$  using the Cytoscape software (version 3.1.1). Cytoscape plug-in ClueGO and CluePedia were used to visualize functions enriched in the deregulated genes. The GO terms presented are significantly enriched in up-regulated and down-regulated genes with  $FDR \leq 0.05$  (Benjamini-Hochberg p-value correction).



### 3.9 Mlp37347 does not modify the morphology of *A. thaliana* leaves

To evaluate the biological outcomes of the presence and absence of Mlp37347 and GAD1, respectively, in plant cells. We compared the phenotype of Mlp37347 expressing and *gad1* lines with wild type Col-0 plants. No significant morphological difference was observed in 3-weeks-old plants (Figure 3.14; upper panel), but the *gad1* line displayed delayed bolting in the 5-weeks-old plant (Figure 3.14; lower panel) compare to Col-0 and Mlp37347. This observation suggests that the constitutive expression in planta of Mlp37347 does not modify the morphology of the plant. Whereas the absence of GAD1 protein has an impact on plant growth and development.

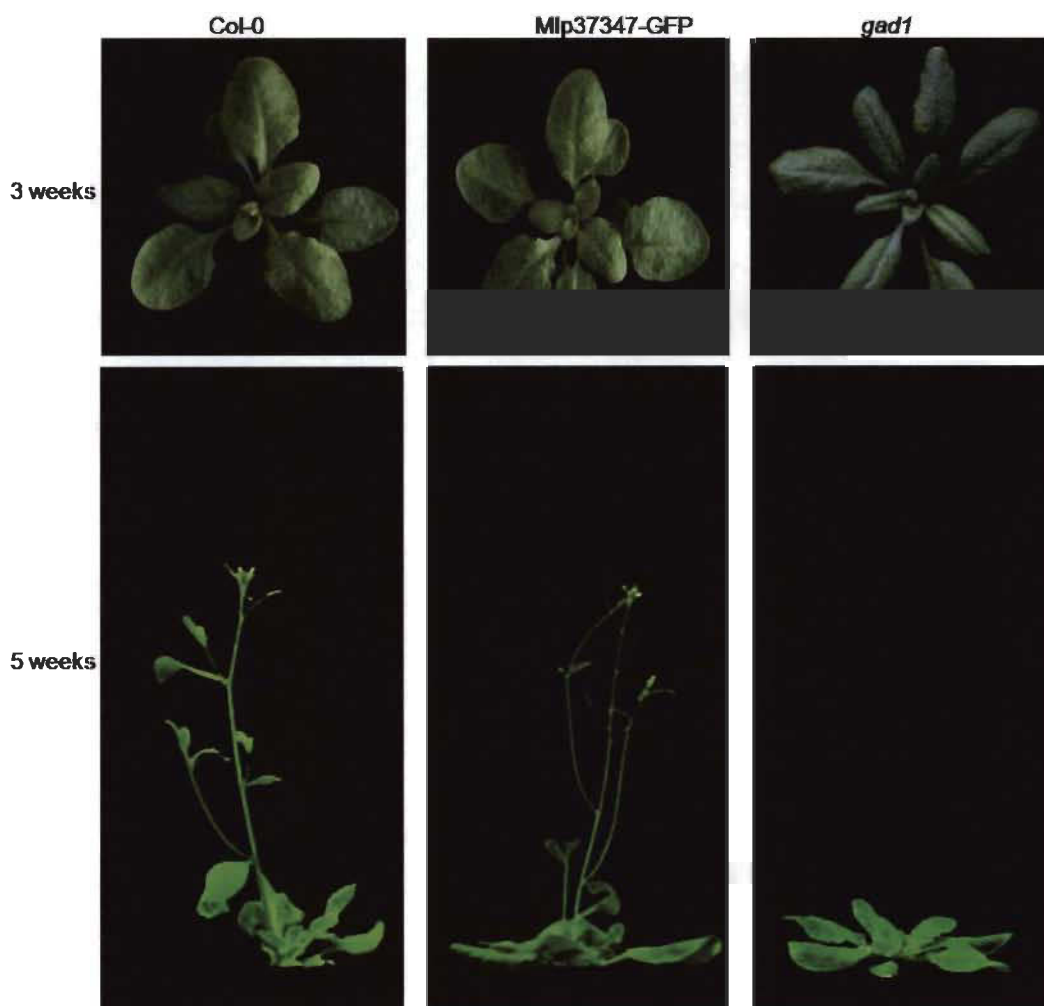


**Figure 3.14. Phenotype of Mlp37347 and *gad1* knock-out in *A. thaliana* transgenic.** Morphology of 3-5-weeks old Col-0, stable transgenic Mlp37347, and *gad1* knock-out plants were soil-grown at 22 °C.

### 3.10 Mlp37347 increases the susceptibility of *A. thaliana* to *H. arabidopsidis*

To assess Mlp37347 in planta expression on plant susceptibility to pathogens, we performed growth assays with two different kinds of organisms: an oomycete and a bacterium. We measured the plant susceptibility in control plants (Col-0 and Col-0-GFP) and *enhanced disease susceptibility 1-1* (*eds 1-1*) plants (positive controls hypersensitive to *H. arabidopsidis*) as well as in the following transgenic lines: Mlp37347-GFP, NLS-Mlp37347-GFP, *gad1*, and Mlp37347-GFP x *gad1*. At 7 dpi, we quantified the number of spores. We observed that Mlp37347-GFP significantly increases *Arabidopsis* susceptibility to *H. a. Noco2* (Figure 3.15). In contrast, this increase in pathogen growth was not observed when Mlp37347 was sequestered in the nucleus (NLS-37347-GFP) nor in the *gad1* line (expressing Mlp37347-GFP or not) (Figure 3.15). This result suggests that the localization of the effector at the plasmodesmata and its interaction with GADI protein are necessary for Mlp37347 to increase the susceptibility of *Arabidopsis* to the oomycete *Hyaloperonospora arabidopsidis*.

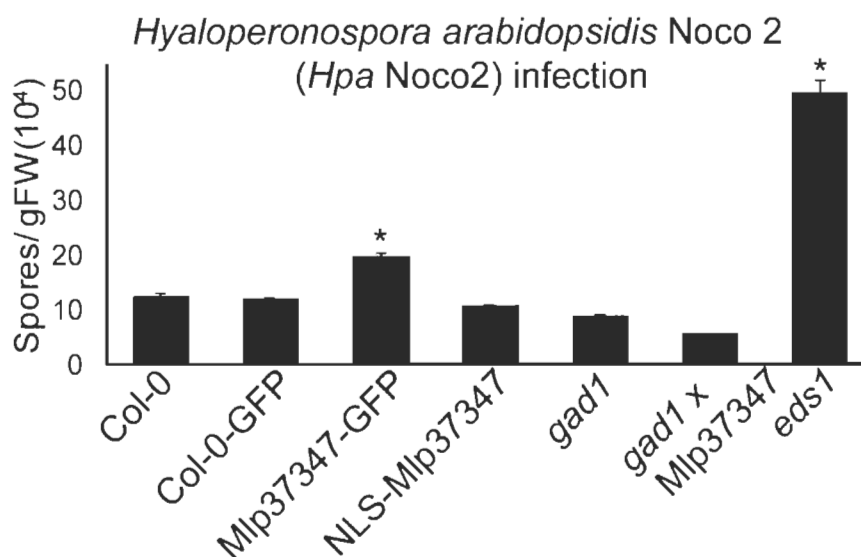


**Figure 3.15. Mlp37347 increases the susceptibility of *A. thaliana* to *H. arabidopsidis*.** The growth of *Hyaloperonospora arabidopsidis* Noco2 (20000 conidiospores/ml). The number of spores/g fresh weight was quantified seven days after inoculation. Bars represent the mean of four replicates. Data represent mean±SD. Statistical significance between Col-0 and Mlp37347 or eds1 was evaluated using Student's t-test ( $P < 0.05$ ); was denoted as an asterisk.

To investigate whether Mlp37347 could enhance susceptibility to bacterial pathogens, we infiltrated 4-week-old control plants (Col-0 and Col-0-GFP) and the following transgenic lines: Mlp37347-GFP, NLS-Mlp37347-GFP, *gad1* as well as Mlp37347-GFP x *gad1* leaves with *Pseudomonas syringae* pv. *tomato* (*Pst*) DC3000 bacteria. Infection assays showed no significant alteration in the pathogen growth in any genotypes (Figure 3.16).

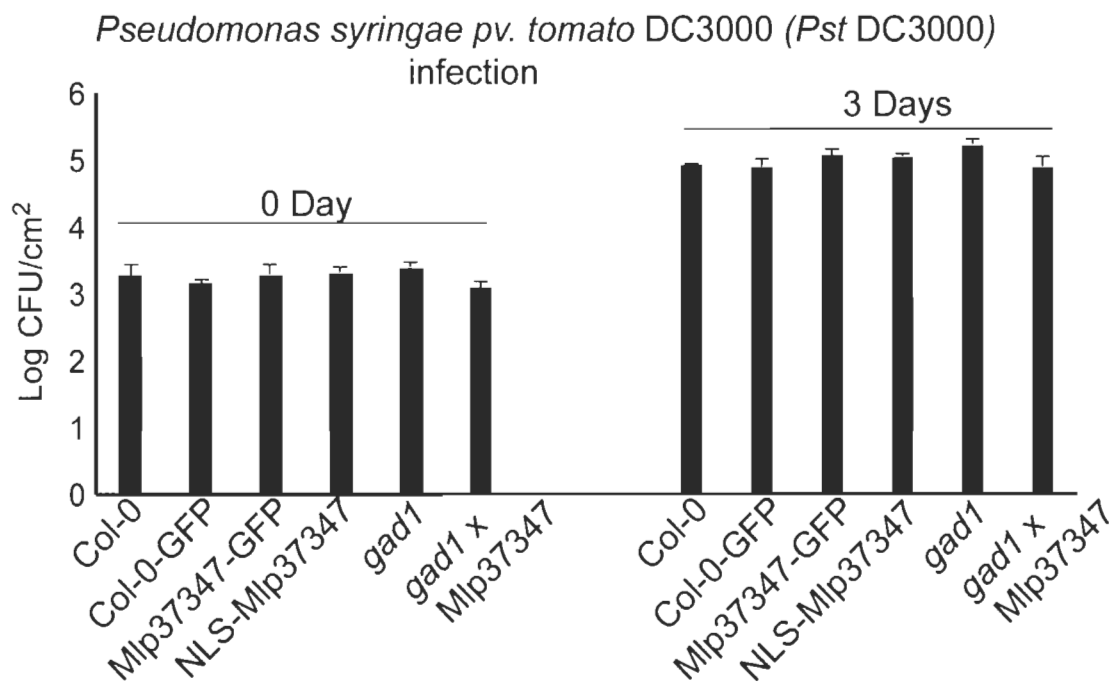


**Figure 3.16. Mlp37347 does not promote the growth of *Pst* DC3000 in *A. thaliana*.** Growth of *Pst* DC3000 in *Arabidopsis* was measured on the day of infection and three days after infection of 4-week-old soil-grown plants by leaf infiltration. A bacterial suspension with  $OD_{600} = 0.001$  was used as inoculum. Data represent mean  $\pm$  SD. Statistical significance was evaluated using Student's t-test ( $P < 0.05$ ).

From this experiment, we conclude that Mlp37347 promotes the growth of the filamentous fungi-like pathogen *H. arabidopsidis*, which produces haustoria like *Mlp*, but not of the bacterial pathogen *P. syringae* in *A. thaliana*.

## CHAPTER IV

### DISCUSSION

Although our laboratory had previously characterized the localization of the effector and the Kamoun group had found an interactor, no functional assay had been performed with this effector, let alone decipher its potential role during infection. We also knew that Mlp37347 encodes for the putative homolog of the avirulence protein AvrL567 protein of *Melampsora lini* (Wang et al., 2007). AvrL567 has been thoroughly characterized in the context of avirulence in flax. The recognition of individual matching AvrL proteins is performed by 13 allelic protein variants- L, L1 to L11, LH. These variants are encoded by a single gene located in L resistance locus (Ellis et al., 1999). More than 90% of amino acid identity is shared between the L alleles, while the LRR domain is seen to have a positively selected variation. The LRR domain is observed to control the recognition specificities, demonstrated through domain-swap experiments conducted on L2, L6, and L10 alleles (Luck et al., 2000, Ellis et al., 1999). Furthermore, in the LRR domain, it was shown that the L6 and L11 proteins differed by only 32 amino acids. Also found in the C-terminal region of the LRR domain, a chimeric protein with 11 amino acid changes was shown to exhibit novel specificity with a lower recognition spectrum (Ellis et al., 2007, Dodds et al., 2006).

The *Melampsora lini* contains the L5, L6, and L7 proteins that perceive allelic variants of AvrL567, the effector protein. The AvrL567 is a secreted protein with 127 amino acids that express in haustoria and translocate to host cells during the infection (Lawrence et al., 2010, Rafiqi et al., 2010, Dodds et al., 2004). Seven variant forms of AvrL567 (-A, -B, -D, -E, -F, -J, -L) are avirulent alleles as they prompt L5 and/or L6, and/or L7-dependent hypersensitive response (HR) in transient expression assays. Meanwhile, the other 5 variant forms (-C, -G, -H, -I, -K) do not trigger a hypersensitive response, meaning they are virulent alleles (Dodds et al., 2006). The interaction between AvrL567 and L5, L6, and L7 were shown in yeast-two-hybrid (Y2H) assays and

demonstrate that the HR-inducing perception *in planta* correlates with the specificity of the protein-protein recognition (Dodds et al., 2006). In the TIR domain, only 11 polymorphisms differentiate the L6 and L7 allele and show identical recognition specificities in AvrL567. Despite this, weaker interactions in yeast and *in planta* hypersensitive responses can be observed in L7 (Bernoux et al., 2011, Luck et al., 2000). The divergence in L proteins is most apparent between the L5 and L6 proteins, which differ by 89 amino acid polymorphisms, 61 amino acid polymorphisms in the LRR, and four small indels, although they continue to have recognition specificities that overlap. The distinction between L5 and L6 is observed through the interaction of L6 with AvrL567-D, as L5 does not partake in such interaction. Despite these thorough investigations over many years, no experiment has paid attention to the virulence target of AvrL567 in the host cell. In an agronomical context, the most important is to counter an effector, understanding the role of an effector is not a priority. However, understand its role is key to understanding pathogenesis and find the weak spot of the plant, the ones targeted by the pathogens. Improving those weak spots may lead to lasting resistance, perhaps more than resistance base on R-Avr matches. This is why we sought to investigate the role of an effector *in planta*, using various approaches.

#### 4.1 Heterologous systems

The study of the molecular mechanism of pathogenicity of rust fungi has been hampered by the fact that rust fungi can neither be grown *in vitro* nor genetically modified. In the case of poplar leaf rust, the genetic transformation of poplar is only possible with poplar cultivars that are not susceptible to rust. This significantly limits our ability to genetically manipulate either the pathogen or susceptible host. To overcome this obstacle, heterologous systems are used to study the function, localization, and interaction of the effectors from a biotrophic pathogen (Win et al., 2012, Petre et al., 2016b). In this study, we found that the Mlp37347 expression in the heterologous systems *A. thaliana* and *N. benthamiana* doubled the plasmodesmal diffusion rate and increased the plasmodesmata size exclusion limit. The information retrieved was vital for the formulation of hypotheses concerning the function of specific effector and for the

initiation of mechanistic studies. The manipulation executed by the effectors on the host structures and functions were demonstrated through these studies and expanded our knowledge regarding the molecular interactions between plants and pathogens. Although, it is widely debated during scientific meetings whether the use of non-host systems for effector screens is the most effective way to study. Most importantly, false effector interactors and localisations can be observed during ‘artificial’ screens (advantages and disadvantages are discussed below). Despite this, the utilization of heterologous plants to study effectors is a sensible way to avoid bottlenecks and other events when looking at pathosystems with limited methodological alternatives.

#### **4.1.1 Advantage and disadvantages of heterologous protein expression systems**

The heterologous expression means that a gene is expressed outside of its natural context, in a "foreign" host system (often a model system). For example, a fungal gene (e.g., encoding a candidate effector) is expressed in plant cells (e.g., leaf cells of *Nicotiana benthamiana*).

##### **4.1.1.1 Advantage**

- *A reliable assay*: Researchers have developed and optimized tests in model systems used for the expression of heterologous proteins. The disadvantages and the pitfalls of data interpretation are known, specifically for protein-protein interaction assays.
- *Using model systems is quick, inexpensive, and easy*: Required information can be obtained quickly and easily in a cost-effective way, which makes it ideal for performing screens.
- *Anyone can review the results*: As they are more accessible to a wide community than more emerging systems. Thus, the systems promote reproducibility. Other research groups may reproduce experiences and evaluate, develop, or challenge them.

#### 4.1.1.2 Disadvantage

- *An incomplete conclusion:* Using a heterologous system, the biological significance of the observed phenomenon cannot be tested. Further confirmations are suggested. Therefore, conclusions are limited to the level of the molecular or cellular mechanisms.
- *The data may be uninformative:* heterologous systems may not be suitable for studying molecules or processes that only occur in specific biological contexts. For example, in heterologous systems, critical components may not reach in a way such as found in native systems, many proteins may not fold properly, will not be in the correct cellular context, will not find their true molecular targets, and so on.
- *You are spoiled:* Being used to working with heterologous systems can lead to less investment in time and energy to develop methods and tools for the original systems. Go around to both systems studies are necessary.

#### 4.2 Plasmodesmata localization Mlp37347 is required for enhanced plasmodesmata flux

Several groups have recently reported that pathogen proteins, mainly from viruses and bacteria, associate with plasmodesmata to influence intercellular communication (Han et al., 2019). However, reports of fungal proteins interfering with the plasmodesmata flux are scarce. Mlp37347 seems to be one of such proteins. Mlp37347 is one of the *Melampsora larici-populina* CSEPs studied by Petre in 2015, whose role as a true effector has been supported by its effect during infection, Mlp37347, did not display bacterial growth, but increased oomycete growth. (Germain et al., 2018). The sequencing of the *M. larici-populina* genome provided access to DNA sequences encoding 1,184 small secreted proteins. It allowed the functional characterization of potential candidate secretory effector proteins (CSEP). Among them exists Mlp37347, it does not have any close relative (other than AvrL567) and does not belong to a specific effector family. More importantly, Mlp37347 displays a unique plasmodesmata localization (Germain

et al., 2018). For pathogens, an augmentation in plasmodesmal flow can be favorable, as once they gain access to one cell, they could more easily draw the soluble nutrients from neighboring cells. Studies have shown that cell to cell propagation through plasmodesmata is used by viruses (Benitez-Alfonso et al., 2010). It would also be an interesting feature for biotrophs as it could allow effectors, which are small soluble proteins, to move through the plant to favor infection, for example, by neutralizing the plant systemic responses and to facilitate access to the resources of the surrounding cells. Pathogenic effectors act as disease-promoting factors that target specific host proteins with roles in plant immunity, nutrients scavenging or other.

Tomczynska and his colleagues studied the function of the RxLR3 effector of the oomycete phytopathogen, *Phytophthora brassicae*. RxLR3 interacts with three callose synthase family, CalS1, CalS2, and CalS3. RxLR3 co-localized with the plasmodesmal marker, PDLP5, and with deposits associated with the plasmodesmata of the  $\beta$ -1,3-glucan polymer, callose. Effector inhibitors function of plasmodesmal callose synthase enzymes (CalS) and callose deposits were reduced, and intracellular trafficking (evaluated using GFP tracer) was improved in the presence of RxLR3. In *Arabidopsis* lines expressing RxLR3, callose level was decreased in response to infection compared to wild type. Tomczynska et al. concluded that the virulence function of the RxLR3 effector was to act as a positive regulator of plasmodesmal transport and provided evidence of competition between *P. brassicae* and *Arabidopsis* for the control of cell-to-cell trafficking (Tomczynska et al., 2020).

A more recent study showed that the effector protein HopO1-1 from *Pseudomonas syringae* modulates the plasmodesmata function. HopO1-1 is necessary for *P. syringae* to spread locally to nearby tissues during infection. In *Arabidopsis* lines expressing HopO1-1, there is an observed increase in the distance of plasmodesmata-dependent molecular flux between neighboring plant cells. The catalytic activity of HopO1-1 is necessary for the regulation of plasmodesmata. HopO1-1 physically interacts with and destabilizes the PDLP7 and PDLP5 proteins in order to manipulate host cell-to-cell



mediated communication and maximize the spread of bacterial infection (Aung et al., 2020).

Another interesting study has shown that the effectors Avr2 and Six5 of the fungus *Fusarium oxysporum* are essential for resistance to I-2-induced disease in tomato. Both Avr2 and Six5 have been found to interact at the plasmodesmata. Single-cell transformation revealed that a 2XmCherry marker protein and Avr2-GFP move only to neighboring cells in the presence of Six5. Six5 alone does not modify plasmodesmal transduction because 2xmCherry requires the presence of both effectors to be translocated. In the presence of Six5, Avr2 moves from cell to cell, which in susceptible plants contributes to virulence (Cao et al., 2018).

Our primary goal was to answer the question: Does Mlp37347 manipulate the plasmodesmata? To address this question, we carried out the diffusion assay in *N. benthamiana*. Firstly, we evaluated the Mlp37347 localization at the plasmodesmata, as previously observed in *A. thaliana* (Germain et al., 2018). To this end, we expressed Mlp37347-GFP by agroinfiltration, and its subcellular localization was determined by confocal microscopy. Most importantly, we evaluated its co-localization with the plasmodesmata marker PDCB1-mCherry. Both fluorescent proteins overlapped in punctate structures, confirming that Mlp37347 accumulates at the plasmodesmata in *N. benthamiana* as well.

It is presumed that soluble molecules are transported passively through the plasmodesmal cytoplasmic sleeves, approximately 3-4 nm in diameter (Robards & Lucas, 1990, Wright et al., 2003, Maule, 2008). Ideally, plasmodesmata channels should restrict the cytoplasmic diffusion of molecules larger than 4 nm in size. As we expected, 2XmCherry (MW: 65 KDa, and diameter: 8 nm) (<sup>2</sup>calculated by Calctool, [http://www.calctool.org/CALC/prof/bio/protein\\_size](http://www.calctool.org/CALC/prof/bio/protein_size)) did not show diffusion to neighboring cells in the absence of Mlp37347. The diffusion of 2XmCherry is not possible without modifying the plasmodesmata size. A few plasmodesmata-localized proteins have been found to regulate plasmodesmal permeability (Ueki & Citovsky, 2014). Our data

indicate that the presence of Mlp37347 at plasmodesmata modifies the physical properties of plasmodesmata, allowing the general size constrained 2XmCherry to move between cells.

Induction of beta-1,3-glucanases is also observed in the transgenic line expressing Mlp37347, as it is observed in viruses that hijack the plasmodesmata for their propagation. This makes sense because beta-1,3-glucanases are responsible for glucan degradation at the plasmodesmata; once glucan has been degraded, the plasmodesmata is more open. The opening of the plasmodesmata caused by Mlp37347 can prove to be a double-edged sword, as intercellular signaling is required for the coordination of plant defense. Plasmodesmata exploitation by fungi for intercellular propagation has been reported for *Magnaporthe oryzae* (Ascomycota), the hemibiotrophic fungus that causes the rice blast disease (Kankanala et al., 2007). In their work Kankanala et al. (2007) report that intracellular invasive hyphae can propagate from cell to cell by invading neighboring cells, most likely through plasmodesmata. More precisely, Kankanala reported that the hemibiotrophic fungus *Magnaporthe oryzae*, invades living plant cells using invasive intracellular hyphae (HI), which grow from cell to cell. Their time-lapse imaging and transmission electron microscopy (TEM) showed that HI preferably contacted or crossed cell walls in pit fields using plasmodesmata for cell-to-cell movement. Yamaoka demonstrated a different strategy; the work of *Blumeria graminis* (Ascomycota) intercellular propagation was reduced when plasmodesmata were mechanically destroyed, again supporting a propagation through plasmodesmata.

To the best of our knowledge, rusts have never been shown to use or manipulate plasmodesmata. In our case, this *Mlp* effector seems to manipulate plasmodesmata flux through the deregulation of callose metabolism, which is more akin to what has been observed for viruses. Our work does not show any evidence of propagation through the plasmodesmata, nor did we attempt to assess this phenomenon because of the limitations imposed by the use of our heterologous systems.

### **4.3 Mlp37347 decreases plasmodesmata callose deposition and affects callose metabolism gene expression**

The callose-dependent constriction of the plasmodesmata is the primary regulatory mechanism of plasmodesmal permeability (Zavaliev et al., 2011). It is used by plants both during development and cell differentiation and as part of the PR defense response (Vatén et al., 2011, Sevillem et al., 2013). The two opposite pathways, callose synthesis, and callose degradation, are targeted by viruses, either directly or through transcriptional regulation (Wu & Gallagher, 2011, Conti et al., 2012).

It has already been shown that fungal effectors can also alter transcription (Madina et al., 2020, Wu & Gallagher, 2011, Conti et al., 2012, Ahmed et al., 2018). Our transcriptional analysis of *Arabidopsis* expressing Mlp37347-GFP indicates that the genes (ISA3, DPE1, PHS1, PHS2) for the catabolic processing of glucan are significantly up-regulated. In particular, a second allele, PHS1-3, is hypersensitive to abscisic acid, indicating a possible involvement of PHS1 in the degradation of callose via ABA signaling (Tang et al., 2016), while the genes (GSL4, XTH9) linked to the synthesis of glucan are downregulated.

GSL4/CalS4 encodes a protein similar to callose synthase 1 (CalS1) and CalS8. CalS1 and CalS8 have been identified as key genes involved in the callose synthase process and have been integrated into signaling pathways that control biotic and abiotic stress responses (Cui & Lee, 2016). The Xyloglucan Endotransglucosylase-Hydrolase (XTH), a gene whose expression is regulated by the transcription factor HY5 (Xu et al., 2016). HY5 family is a large group of enzymes involved in cell wall remodeling (Cosgrove, 2016).

Consistently, we have observed that the amount of callose was significantly reduced in the stable Mlp37347 expressing line compared to Col-0. Although we did not assess if Mlp37347's disruption of callose deposition is sufficient to recreate the aberrant guard cells localization and proliferative clusters observed in the epithelium of plants deficient in the callose synthase GSL8 (De Storme et al., 2013) we did not observe any guard cell

abnormality. This result suggests that the plasmodesmata localization of Mlp3747 is required for enhanced plasmodesmata flux, as this increase was not observed when the effector (NLS-Mlp37347-GFP) was segregated in the nucleus.

The exact mechanism by which Mlp37347 regulates callose remains to be elucidated. Plasmodesmata functions are also regulated by the composition of their membranes, as nanodomains lipids and protein constituents are crucial for controlling the flexibility of the PD membrane and by the cell cytoskeleton (Grison et al., 2019). It has been shown that some viruses increase the size exclusion limit of plasmodesmata through depolymerization of actin filaments (F-actin) (Su et al., 2010). It would be interesting to see if Mlp37347 also has an impact on these plasmodesmata regulatory components.

#### **4.4 Mlp37347-GAD1 interaction**

To study the molecular virulence mechanisms of Mlp37347, we have focused on the effector's known interactant, GAD1. GAD catalyzes the conversion of glutamate to gamma-aminobutyric acid (GABA) in the presence of the pyridoxal phosphate (PLP) cofactor. GAD is present in two isoforms in plants (Kumar & Punekar, 1997). The enzyme has a unique characteristic, a Calmodulin (CaM) binding domain at the C-terminus (Gallego et al., 1995, Arazi et al., 1995, Baum et al., 1993). *In vitro* analysis has shown that  $\text{Ca}^{2+}$  and CaM stimulate GAD activity 1- to 9-fold (Bitanhirwe & Cunningham, 2009, Snedden et al., 1995, Ling et al., 1994) in partially purified protein preparations, and nearly 20-fold in purified preparations and have suggested that GAD can be stimulated *in vivo* by  $\text{Ca}^{2+}$  signal pathways (Snedden et al., 1995).

Studies demonstrated rapid increases in cytoplasmic concentrations of  $\text{Ca}^{2+}$  and GABA (Price et al., 1994, Knight et al., 1992) in plant cells upon exposure to various environmental stimuli such as abiotic and biotic stress response, growth, and development (Yang & Poovaiah, 2002, Bouché et al., 2002). We followed our interest in *in silico* study on Mlp37347-AtGAD1 or PtGAD1 interaction. The top-ranked docking results from different servers showed similar binding poses of Mlp37347 bound to GAD1, and a

common hydrogen bonding networks show Glu46, Asn79, Arg80, and Ser104 of Mlp37347 binding to Arg, Phe, His, Asn, and Arg of both AtGAD1 and PtGAD1. It should be noted that all different servers use different algorithms to calculate binding interfaces. Thus, a common Mlp37347-GAD1 interaction pattern obtained from all four servers is convincing to proceed with further analysis.

A well-known pathway involved in the abiotic and biotic stress response is the activation of GAD by CaM. Although, in recent years, little has been understood about the role of GABA in plant pathogenesis. An increased-GABA level is a typical response to various stresses, and strict control of GABA synthesis by GAD and CaM appears to be essential for the development of the plant. The N-terminal (1-57) of GAD1 is involved in the formation of the multimer. The C-terminus (471-502) binds to CaM in a calcium-dependent manner and possibly encompasses an auto-inhibitory domain. In our docking results, GAD1 residues (Arg139, Phe302, His303, Asn305) bind to the effector Mlp37347. It would be interesting to see whether this effector interaction interferes with calmodulin-binding and GABA production by altering the overall structure as well as solving the three-dimensional structure of Mlp37347. Although, recently, de Guillen and colleagues used a strategy based on the production of eleven recombinant *Mlp* effectors in *Escherichia coli* and successfully purified and solved the structure of two effectors, Mlp124266 and Mlp124017, using NMR spectroscopy. They were unable to improve the solubility and sufficiently stabilize the purification procedure of Mlp124111, Mlp124561, Mlp37347, Mlp107772, and Mlp124202. They decided to keep these proteins for subsequent analyses (de Guillen et al., 2019).

#### **4.5 Mlp37347 increases the susceptibility of *A. thaliana* to *H. arabidopsidis***

The two main factors that affect the virulence studies of poplar rust fungi are 1) the prolonged amount of time required for genetic transformation and development of a transgenic poplar and 2) the fact that the one poplar genotype which is amenable to genetic transformation is resistant to *Mlp*. Until recently, such methods are not fully available in

poplar rust pathosystems. Thus, we generated *A. thaliana* transgenic lines to investigate the virulence activities of rust in a heterologous system.

*M. larici-populina* and *Hyaloperonospora arabidopsidis* are both obligate biotrophic filamentous pathogens of dicotyledonous plants. They share similar modes of propagation in leaf tissue. Consequently, the pathogenicity of *H. arabidopsidis* would be more likely than the bacterial pathogenicity of *P. syringae* to be affected by rust effectors. Indeed, the Mlp37347-GFP line promoted the growth of *H. arabidopsidis*, but not to an equivalent level with the infection control line *enhanced diseased susceptibility 1 (eds1)*, which is hyper susceptible to *H. arabidopsidis*. We conclude that Mlp37347 significantly increases susceptibility to *H. arabidopsidis* var. Noco2. Furthermore, this increase in sensitivity was not observed when Mlp37347 was sequestered in the nucleus (NLS-37347-GFP) or in the *gad1* line. Meanwhile, in *Pseudomonas syringae* pv. *tomato* DC3000, bacterial infection assays showed no significant alteration in pathogen growth between genotypes. It is possible that Mlp37347 interaction with GAD assists in leaf infection by fungal-like biotrophic pathogens.

#### 4.6 DoorMan Hypothetical Model

Based on concurrent studies and our results, we drew a hypothetical model, which we called DoorMan (Figure 4.1). This model aims to answer the main question presented in this thesis. After being secreted from the *M. larici-populina*, effector Mlp37347 localizes at the plasmodesmata. Once the Mlp37347 is at the plasmodesmata, it works like a “doorman” to act on the opening of the plasmodesmata channel and may favor other invasive effector proteins, invasive hyphae (IH), or enhance molecular cell to cell flux by increasing their intracellular movement. This unique characteristic of the effector appears to promote the growth of *Mlp*. It is not impossible that the invasive hyphae (IH) of *Mlp* use dilated plasmodesmata caused by Mlp37347 for their cell-to-cell movement to reach more intracellular spaces and spread infection, but we have no evidence supporting this possibility, and although this strategy is used by Ascomycota, it has never been demonstrated for Basidiomycota.

Since it does not explain how Mlp37347 manipulates the transcriptional process since the effector is localized at the plasmodesmata, not the nuclei, to find the answer, we hypothesized the possible involvement of  $\text{Ca}^{2+}$ /calmodulin-dependent protein kinases (CDPK) in this process. Calmodulin is an intracellular target of the secondary  $\text{Ca}^{2+}$  messenger, and  $\text{Ca}^{2+}$  binding is required to activate calmodulin. Upon the binding to  $\text{Ca}^{2+}$ , calmodulin turns into a vital part of a calcium signal transduction pathway by modifying its interactions with various target proteins such as kinases or phosphatases (Chin & Means, 2000, Stevens, 1983). As a result of interactions between Mlp37347 and GAD1, the conformation of the Mlp37347-GAD-Calmodulin complex may interfere with the activation of CDPK.

Our second hypothesis involves retrograde signaling. Retrograde signaling states the regulation of nuclear gene expression in response to functional changes in organelles, which are carefully coordinated to balance their activities. Recently, Ganusova et al. have shown that retrograde signaling from the chloroplast to the nucleus controls intercellular trafficking via the formation of plasmodesmata (Ganusova et al., 2020).

In addition, more recently, Liu Xian showed that the RipI effector of *Ralstonia solanacearum* promotes the interaction of GADs with calmodulin, increasing the production of GABA. *R. solanacearum* can replicate efficiently using GABA as a nutrient, RipI and plant GABA contribute to successful infection (Xian et al., 2020). One of our hypotheses is that the Mlp37347-GAD1 interaction could increase the level of GABA, which can be used by *Mlp* as nutrients; this might be the reason that *gad1* mutation does not promote the infection.

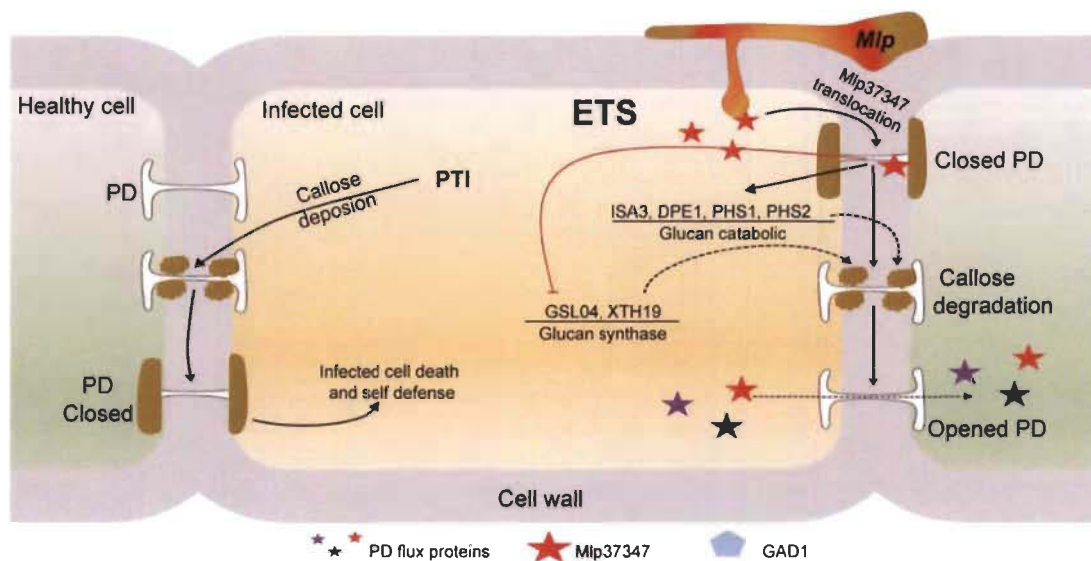


Figure 4.1. A hypothetical model illustrating a potential role of Mlp37347 and plasmodesmata during infection.



## CHAPTER V

### CONCLUSION

Fungi can colonize plants, and they have adopted very diverse lifestyles. Colonization is ruled in all systems by the secretion of hundreds of effector proteins. These effectors suppress plant defense responses and alter plant physiology to accommodate fungal invaders and provide them with nutrients. Effectors function at the site of interaction between fungal hyphae and the host, or they are transferred to cellular compartments. Therefore, the identification and functional characterization of effectors will increase our knowledge of the concepts of biotrophy, thus allowing a better understanding of the plant-microbe interaction. In this thesis, we focus on the mechanisms of Mlp37347, an effector candidate of the rust fungi *M. larici-populina* that promotes virulence. We address the issue of uptake of effectors in plant cells and highlight open questions and future challenges. With the following conclusion, this research establishes a better understanding of plant-pathogen interactions.

Here we show that Mlp37347 is present at plasmodesmata. The Mlp37347's presence in a plant cell, only when localized at the plasmodesmata, alters the physical properties of the plasmodesmata, allowing 2xmCherry to move neighboring cells. Whereas, 2xmCherry flux is restricted to adjacent cells in the absence of Mlp37347. Several research groups reported that 2XmCherry does not diffuse through plasmodesmata because its size prevents the distribution of the protein to the neighboring cells unless the size exclusion limit (SEL) of plasmodesmata is increased. From these observations, we conclude that the diffusion through the plasmodesmata is facilitated in the presence of Mlp37347.

Once we understood that the presence of Mlp37347 facilitates plasmodesmal flux, we then investigated if the localization of Mlp37347 at the plasmodesmata is important for the increased SEL observed using the Drop-ANd-See (DANS) assay. Here we measure

symplastic dye diffused area in different stable transgenic lines. Results showed a significant flux increase, revealed by the larger area stained by the CF dye, in the presence of Mlp37347-GFP; however, this increase is not observed when the effector is restricted to the nucleus. This result concludes that the localization of Mlp37347 at the plasmodesmata is required to increase the intercellular flux.

In relation to the plasmodesmata flux mechanism, we followed our interest to understand the responsible components for the effect of Mlp37347-GFP on plasmodesmata flux. We started with the effector's known interactant, GAD1. We confirmed the Mlp37347- *A. thaliana* (At) GAD1 interaction by the yeast-two hybrid (Y2H) experiment. Later, different *in-silico* docking analyses showed a common hydrogen-bonding network of Mlp37347 linked to both AtGAD1 and PtGAD1. Given the importance of callose for plasmodesmata permeability, we looked at the callose level in response to Mlp37347, NLS-Mlp37347-GFP, and *gad1* knock out. The amount of callose was significantly reduced in the stable Mlp37347-GFP line compared to Col-0. On the other hand, in the stable *gad1* mutant, *gad1* x Mlp37347-GFP, and NLS-Mlp37347-GFP, the amount of callose deposition did not vary significantly. In relation to callose deposition, our transcriptomic profiling of 4-days old *A. thaliana* stable transgenic seedlings expressing Mlp37347-GFP revealed that genes for the catabolic process of glucan are significantly up-regulated. These results establish a direct link to our previous observation that Mlp37347 localization to the plasmodesmata is important for its action on plasmodesmata opening and indicates the importance of GAD1 in diffusion processes facilitated by *Melampsora* effector.

The GAD1 was then investigated as a potential virulence target of Mlp37347 through a series of infection assays in *Arabidopsis* where GAD1 was either knocked out and crossed *gad1* x Mlp37347. The presence of Mlp37347-GFP significantly increases *Arabidopsis* susceptibility to *H. arabidopsidis*. In contrast, this increase in pathogen growth was not observed when Mlp37347 was sequestered in the nucleus (NLS-37347-GFP) nor in the *gad1* line (expressing Mlp37347-GFP or not). We conclude that Mlp37347 promotes the growth of *H. arabidopsidis*, which is a filamentous fungal-like

pathogen that produces haustorium like *Melampsora larici-populina* by enlarging plasmodesmata channel, which may allow growing hyphae to gain more intercellular access and delivers other virulent effectors to manipulate host defenses.

This study can essentially expand our knowledge of the poplar-*Melampsora larici-populina* pathosystem and highlight the importance of associated proteins as plant susceptibility. The forthcoming work will be aimed at understanding the specific mechanism by which Mlp37347 affects plant defense, which could help plan rust pathogen control strategies.

## **5.1 Perspectives**

### **5.1.1 Short term perspectives**

#### ***5.1.1.1 Validation of gene expression based on transcriptome sequence data***

Our transcriptomic analysis showed genes for the catabolic process of glucan are significantly up-regulated in 4-days old *A. thaliana* stable transgenic seedlings expressing Mlp37347-GFP. Plant defense-related and callose synthase-like genes are down-regulated in the line expressing Mlp37347-GFP. Therefore, we would like to validate gene expression based on transcriptome sequence data. To this end, we will select the up/down-regulated genes of greater fold change from the gene list, and then we will synthesize cDNA from the RNAs isolated from different genotypes. Afterward, RT-qPCR will be performed using a gene-specific primer for the analysis of gene expression.

#### ***5.1.1.2 Quantification of GABA level***

Since GABA has been in the spotlight lately, we sought to measure GABA content in different genotypes further using the HPLC method as described by Koike et al. (2013).

## 5.1.2 Long term perspectives

### 5.1.2.1 Confirmation of Mlp37347's doorman effect

We concluded from the hypothetical DoorMan model that Mlp37347 may assist other invasive effectors and IH to gain intracellular access to spread the infection. The *agrobacterium*-mediated transient expression of multiple *Mlp* effectors with or without Mlp37347 could be implemented to verify the DoorMan effect.

### 5.1.2.2 Retrograde signaling

It is not yet known where the Mlp37347-GAD1 interaction takes place in the plant, maybe in the cytosol or at the plasmodesmata, and how a PD-localized effector manipulates the transcriptional process. We could look at the retrograde signaling path for the answer since the retrograde response pathway initiates a signaling cascade to modulate the expression of nuclear genes in response to changes in mitochondrial and chloroplast function.

### 5.1.2.3 Crystal structure studies

A successfully solved Mlp3747 structure could show us that unrelated effectors can adopt folds similar to known proteins. That kind of information will encourage the use of biochemical and structural approaches for functionally characterized rust effectors. Apart from this, the proteomic analysis of plasmodesmata purified from the walls of transgenic *Arabidopsis* suspension cells could tell us more about membrane-rich structures and immunoreactive markers for the plasma membrane using nano-liquid chromatography and an Orbitrap ion-trap tandem mass spectrometer.

### 5.1.2.4 Host-induced gene silencing (HIGS) of Mlp37347

Mlp37347 was found to increase virulence activity. Therefore, it would be interesting to use one of the RNA interference (RNAi) approaches to downregulate or

silence the level of Mlp37347 transcription to control *M. larici-populina*. Host-induced gene inhibition (HIGS) is one of the new RNA-based approaches that have been used successfully to control pathogenic fungi that infect various crops of agronomic importance, for example, powdery mildew *Blumeria graminis*, (Nowara et al. 2010).

## **5.2 Final conclusions**

Collectively, the present thesis presents the important role effector Mlp37347 plays in *M. larici-populina* pathogenesis. After being secreted from *M. larici-populina*, Mlp37347 localizes at the plasmodesmata, and it binds to the Glutamate decarboxylase 1 and facilitates plasmodesmata flux to improve plant sensitivity. Our findings are also relevant to the development of a pathogen model to study other rust pathogens and will contribute to future rust disease prevention efforts.

## FOOTNOTES

<sup>1</sup> <https://www.rcsb.org/>

<sup>2</sup> [http://www.calctool.org/CALC/prof/bio/protein\\_size](http://www.calctool.org/CALC/prof/bio/protein_size)

## REFERENCES

- Abramovitch RB, Anderson JC, Martin GB, 2006. Bacterial elicitation and evasion of plant innate immunity. *Nature Reviews Molecular Cell Biology* **7**, 601-11.
- Ahmed MB, Dos Santos KCG, Sanchez IB, *et al.*, 2018. A rust fungal effector binds plant DNA and modulates transcription. *Scientific reports* **8**, 1-14.
- Anderson JC, Bartels S, Besteiro MaG, Shahollari B, Ulm R, Peck SC, 2011. Arabidopsis MAP Kinase Phosphatase 1 (AtMKP1) negatively regulates MPK6-mediated PAMP responses and resistance against bacteria. *The Plant Journal* **67**, 258-68.
- Arazi T, Baum G, Snedden WA, Shelp BJ, Fromm H, 1995. Molecular and biochemical analysis of calmodulin interactions with the calmodulin-binding domain of plant glutamate decarboxylase. *Plant physiology* **108**, 551-61.
- Arias SL, Theumer MG, Mary VS, Rubinstein HR, 2012. Fumonisin: probable role as effectors in the complex interaction of susceptible and resistant maize hybrids and *Fusarium verticillioides*. *Journal of agricultural and food chemistry* **60**, 5667-75.
- Asai T, Tena G, Plotnikova J, *et al.*, 2002. MAP kinase signalling cascade in Arabidopsis innate immunity. *Nature* **415**, 977-83.
- Aung K, Kim P, Li Z, *et al.*, 2020. Pathogenic bacteria target plant plasmodesmata to colonize and invade surrounding tissues. *The Plant Cell* **32**, 595-611.
- Ausubel FM, 2005. Are innate immune signaling pathways in plants and animals conserved? *Nature immunology* **6**, 973-9.
- Axtell MJ, Staskawicz BJ, 2003. Initiation of RPS2-specified disease resistance in Arabidopsis is coupled to the AvrRpt2-directed elimination of RIN4. *Cell* **112**, 369-77.
- Bartels S, Anderson JC, Besteiro MaG, *et al.*, 2009. MAP kinase phosphatase1 and protein tyrosine phosphatase1 are repressors of salicylic acid synthesis and SNC1-mediated responses in Arabidopsis. *The Plant Cell* **21**, 2884-97.
- Bartels S, Besteiro MaG, Lang D, Ulm R, 2010. Emerging functions for plant MAP kinase phosphatases. *Trends in plant science* **15**, 322-9.

- Baum G, Chen Y, Arazi T, Takatsuji H, Fromm H, 1993. A plant glutamate decarboxylase containing a calmodulin binding domain. Cloning, sequence, and functional analysis. *Journal of Biological Chemistry* **268**, 19610-7.
- Beckers G, Spoel S, 2006. Fine-tuning plant defence signalling: salicylate versus jasmonate. *Plant biology* **8**, 1-10.
- Benitez-Alfonso Y, Faulkner C, Pendle A, Miyashima S, Helariutta Y, Maule A, 2013. Symplastic intercellular connectivity regulates lateral root patterning. *Developmental cell* **26**, 136-47.
- Benitez-Alfonso Y, Faulkner C, Ritzenthaler C, Maule AJ, 2010. Plasmodesmata: gateways to local and systemic virus infection. *Molecular plant-microbe interactions* **23**, 1403-12.
- Berens ML, Berry HM, Mine A, Argueso CT, Tsuda K, 2017. Evolution of hormone signaling networks in plant defense. *Annual Review of Phytopathology* **55**, 401-25.
- Bernoux M, Ve T, Williams S, *et al.*, 2011. Structural and functional analysis of a plant resistance protein TIR domain reveals interfaces for self-association, signaling, and autoregulation. *Cell host & microbe* **9**, 200-11.
- Bethke G, Pecher P, Eschen-Lippold L, *et al.*, 2012. Activation of the Arabidopsis thaliana mitogen-activated protein kinase MPK11 by the flagellin-derived elicitor peptide, flg22. *Molecular plant-microbe interactions* **25**, 471-80.
- Bethke G, Unthan T, Uhrig JF, *et al.*, 2009. Flg22 regulates the release of an ethylene response factor substrate from MAP kinase 6 in Arabidopsis thaliana via ethylene signaling. *Proceedings of the National Academy of Sciences* **106**, 8067-72.
- Bindea G, Galon J, Mlecnik B, 2013. CluePedia Cytoscape plugin: pathway insights using integrated experimental and in silico data. *Bioinformatics* **29**, 661-3.
- Bitanhirwe BK, Cunningham MG, 2009. Zinc: the brain's dark horse. *Synapse* **63**, 1029-49.
- Boller T, Felix G, 2009. A renaissance of elicitors: perception of microbe-associated molecular patterns and danger signals by pattern-recognition receptors. *Annual review of plant biology* **60**, 379-406.
- Bolton MD, Van Esse HP, Vossen JH, *et al.*, 2008. The novel Cladosporium fulvum lysin motif effector Ecp6 is a virulence factor with orthologues in other fungal species. *Molecular microbiology* **69**, 119-36.



- Bos JI, Kanneganti TD, Young C, *et al.*, 2006. The C-terminal half of *Phytophthora infestans* RXLR effector AVR3a is sufficient to trigger R3a-mediated hypersensitivity and suppress INF1-induced cell death in *Nicotiana benthamiana*. *The Plant Journal* **48**, 165-76.
- Bouché N, Scharlat A, Snedden W, Bouchez D, Fromm H, 2002. A novel family of calmodulin-binding transcription activators in multicellular organisms. *Journal of Biological Chemistry* **277**, 21851-61.
- Boudsocq M, Willmann MR, McCormack M, *et al.*, 2010. Differential innate immune signalling via Ca<sup>2+</sup> sensor protein kinases. *Nature* **464**, 418-22.
- Brandner K, Sambade A, Boutant E, *et al.*, 2008. Tobacco mosaic virus movement protein interacts with green fluorescent protein-tagged microtubule end-binding protein 1. *Plant physiology* **147**, 611-23.
- Brock AK, Willmann R, Kolb D, *et al.*, 2010. The Arabidopsis mitogen-activated protein kinase phosphatase PP2C5 affects seed germination, stomatal aperture, and abscisic acid-inducible gene expression. *Plant physiology* **153**, 1098-111.
- Brodersen P, Petersen M, Bjørn Nielsen H, *et al.*, 2006. Arabidopsis MAP kinase 4 regulates salicylic acid- and jasmonic acid/ethylene-dependent responses via EDS1 and PAD4. *The Plant Journal* **47**, 532-46.
- Browse J, 2009. Jasmonate passes muster: a receptor and targets for the defense hormone. *Annual review of plant biology* **60**, 183-205.
- Brutus A, Sicilia F, Macone A, Cervone F, De Lorenzo G, 2010. A domain swap approach reveals a role of the plant wall-associated kinase 1 (WAK1) as a receptor of oligogalacturonides. *Proceedings of the National Academy of Sciences* **107**, 9452-7.
- Büttner D, He SY, 2009. Type III protein secretion in plant pathogenic bacteria. *Plant physiology* **150**, 1656-64.
- Caillaud M-C, Wirthmueller L, Fabro G, *et al.* Mechanisms of nuclear suppression of host immunity by effectors from the Arabidopsis downy mildew pathogen *Hyaloperonospora arabidopsidis* (Hpa). *Proceedings of the Cold Spring Harbor symposia on quantitative biology, 2012a*: Cold Spring Harbor Laboratory Press, 285-93.
- Caillaud MC, Piquerez SJ, Fabro G, *et al.*, 2012b. Subcellular localization of the Hpa RxLR effector repertoire identifies a tonoplast-associated protein HaRxL17 that confers enhanced plant susceptibility. *The Plant Journal* **69**, 252-65.

- Canton J, Grinstein S, 2014. Priming and activation of NADPH oxidases in plants and animals. *Trends in immunology* **35**, 405-7.
- Cao L, Blekemolen MC, Tintor N, Cornelissen BJ, Takken FL, 2018. The *Fusarium oxysporum* Avr2-Six5 effector pair alters plasmodesmatal exclusion selectivity to facilitate cell-to-cell movement of Avr2. *Molecular plant* **11**, 691-705.
- Chiang Y-H, Coaker G, 2015. Effector triggered immunity: NLR immune perception and downstream defense responses. *The Arabidopsis Book* **2015**.
- Chibucos MC, Tyler BM, 2009. Common themes in nutrient acquisition by plant symbiotic microbes, described by the Gene Ontology. *BMC microbiology* **9**, S6.
- Chin D, Means AR, 2000. Calmodulin: a prototypical calcium sensor. *Trends in cell biology* **10**, 322-8.
- Chinchilla D, Zipfel C, Robatzek S, *et al.*, 2007. A flagellin-induced complex of the receptor FLS2 and BAK1 initiates plant defence. *Nature* **448**, 497-500.
- Chini A, Fonseca S, Chico JM, Fernández-Calvo P, Solano R, 2009. The ZIM domain mediates homo-and heteromeric interactions between Arabidopsis JAZ proteins. *The Plant Journal* **59**, 77-87.
- Chisholm ST, Coaker G, Day B, Staskawicz BJ, 2006. Host-microbe interactions: shaping the evolution of the plant immune response. *Cell* **124**, 803-14.
- Choi J, Tanaka K, Cao Y, *et al.*, 2014. Identification of a plant receptor for extracellular ATP. *Science* **343**, 290-4.
- Collemare J, Lebrun MH, 2011. Fungal secondary metabolites: ancient toxins and novel effectors in plant-microbe interactions. *Effectors in plant-microbe interactions*, 377-400.
- Conrath U, Beckers GJ, Flors V, *et al.*, 2006. Priming: getting ready for battle. *Molecular plant-microbe interactions* **19**, 1062-71.
- Conti G, Rodriguez MC, Manacorda CA, Asurmendi S, 2012. Transgenic expression of Tobacco mosaic virus capsid and movement proteins modulate plant basal defense and biotic stress responses in *Nicotiana tabacum*. *Molecular plant-microbe interactions* **25**, 1370-84.
- Cosgrove DJ, 2016. Plant cell wall extensibility: connecting plant cell growth with cell wall structure, mechanics, and the action of wall-modifying enzymes. *Journal of experimental botany* **67**, 463-76.

- Cui W, Lee J-Y, 2016. Arabidopsis callose synthases CalS1/8 regulate plasmodesmal permeability during stress. *Nature plants* **2**, 1-9.
- Cui W, Wang X, Lee J-Y, 2015. Drop-ANd-See: a simple, real-time, and noninvasive technique for assaying plasmodesmal permeability. In. *Plasmodesmata*. Springer, 149-56.
- Cuomo CA, Lin Y-C, Aerts A, *et al.*, 2011. Obligate biotrophy features unraveled by the genomic analysis of rust fungi.
- Dangl JL, Jones JD, 2001. Plant pathogens and integrated defence responses to infection. *Nature* **411**, 826-33.
- De Guillen K, Lorrain C, Tsan P, *et al.*, 2019. Structural genomics applied to the rust fungus *Melampsora larici-populina* reveals two candidate effector proteins adopting cystine knot and NTF2-like protein folds. *Scientific reports* **9**, 1-12.
- De Jonge R, Van Esse HP, Kombrink A, *et al.*, 2010. Conserved fungal LysM effector Ecp6 prevents chitin-triggered immunity in plants. *Science* **329**, 953-5.
- De Jonge R, Van Esse HP, Maruthachalam K, *et al.*, 2012. Tomato immune receptor Ve1 recognizes effector of multiple fungal pathogens uncovered by genome and RNA sequencing. *Proceedings of the National Academy of Sciences* **109**, 5110-5.
- De Storme N, De Schrijver J, Van Criekinge W, Wewer V, Dörmann P, Geelen D, 2013. GLUCAN SYNTHASE-LIKE8 and STEROL METHYLTRANSFERASE2 are required for ploidy consistency of the sexual reproduction system in Arabidopsis. *The Plant Cell* **25**, 387-403.
- De Storme N, Geelen D, 2014. Callose homeostasis at plasmodesmata: molecular regulators and developmental relevance. *Frontiers in plant science* **5**, 138.
- De Wit PJ, 2016. Apoplastic fungal effectors in historic perspective; a personal view. *New Phytologist* **212**, 805-13.
- Dempsey DMA, Klessig DF, 2012. SOS—too many signals for systemic acquired resistance? *Trends in plant science* **17**, 538-45.
- Depluvere S, Devos S, Devreese B, 2016. The role of bacterial secretion systems in the virulence of Gram-negative airway pathogens associated with cystic fibrosis. *Frontiers in microbiology* **7**, 1336.
- Deslandes L, Rivas S, 2012. Catch me if you can: bacterial effectors and plant targets. *Trends in plant science* **17**, 644-55.

- Dodds PN, Lawrence GJ, Catanzariti A-M, Ayliffe MA, Ellis JG, 2004. The *Melampsora lini* AvrL567 avirulence genes are expressed in haustoria and their products are recognized inside plant cells. *The Plant Cell* **16**, 755-68.
- Dodds PN, Lawrence GJ, Catanzariti A-M, *et al.*, 2006. Direct protein interaction underlies gene-for-gene specificity and coevolution of the flax resistance genes and flax rust avirulence genes. *Proceedings of the National Academy of Sciences* **103**, 8888-93.
- Dong X, 2004. NPR1, all things considered. *Current opinion in plant biology* **7**, 547-52.
- Du Y, Berg J, Govers F, Bouwmeester K, 2015. Immune activation mediated by the late blight resistance protein R1 requires nuclear localization of R1 and the effector AVR1. *New Phytologist* **207**, 735-47.
- Duhovny D, Nussinov R, Wolfson HJ. Efficient unbound docking of rigid molecules. *Proceedings of the International workshop on algorithms in bioinformatics, 2002*: Springer, 185-200.
- Duplessis S, Cuomo CA, Lin Y-C, *et al.*, 2011a. Obligate biotrophy features unraveled by the genomic analysis of rust fungi. *Proceedings of the National Academy of Sciences* **108**, 9166-71.
- Duplessis S, Hacquard S, Delaruelle C, *et al.*, 2011b. *Melampsora larici-populina* transcript profiling during germination and timecourse infection of poplar leaves reveals dynamic expression patterns associated with virulence and biotrophy. *Molecular Plant-Microbe Interactions* **24**, 808-18.
- Ellis JG, Lawrence GJ, Dodds PN, 2007. Further analysis of gene-for-gene disease resistance specificity in flax. *Molecular plant pathology* **8**, 103-9.
- Ellis JG, Lawrence GJ, Luck JE, Dodds PN, 1999. Identification of regions in alleles of the flax rust resistance gene L that determine differences in gene-for-gene specificity. *The Plant Cell* **11**, 495-506.
- Epel BL. Plant viruses spread by diffusion on ER-associated movement-protein-rafts through plasmodesmata gated by viral induced host  $\beta$ -1, 3-glucanases. *Proceedings of the Seminars in cell & developmental biology, 2009*: Elsevier, 1074-81.
- Fabro G, Steinbrenner J, Coates M, *et al.*, 2011. Multiple candidate effectors from the oomycete pathogen *Hyaloperonospora arabidopsidis* suppress host plant immunity. *PLoS pathog* **7**, e1002348.

- Faulkner C, Petutschnig E, Benitez-Alfonso Y, *et al.*, 2013. LYM2-dependent chitin perception limits molecular flux via plasmodesmata. *Proceedings of the National Academy of Sciences* **110**, 9166-70.
- Felix G, Duran JD, Volko S, Boller T, 1999. Plants have a sensitive perception system for the most conserved domain of bacterial flagellin. *The Plant Journal* **18**, 265-76.
- Flor H, 1971a. Current status of the gene-for-gene concept. *Annu. Rev.*
- Flor HH, 1971b. Current status of the gene-for-gene concept. *Annual review of phytopathology* **9**, 275-96.
- Fonseca S, Chini A, Hamberg M, *et al.*, 2009. (+)-7-iso-Jasmonoyl-L-isoleucine is the endogenous bioactive jasmonate. *Nature chemical biology* **5**, 344-50.
- Fradin EF, Abd-El-Haliem A, Masini L, Van Den Berg GC, Joosten MH, Thomma BP, 2011. Interfamily transfer of tomato Ve1 mediates *Verticillium* resistance in *Arabidopsis*. *Plant physiology* **156**, 2255-65.
- Fu ZQ, Yan S, Saleh A, *et al.*, 2012. NPR3 and NPR4 are receptors for the immune signal salicylic acid in plants. *Nature* **486**, 228-32.
- Gaffney T, Friedrich L, Vernooij B, *et al.*, 1993. Requirement of salicylic acid for the induction of systemic acquired resistance. *Science* **261**, 754-6.
- Gallego PP, Whotton L, Picton S, Grierson D, Gray JE, 1995. A role for glutamate decarboxylase during tomato ripening: the characterisation of a cDNA encoding a putative glutamate decarboxylase with a calmodulin-binding site. *Plant molecular biology* **27**, 1143-51.
- Ganusova EE, Reagan BC, Fernandez JC, *et al.*, 2020. Chloroplast-to-nucleus retrograde signalling controls intercellular trafficking via plasmodesmata formation. *Philosophical Transactions of the Royal Society B* **375**, 20190408.
- Gao M, Liu J, Bi D, *et al.*, 2008. MEKK1, MKK1/MKK2 and MPK4 function together in a mitogen-activated protein kinase cascade to regulate innate immunity in plants. *Cell research* **18**, 1190-8.
- Gao Q-M, Zhu S, Kachroo P, Kachroo A, 2015. Signal regulators of systemic acquired resistance. *Frontiers in plant science* **6**, 228.
- Gaouar O, Morency M-J, Letanneur C, Séguin A, Germain H, 2016. The 124202 candidate effector of *Melampsora larici-populina* interacts with membranes in *Nicotiana* and *Arabidopsis*. *Canadian Journal of Plant Pathology* **38**, 197-208.

- Germain H, Gray-Mitsumune M, Lafleur E, Matton DP, 2008. ScORK17, a transmembrane receptor-like kinase predominantly expressed in ovules is involved in seed development. *Planta* **228**, 851-62.
- Germain H, Joly DL, Mireault C, *et al.*, 2018. Infection assays in Arabidopsis reveal candidate effectors from the poplar rust fungus that promote susceptibility to bacteria and oomycete pathogens. *Molecular plant pathology* **19**, 191-200.
- Glazebrook J, 2005. Contrasting mechanisms of defense against biotrophic and necrotrophic pathogens. *Annu. Rev. Phytopathol.* **43**, 205-27.
- Gómez-Gómez L, Boller T, 2000. FLS2: an LRR receptor-like kinase involved in the perception of the bacterial elicitor flagellin in Arabidopsis. *Molecular cell* **5**, 1003-11.
- Gómez-Gómez L, Felix G, Boller T, 1999. A single locus determines sensitivity to bacterial flagellin in Arabidopsis thaliana. *The Plant Journal* **18**, 277-84.
- González Besteiro MA, Bartels S, Albert A, Ulm R, 2011. Arabidopsis MAP kinase phosphatase 1 and its target MAP kinases 3 and 6 antagonistically determine UV-B stress tolerance, independent of the UVR8 photoreceptor pathway. *The Plant Journal* **68**, 727-37.
- Grant M, Lamb C, 2006. Systemic immunity. *Current opinion in plant biology* **9**, 414-20.
- Grison MS, Kirk P, Brault ML, *et al.*, 2019. Plasma membrane-associated receptor-like kinases relocalize to plasmodesmata in response to osmotic stress. *Plant physiology* **181**, 142-60.
- Guseman JM, Lee JS, Bogenschutz NL, *et al.*, 2010. Dysregulation of cell-to-cell connectivity and stomatal patterning by loss-of-function mutation in Arabidopsis chorus (glucan synthase-like 8). *Development* **137**, 1731-41.
- Hacquard S, Delaruelle C, Frey P, Tisserant E, Kohler A, Duplessis S, 2013. Transcriptome analysis of poplar rust telia reveals overwintering adaptation and tightly coordinated karyogamy and meiosis processes. *Frontiers in plant science* **4**, 456.
- Hacquard S, Delaruelle C, Legué V, *et al.*, 2010. Laser capture microdissection of uredinia formed by *Melampsora larici-populina* revealed a transcriptional switch between biotrophy and sporulation. *Molecular Plant-Microbe Interactions* **23**, 1275-86.

- Hacquard S, Joly DL, Lin Y-C, *et al.*, 2012. A comprehensive analysis of genes encoding small secreted proteins identifies candidate effectors in *Melampsora larici-populina* (poplar leaf rust). *Molecular plant-microbe interactions* **25**, 279-93.
- Hacquard S, Petre B, Frey P, Hecker A, Rouhier N, Duplessis S, 2011. The poplar-poplar rust interaction: insights from genomics and transcriptomics. *Journal of pathogens* **2011**.
- Han X, Huang L-J, Feng D, Jiang W, Miu W, Li N, 2019. Plasmodesmata-Related Structural and Functional Proteins: The Long Sought-After Secrets of a Cytoplasmic Channel in Plant Cell Walls. *International journal of molecular sciences* **20**, 2946.
- Han X, Hyun TK, Zhang M, *et al.*, 2014. Auxin-callose-mediated plasmodesmal gating is essential for tropic auxin gradient formation and signaling. *Developmental cell* **28**, 132-46.
- Harries PA, Schoelz JE, Nelson RS, 2010. Intracellular transport of viruses and their components: utilizing the cytoskeleton and membrane highways. *Molecular plant-microbe interactions* **23**, 1381-93.
- Haruta M, Sabat G, Stecker K, Minkoff BB, Sussman MR, 2014. A peptide hormone and its receptor protein kinase regulate plant cell expansion. *Science* **343**, 408-11.
- Hauck P, Thilmony R, He SY, 2003. A *Pseudomonas syringae* type III effector suppresses cell wall-based extracellular defense in susceptible *Arabidopsis* plants. *Proceedings of the National Academy of Sciences* **100**, 8577-82.
- Haupt S, Cowan GH, Ziegler A, Roberts AG, Oparka KJ, Torrance L, 2005. Two plant-viral movement proteins traffic in the endocytic recycling pathway. *The Plant Cell* **17**, 164-81.
- Hayashi F, Smith KD, Ozinsky A, *et al.*, 2001. The innate immune response to bacterial flagellin is mediated by Toll-like receptor 5. *Nature* **410**, 1099-103.
- Hogenhout SA, Van Der Hoorn RA, Terauchi R, Kamoun S, 2009. Emerging concepts in effector biology of plant-associated organisms. *Molecular plant-microbe interactions* **22**, 115-22.
- Huitema E, Bos JI, Tian M, Win J, Waugh ME, Kamoun S, 2004. Linking sequence to phenotype in *Phytophthora*-plant interactions. *Trends in microbiology* **12**, 193-200.

- Ichimura K, Casais C, Peck SC, Shinozaki K, Shirasu K, 2006. MEKK1 is required for MPK4 activation and regulates tissue-specific and temperature-dependent cell death in Arabidopsis. *Journal of Biological Chemistry* **281**, 36969-76.
- Jehle AK, Lipschis M, Albert M, *et al.*, 2013. The receptor-like protein ReMAX of Arabidopsis detects the microbe-associated molecular pattern eMax from Xanthomonas. *The Plant Cell* **25**, 2330-40.
- Jiang RH, Tripathy S, Govers F, Tyler BM, 2008. RXLR effector reservoir in two Phytophthora species is dominated by a single rapidly evolving superfamily with more than 700 members. *Proceedings of the National Academy of Sciences* **105**, 4874-9.
- Joly DL, Feau N, Tanguay P, Hamelin RC, 2010. Comparative analysis of secreted protein evolution using expressed sequence tags from four poplar leaf rusts (Melampsora spp.). *BMC genomics* **11**, 422.
- Jones JD, Dangl JL, 2006. The plant immune system. *Nature* **444**, 323-9.
- Ju H-J, Samuels TD, Wang Y-S, *et al.*, 2005. The potato virus X TGBp2 movement protein associates with endoplasmic reticulum-derived vesicles during virus infection. *Plant physiology* **138**, 1877-95.
- Kadota Y, Shirasu K, Zipfel C, 2015. Regulation of the NADPH oxidase RBOHD during plant immunity. *Plant and Cell Physiology* **56**, 1472-80.
- Kaku H, Nishizawa Y, Ishii-Minami N, *et al.*, 2006. Plant cells recognize chitin fragments for defense signaling through a plasma membrane receptor. *Proceedings of the National Academy of Sciences* **103**, 11086-91.
- Kale SD, Gu B, Capelluto DG, *et al.*, 2010. External lipid PI3P mediates entry of eukaryotic pathogen effectors into plant and animal host cells. *Cell* **142**, 284-95.
- Kamoun S, 2003. Molecular genetics of pathogenic oomycetes. *Eukaryotic cell* **2**, 191-9.
- Kankanala P, Czymbek K, Valent B, 2007. Roles for rice membrane dynamics and plasmodesmata during biotrophic invasion by the blast fungus. *The Plant Cell* **19**, 706-24.
- Karimi M, Inzé D, Depicker A, 2002. GATEWAY™ vectors for Agrobacterium-mediated plant transformation. *Trends in plant science* **7**, 193-5.



- Katsir L, Schillmiller AL, Staswick PE, He SY, Howe GA, 2008. COI1 is a critical component of a receptor for jasmonate and the bacterial virulence factor coronatine. *Proceedings of the National Academy of Sciences* **105**, 7100-5.
- Kawamura A, Mizuno Y, Minamidani T, *et al.*, 2009a. The second survey of the molecular clouds in the Large Magellanic Cloud by NANTEN. II. Star formation. *The Astrophysical Journal Supplement Series* **184**, 1.
- Kawamura Y, Hase S, Takenaka S, *et al.*, 2009b. INF1 elicitor activates jasmonic acid- and ethylene-mediated signalling pathways and induces resistance to bacterial wilt disease in tomato. *Journal of Phytopathology* **157**, 287-97.
- Khang CH, Berruyer R, Giraldo MC, *et al.*, 2010. Translocation of *Magnaporthe oryzae* effectors into rice cells and their subsequent cell-to-cell movement. *The Plant Cell* **22**, 1388-403.
- Kloek AP, Verbsky ML, Sharma SB, *et al.*, 2001. Resistance to *Pseudomonas syringae* conferred by an *Arabidopsis thaliana* coronatine-insensitive (*coi1*) mutation occurs through two distinct mechanisms. *The Plant Journal* **26**, 509-22.
- Knight MR, Smith SM, Trewavas AJ, 1992. Wind-induced plant motion immediately increases cytosolic calcium. *Proceedings of the National Academy of Sciences* **89**, 4967-71.
- Koornneef M, Meinke D, 2010. The development of *Arabidopsis* as a model plant. *The Plant Journal* **61**, 909-21.
- Kong Q, Qu N, Gao M, *et al.*, 2012. The MEKK1-MKK1/MKK2-MPK4 kinase cascade negatively regulates immunity mediated by a mitogen-activated protein kinase kinase kinase in *Arabidopsis*. *The Plant Cell* **24**, 2225-36.
- Kozakov D, Hall DR, Xia B, *et al.*, 2017. The ClusPro web server for protein-protein docking. *Nature protocols* **12**, 255.
- Krenek P, Samajova O, Luptovciak I, Duskocilova A, Komis G, Samaj J, 2015. Transient plant transformation mediated by *Agrobacterium tumefaciens*: Principles, methods and applications. *Biotechnology Advances* **33**, 1024-42.
- Krol E, Mentzel T, Chinchilla D, *et al.*, 2010. Perception of the *Arabidopsis* danger signal peptide 1 involves the pattern recognition receptor AtPEPR1 and its close homologue AtPEPR2. *Journal of Biological Chemistry* **285**, 13471-9.
- Kumar S, Punekar NS, 1997. The metabolism of 4-aminobutyrate (GABA) in fungi. *Mycological Research* **101**, 403-9.

- Kunjeti SG, Iyer G, Johnson E, *et al.*, 2016. Identification of Phakopsora pachyrhizi candidate effectors with virulence activity in a distantly related pathosystem. *Frontiers in plant science* **7**, 269.
- Kunkel BN, Brooks DM, 2002. Cross talk between signaling pathways in pathogen defense. *Current opinion in plant biology* **5**, 325-31.
- Lawrence GJ, Dodds PN, Ellis JG, 2007. Rust of flax and linseed caused by Melampsora lini. *Molecular plant pathology* **8**, 349-64.
- Lawrence GJ, Dodds PN, Ellis JG, 2010. TECHNICAL ADVANCE: transformation of the flax rust fungus, Melampsora lini: selection via silencing of an avirulence gene. *The Plant Journal* **61**, 364-9.
- Lecourieux D, Mazars C, Pauly N, Ranjeva R, Pugin A, 2002. Analysis and effects of cytosolic free calcium increases in response to elicitors in Nicotiana plumbaginifolia cells. *The Plant Cell* **14**, 2627-41.
- Lecourieux D, Ranjeva R, Pugin A, 2006. Calcium in plant defence-signalling pathways. *New Phytologist* **171**, 249-69.
- Lee J-Y, Lu H, 2011. Plasmodesmata: the battleground against intruders. *Trends in plant science* **16**, 201-10.
- Lee J-Y, Yoo B-C, Lucas WJ, 2000. Parallels between nuclear-pore and plasmodesmal trafficking of information molecules. *Planta* **210**, 177-87.
- Levy A, Erlanger M, Rosenthal M, Epel BL, 2007. A plasmodesmata-associated  $\beta$ -1, 3-glucanase in Arabidopsis. *The Plant Journal* **49**, 669-82.
- Li G, Meng X, Wang R, *et al.*, 2012. Dual-level regulation of ACC synthase activity by MPK3/MPK6 cascade and its downstream WRKY transcription factor during ethylene induction in Arabidopsis. *PLoS Genet* **8**, e1002767.
- Ling V, Snedden WA, Shelp BJ, Assmann SM, 1994. Analysis of a soluble calmodulin binding protein from fava bean roots: identification of glutamate decarboxylase as a calmodulin-activated enzyme. *The Plant Cell* **6**, 1135-43.
- Liu Y, Zhang S, 2004. Phosphorylation of 1-aminocyclopropane-1-carboxylic acid synthase by MPK6, a stress-responsive mitogen-activated protein kinase, induces ethylene biosynthesis in Arabidopsis. *The Plant Cell* **16**, 3386-99.
- Lorrain C, Hecker A, Duplessis S, 2015. Effector-mining in the poplar rust fungus Melampsora larici-populina secretome. *Frontiers in plant science* **6**, 1051.

- Lucas WJ, Lee J-Y, 2004. Plasmodesmata as a supracellular control network in plants. *Nature Reviews Molecular Cell Biology* **5**, 712-26.
- Luck JE, Lawrence GJ, Dodds PN, Shepherd KW, Ellis JG, 2000. Regions outside of the leucine-rich repeats of flax rust resistance proteins play a role in specificity determination. *The Plant Cell* **12**, 1367-77.
- Lumbreras V, Vilela B, Irar S, *et al.*, 2010. MAPK phosphatase MKP2 mediates disease responses in Arabidopsis and functionally interacts with MPK3 and MPK6. *The Plant Journal* **63**, 1017-30.
- Mackey D, Belkhadir Y, Alonso JM, Ecker JR, Dangl JL, 2003. Arabidopsis RIN4 is a target of the type III virulence effector AvrRpt2 and modulates RPS2-mediated resistance. *Cell* **112**, 379-89.
- Mackey D, Holt III BF, Wiig A, Dangl JL, 2002. RIN4 interacts with Pseudomonas syringae type III effector molecules and is required for RPM1-mediated resistance in Arabidopsis. *Cell* **108**, 743-54.
- Madina MH, Rahman MS, Huang X, Zhang Y, Zheng H, Germain H, 2020. A poplar rust effector protein associates with protein disulfide isomerase and enhances plant susceptibility. *Biology* **9**, 294.
- Maule A, Faulkner C, Benitez-Alfonso Y, 2012. Plasmodesmata “in communicado”. *Frontiers in plant science* **3**, 30.
- Maule AJ, 2008. Plasmodesmata: structure, function and biogenesis. *Current opinion in plant biology* **11**, 680-6.
- Mccann HC, Guttman DS, 2008. Evolution of the type III secretion system and its effectors in plant–microbe interactions. *New Phytologist* **177**, 33-47.
- Meikle RD. Willows and poplars of Great Britain and Ireland, 1984: Botanical Society of the British Isles.
- Melotto M, Underwood W, Koczan J, Nomura K, He SY, 2006. Plant stomata function in innate immunity against bacterial invasion. *Cell* **126**, 969-80.
- Mészáros T, Helfer A, Hatzimasoura E, *et al.*, 2006. The Arabidopsis MAP kinase kinase MKK1 participates in defence responses to the bacterial elicitor flagellin. *The Plant Journal* **48**, 485-98.
- Meyerowitz EM, 1989. Arabidopsis, a useful weed. *Cell* **56**, 263-9.

- Meyerowitz EM, 2001. Prehistory and history of Arabidopsis research. *Plant Physiology* **125**, 15-9.
- Mireault C, Paris L-E, Germain H, 2014. Enhancement of the Arabidopsis floral dip method with XIAMETER OFX-0309 as alternative to Silwet L-77 surfactant. *Botany* **92**, 523-5.
- Misas-Villamil JC, Van Der Hoorn RA, 2008. Enzyme-inhibitor interactions at the plant-pathogen interface. *Current opinion in plant biology* **11**, 380-8.
- Mishina TE, Zeier J, 2007. Pathogen-associated molecular pattern recognition rather than development of tissue necrosis contributes to bacterial induction of systemic acquired resistance in Arabidopsis. *The Plant Journal* **50**, 500-13.
- Miya A, Albert P, Shinya T, *et al.*, 2007. CERK1, a LysM receptor kinase, is essential for chitin elicitor signaling in Arabidopsis. *Proceedings of the National Academy of Sciences* **104**, 19613-8.
- Miyashita Y, Good AG, 2008. Contribution of the GABA shunt to hypoxia-induced alanine accumulation in roots of Arabidopsis thaliana. *Plant and Cell Physiology* **49**, 92-102.
- Nakagami H, Soukupová H, Schikora A, Zárský V, Hirt H, 2006. A mitogen-activated protein kinase kinase kinase mediates reactive oxygen species homeostasis in Arabidopsis. *Journal of Biological Chemistry* **281**, 38697-704.
- Ossowski S, Schneeberger K, Clark RM, Lanz C, Warthmann N, Weigel D, 2008. Sequencing of natural strains of Arabidopsis thaliana with short reads. *Genome research* **18**, 2024-33.
- Pedley KF, Martin GB, 2005. Role of mitogen-activated protein kinases in plant immunity. *Current opinion in plant biology* **8**, 541-7.
- Pernaci M, De Mita S, Andrieux A, *et al.*, 2014. Genome-wide patterns of segregation and linkage disequilibrium: the construction of a linkage genetic map of the poplar rust fungus Melampsora larici-populina. *Frontiers in plant science* **5**, 454.
- Persoons A, Hayden KJ, Fabre B, *et al.*, 2017. The escalatory Red Queen: Population extinction and replacement following arms race dynamics in poplar rust. *Molecular ecology* **26**, 1902-18.
- Petersen M, Brodersen P, Næsted H, *et al.*, 2000. Arabidopsis MAP kinase 4 negatively regulates systemic acquired resistance. *Cell* **103**, 1111-20.

- Petre B, Kamoun S, 2014. How do filamentous pathogens deliver effector proteins into plant cells? *PLoS biology* **12**, e1001801.
- Petre B, Lorrain C, Saunders DG, *et al.*, 2016a. Rust fungal effectors mimic host transit peptides to translocate into chloroplasts. *Cellular microbiology* **18**, 453-65.
- Petre B, Saunders DG, Sklenar J, *et al.*, 2016b. Heterologous expression screens in *Nicotiana benthamiana* identify a candidate effector of the wheat yellow rust pathogen that associates with processing bodies. *PloS one* **11**, e0149035.
- Petre B, Saunders DG, Sklenar J, *et al.*, 2015. Candidate effector proteins of the rust pathogen *Melampsora larici-populina* target diverse plant cell compartments. *Molecular plant-microbe interactions* **28**, 689-700.
- Petutschnig EK, Jones AM, Serazetdinova L, Lipka U, Lipka V, 2010. The LysM-RLK CERK1 is a major chitin binding protein in *Arabidopsis thaliana* and subject to chitin-induced phosphorylation. *Journal of Biological Chemistry*, jbc. M110. 116657.
- Pierce BG, Hourai Y, Weng Z, 2011. Accelerating protein docking in ZDOCK using an advanced 3D convolution library. *PloS one* **6**.
- Pierce BG, Wiehe K, Hwang H, Kim B-H, Vreven T, Weng Z, 2014. ZDOCK server: interactive docking prediction of protein–protein complexes and symmetric multimers. *Bioinformatics* **30**, 1771-3.
- Pieterse CM, Leon-Reyes A, Van Der Ent S, Van Wees SC, 2009. Networking by small-molecule hormones in plant immunity. *Nature chemical biology* **5**, 308-16.
- Pinon J, Frey P, 2005. Interactions between poplar clones and *Melampsora* populations and their implications for breeding for durable resistance. *Rust diseases of willow and poplar*, 139-54.
- Price AH, Taylor A, Ripley SJ, Griffiths A, Trewavas AJ, Knight MR, 1994. Oxidative signals in tobacco increase cytosolic calcium. *The Plant Cell* **6**, 1301-10.
- Pritchard L, Birch PR, 2014. The zigzag model of plant–microbe interactions: is it time to move on? *Molecular plant pathology* **15**, 865.
- Qiu JL, Fiil BK, Petersen K, *et al.*, 2008. *Arabidopsis* MAP kinase 4 regulates gene expression through transcription factor release in the nucleus. *The EMBO journal* **27**, 2214-21.

- Rafiqi M, Ellis JG, Ludowici VA, Hardham AR, Dodds PN, 2012. Challenges and progress towards understanding the role of effectors in plant–fungal interactions. *Current opinion in plant biology* **15**, 477-82.
- Rafiqi M, Gan PH, Ravensdale M, *et al.*, 2010. Internalization of flax rust avirulence proteins into flax and tobacco cells can occur in the absence of the pathogen. *The Plant Cell* **22**, 2017-32.
- Ravensdale M, Nemri A, Thrall PH, Ellis JG, Dodds PN, 2011. Co-evolutionary interactions between host resistance and pathogen effector genes in flax rust disease. *Molecular plant pathology* **12**, 93-102.
- Rédei GP, 1975. Arabidopsis as a genetic tool. *Annual review of genetics* **9**, 111-27.
- Robards A, Lucas W, 1990. Plasmodesmata. *Annual review of plant biology* **41**, 369-419.
- Robert-Seilaniantz A, Grant M, Jones JD, 2011. Hormone crosstalk in plant disease and defense: more than just jasmonate-salicylate antagonism. *Annual review of phytopathology* **49**, 317-43.
- Ron M, Avni A, 2004. The receptor for the fungal elicitor ethylene-inducing xylanase is a member of a resistance-like gene family in tomato. *The Plant Cell* **16**, 1604-15.
- Ross AF, 1961. Systemic acquired resistance induced by localized virus infections in plants. *Virology* **14**, 340-58.
- Roux M, Schwessinger B, Albrecht C, *et al.*, 2011. The Arabidopsis leucine-rich repeat receptor–like kinases BAK1/SERK3 and BKK1/SERK4 are required for innate immunity to hemibiotrophic and biotrophic pathogens. *The Plant Cell* **23**, 2440-55.
- Sager RE, Lee J-Y, 2018. Plasmodesmata at a glance. *Journal of Cell Science* **131**.
- Sasaki N, Park J-W, Maule AJ, Nelson RS, 2006. The cysteine–histidine-rich region of the movement protein of Cucumber mosaic virus contributes to plasmodesmal targeting, zinc binding and pathogenesis. *Virology* **349**, 396-408.
- Saunders DG, Win J, Cano LM, Szabo LJ, Kamoun S, Raffaele S, 2012. Using hierarchical clustering of secreted protein families to classify and rank candidate effectors of rust fungi. *PLoS One* **7**, e29847.
- Schenk PM, Kazan K, Wilson I, *et al.*, 2000. Coordinated plant defense responses in Arabidopsis revealed by microarray analysis. *Proceedings of the National Academy of Sciences* **97**, 11655-60.

- Schneidman-Duhovny D, Inbar Y, Nussinov R, Wolfson HJ, 2005. PatchDock and SymmDock: servers for rigid and symmetric docking. *Nucleic acids research* **33**, W363-W7.
- Schweighofer A, Kazanaviciute V, Scheikl E, *et al.*, 2007. The PP2C-type phosphatase AP2C1, which negatively regulates MPK4 and MPK6, modulates innate immunity, jasmonic acid, and ethylene levels in Arabidopsis. *The Plant Cell* **19**, 2213-24.
- Seybold H, Trempel F, Ranf S, Scheel D, Romeis T, Lee J, 2014. Ca<sup>2+</sup> signalling in plant immune response: from pattern recognition receptors to Ca<sup>2+</sup> decoding mechanisms. *New Phytologist* **204**, 782-90.
- Sevilem I, Miyashima S, Helariutta Y, 2013. Cell-to-cell communication via plasmodesmata in vascular plants. *Cell adhesion & migration* **7**, 27-32.
- Shan L, He P, Li J, *et al.*, 2008. Bacterial effectors target the common signaling partner BAK1 to disrupt multiple MAMP receptor-signaling complexes and impede plant immunity. *Cell host & microbe* **4**, 17-27.
- Sheard LB, Tan X, Mao H, *et al.*, 2010. Jasmonate perception by inositol-phosphate-potentiated COI1-JAZ co-receptor. *Nature* **468**, 400-5.
- Shigenaga AM, Argueso CT. No hormone to rule them all: Interactions of plant hormones during the responses of plants to pathogens. *Proceedings of the Seminars in Cell & Developmental Biology, 2016*: Elsevier, 174-89.
- Shimizu T, Nakano T, Takamizawa D, *et al.*, 2010. Two LysM receptor molecules, CEBiP and OsCERK1, cooperatively regulate chitin elicitor signaling in rice. *The Plant Journal* **64**, 204-14.
- Singh A, Lim GH, Kachroo P, 2017. Transport of chemical signals in systemic acquired resistance. *Journal of integrative plant biology* **59**, 336-44.
- Snedden WA, Arazi T, Fromm H, Shelp BJ, 1995. Calcium/calmodulin activation of soybean glutamate decarboxylase. *Plant physiology* **108**, 543-9.
- Sohn KH, Lei R, Nemri A, Jones JD, 2007. The downy mildew effector proteins ATR1 and ATR13 promote disease susceptibility in Arabidopsis thaliana. *The Plant Cell* **19**, 4077-90.
- Sonah H, Deshmukh RK, Bélanger RR, 2016. Computational prediction of effector proteins in fungi: opportunities and challenges. *Frontiers in plant science* **7**, 126.

- Song J, Win J, Tian M, *et al.*, 2009. Apoplastic effectors secreted by two unrelated eukaryotic plant pathogens target the tomato defense protease Rcr3. *Proceedings of the National Academy of Sciences* **106**, 1654-9.
- Soriano M, 2017. Plasmids 101: Gateway Cloning. *Addgene's Blog*, jan
- Stergiopoulos I, Van Den Burg HA, Ökmen B, *et al.*, 2010. Tomato Cf resistance proteins mediate recognition of cognate homologous effectors from fungi pathogenic on dicots and monocots. *Proceedings of the National Academy of Sciences* **107**, 7610-5.
- Stevens FC, 1983. Calmodulin: an introduction. *Canadian journal of biochemistry and cell biology* **61**, 906-10.
- Su S, Liu Z, Chen C, *et al.*, 2010. Cucumber mosaic virus movement protein severs actin filaments to increase the plasmodesmal size exclusion limit in tobacco. *The Plant Cell* **22**, 1373-87.
- Suarez-Rodriguez MC, Adams-Phillips L, Liu Y, *et al.*, 2007. MEKK1 is required for flg22-induced MPK4 activation in Arabidopsis plants. *Plant physiology* **143**, 661-9.
- Tang Q, Guittard-Crilat E, Maldiney R, *et al.*, 2016. The mitogen-activated protein kinase phosphatase PHS1 regulates flowering in Arabidopsis thaliana. *Planta* **243**, 909-23.
- Taj G, Agarwal P, Grant M, Kumar A, 2010. MAPK machinery in plants: recognition and response to different stresses through multiple signal transduction pathways. *Plant signaling & behavior* **5**, 1370-8.
- Thines B, Katsir L, Melotto M, *et al.*, 2007. JAZ repressor proteins are targets of the SCF COII complex during jasmonate signalling. *Nature* **448**, 661-5.
- Thomas CL, Bayer EM, Ritzenthaler C, Fernandez-Calvino L, Maule AJ, 2008. Specific targeting of a plasmodesmal protein affecting cell-to-cell communication. *PLoS biol* **6**, e7.
- Thomma BP, Eggermont K, Penninckx IA, *et al.*, 1998. Separate jasmonate-dependent and salicylate-dependent defense-response pathways in Arabidopsis are essential for resistance to distinct microbial pathogens. *Proceedings of the National Academy of Sciences* **95**, 15107-11.
- Thomma BP, Van Esse HP, Crous PW, De Wit PJ, 2005. Cladosporium fulvum (syn. Passalora fulva), a highly specialized plant pathogen as a model for functional studies on plant pathogenic Mycosphaerellaceae. *Molecular plant pathology* **6**, 379-93.



- Tomczynska I, Stumpe M, Doan TG, Mauch F, 2020. A Phytophthora effector protein promotes symplastic cell-to-cell trafficking by physical interaction with plasmodesmata-localised callose synthases. *New Phytologist*, -.
- Torto-Alalibo T, Collmer CW, Lindeberg M, Bird D, Collmer A, Tyler BM, 2009. Common and contrasting themes in host cell-targeted effectors from bacterial, fungal, oomycete and nematode plant symbionts described using the Gene Ontology. *BMC microbiology* **9**, 1-8.
- Tovchigrechko A, Vakser IA, 2006. GRAMM-X public web server for protein-protein docking. *Nucleic acids research* **34**, W310-W4.
- Tuskan GA, Difazio S, Jansson S, *et al.*, 2006. The genome of black cottonwood, *Populus trichocarpa* (Torr. & Gray). *science* **313**, 1596-604.
- Tuzun S, Kuć J, 1985. Movement of a factor in tobacco infected with *Peronospora tabacina* Adam which systemically protects against blue mold. *Physiological Plant Pathology* **26**, 321-30.
- Ueki S, Citovsky V, 2014. Plasmodesmata-associated proteins: Can we see the whole elephant? *Plant signaling & behavior* **9**, e27899.
- Valent B, Khang CH, 2010. Recent advances in rice blast effector research. *Current opinion in plant biology* **13**, 434-41.
- Vallad GE, Goodman RM, 2004. Systemic acquired resistance and induced systemic resistance in conventional agriculture. *Crop science* **44**, 1920-34.
- Van Den Burg HA, Harrison SJ, Joosten MH, Vervoort J, De Wit PJ, 2006. *Cladosporium fulvum* Avr4 protects fungal cell walls against hydrolysis by plant chitinases accumulating during infection. *Molecular plant-microbe interactions* **19**, 1420-30.
- Van Der Hoorn RA, Kamoun S, 2008. From guard to decoy: a new model for perception of plant pathogen effectors. *The Plant Cell* **20**, 2009-17.
- Vatén A, Dettmer J, Wu S, *et al.*, 2011. Callose biosynthesis regulates symplastic trafficking during root development. *Developmental cell* **21**, 1144-55.
- Vialle A, Frey P, Hambleton S, Bernier L, Hamelin RC, 2011. Poplar rust systematics and refinement of *Melampsora* species delineation. *Fungal Diversity* **50**, 227.
- Wang C-IA, Gunčar G, Forwood JK, *et al.*, 2007. Crystal structures of flax rust avirulence proteins AvrL567-A and-D reveal details of the structural basis for flax disease resistance specificity. *The Plant Cell* **19**, 2898-912.

- Weiberg A, Wang M, Lin F-M, *et al.*, 2013. Fungal small RNAs suppress plant immunity by hijacking host RNA interference pathways. *Science* **342**, 118-23.
- Willmann R, Lajunen HM, Erbs G, *et al.*, 2011. Arabidopsis lysin-motif proteins LYM1 LYM3 CERK1 mediate bacterial peptidoglycan sensing and immunity to bacterial infection. *Proceedings of the National Academy of Sciences* **108**, 19824-9.
- Win J, Chaparro-Garcia A, Belhaj K, *et al.* Effector biology of plant-associated organisms: concepts and perspectives. *Proceedings of the Cold Spring Harbor symposia on quantitative biology, 2012*: Cold Spring Harbor Laboratory Press, 235-47.
- Wright KM, Roberts AG, Martens HJ, Sauer N, Oparka KJ, 2003. Structural and functional vein maturation in developing tobacco leaves in relation to AtSUC2 promoter activity. *Plant physiology* **131**, 1555-65.
- Wu S, Gallagher KL, 2011. Mobile protein signals in plant development. *Current opinion in plant biology* **14**, 563-70.
- Wu Y, Zhang D, Chu JY, *et al.*, 2012. The Arabidopsis NPR1 protein is a receptor for the plant defense hormone salicylic acid. *Cell reports* **1**, 639-47.
- Xian L, Yu G, Wei Y, *et al.*, 2020. A bacterial effector protein hijacks plant metabolism to support pathogen nutrition. *Cell host & microbe* **28**, 548-57. e7.
- Xiang T, Zong N, Zou Y, *et al.*, 2008. Pseudomonas syringae effector AvrPto blocks innate immunity by targeting receptor kinases. *Current biology* **18**, 74-80.
- Xie D-X, Feys BF, James S, Nieto-Rostro M, Turner JG, 1998. COI1: an Arabidopsis gene required for jasmonate-regulated defense and fertility. *Science* **280**, 1091-4.
- Xu X, Chi W, Sun X, *et al.*, 2016. Convergence of light and chloroplast signals for de-etiolation through ABI4-HY5 and COP1. *Nature plants* **2**, 1-7.
- Yan Y, Stolz S, Chételat A, *et al.*, 2007. A downstream mediator in the growth repression limb of the jasmonate pathway. *The Plant Cell* **19**, 2470-83.
- Yang J, Yan R, Roy A, Xu D, Poisson J, Zhang Y, 2015. The I-TASSER Suite: protein structure and function prediction. *Nature methods* **12**, 7.
- Yang T, Poovaiah B, 2002. Hydrogen peroxide homeostasis: activation of plant catalase by calcium/calmodulin. *Proceedings of the National Academy of Sciences* **99**, 4097-102.

- Yoo S-D, Cho Y-H, Tena G, Xiong Y, Sheen J, 2008. Dual control of nuclear EIN3 by bifurcate MAPK cascades in C<sub>2</sub>H<sub>4</sub> signalling. *Nature* **451**, 789-95.
- Zambryski P, Crawford K, 2000. Plasmodesmata: gatekeepers for cell-to-cell transport of developmental signals in plants. *Annual review of cell and developmental biology* **16**, 393-421.
- Zavaliev R, Epel BL, 2015. Imaging callose at plasmodesmata using aniline blue: quantitative confocal microscopy. In. *Plasmodesmata*. Springer, 105-19.
- Zavaliev R, Ueki S, Epel BL, Citovsky V, 2011. Biology of callose ( $\beta$ -1, 3-glucan) turnover at plasmodesmata. *Protoplasma* **248**, 117-30.
- Zhang W, Fraiture M, Kolb D, *et al.*, 2013. Arabidopsis receptor-like protein30 and receptor-like kinase suppressor of BIR1-1/EVERSHED mediate innate immunity to necrotrophic fungi. *The Plant Cell* **25**, 4227-41.
- Zhang Y, 2008. I-TASSER server for protein 3D structure prediction. *BMC bioinformatics* **9**, 40.
- Zhang Z, Wu Y, Gao M, *et al.*, 2012. Disruption of PAMP-induced MAP kinase cascade by a *Pseudomonas syringae* effector activates plant immunity mediated by the NB-LRR protein SUMM2. *Cell host & microbe* **11**, 253-63.
- Zhou J-M, Chai J, 2008. Plant pathogenic bacterial type III effectors subdue host responses. *Current opinion in microbiology* **11**, 179-85.
- Zipfel C, 2014. Plant pattern-recognition receptors. *Trends in immunology* **35**, 345-51.
- Zipfel C, Kunze G, Chinchilla D, *et al.*, 2006. Perception of the bacterial PAMP EF-Tu by the receptor EFR restricts *Agrobacterium*-mediated transformation. *Cell* **125**, 749-60.
- Zipfel C, Rathjen JP, 2008. Plant immunity: AvrPto targets the frontline. *Current biology* **18**, R218-R20.

## ANNEX A

### SUPPLEMENTARY TABLES AND FIGURES

**Supplementary Table: 1. List of Primers**

Name	Sequence
<b>pCambia 1380 (NOS) Seq. R</b>	GAT CTA GTA ACA TAG ATG ACA CC
<b>pCambia 35SP F</b>	TGAGACTTTTCAACAAAGGG
<b>72bp-Re.S.pCam-F</b>	CCACTGACGTAAGGGATGACG
Name	Primer (5'-3')
<b>NLS-347. F</b>	ATG CCA AAA AAG AAG AGA AAG G
<b>NLS-347. R</b>	CCA CTT CTT GGG TTT TGG TAC
<b>Attb1-NLS-347. F</b>	GGG GAC AAG TTT GTA CAA AAA AGC AGG CTT CAT GCC AAA AAA GAA GAG AAA GGT AG
<b>Attb2-NLS-347. R</b>	GGG GAC CAC TTT GTA CAA GAA AGC TGG GTC CCA CTT CTT GGG TTT TGG TAC TTG
<b>SALK_022227-LP</b>	CATGGAATCTGATTTCCATGC
<b>SALK_022227-RP</b>	CATGTTACACATCGGTTCTG
<b>pCambia-overlap-mCherry_F1</b>	CTATATAAGGAAGTTCATTTTCAATTTGGAGAGGACAGCCCAATGGTGAGCAAGGGCGAGGA
<b>pCambia-overlap-mCherry_R1</b>	GATGATGGCCATGTTATCCTCCTCGCCCTTGCTCACCATGCTTGTACAGCTCGTCCATGC
<b>2xmCherry-F</b>	GCA TGAAAGCTTATGGTGAGCAAGGGCGAGGAG

<b>2xmCherry-R</b>	GCA TGAGGATCCTTACTTGTACAGCTCGTCCATG
<b>Re.S.pCam-F</b> <b>Re.S.pCam-R</b>	CCAAGCTTCGACTCTAGAGGATC CTTGACAGCTCGTCCATGC
<b>pCam.ovlap-mCh-F</b> <b>pCam.ovlap-mCh-R</b>	GAAGTTCATTTTCATTTGGAGAGGACAGCCCAATGGTGAGCAAGGGCGAGG GCCATGTTATCCTCCTCGCCCTTGCTCACCATGCTTGTACAGCTCGTCCATGC
<b>Attb1-GAD1-F</b> <b>Attb2-GAD1-R</b>	GGG GAC AAG TTT GTA CAA AAA AGC AGG CTTC ATGGTGCTCTCCCACGCCGTATC GGG GAC CAC TTT GTA CAA GAA AGC TGG GTCGCAGATAACCACTCGTCTTCTTCC
<b>Attb1-347-F</b> <b>Attb2-347-R</b>	GGG GAC AAG TTT GTA CAA AAA AGC AGG CTTC ATGAAGATTCATCTATCATTGAAAG GGG GAC CAC TTT GTA CAA GAA AGC TGG GTCCCACTTCTTGGGTTTTGGTAC
<b>pGBKT7_OL_347-F</b> <b>pGBKT7_OL_347-R</b>	CAGAGGAGGACCTGCATATGGCCATGGAGGCCGAATTCCTATGGTAGAACCACTCCCAC TTATGCTAGTTATGCGGCCGCTGCAGGTGCACGGATCCCCCACTTCTTGGGTTTTGGTAC
<b>pGADT7_OL_bnding-1-F</b> <b>pGADT7_OL_bnding-1-R</b>	ATTACGCTCATATGGCCATGGAGGCCAGTGAATTCCACCCTATGAATATGATGTTGAACCTGGC TGCAGCTCGAGCTCGATGGATCCCGTATCGATGCCACCCAATAAGTTCCTCCAACCTCACGC
<b>pGADT7_OL_center-10-F</b> <b>pGADT7_OL_center-10-R</b>	ATTACGCTCATATGGCCATGGAGGCCAGTGAATTCCACCCTATGAACATGTTGTTGAATTTAGC TGCAGCTCGAGCTCGATGGATCCCGTATCGATGCCACCCCTAAAATGCGTTCTAAAATCTCAAG
<b>pGADT7_OL_GAD1-F</b> <b>pGADT7_OL_GAD1-R</b>	ATTACGCTCATATGGCCATGGAGGCCAGTGAATTCCACCCTATGGTGCTCTCCCACGCCG TGCAGCTCGAGCTCGATGGATCCCGTATCGATGCCACCCGCAGATAACCACTCGTCTTC
<b>pGADT7 overlap PtGAD-F:</b> <b>pGADT7 overlap PtGAD-R:</b>	ATTACGCTCATATGGCCATGGAGGCCAGTGAATTCCACCCTATGGTTCTCTCCAAGACAT TGCAGCTCGAGCTCGATGGATCCCGTATCGATGCCACCCCTAACACACACCATTTCATCT

**Supplementary Table 2. List of up-regulated and down regulated gene**

---

Up-regulated gene				
Initial Alias	Fold Change	P-value	Name	Description
AT1G53480	4.33866979	9.32E-20	MRD1	Mto 1 responding down 1 [Source:UniProtKB/TrEMBL;Acc:Q9LPG4]
AT1G72416	3.55546213	1.45E-07	AT1G72416	Chaperone DnaJ-domain superfamily protein [Source:UniProtKB/TrEMBL;Acc:B3H5X6]
AT4G27440	3.33595934	3.20E-19	PORB	Protochlorophyllide reductase B, chloroplastic [Source:UniProtKB/Swiss-Prot;Acc:P21218]
AT1G49230	3.29108142	2.83E-08	ATL78	RING-H2 finger protein ATL78 [Source:UniProtKB/Swiss-Prot;Acc:Q6NQG7]
AT1G56300	3.22108984	1.38E-06	AT1G56300	At1g56300 [Source:UniProtKB/TrEMBL;Acc:Q8L7R1]
AT4G34950	3.01791245	3.66E-12	AT4G34950	Major facilitator superfamily protein [Source:UniProtKB/TrEMBL;Acc:Q9SW40]
AT1G12030	2.98669847	7.36E-06	AT1G12030	At1g12030 [Source:UniProtKB/TrEMBL;Acc:O65376]

AT5G61290	2.94586299	2.44E-08	AT5G61290	Flavin-containing monooxygenase FMO GS-OX-like 8 [Source:UniProtKB/Swiss-Prot;Acc:Q9FLK4]
AT2G34510	2.92746854	4.86E-17	AT2G34510	Uncharacterized protein At2g34510 [Source:UniProtKB/TrEMBL;Acc:O64696]
AT2G18150	2.91640874	1.99E-06	PER15	Peroxidase 15 [Source:UniProtKB/Swiss-Prot;Acc:Q9SI16]
AT3G02885	2.9083609	3.75E-07	GASA5	Gibberellin-regulated protein 5 [Source:UniProtKB/Swiss-Prot;Acc:Q84J95]
AT5G62360	2.90683488	2.59E-06	AT5G62360	Plant invertase/pectin methylesterase inhibitor superfamily protein [Source:UniProtKB/TrEMBL;Acc:Q9LVA3]
AT1G76790	2.87745578	2.90E-08	IGMT5	Indole glucosinolate O-methyltransferase 5 [Source:UniProtKB/Swiss-Prot;Acc:Q9SRD4]
AT2G14230	2.84727891	0.000269906	None	None
AT5G24470	2.82105887	8.69E-05	APRR5	Two-component response regulator-like APRR5 [Source:UniProtKB/Swiss-Prot;Acc:Q6LA42]

AT5G62730	2.77426802	0.00010753	NPF4.7	Protein NRT1/ PTR FAMILY 4.7 [Source:UniProtKB/Swiss-Prot;Acc:Q9FM20]
AT4G30660	2.73903386	1.35E-06	AT4G30660	UPF0057 membrane protein At4g30660 [Source:UniProtKB/Swiss-Prot;Acc:Q9SUI0]
AT1G22570	2.73054075	1.45E-14	NPF5.15	Protein NRT1/ PTR FAMILY 5.15 [Source:UniProtKB/Swiss-Prot;Acc:Q9SK99]
AT1G13609	2.70561931	0.000582729	AT1G13609	Defensin-like protein 287 [Source:UniProtKB/Swiss-Prot;Acc:Q2V4N4]
AT5G51550	2.62900496	4.70E-17	EXL3	Protein EXORDIUM-like 3 [Source:UniProtKB/Swiss-Prot;Acc:Q9FHM9]
AT5G04150	2.60361833	0.000259825	BHLH101	basic helix-loop-helix (bHLH) DNA-binding superfamily protein [Source:TAIR;Acc:AT5G04150]
AT4G26670	2.58927171	2.22E-07	TIM22-2	Chloroplastic import inner membrane translocase subunit TIM22-2 [Source:UniProtKB/Swiss-Prot;Acc:Q94EH2]



AT2G47870	2.56453748	0.000301836	GRXC12	Putative glutaredoxin-C12 [Source:UniProtKB/Swiss-Prot;Acc:O82254]
AT2G21660	2.5608628	9.25E-06	RBG7	Glycine-rich RNA-binding protein 7 [Source:UniProtKB/Swiss-Prot;Acc:Q03250]
AT2G30210	2.53517516	0.000139373	LAC3	Laccase-3 [Source:UniProtKB/Swiss-Prot;Acc:Q56YT0]
AT5G38020	2.52125869	0.000121462	AT5G38020	At5g38020 [Source:UniProtKB/TrEMBL;Acc:Q84MB1]
AT4G03210	2.51916312	7.49E-13	XTH9	Xyloglucan endotransglucosylase/hydrolase (Fragment) [Source:UniProtKB/TrEMBL;Acc:C0SVH2]
AT1G47395	2.49820609	0.001241213	AT1G47395	At1g47390 [Source:UniProtKB/TrEMBL;Acc:Q8GUL3]
AT1G11600	2.48989933	7.06E-11	CYP77B1	Cytochrome P450 like protein [Source:UniProtKB/TrEMBL;Acc:Q9SAB7]
AT2G14245	2.46832113	0.001612216	None	None
AT4G09020	2.4655905	8.72E-10	ISA3	Isoamylase 3, chloroplastic [Source:UniProtKB/Swiss-Prot;Acc:Q9M0S5]

AT2G01520	2.46271703	0.000726475	MLP328	MLP-like protein 328 [Source:UniProtKB/Swiss-Prot;Acc:Q9ZVF3]
AT3G45970	2.42426187	5.99E-06	EXLA1	Expansin-like A1 [Source:UniProtKB/Swiss-Prot;Acc:Q9LZT4]
AT2G38380	2.41231909	3.57E-05	PER22	Peroxidase 22 [Source:UniProtKB/Swiss-Prot;Acc:P24102]
AT4G01130	2.37266441	2.07E-07	AT4G01130	GDSL esterase/lipase At4g01130 [Source:UniProtKB/Swiss-Prot;Acc:Q9M153]
AT2G21130	2.37062641	2.59E-05	CYP19-2	Peptidyl-prolyl cis-trans isomerase CYP19-2 [Source:UniProtKB/Swiss-Prot;Acc:Q9SKQ0]
AT1G31690	2.36834605	0.00014107	AT1G31690	Amine oxidase [Source:UniProtKB/TrEMBL;Acc:F4IAX0]
AT5G64860	2.36255947	7.56E-12	DPE1	4-alpha-glucanotransferase DPE1, chloroplastic/amyloplastic [Source:UniProtKB/Swiss-Prot;Acc:Q9LV91]
AT5G05250	2.35412743	0.000776809	AT5G05250	AT5g05250/K18I23_5 [Source:UniProtKB/TrEMBL;Acc:Q9FLC9]
AT5G08030	2.34191701	0.001079325	AT5G08030	PLC-like phosphodiesterases superfamily protein [Source:TAIR;Acc:AT5G08030]

AT1G47400	2.33727669	0.003454085	AT1G47400	unknown protein; BEST Arabidopsis thaliana protein match is: unknown protein (TAIR:AT1G47395.1); Ha. [Source:TAIR;Acc:AT1G47400]
AT1G20030	2.32944201	3.30E-05	AT1G20030	Pathogenesis-related thaumatin superfamily protein [Source:UniProtKB/TrEMBL;Acc:Q9LNT0]
AT3G22800	2.31852458	0.000681221	LRX6	Leucine-rich repeat extensin-like protein 6 [Source:UniProtKB/Swiss-Prot;Acc:Q9LUI1]
AT1G62262	2.29283893	0.003960262	SLAH4	S-type anion channel SLAH4 [Source:UniProtKB/Swiss-Prot;Acc:A8MRV9]
AT1G06100	2.28486266	0.001418675	AT1G06100	Delta-9 desaturase-like 2 protein [Source:UniProtKB/Swiss-Prot;Acc:Q9LND8]
AT5G23210	2.28031015	1.49E-13	SCPL34	Serine carboxypeptidase-like 34 [Source:UniProtKB/Swiss-Prot;Acc:Q0WPR4]
AT3G63160	2.26019175	1.38E-07	AT3G63160	OEP6 [Source:UniProtKB/TrEMBL;Acc:A0A384KZL8]

AT1G28230	2.25734435	0.000569211	PUP1	Purine permease 1 [Source:UniProtKB/Swiss-Prot;Acc:Q9FZ96]
AT4G16563	2.25217007	2.38E-06	AT4G16563	Probable aspartyl protease At4g16563 [Source:UniProtKB/Swiss-Prot;Acc:Q940R4]
AT2G34700	2.25215419	0.003686267	AT2G34700	Pollen Ole e 1 allergen and extensin family protein [Source:UniProtKB/TrEMBL;Acc:O64586]
AT3G53460	2.25144864	9.04E-13	CP29	Chloroplast RNA-binding protein 29 [Source:UniProtKB/TrEMBL;Acc:F4JAF3]
AT5G49525	2.24643786	0.002066782	AT5G49525	At5g49525 [Source:UniProtKB/TrEMBL;Acc:Q8L7F0]
AT2G14247	2.23955357	0.00553205	AT2G14247	Expressed protein [Source:UniProtKB/TrEMBL;Acc:Q8GWC0]
AT4G29610	2.23679669	0.000609663	CDA6	Cytidine deaminase 6 [Source:UniProtKB/Swiss-Prot;Acc:Q9SU86]
AT2G39900	2.20929072	3.01E-08	WLIN2A	WLIM2a [Source:UniProtKB/TrEMBL;Acc:A0A178VU35]
AT5G45750	2.20586821	2.52E-13	RABA1C	RABA1c [Source:UniProtKB/TrEMBL;Acc:A0A178UDB2]

AT3G18900	2.20216276	1.32E-06	AT3G18900	Ternary complex factor MIP1 leucine-zipper protein [Source:UniProtKB/TrEMBL;Acc:A0A1I9LMH3]
AT3G45070	2.19342961	0.003602024	AT3G45070	Sulfotransferase [Source:UniProtKB/TrEMBL;Acc:A0A1I9LRV5]
AT2G38390	2.18582288	0.000515462	PER23	Peroxidase 23 [Source:UniProtKB/Swiss-Prot;Acc:O80912]
AT3G23870	2.18544245	2.68E-05	AT3G23870	Probable magnesium transporter NIPA1 [Source:UniProtKB/Swiss-Prot;Acc:Q9LIR9]
AT5G38030	2.16674855	0.000813957	DTX30	Protein DETOXIFICATION 30 [Source:UniProtKB/Swiss-Prot;Acc:Q9LS19]
AT1G22370	2.16576078	7.23E-07	UGT85A5	UDP-glycosyltransferase 85A5 [Source:UniProtKB/Swiss-Prot;Acc:Q9LMF0]
AT3G46970	2.15121317	1.24E-05	PHS2	Alpha-glucan phosphorylase 2, cytosolic [Source:UniProtKB/Swiss-Prot;Acc:Q9SD76]
AT4G04330	2.14903855	0.002234617	RBCX1	Chaperonin-like RBCX protein 1, chloroplastic [Source:UniProtKB/Swiss-Prot;Acc:Q94AU9]

AT5G13170	2.14896201	0.006541172	SWEET15	Bidirectional sugar transporter SWEET15 [Source:UniProtKB/Swiss-Prot;Acc:Q9FY94]
AT3G29320	2.14124926	5.45E-09	PHS1	Alpha-glucan phosphorylase 1 [Source:UniProtKB/Swiss-Prot;Acc:Q9LIB2]
AT5G24770	2.1159172	0.000150451	VSP2	Vegetative storage protein 2 [Source:UniProtKB/Swiss-Prot;Acc:O82122]
AT4G14060	2.11300712	0.007794694	AT4G14060	AT4g14060/dl3070w [Source:UniProtKB/TrEMBL;Acc:O23267]
AT3G12700	2.10894259	7.61E-08	NANA	Aspartic proteinase NANA, chloroplast [Source:UniProtKB/Swiss-Prot;Acc:Q9LTW4]
AT4G10695	2.10748014	0.006638724	AT4G10695	CDC68-like protein [Source:UniProtKB/TrEMBL;Acc:Q3EA58]
AT2G31360	2.10180509	3.06E-08	ADS2	Delta-9 acyl-lipid desaturase 2 [Source:UniProtKB/Swiss-Prot;Acc:Q9SID2]

AT5G17700	2.08863313	0.00224124	DTX25	Protein DETOXIFICATION [Source:UniProtKB/TrEMBL;Acc:A0A178UJQ3]
AT5G62210	2.08219118	0.00074632	AT5G62210	Embryo-specific protein 3, (ATS3) [Source:UniProtKB/TrEMBL;Acc:Q9LVB5]
AT1G69880	2.07488505	0.008133009	TRX8	Thioredoxin H8 [Source:UniProtKB/Swiss-Prot;Acc:Q9CAS1]
AT5G46600	2.06863709	0.000553259	ALMT13	Aluminum-activated malate transporter 13 [Source:UniProtKB/Swiss-Prot;Acc:Q9LS23]
AT5G55340	2.05990256	0.001669494	AT5	Probable long-chain-alcohol O-fatty-acyltransferase 5 [Source:UniProtKB/Swiss-Prot;Acc:Q9FJ76]
AT3G11415	2.05654234	0.004609403	AT3G11415	None
AT5G42800	2.05262884	0.008288956	DFRA	Dihydroflavonol reductase [Source:UniProtKB/TrEMBL;Acc:B1GV15]
AT3G02480	2.03300048	0.010378758	AT3G02480	AT3g02480/F16B3_11 [Source:UniProtKB/TrEMBL;Acc:Q9M892]

AT4G17920	2.03152542	0.013121577	ATL29	RING-H2 finger protein ATL29 [Source:UniProtKB/Swiss-Prot;Acc:O49691]
AT1G13130	2.02412615	0.010400032	AT1G13130	At1g13130 [Source:UniProtKB/TrEMBL;Acc:Q66GP7]
AT2G41240	2.01256417	0.014462172	BHLH100	BHLH100 [Source:UniProtKB/TrEMBL;Acc:A0A384LFW4]
AT5G62350	2.01171319	5.43E-11	AT5G62350	Plant invertase/pectin methylesterase inhibitor superfamily protein [Source:UniProtKB/TrEMBL;Acc:Q9LVA4]
AT4G30650	2.00144368	0.003049274	AT4G30650	UPF0057 membrane protein At4g30650 [Source:UniProtKB/Swiss-Prot;Acc:Q9M095]

Down-regulated gene

Initial Alias	Fold Change	P-value	Name	Description
AT1G61550	-5.10880695	4.57E-18	AT1G61550	G-type lectin S-receptor-like serine/threonine-protein kinase At1g61550 [Source:UniProtKB/Swiss-Prot;Acc:Q9SY95]



AT5G07010	-4.60172873	1.64E-15	SOT15	Sulfotransferase [Source:UniProtKB/TrEMBL;Acc:A0A178UG65]
AT1G69490	-4.45858245	1.83E-23	NAC029	NAP [Source:UniProtKB/TrEMBL;Acc:A0A178W8K0]
AT1G77760	-4.45533948	8.27E-27	NIA1	Nitrate reductase [Source:UniProtKB/TrEMBL;Acc:A0A178WBR8]
AT2G46970	-4.26003539	6.88E-14	PIL1	Transcription factor PIL1 [Source:UniProtKB/Swiss-Prot;Acc:Q8L5W8]
AT4G31380	-4.00265979	1.99E-09	FLP1	Flowering-promoting factor 1-like protein 1 [Source:UniProtKB/Swiss-Prot;Acc:Q5Q0B3]
AT5G50335	-3.94684846	5.66E-16	AT5G50335	At5g50335 [Source:UniProtKB/TrEMBL;Acc:Q8LEB7]
AT3G49160	-3.94562642	9.64E-26	PKP4	Plastidial pyruvate kinase 4, chloroplastic [Source:UniProtKB/Swiss-Prot;Acc:Q9M3B6]
AT1G37130	-3.84532013	3.06E-21	NIA2	Nitrate reductase [NADH] 2 [Source:UniProtKB/Swiss-Prot;Acc:P11035]

AT3G54510	-3.61607391	2.35E-10	AT3G54510	Hyperosmolality-gated Ca <sup>2+</sup> permeable channel 2.5 [Source:UniProtKB/TrEMBL;Acc:A0A097NUQ7]
AT3G09450	-3.56474605	8.73E-07	AT3G09450	F3L24.34 protein [Source:UniProtKB/TrEMBL;Acc:Q9S710]
AT3G17609	-3.54412836	1.77E-09	HYH	HYH [Source:UniProtKB/TrEMBL;Acc:A0A178VIU6]
AT2G28190	-3.53195723	4.69E-22	CSD2	Superoxide dismutase [Cu-Zn] 2, chloroplastic [Source:UniProtKB/Swiss-Prot;Acc:O78310]
AT1G75450	-3.4983461	5.72E-17	CKX5	Cytokinin dehydrogenase 5 [Source:UniProtKB/Swiss-Prot;Acc:Q67YU0]
ATCG00770	-3.49003796	7.67E-07	RPS8	30S ribosomal protein S8, chloroplastic [Source:UniProtKB/Swiss-Prot;Acc:P56801]
AT1G14540	-3.459773	1.47E-09	PER4	Peroxidase [Source:UniProtKB/TrEMBL;Acc:A0A178WND9]
AT1G52830	-3.4312261	2.71E-09	IAA6	SHY1 [Source:UniProtKB/TrEMBL;Acc:A0A384LEJ2]
AT1G01060	-3.40336552	1.23E-07	LHY	LHY1 [Source:UniProtKB/TrEMBL;Acc:A0A178W761]

AT5G53980	-3.35957747	6.19E-08	ATHB-52	Homeobox-leucine zipper protein ATHB-52 [Source:UniProtKB/Swiss-Prot;Acc:Q9FN29]
AT1G55960	-3.34946129	7.97E-17	AT1G55960	Polyketide cyclase/dehydrase and lipid transport superfamily protein [Source:UniProtKB/TrEMBL;Acc:Q93YV2]
AT1G52565	-3.34251487	2.63E-11	AT1G52565	At1g52565 [Source:UniProtKB/TrEMBL;Acc:A0JPU2]
AT2G28056	-3.34098571	3.81E-09	MIR172A	MIR172/MIR172A; miRNA [Source:TAIR;Acc:AT2G28056]
ATCG00760	-3.3317866	6.39E-06	RPL36	50S ribosomal protein L36, chloroplastic [Source:UniProtKB/TrEMBL;Acc:A0A1B1W4X9]
AT2G47270	-3.31313202	5.29E-07	UPB1	UPB1 [Source:UniProtKB/TrEMBL;Acc:A0A178VV95]
AT4G15550	-3.29403548	2.39E-12	UGT75D1	UDP-glycosyltransferase 75D1 [Source:UniProtKB/Swiss- Prot;Acc:O23406]
ATCG00750	-3.25493638	6.67E-06	RPS11	30S ribosomal protein S11, chloroplastic [Source:UniProtKB/TrEMBL;Acc:A0A1B1W4X8]
AT2G21910	-3.25059589	1.40E-05	CYP96A5	Cytochrome P450, family 96, subfamily A, polypeptide 5 [Source:UniProtKB/TrEMBL;Acc:Q9SJ08]

AT5G54470	-3.19349774	1.28E-07	AT5G54470	BBX29 [Source:UniProtKB/TrEMBL;Acc:A0A178UJV0]
AT5G01540	-3.1909726	1.43E-07	LECRK62	L-type lectin-domain containing receptor kinase VI.2 [Source:UniProtKB/Swiss-Prot;Acc:Q9M021]
AT5G24110	-3.18360444	2.49E-10	WRKY30	Probable WRKY transcription factor 30 [Source:UniProtKB/Swiss-Prot;Acc:Q9FL62]
AT5G25260	-3.17918713	1.65E-07	FLOT2	Flotillin-like protein 2 [Source:UniProtKB/Swiss-Prot;Acc:Q4V3D6]
AT5G01600	-3.14371931	3.64E-12	FER1	Ferritin-1, chloroplastic [Source:UniProtKB/Swiss-Prot;Acc:Q39101]
AT2G40610	-3.13170838	4.72E-12	EXPA8	Expansin-A8 [Source:UniProtKB/Swiss-Prot;Acc:O22874]
AT5G02540	-3.12556569	4.18E-08	AT5G02540	NAD(P)-binding Rossmann-fold superfamily protein [Source:UniProtKB/TrEMBL;Acc:F4KCF2]
AT5G02020	-3.12501642	9.68E-07	SIS	AT5g02020/T7H20_70 [Source:UniProtKB/TrEMBL;Acc:Q9LZM9]
AT2G15020	-3.09029228	4.21E-05	AT2G15020	At2g15020 [Source:UniProtKB/TrEMBL;Acc:Q9ZUK9]

AT3G09600	-3.07652366	1.47E-09	RVE8	Protein REVEILLE 8 [Source:UniProtKB/Swiss-Prot;Acc:Q8RWU3]
AT3G10815	-3.04888789	5.68E-06	AT3G10815	Putative RING zinc finger protein [Source:UniProtKB/TrEMBL;Acc:Q8L729]
AT1G64660	-3.0123163	1.14E-06	MGL	Methionine gamma-lyase [Source:UniProtKB/Swiss-Prot;Acc:Q9SGU9]
AT1G56060	-3.01203328	6.39E-06	AT1G56060	unknown protein; BEST Arabidopsis thaliana protein match is: unknown protein (TAIR:AT2G32210.1); Ha. [Source:TAIR;Acc:AT1G56060]
AT2G24165	-3.00328874	5.12E-05	None	None
AT1G57640	-2.9571278	1.57E-05	None	None
AT1G57650	-2.95657421	1.54E-05	AT1G57650	ATP binding protein [Source:UniProtKB/TrEMBL;Acc:F4I847]
AT5G16023	-2.95301071	5.18E-05	RTFL18	DVL1 [Source:UniProtKB/TrEMBL;Acc:Q6X5V0]
AT1G68238	-2.94882412	2.51E-06	AT1G68238	Putative uncharacterized protein [Source:UniProtKB/TrEMBL;Acc:Q1G3X3]

AT3G21150	-2.94581094	5.57E-05	BBX32	B-box zinc finger protein 32 [Source:UniProtKB/Swiss-Prot;Acc:Q9LJB7]
AT5G24580	-2.93558353	7.59E-11	HIPP09	Heavy metal-associated isoprenylated plant protein 9 [Source:UniProtKB/Swiss-Prot;Acc:Q9FLU5]
AT1G03010	-2.93457373	4.82E-07	AT1G03010	BTB/POZ domain-containing protein At1g03010 [Source:UniProtKB/Swiss-Prot;Acc:Q9SA69]
AT5G35525	-2.93206005	2.67E-07	PCR3	Protein PLANT CADMIUM RESISTANCE 3 [Source:UniProtKB/Swiss-Prot;Acc:P0CW97]
AT5G37260	-2.93096439	3.18E-09	RVE2	Protein REVEILLE 2 [Source:UniProtKB/Swiss-Prot;Acc:F4K5X6]
AT5G53200	-2.93046741	1.95E-05	TRY	TRY [Source:UniProtKB/TrEMBL;Acc:A0A178UFU9]
AT1G26790	-2.92903107	0.000169229	AT1G26790	Dof-type zinc finger DNA-binding family protein [Source:TAIR;Acc:AT1G26790]
AT5G02580	-2.92865436	7.39E-06	AT5G02580	Argininosuccinate lyase [Source:UniProtKB/TrEMBL;Acc:Q84TG0]

ATCG00810	-2.92607887	7.84E-05	RPL22	50S ribosomal protein L22, chloroplastic [Source:UniProtKB/Swiss-Prot;Acc:P56795]
AT3G15310	-2.9127224	0.000175337	None	None
AT3G21320	-2.88767174	2.18E-05	AT3G21320	EARLY FLOWERING protein [Source:UniProtKB/TrEMBL;Acc:Q5Q0C8]
AT5G22520	-2.87235686	1.31E-05	AT5G22520	At5g22520 [Source:UniProtKB/TrEMBL;Acc:Q9FK87]
AT4G16780	-2.87225955	2.29E-10	HAT4	Homeobox-leucine zipper protein HAT4 [Source:UniProtKB/Swiss-Prot;Acc:Q05466]
AT3G55150	-2.86900705	5.73E-07	ATEXO70H1	Exocyst complex component EXO70H1 [Source:UniProtKB/Swiss-Prot;Acc:Q8VY27]
AT3G62090	-2.86458499	2.65E-10	PIF6	PIL2 [Source:UniProtKB/TrEMBL;Acc:A0A178VFI3]
AT5G01595	-2.86355516	7.57E-05	AT5G01595	other RNA [Source:TAIR;Acc:AT5G01595]
AT3G59220	-2.85492603	2.82E-05	PRN1	Pirin-1 [Source:UniProtKB/Swiss-Prot;Acc:Q9LX49]

AT4G26120	-2.85202591	1.65E-11	AT4G26120	Ankyrin repeat family protein / BTB/POZ domain-containing protein [Source:TAIR;Acc:AT4G26120]
AT4G12520	-2.84901335	7.74E-05	AT4G12520	At4g12520 [Source:UniProtKB/TrEMBL;Acc:Q9S7U3]
AT3G60420	-2.84647987	6.18E-06	AT3G60420	Phosphoglycerate mutase family protein [Source:UniProtKB/TrEMBL;Acc:F4JBT8]
AT1G01520	-2.82133457	0.000216315	AT1G01520	ASG4 [Source:UniProtKB/TrEMBL;Acc:A0A384LJW3]
AT3G15540	-2.81981592	2.52E-09	IAA19	Auxin-responsive protein [Source:UniProtKB/TrEMBL;Acc:Q2VWA2]
AT1G64500	-2.81739937	5.82E-07	AT1G64500	F1N19.7 [Source:UniProtKB/TrEMBL;Acc:Q9SGW5]
AT1G65870	-2.80353633	0.0002315	DIR21	Dirigent protein 21 [Source:UniProtKB/Swiss-Prot;Acc:Q9SS03]
AT5G41730	-2.79838718	0.000330101	AT5G41730	Protein kinase family protein [Source:UniProtKB/TrEMBL;Acc:Q9FGG5]
AT5G19600	-2.79791574	1.28E-05	SULTR3;5	Probable sulfate transporter 3.5 [Source:UniProtKB/Swiss-Prot;Acc:Q94LW6]



AT1G33960	-2.78932346	0.000139795	AIG1	P-loop containing nucleoside triphosphate hydrolases superfamily protein [Source:TAIR;Acc:AT1G33960]
AT3G11340	-2.78874967	0.000126528	UGT76B1	UDP-glycosyltransferase 76B1 [Source:UniProtKB/Swiss-Prot;Acc:Q9C768]
ATCG00290	-2.77822214	0.000352683	TRNS.2	tRNA-Ser [Source:TAIR;Acc:ATCG00290]
AT1G16420	-2.76386703	0.000116941	AMC8	Metacaspase-8 [Source:UniProtKB/Swiss-Prot;Acc:Q9SA41]
ATCG00740	-2.76051757	0.000187118	RPOA	DNA-directed RNA polymerase subunit alpha [Source:UniProtKB/Swiss-Prot;Acc:P56762]
AT5G44255	-2.74877543	0.000154127	None	None
AT1G44830	-2.74205178	2.51E-05	ERF014	Ethylene-responsive transcription factor ERF014 [Source:UniProtKB/Swiss-Prot;Acc:Q9LPE8]
AT2G35980	-2.74178003	5.09E-05	NHL10	NDR1/HIN1-like protein 10 [Source:UniProtKB/Swiss-Prot;Acc:Q9SJ52]
AT5G65080	-2.74004773	3.79E-09	MAF5	K-box region and MADS-box transcription factor family protein [Source:TAIR;Acc:AT5G65080]

AT1G01680	-2.73866643	0.000191084	PUB54	U-box domain-containing protein 54 [Source:UniProtKB/Swiss-Prot;Acc:Q9LQ92]
AT1G53625	-2.73408793	0.000101231	AT1G53625	At1g53625 [Source:UniProtKB/TrEMBL;Acc:Q9LPH9]
AT2G26020	-2.72862163	0.000520884	PDF1.2B	PDF1.2b [Source:UniProtKB/TrEMBL;Acc:A0A178VQC3]
AT1G68620	-2.71745803	1.78E-08	CXE6	Probable carboxylesterase 6 [Source:UniProtKB/Swiss-Prot;Acc:Q9SX25]
AT5G61160	-2.71373224	9.70E-05	ACT	Agmatine coumaroyltransferase [Source:UniProtKB/Swiss-Prot;Acc:Q9FNP9]
AT1G02340	-2.71211399	2.80E-05	HFR1	Transcription factor HFR1 [Source:UniProtKB/Swiss-Prot;Acc:Q9FE22]
AT2G04450	-2.7007366	6.52E-07	NUDT6	Nudix hydrolase 6 [Source:UniProtKB/Swiss-Prot;Acc:Q9SJC4]
AT5G56960	-2.68610947	0.000116624	AT5G56960	basic helix-loop-helix (bHLH) DNA-binding family protein [Source:TAIR;Acc:AT5G56960]

AT1G02400	-2.68464895	1.17E-09	GA2OX6	Gibberellin 2-beta-dioxygenase 6 [Source:UniProtKB/Swiss-Prot;Acc:Q9FZ21]
AT1G48320	-2.66950415	2.75E-05	DHNAT1	DHNAT1 [Source:UniProtKB/TrEMBL;Acc:A0A178WIC5]
AT1G69572	-2.66825412	0.000723276	AT1G69572	other RNA [Source:TAIR;Acc:AT1G69572]
AT3G54770	-2.65100307	2.75E-05	ARP1	Probable RNA-binding protein ARP1 [Source:UniProtKB/Swiss-Prot;Acc:Q9M1S3]
ATCG01300	-2.64893394	2.96E-05	RPL23-A	50S ribosomal protein L23, chloroplastic [Source:UniProtKB/Swiss-Prot;Acc:P61845]
ATCG00840	-2.64860139	2.96E-05	RPL23-A	50S ribosomal protein L23, chloroplastic [Source:UniProtKB/Swiss-Prot;Acc:P61845]
AT1G13550	-2.6458285	0.000274688	AT1G13550	Putative uncharacterized protein [Source:UniProtKB/TrEMBL;Acc:Q3EDD3]
AT5G56544	-2.64456988	0.000733607	None	None
AT1G66725	-2.63790933	3.56E-05	MIR163	MIR163; miRNA [Source:TAIR;Acc:AT1G66725]

AT5G24120	-2.63507477	5.53E-08	SIGE	RNA polymerase sigma factor sigE, chloroplastic/mitochondrial [Source:UniProtKB/Swiss-Prot;Acc:Q9ZNX9]
AT1G04310	-2.63493072	6.23E-09	ERS2	Ethylene response sensor 2 [Source:UniProtKB/Swiss- Prot;Acc:P93825]
AT1G12520	-2.6339652	1.83E-34	CCS	Copper chaperone for superoxide dismutase, chloroplastic/cytosolic [Source:UniProtKB/Swiss- Prot;Acc:Q9LD47]
AT3G61390	-2.63133889	0.000779672	PUB36	U-box domain-containing protein 36 [Source:UniProtKB/Swiss- Prot;Acc:Q8GZ84]
AT5G42380	-2.63032016	0.00020361	CML37	Calcium-binding protein CML37 [Source:UniProtKB/Swiss- Prot;Acc:Q9FIH9]
ATCG00330	-2.62775476	4.53E-05	RPS14	30S ribosomal protein S14, chloroplastic [Source:UniProtKB/TrEMBL;Acc:A0A1B1W4T5]
ATCG01120	-2.62502323	0.000861805	RPS15	30S ribosomal protein S15, chloroplastic [Source:UniProtKB/Swiss-Prot;Acc:P56805]

AT1G75590	-2.61606347	5.53E-06	AT1G75590	SAUR-like auxin-responsive protein family [Source:UniProtKB/TrEMBL;Acc:F4HZ54]
ATCG00340	-2.61604027	9.50E-05	PSAB	Photosystem I P700 chlorophyll a apoprotein A2 [Source:UniProtKB/TrEMBL;Acc:A0A1B1W4U2]
AT5G22530	-2.61033363	0.000508169	AT5G22530	Uncharacterized protein At5g22530 [Source:UniProtKB/TrEMBL;Acc:Q9FK86]
AT3G14780	-2.5986099	1.47E-06	AT3G14780	Callose synthase [Source:UniProtKB/TrEMBL;Acc:Q8GW77]
AT1G21120	-2.59477707	7.39E-06	AT1G21120	O-methyltransferase family protein [Source:TAIR;Acc:AT1G21120]
AT3G21520	-2.5918463	0.000397896	DMP1	Protein DMP1 [Source:UniProtKB/Swiss-Prot;Acc:Q9LVF4]
AT5G38200	-2.58998636	9.36E-07	AT5G38200	Class I glutamine amidotransferase-like superfamily protein [Source:UniProtKB/TrEMBL;Acc:F4KA45]
AT4G12510	-2.58982118	0.000560158	AT4G12510	At4g12520 [Source:UniProtKB/TrEMBL;Acc:Q9S7U3]
AT4G03450	-2.56750404	0.000613326	AT4G03450	Ankyrin repeat family protein [Source:UniProtKB/TrEMBL;Acc:Q9ZT73]

AT3G13438	-2.56430806	0.0010538	None	None
AT1G05880	-2.56270397	0.001150901	ARI12	Probable E3 ubiquitin-protein ligase ARI12 [Source:UniProtKB/Swiss-Prot;Acc:Q84RQ9]
AT1G72070	-2.55965707	3.13E-05	AT1G72070	Chaperone DnaJ-domain superfamily protein [Source:UniProtKB/TrEMBL;Acc:F4IBN6]
AT3G25510	-2.55332494	1.37E-06	AT3G25510	Disease resistance protein (TIR-NBS-LRR class) family protein [Source:UniProtKB/TrEMBL;Acc:F4J910]
AT3G02670	-2.5518899	0.000566831	AT3G02670	F16B3.30 protein [Source:UniProtKB/TrEMBL;Acc:Q9M875]
AT5G13320	-2.55064066	0.000458671	PBS3	Auxin-responsive GH3 family protein [Source:TAIR;Acc:AT5G13320]
AT1G80130	-2.54435448	0.000480917	AT1G80130	F18B13.21 protein [Source:UniProtKB/TrEMBL;Acc:Q9SSC6]
AT1G08830	-2.54352593	2.29E-10	CSD1	Superoxide dismutase [Cu-Zn] 1 [Source:UniProtKB/Swiss-Prot;Acc:P24704]
AT3G23800	-2.53822352	0.000207552	SBP3	SBP3 [Source:UniProtKB/TrEMBL;Acc:A0A178VEQ9]

AT5G26920	-2.53709235	1.10E-07	CBP60G	Calmodulin-binding protein 60 G [Source:UniProtKB/Swiss-Prot;Acc:F4K2R6]
AT5G38212	-2.53309468	0.001262187	AT5G38212	Potential natural antisense gene, locus overlaps with AT5G38210 [Source:TAIR;Acc:AT5G38212]
AT4G23210	-2.53288205	1.45E-07	CRK13	Cysteine-rich receptor-like protein kinase 13 [Source:UniProtKB/Swiss-Prot;Acc:Q0PW40]
AT4G37553	-2.53059095	0.001133897	AT4G37553	Potential natural antisense gene, locus overlaps with AT4G37550 and AT4G37560 [Source:TAIR;Acc:AT4G37553]
AT1G23060	-2.52192225	6.60E-06	AT1G23060	MDP40 [Source:UniProtKB/TrEMBL;Acc:A0A384LAT5]
AT1G78290	-2.52166155	3.46E-07	SRK2C	SRK2C [Source:UniProtKB/TrEMBL;Acc:A0A178W6S8]
ATCG00350	-2.52090501	0.000244497	PSAA	Photosystem I P700 chlorophyll a apoprotein A1 [Source:UniProtKB/Swiss-Prot;Acc:P56766]
AT5G39660	-2.51989714	4.04E-10	CDF2	Cyclic dof factor 2 [Source:UniProtKB/Swiss-Prot;Acc:Q93ZL5]

AT2G39518	-2.51424033	3.64E-05	AT2G39518	CASP-like protein 4D2 [Source:UniProtKB/Swiss-Prot;Acc:Q56X75]
AT3G24518	-2.51237769	0.000786655	AT3G24518	other RNA [Source:TAIR;Acc:AT3G24518]
AT3G53150	-2.50646954	0.000919831	UGT73D1	UDP-glucosyl transferase 73D1 [Source:TAIR;Acc:AT3G53150]
AT1G57630	-2.49724637	0.000783384	AT1G57630	Disease resistance protein RPP1-WsB, putative [Source:UniProtKB/TrEMBL;Acc:Q9FVT9]
AT1G75490	-2.49247252	8.04E-05	DREB2D	Dehydration-responsive element-binding protein 2D [Source:UniProtKB/Swiss-Prot;Acc:Q9LQZ2]
AT2G46830	-2.48804354	3.57E-05	CCA1	Protein CCA1 [Source:UniProtKB/Swiss-Prot;Acc:P92973]
AT5G54585	-2.48043831	1.17E-06	AT5G54585	Uncharacterized protein At5g54585 [Source:UniProtKB/TrEMBL;Acc:Q8VZU6]
AT1G69570	-2.46178952	4.19E-09	CDF5	Cyclic dof factor 5 [Source:UniProtKB/Swiss-Prot;Acc:Q9SEZ3]



AT4G25070	-2.45715498	1.67E-05	AT4G25070	Caldesmon-like protein [Source:UniProtKB/TrEMBL;Acc:A0MFT2]
AT5G54610	-2.4554414	0.00193698	BAD1	Ankyrin repeat-containing protein BDA1 [Source:UniProtKB/Swiss-Prot;Acc:Q8GYH5]
AT4G04540	-2.45228323	0.001008187	CRK39	Putative cysteine-rich receptor-like protein kinase 39 [Source:UniProtKB/Swiss-Prot;Acc:Q9SYS7]
AT5G01542	-2.45143419	0.002050571	AT5G01542	Potential natural antisense gene, locus overlaps with AT5G01540 [Source:TAIR;Acc:AT5G01542]
AT3G46650	-2.4480778	0.000399355	AT3G46650	UDP-Glycosyltransferase superfamily protein [Source:UniProtKB/TrEMBL;Acc:F4J962]
ATCG00820	-2.44322152	0.000319541	RPS19	ribosomal protein S19 [Source:TAIR;Acc:ATCG00820]
AT5G53048	-2.44271651	0.001746331	AT5G53048	other RNA [Source:TAIR;Acc:AT5G53048]
AT5G15845	-2.44074257	0.001906673	AT5G15845	other RNA [Source:TAIR;Acc:AT5G15845]
AT3G12910	-2.43263142	0.000749971	AT3G12910	NAC (No Apical Meristem) domain transcriptional regulator superfamily protein [Source:UniProtKB/TrEMBL;Acc:Q9LSI4]

AT4G38545	-2.43184264	0.000308932	AT4G38545	other RNA [Source:TAIR;Acc:AT4G38545]
AT1G23965	-2.43170181	0.000515462	AT1G23965	Transcription factor [Source:UniProtKB/TrEMBL;Acc:Q1G3U2]
AT3G08885	-2.42995273	3.33E-05	None	None
AT5G36220	-2.42664	1.62E-07	CYP81D1	Cytochrome P450 81D1 [Source:UniProtKB/Swiss-Prot;Acc:Q9FG65]
AT3G28857	-2.42652011	5.05E-05	PRE5	Transcription factor PRE5 [Source:UniProtKB/Swiss-Prot;Acc:Q9LJX1]
AT2G39530	-2.42614952	0.002010435	AT2G39530	CASP-like protein 4D1 [Source:UniProtKB/Swiss-Prot;Acc:Q8GWD5]
AT4G10310	-2.42567097	1.59E-08	HKT1	Sodium transporter HKT1 [Source:UniProtKB/Swiss-Prot;Acc:Q84TI7]
AT3G21670	-2.42203135	0.000130597	NPF6.4	Protein NRT1/ PTR FAMILY 6.4 [Source:UniProtKB/Swiss-Prot;Acc:Q9LVE0]

AT2G41250	-2.42056176	5.21E-10	AT2G41250	Haloacid dehalogenase-like hydrolase (HAD) superfamily protein [Source:UniProtKB/TrEMBL;Acc:Q9ZVB6]
AT2G34940	-2.41906023	0.000354317	VSR5	VSR5 [Source:UniProtKB/TrEMBL;Acc:A0A384KPH5]
ATCG01110	-2.41070161	0.002336603	NDHH	NAD(P)H-quinone oxidoreductase subunit H, chloroplastic [Source:UniProtKB/Swiss-Prot;Acc:P56753]
AT1G24145	-2.40991645	9.81E-05	AT1G24145	At1g24145 [Source:UniProtKB/TrEMBL;Acc:Q8GYP2]
AT1G10340	-2.40946059	2.00E-09	AT1G10340	Ankyrin repeat family protein [Source:UniProtKB/TrEMBL;Acc:Q9SY76]
AT5G04190	-2.40828618	7.10E-06	PKS4	Protein PHYTOCHROME KINASE SUBSTRATE 4 [Source:UniProtKB/Swiss-Prot;Acc:Q9FYE2]
AT5G08760	-2.39566957	0.000142702	AT5G08760	unknown protein; FUNCTIONS IN: molecular_function unknown; INVOLVED IN: biological_process unknown; LOCATED IN: endomembrane system; Ha. [Source:TAIR;Acc:AT5G08760]

AT4G10150	-2.39252677	6.73E-06	ATL7	RING-H2 finger protein ATL7 [Source:UniProtKB/Swiss-Prot;Acc:Q9SN28]
AT3G29370	-2.39100783	0.000155838	AT3G29370	Uncharacterized protein At3g29370 [Source:UniProtKB/TrEMBL;Acc:Q8LD48]
AT1G03020	-2.38817803	0.001582297	GRXS1	Monothiol glutaredoxin-S1 [Source:UniProtKB/Swiss-Prot;Acc:Q9SA68]
AT5G63650	-2.38798161	4.18E-08	SRK2H	Serine/threonine-protein kinase SRK2H [Source:UniProtKB/Swiss-Prot;Acc:Q9FFP9]
AT1G78970	-2.38707835	8.47E-17	LUP1	Lupeol synthase 1 [Source:UniProtKB/Swiss-Prot;Acc:Q9C5M3]
AT5G44420	-2.37756193	0.002828762	PDF1.2A	Defensin-like protein 16 [Source:UniProtKB/Swiss-Prot;Acc:Q9FI23]
AT4G25260	-2.37618454	9.13E-09	PMEI7	Pectinesterase inhibitor 7 [Source:UniProtKB/Swiss-Prot;Acc:Q9SB37]

AT1G20120	-2.37527053	6.50E-07	AT1G20120	GDSL esterase/lipase At1g20120 [Source:UniProtKB/Swiss-Prot;Acc:P0DKJ6]
AT1G26945	-2.37469345	2.79E-08	PRE6	Transcription factor PRE6 [Source:UniProtKB/Swiss-Prot;Acc:Q8GW32]
AT5G42830	-2.37428626	0.000292731	AT5G42830	HXXXD-type acyl-transferase family protein [Source:UniProtKB/TrEMBL;Acc:Q9FMN6]
AT1G01340	-2.37131875	1.81E-07	CNGC10	Probable cyclic nucleotide-gated ion channel 10 [Source:UniProtKB/Swiss-Prot;Acc:Q9LNJ0]
AT4G34380	-2.36785098	0.00040348	AT4G34380	At4g34380 [Source:UniProtKB/TrEMBL;Acc:Q9SZ03]
AT2G31980	-2.36605309	1.70E-05	CYS2	Cysteine proteinase inhibitor [Source:UniProtKB/TrEMBL;Acc:A0A178VSQ8]
AT3G27170	-2.36358926	9.98E-06	CLC-B	CLC-B [Source:UniProtKB/TrEMBL;Acc:A0A178VKG6]
AT2G33020	-2.35277495	0.000213345	AtRLP24	Receptor like protein 24 [Source:UniProtKB/Swiss-Prot;Acc:O49329]

AT2G28400	-2.34944824	1.07E-06	AT2G28400	Uncharacterized protein At2g28400 [Source:UniProtKB/TrEMBL;Acc:Q9SKN0]
AT5G15265	-2.34930699	0.001202481	AT5G15265	Transmembrane protein [Source:UniProtKB/TrEMBL;Acc:Q56YM4]
AT5G25190	-2.34373716	4.42E-06	ERF003	Ethylene-responsive transcription factor ERF003 [Source:UniProtKB/Swiss-Prot;Acc:Q94AW5]
AT3G12710	-2.34054501	3.10E-16	AT3G12710	DNA glycosylase superfamily protein [Source:UniProtKB/TrEMBL;Acc:Q9LTW3]
AT5G22380	-2.33355474	0.002138065	NAC090	NAC-domain protein-like [Source:UniProtKB/TrEMBL;Acc:Q680R1]
AT2G02990	-2.32558203	0.00209011	RNS1	Ribonuclease 1 [Source:UniProtKB/Swiss-Prot;Acc:P42813]
AT5G17300	-2.32006458	0.000204984	RVE1	Protein REVEILLE 1 [Source:UniProtKB/Swiss-Prot;Acc:F4KGY6]
AT3G29575	-2.31255119	0.000221358	AFP3	Ninja-family protein AFP3 [Source:UniProtKB/Swiss-Prot;Acc:Q94F39]

AT2G35945	-2.31207975	0.003901223	AT2G35945	other RNA [Source:TAIR;Acc:AT2G35945]
AT3G15760	-2.30950576	5.81E-09	AT3G15760	At3g15760 [Source:UniProtKB/TrEMBL;Acc:Q9LW03]
AT1G53700	-2.30933288	3.34E-05	WAG1	Serine/threonine-protein kinase WAG1 [Source:UniProtKB/Swiss-Prot;Acc:Q9C8M5]
AT4G38560	-2.30870913	0.000851668	AT4G38560	Phospholipase like protein [Source:UniProtKB/TrEMBL;Acc:Q0WV01]
AT1G09932	-2.30546423	0.000329389	AT1G09932	Phosphoglycerate mutase family protein [Source:UniProtKB/TrEMBL;Acc:Q8GWG7]
AT3G12220	-2.30527251	0.002934498	SCPL16	Serine carboxypeptidase-like 16 [Source:UniProtKB/Swiss- Prot;Acc:Q9C7D4]
AT1G49000	-2.29795237	1.11E-06	AT1G49000	At1g49000 [Source:UniProtKB/TrEMBL;Acc:Q9M9A2]
AT5G26200	-2.29581726	6.27E-06	AT5G26200	AT5g26200/T19G15_50 [Source:UniProtKB/TrEMBL;Acc:Q93YZ9]
AT4G11890	-2.29545547	3.20E-06	AT4G11890	Protein kinase superfamily protein [Source:UniProtKB/TrEMBL;Acc:F4JPT7]

AT5G57510	-2.29261363	0.002908408	AT5G57510	Cotton fiber protein [Source:UniProtKB/TrEMBL;Acc:Q9FKM0]
AT4G39670	-2.29103147	0.000756913	AT4G39670	ACD11 homolog protein [Source:UniProtKB/Swiss-Prot;Acc:Q8L7U7]
AT5G02490	-2.29064996	0.000726475	MED37D	Probable mediator of RNA polymerase II transcription subunit 37c [Source:UniProtKB/Swiss-Prot;Acc:P22954]
AT4G15248	-2.28998635	0.004638883	MIP1A	B-box domain protein 30 [Source:UniProtKB/Swiss-Prot;Acc:Q1G3I2]
AT2G28053	-2.28566335	0.003701082	None	None
AT5G43630	-2.28115411	2.02E-05	TZP	Zinc knuckle (CCHC-type) family protein [Source:UniProtKB/TrEMBL;Acc:Q9FIX7]
AT4G11170	-2.28029541	0.00217263	AT4G11170	Putative disease resistance protein At4g11170 [Source:UniProtKB/Swiss-Prot;Acc:O82500]
AT4G32280	-2.27560031	0.000791879	IAA29	Auxin-responsive protein [Source:UniProtKB/TrEMBL;Acc:Q2VWA0]



AT5G39670	-2.27130776	0.001290645	CML46	Probable calcium-binding protein CML46 [Source:UniProtKB/Swiss-Prot;Acc:Q93Z27]
AT1G02820	-2.27100938	0.000478902	LEA2	LEA3 [Source:UniProtKB/TrEMBL;Acc:A0A178WJ88]
AT4G13395	-2.26645154	0.001906673	DVL10	DVL10 [Source:UniProtKB/TrEMBL;Acc:Q61M91]
AT3G50770	-2.26418375	0.001474861	CML41	Probable calcium-binding protein CML41 [Source:UniProtKB/Swiss-Prot;Acc:Q8L3R2]
AT4G02520	-2.26243262	4.21E-05	GSTF2	Glutathione S-transferase F2 [Source:UniProtKB/Swiss-Prot;Acc:P46422]
AT4G31370	-2.26048688	0.00252467	FLA5	Fasciclin-like arabinogalactan protein 5 [Source:UniProtKB/Swiss-Prot;Acc:O49586]
AT3G46080	-2.25533768	0.001932282	ZAT8	Zinc finger protein ZAT8 [Source:UniProtKB/Swiss-Prot;Acc:Q9LX85]
AT4G15380	-2.25435732	0.000308435	CYP705A4	Cytochrome P450, family 705, subfamily A, polypeptide 4 [Source:UniProtKB/TrEMBL;Acc:Q8L7H7]
AT4G22040	-2.25349178	0.003401149	None	None

AT1G06080	-2.25309769	0.000705647	ADS1	Delta-9 acyl-lipid desaturase 1 [Source:UniProtKB/Swiss-Prot;Acc:O65797]
AT3G48640	-2.2528849	0.003960337	AT3G48640	Transmembrane protein [Source:UniProtKB/TrEMBL;Acc:Q9SMN5]
AT2G20150	-2.24783633	0.004455106	AT2G20150	Uncharacterized protein At2g20150/T2G17.5 [Source:UniProtKB/TrEMBL;Acc:Q84X45]
AT3G17050	-2.24645606	3.47E-06	None	None
AT5G18050	-2.24481922	3.20E-06	SAUR22	Auxin-responsive protein SAUR22 [Source:UniProtKB/Swiss-Prot;Acc:Q9FJF7]
AT5G35935	-2.23822396	2.38E-06	None	None
AT2G36630	-2.23764031	4.59E-08	AT2G36630	Sulfite exporter TauE/SafE family protein 4 [Source:UniProtKB/Swiss-Prot;Acc:Q8S9J0]
AT3G23120	-2.23081776	0.003462465	AtRLP38	Receptor-like protein 38 [Source:UniProtKB/Swiss-Prot;Acc:Q9LS79]

AT5G26690	-2.22844217	0.003649956	HIPP02	Heavy metal-associated isoprenylated plant protein 2 [Source:UniProtKB/Swiss-Prot;Acc:Q8GWS3]
AT2G47015	-2.22735099	0.006016585	MIR408	MIR408; miRNA [Source:TAIR;Acc:AT2G47015]
AT3G54500	-2.22545106	2.35E-07	AT3G54500	BEST Arabidopsis thaliana protein match is: dentin sialophosphoprotein-related (TAIR:AT5G64170.1); Ha. [Source:TAIR;Acc:AT3G54500]
AT5G54203	-2.2252884	0.002405826	None	None
ATCG00420	-2.2250407	0.003271058	NDHJ	NAD(P)H-quinone oxidoreductase subunit J, chloroplastic [Source:UniProtKB/Swiss-Prot;Acc:P56754]
AT2G16720	-2.22340086	3.64E-05	MYB7	Transcription factor MYB7 [Source:UniProtKB/Swiss- Prot;Acc:Q42379]
AT2G46940	-2.22277386	0.000308932	AT2G46940	unknown protein; BEST Arabidopsis thaliana protein match is: unknown protein (TAIR:AT3G62070.1); Ha. [Source:TAIR;Acc:AT2G46940]

AT4G17090	-2.21945763	3.44E-05	BAM3	Beta-amylase 3, chloroplastic [Source:UniProtKB/Swiss-Prot;Acc:O23553]
AT2G18970	-2.21809561	0.00613071	AT2G18970	At2g18970 [Source:UniProtKB/TrEMBL;Acc:O64627]
AT2G42250	-2.2175626	0.006311388	CYP712A1	Cytochrome P450, family 712, subfamily A, polypeptide 1 [Source:UniProtKB/TrEMBL;Acc:O48532]
AT3G24520	-2.21719574	0.000742122	HSFC1	Heat stress transcription factor C-1 [Source:UniProtKB/Swiss-Prot;Acc:Q9LV52]
AT5G01215	-2.21408156	0.004199682	AT5G01215	other RNA [Source:TAIR;Acc:AT5G01215]
AT3G57460	-2.21016888	0.001472543	AT3G57460	Catalytic/ metal ion binding / metalloendopeptidase/ zinc ion binding protein [Source:UniProtKB/TrEMBL;Acc:F4J3D6]
AT5G64905	-2.20969675	0.005301192	PEP3	Elicitor peptide 3 [Source:UniProtKB/Swiss-Prot;Acc:Q8LAX3]
AT1G72770	-2.20938907	4.97E-10	HAB1	Protein phosphatase 2C 16 [Source:UniProtKB/Swiss-Prot;Acc:Q9CAJ0]

AT2G27660	-2.20928146	0.001027535	AT2G27660	Cysteine/Histidine-rich C1 domain family protein [Source:UniProtKB/TrEMBL;Acc:Q9ZUW8]
AT2G07682	-2.20863546	0.004616101	None	None
AT3G28580	-2.2082802	0.005077725	AT3G28580	AAA-ATPase At3g28580 [Source:UniProtKB/Swiss-Prot;Acc:Q9LJJ7]
AT2G30140	-2.20633123	1.17E-06	UGT87A2	UDP-glycosyltransferase 87A2 [Source:UniProtKB/Swiss-Prot;Acc:O64733]
AT5G63195	-2.20614237	0.006412343	AT5G63195	other RNA [Source:TAIR;Acc:AT5G63195]
AT1G61680	-2.20320995	0.001590559	TPS14	S-(+)-linalool synthase, chloroplastic [Source:UniProtKB/Swiss-Prot;Acc:Q84UV0]
AT5G17760	-2.2030497	1.40E-05	AT5G17760	AAA-ATPase At5g17760 [Source:UniProtKB/Swiss-Prot;Acc:Q9FN75]
AT3G23240	-2.19656923	0.002095607	ERF1B	Ethylene-responsive transcription factor 1B [Source:UniProtKB/Swiss-Prot;Acc:Q8LDC8]

AT5G66620	-2.19531029	2.58E-05	DAR6	Protein DA1-related 6 [Source:UniProtKB/Swiss-Prot;Acc:Q9FJX8]
AT3G20395	-2.19333443	0.0020256	AT3G20395	RING/U-box superfamily protein [Source:UniProtKB/TrEMBL;Acc:Q1G3M1]
AT4G15430	-2.18594351	7.57E-05	AT4G15430	CSC1-like protein At4g15430 [Source:UniProtKB/Swiss-Prot;Acc:Q8VZM5]
AT1G33950	-2.18544595	0.006165375	IAN7	Immune-associated nucleotide-binding protein 7 [Source:UniProtKB/Swiss-Prot;Acc:Q9C8V2]
AT2G19190	-2.18402966	0.000789592	SIRK	Senescence-induced receptor-like serine/threonine-protein kinase [Source:UniProtKB/Swiss-Prot;Acc:O64483]
AT4G27590	-2.17690162	0.000780566	AT4G27590	Heavy metal transport/detoxification superfamily protein [Source:UniProtKB/TrEMBL;Acc:F4JJN9]
AT4G27260	-2.17662789	0.0004431	GH3.5	Indole-3-acetic acid-amido synthetase GH3.5 [Source:UniProtKB/Swiss-Prot;Acc:O81829]

AT1G51890	-2.17387098	0.000516699	AT1G51890	Leucine-rich repeat protein kinase family protein [Source:TAIR;Acc:AT1G51890]
AT4G21500	-2.17335317	2.13E-08	AT4G21500	At4g21500 [Source:UniProtKB/TrEMBL;Acc:O65415]
AT1G32960	-2.17231332	0.004783473	SBT3.3	Subtilisin-like protease SBT3.3 [Source:UniProtKB/Swiss-Prot;Acc:Q9MAP5]
AT3G30180	-2.16998555	3.20E-19	CYP85A2	Cytochrome P450 85A2 [Source:UniProtKB/Swiss-Prot;Acc:Q940V4]
AT3G56408	-2.16960133	0.007675897	AT3G56408	other RNA [Source:TAIR;Acc:AT3G56408]
AT4G24700	-2.16888738	0.000451968	AT4G24700	Uncharacterized protein At4g24700 [Source:UniProtKB/TrEMBL;Acc:Q9SB65]
AT1G09540	-2.16846026	0.003329841	MYB61	MYB61 [Source:UniProtKB/TrEMBL;Acc:A0A178WLE4]
AT2G38470	-2.16782242	8.60E-05	WRKY33	WRKY33 [Source:UniProtKB/TrEMBL;Acc:A0A384L4W4]
AT4G30180	-2.16659025	2.75E-05	BHLH146	Transcription factor bHLH146 [Source:UniProtKB/Swiss-Prot;Acc:Q9SUM5]

AT1G13340	-2.16515636	0.001906673	AT1G13340	Regulator of Vps4 activity in the MVB pathway protein [Source:UniProtKB/TrEMBL;Acc:Q9FX63]
AT5G64810	-2.16358582	0.007786217	WRKY51	Probable WRKY transcription factor 51 [Source:UniProtKB/Swiss-Prot;Acc:Q93WU9]
AT1G79270	-2.16222786	2.98E-05	ECT8	Evolutionarily conserved C-terminal region 8 [Source:UniProtKB/TrEMBL;Acc:Q9FPE7]
AT1G33420	-2.16204733	0.00201343	AT1G33420	PHD finger protein At1g33420 [Source:UniProtKB/Swiss-Prot;Acc:Q9C810]
ATCG00160	-2.16197075	4.58E-05	RPS2	30S ribosomal protein S2, chloroplastic [Source:UniProtKB/Swiss-Prot;Acc:P56797]
AT5G15581	-2.16062816	0.007225424	AT5G15581	Putative uncharacterized protein T20K14_200 [Source:UniProtKB/TrEMBL;Acc:Q9LF23]
AT5G60900	-2.15920542	0.00160841	RLK1	receptor-like protein kinase 1 [Source:TAIR;Acc:AT5G60900]
AT1G21050	-2.15915282	5.35E-09	AT1G21050	Protein of unknown function, DUF617 [Source:TAIR;Acc:AT1G21050]



AT3G54830	-2.15804248	1.30E-06	AT3G54830	None
AT1G10155	-2.15435119	0.001654387	ATPP2-A10	Phloem protein 2-A10 [Source:UniProtKB/TrEMBL;Acc:F4I2R3]
AT1G29195	-2.15365625	1.91E-05	AT1G29195	At1g29190/F28N24_12 [Source:UniProtKB/TrEMBL;Acc:Q9LP48]
AT2G46400	-2.15275612	0.005153719	WRKY46	Probable WRKY transcription factor 46 [Source:UniProtKB/Swiss-Prot;Acc:Q9SKD9]
AT5G59670	-2.15252948	0.001865764	AT5G59670	Receptor-like protein kinase At5g59670 [Source:UniProtKB/Swiss-Prot;Acc:Q9FN94]
ATMG00370	-2.1518881	0.006964196	ORF199	Uncharacterized mitochondrial protein AtMg00370 [Source:UniProtKB/Swiss-Prot;Acc:P93296]
AT1G69260	-2.14747118	0.001920011	AFP1	Ninja-family protein AFP1 [Source:UniProtKB/Swiss-Prot;Acc:Q9LQ98]
AT3G12320	-2.14461238	2.77E-06	LNK3	LNK3 [Source:UniProtKB/TrEMBL;Acc:A0A178VJK8]

AT5G52760	-2.14218511	0.005416496	HIPP14	Heavy metal-associated isoprenylated plant protein 14 [Source:UniProtKB/Swiss-Prot;Acc:Q9LTE1]
AT1G07390	-2.14132959	4.27E-08	AtRLP1	Receptor like protein 1 [Source:UniProtKB/TrEMBL;Acc:F4HQM4]
AT5G14760	-2.14032207	0.000490961	AO	L-aspartate oxidase, chloroplastic [Source:UniProtKB/Swiss-Prot;Acc:Q94AY1]
AT1G01560	-2.1399495	0.002564184	MPK11	Mitogen-activated protein kinase 11 [Source:UniProtKB/Swiss-Prot;Acc:Q9LMM5]
AT2G02930	-2.13893175	0.00038919	GSTF3	Glutathione S-transferase F3 [Source:UniProtKB/Swiss-Prot;Acc:Q9SLM6]
AT5G66640	-2.1380394	0.001443061	DAR3	DA1-related protein 3 [Source:TAIR;Acc:AT5G66640]
AT4G16690	-2.13390019	0.000649132	PPD	Probable pheophorbidase [Source:UniProtKB/Swiss-Prot;Acc:O23512]
AT4G14390	-2.13371601	0.006288326	AT4G14390	Ankyrin repeat family protein [Source:UniProtKB/TrEMBL;Acc:F4JVF4]

AT1G47510	-2.13162194	0.002732398	IP5P11	Type IV inositol polyphosphate 5-phosphatase 11 [Source:UniProtKB/Swiss-Prot;Acc:Q5EAF2]
AT2G21560	-2.13118895	0.000285463	AT2G21560	Nucleolar-like protein [Source:UniProtKB/TrEMBL;Acc:Q9SIK3]
AT2G32680	-2.12965495	0.002979499	AtRLP23	Receptor like protein 23 [Source:UniProtKB/Swiss-Prot;Acc:O48849]
AT2G26692	-2.12957972	0.0069795	AT2G26692	other RNA [Source:TAIR;Acc:AT2G26692]
AT5G61350	-2.12952908	0.004852321	AT5G61350	Probable receptor-like protein kinase At5g61350 [Source:UniProtKB/Swiss-Prot;Acc:Q9FLJ8]
AT3G48630	-2.12929971	0.005554434	AT3G48630	unknown protein; BEST Arabidopsis thaliana protein match is: unknown protein (TAIR:AT3G44150.1); Ha. [Source:TAIR;Acc:AT3G48630]
AT3G02380	-2.12796911	0.000587401	COL2	Zinc finger protein CONSTANS-LIKE 2 [Source:UniProtKB/Swiss-Prot;Acc:Q96502]
AT3G04300	-2.12777006	0.000336321	AT3G04300	At3g04300 [Source:UniProtKB/TrEMBL;Acc:Q9M8Y6]

AT3G14770	-2.12716439	7.93E-07	SWEET2	Bidirectional sugar transporter SWEET [Source:UniProtKB/TrEMBL;Acc:A0A178VM79]
AT4G01680	-2.12662314	2.32E-05	MYB55	Myb domain protein 55 [Source:UniProtKB/TrEMBL;Acc:Q9ZS14]
AT1G29640	-2.12313438	0.002146577	AT1G29640	At1g29640 [Source:UniProtKB/TrEMBL;Acc:Q9C7N7]
AT5G53970	-2.121241	1.42E-05	AT5G53970	Probable aminotransferase TAT2 [Source:UniProtKB/Swiss-Prot;Acc:Q9FN30]
AT5G52640	-2.12120263	0.003370829	HSP90-1	Heat shock protein 90-1 [Source:UniProtKB/Swiss-Prot;Acc:P27323]
AT5G02780	-2.11919135	0.006068088	GSTL1	Glutathione S-transferase L1 [Source:UniProtKB/Swiss-Prot;Acc:Q6NLB0]
AT3G62100	-2.11840471	0.000550619	IAA30	Auxin-responsive protein (Fragment) [Source:UniProtKB/TrEMBL;Acc:C0SVF9]
ATMG01390	-2.11796937	0.001241213	RRN18	Mitochondrial 18S ribosomal RNA, which is a component of the 30S small subunit of mitochondrial ribosome. The rRNA is

				degraded by a polynucleotide phosphorylase-like protein (AtmtPNPase). [Source:TAIR;Acc:ATMG01390]
AT5G22500	-2.11729917	0.00027013	FAR1	Fatty acyl-CoA reductase 1 [Source:UniProtKB/Swiss-Prot;Acc:Q39152]
ATCG01130	-2.11567994	0.009900827	YCF1.2	Ycf1 protein [Source:TAIR;Acc:ATCG01130]
AT5G49620	-2.11449768	0.006638724	AtMYB78	myb domain protein 78 [Source:TAIR;Acc:AT5G49620]
ATCG00280	-2.11322136	0.001796621	PSBC	Photosystem II CP43 reaction center protein [Source:UniProtKB/TrEMBL;Acc:A0A1B1W4T4]
AT2G16060	-2.10872547	0.003332105	AHB1	NSHB1 [Source:UniProtKB/TrEMBL;Acc:A0A384KL50]
AT5G39610	-2.10838629	0.000523837	NAC92	NAC domain-containing protein 92 [Source:UniProtKB/Swiss-Prot;Acc:Q9FKA0]
AT5G57770	-2.10639206	0.010237302	AT5G57770	Plant protein of unknown function (DUF828) with plant pleckstrin homology-like region [Source:TAIR;Acc:AT5G57770]

AT2G32210	-2.10544574	0.00213669	AT2G32210	Cysteine-rich/transmembrane domain A-like protein [Source:UniProtKB/TrEMBL;Acc:Q9SKX9]
AT3G14570	-2.10362612	2.54E-07	CALS8	Putative callose synthase 8 [Source:UniProtKB/Swiss-Prot;Acc:Q9LUD7]
AT3G49980	-2.10309097	0.004982867	AT3G49980	F-box and associated interaction domains-containing protein [Source:UniProtKB/TrEMBL;Acc:A0A1I9LP00]
AT5G55970	-2.10085058	2.38E-06	AT5G55970	RING/U-box superfamily protein [Source:UniProtKB/TrEMBL;Acc:Q8LES9]
AT5G48900	-2.10002583	7.22E-10	AT5G48900	Probable pectate lyase 20 [Source:UniProtKB/Swiss-Prot;Acc:Q93WF1]
AT4G23215	-2.09830432	0.002954218	None	None
AT2G46270	-2.09811855	2.22E-07	GBF3	G-box-binding factor 3 [Source:UniProtKB/Swiss-Prot;Acc:P42776]
AT5G59090	-2.09688592	0.008540727	SBT4.12	Subtilisin-like protease SBT4.12 [Source:UniProtKB/Swiss-Prot;Acc:Q8L7D2]

AT4G11521	-2.09451109	0.000386223	CRK34	Putative cysteine-rich receptor-like protein kinase 34 [Source:UniProtKB/Swiss-Prot;Acc:Q8LPI0]
AT4G13040	-2.09441563	1.80E-09	AT4G13040	Integrase-type DNA-binding superfamily protein [Source:UniProtKB/TrEMBL;Acc:F4JS76]
AT2G26010	-2.09392868	0.008569733	PDF1.3	PDF1.3 [Source:UniProtKB/TrEMBL;Acc:A0A178VSS6]
AT2G29470	-2.09212501	0.010798536	GSTU3	Glutathione S-transferase U3 [Source:UniProtKB/Swiss-Prot;Acc:Q9ZW28]
AT1G72060	-2.0919088	0.006939864	AT1G72060	Serine-type endopeptidase inhibitor [Source:UniProtKB/TrEMBL;Acc:Q9C7G9]
AT4G28280	-2.0881085	0.00193698	LLG3	LLG3 [Source:UniProtKB/TrEMBL;Acc:A0A178V2V8]
AT3G13610	-2.08778818	0.009363393	F6'H1	Feruloyl CoA ortho-hydroxylase 1 [Source:UniProtKB/Swiss-Prot;Acc:Q9LHN8]
AT2G32200	-2.086498	0.00041571	AT2G32200	unknown protein; BEST Arabidopsis thaliana protein match is: unknown protein (TAIR:AT2G32210.1); Ha. [Source:TAIR;Acc:AT2G32200]

AT4G11470	-2.08419036	6.06E-06	CRK31	cysteine-rich RLK (RECEPTOR-like protein kinase) 31 [Source:TAIR;Acc:AT4G11470]
AT5G57010	-2.08394894	0.005080301	IQM5	IQ domain-containing protein IQM5 [Source:UniProtKB/Swiss-Prot;Acc:Q058N0]
AT1G54700	-2.08328644	0.009230618	AT1G54700	FUNCTIONS IN: molecular_function unknown; INVOLVED IN: biological_process unknown; LOCATED IN: mitochondrion; CONTAINS InterPro DOMAIN/s: Serine endopeptidase DegP2 (InterPro:IPR015724); BEST Arabidopsis thaliana protein match is: DegP protease 13 ( /.../T5G40560.1); Ha. [Source:TAIR;Acc:AT1G54700]
AT4G27290	-2.08280467	0.00121741	AT4G27290	Serine/threonine-protein kinase [Source:UniProtKB/TrEMBL;Acc:A0A178V0J5]
AT1G49405	-2.08107478	0.002189653	AT1G49405	CASP-like protein 5C3 [Source:UniProtKB/Swiss-Prot;Acc:Q3ECT8]
AT5G19970	-2.07992236	0.000728379	AT5G19970	unknown protein; Ha. [Source:TAIR;Acc:AT5G19970]



AT2G32540	-2.07985653	1.82E-08	CSLB4	Glycosyltransferase (Fragment) [Source:UniProtKB/TrEMBL;Acc:W8Q3D1]
AT3G15518	-2.07735261	0.00091356	AT3G15518	Putative uncharacterized protein [Source:UniProtKB/TrEMBL;Acc:Q8GYA5]
AT5G03552	-2.07727206	0.00168852	MIR822A	MIR822a; miRNA [Source:TAIR;Acc:AT5G03552]
AT5G06865	-2.07541267	0.001408873	AT5G06865	other RNA [Source:TAIR;Acc:AT5G06865]
AT5G11210	-2.0737925	0.00286626	GLR2.5	Glutamate receptor 2.5 [Source:UniProtKB/Swiss-Prot;Acc:Q9LFN5]
AT1G20310	-2.07253669	0.00747646	AT1G20310	Syringolide-induced protein [Source:UniProtKB/TrEMBL;Acc:Q8L956]
AT3G48650	-2.0708346	0.004646196	None	None
AT1G65970	-2.06626654	0.007438094	PRXIIC	TPX2 [Source:UniProtKB/TrEMBL;Acc:A0A178WKG0]
AT3G26742	-2.0660289	0.003401149	AT3G26742	unknown protein; FUNCTIONS IN: molecular_function unknown; INVOLVED IN: biological_process unknown;

Gene ID	Log2 Fold Change	P-value	Gene Name	Description
				LOCATED IN: endomembrane system; Ha. [Source:TAIR;Acc:AT3G26742]
AT4G38540	-2.06426432	0.000783917	MO2	Monooxygenase 2 [Source:UniProtKB/Swiss-Prot;Acc:O81816]
AT3G60520	-2.0640212	1.81E-07	AT3G60520	At3g60520 [Source:UniProtKB/TrEMBL;Acc:Q9M207]
AT3G51070	-2.06389753	0.00857764	AT3G51070	Probable methyltransferase PMT27 [Source:UniProtKB/Swiss-Prot;Acc:Q9SD39]
AT4G23810	-2.06222247	1.21E-05	WRKY53	Probable WRKY transcription factor 53 [Source:UniProtKB/Swiss-Prot;Acc:Q9SUP6]
AT3G08870	-2.06158632	0.000177241	AT3G08870	Concanavalin A-like lectin protein kinase family protein [Source:UniProtKB/TrEMBL;Acc:A0A1I9LTB8]
AT2G47190	-2.06036969	0.001389722	ATMYB2	ATMYB2 [Source:UniProtKB/TrEMBL;Acc:Q39028]
AT5G41750	-2.05970944	0.000519053	AT5G41750	Disease resistance protein (TIR-NBS-LRR class) family [Source:UniProtKB/TrEMBL;Acc:Q9LSX5]
AT5G07000	-2.05959461	6.93E-08	SOT14	Cytosolic sulfotransferase 14 [Source:UniProtKB/Swiss-Prot;Acc:Q8GZ53]

AT4G39610	-2.05822511	0.01018939	AT4G39610	At4g39610 [Source:UniProtKB/TrEMBL;Acc:Q9SV97]
AT1G04330	-2.05805021	0.006518705	AT1G04330	At1g04330 [Source:UniProtKB/TrEMBL;Acc:O22691]
AT5G24080	-2.05772366	0.006165375	AT5G24080	G-type lectin S-receptor-like serine/threonine-protein kinase At5g24080 [Source:UniProtKB/Swiss-Prot;Acc:Q9FLV4]
AT5G07760	-2.05536211	0.000429138	AT5G07760	formin homology 2 domain-containing protein / FH2 domain- containing protein [Source:TAIR;Acc:AT5G07760]
AT5G59590	-2.05473043	0.003236187	UGT76E2	Glycosyltransferase (Fragment) [Source:UniProtKB/TrEMBL;Acc:W8PUA4]
AT1G07160	-2.0524167	0.005837386	AT1G07160	PP2C-type phosphatase AP2C2 [Source:UniProtKB/TrEMBL;Acc:F6LPR6]
AT4G27410	-2.05153177	0.00022529	RD26	NAC (No Apical Meristem) domain transcriptional regulator superfamily protein [Source:UniProtKB/TrEMBL;Acc:F4JIU9]
AT5G06570	-2.05005617	0.000759017	AT5G06570	alpha/beta-Hydrolases superfamily protein [Source:TAIR;Acc:AT5G06570]

AT5G45475	-2.0485283	0.012717858	AT5G45475	Potential natural antisense gene, locus overlaps with AT5G45480 [Source:TAIR;Acc:AT5G45475]
AT2G25090	-2.04719385	0.001317289	CIPK16	Non-specific serine/threonine protein kinase [Source:UniProtKB/TrEMBL;Acc:A0A178W078]
AT5G24910	-2.04629285	0.007442885	CYP714A1	Cytochrome P450 714A1 [Source:UniProtKB/Swiss-Prot;Acc:Q93Z79]
AT5G22460	-2.04564257	0.001074348	AT5G22460	Alpha/beta-Hydrolases superfamily protein [Source:UniProtKB/TrEMBL;Acc:Q9FMQ5]
AT1G57560	-2.04159277	0.002732398	AtMYB50	At1g57560 [Source:UniProtKB/TrEMBL;Acc:Q9C695]
AT4G19460	-2.03986098	0.000265303	AT4G19460	UDP-Glycosyltransferase superfamily protein [Source:UniProtKB/TrEMBL;Acc:F4JT73]
AT3G48240	-2.03875377	0.002425271	AT3G48240	At3g48240 [Source:UniProtKB/TrEMBL;Acc:Q9STK4]
AT5G58770	-2.03704535	0.000535642	AT5G58770	Dehydrololichyl diphosphate synthase 2 [Source:UniProtKB/Swiss-Prot;Acc:Q56Y11]

AT3G21080	-2.03656817	0.000122343	AT3G21080	ABC transporter-like protein [Source:UniProtKB/TrEMBL;Acc:Q9LJC4]
AT3G28540	-2.03630281	0.008133719	AT3G28540	AAA-ATPase At3g28540 [Source:UniProtKB/Swiss-Prot;Acc:Q9LH82]
AT2G29165	-2.03573253	0.012717858	None	None
AT5G53030	-2.03436473	1.38E-05	AT5G53030	Uncharacterized protein At5g53030 [Source:UniProtKB/TrEMBL;Acc:Q9LVU9]
AT1G48745	-2.03307878	0.000633939	AT1G48745	Putative uncharacterized protein [Source:UniProtKB/TrEMBL;Acc:Q1G3E1]
AT4G17098	-2.03193477	0.005223892	AT4G17098	other RNA [Source:TAIR;Acc:AT4G17098]
ATCG00270	-2.03143242	0.003667246	PSBD	Photosystem II D2 protein [Source:UniProtKB/Swiss-Prot;Acc:P56761]
AT1G63840	-2.02920962	0.000126124	AT1G63840	At1g63840/T12P18_14 [Source:UniProtKB/TrEMBL;Acc:Q9CAJ8]

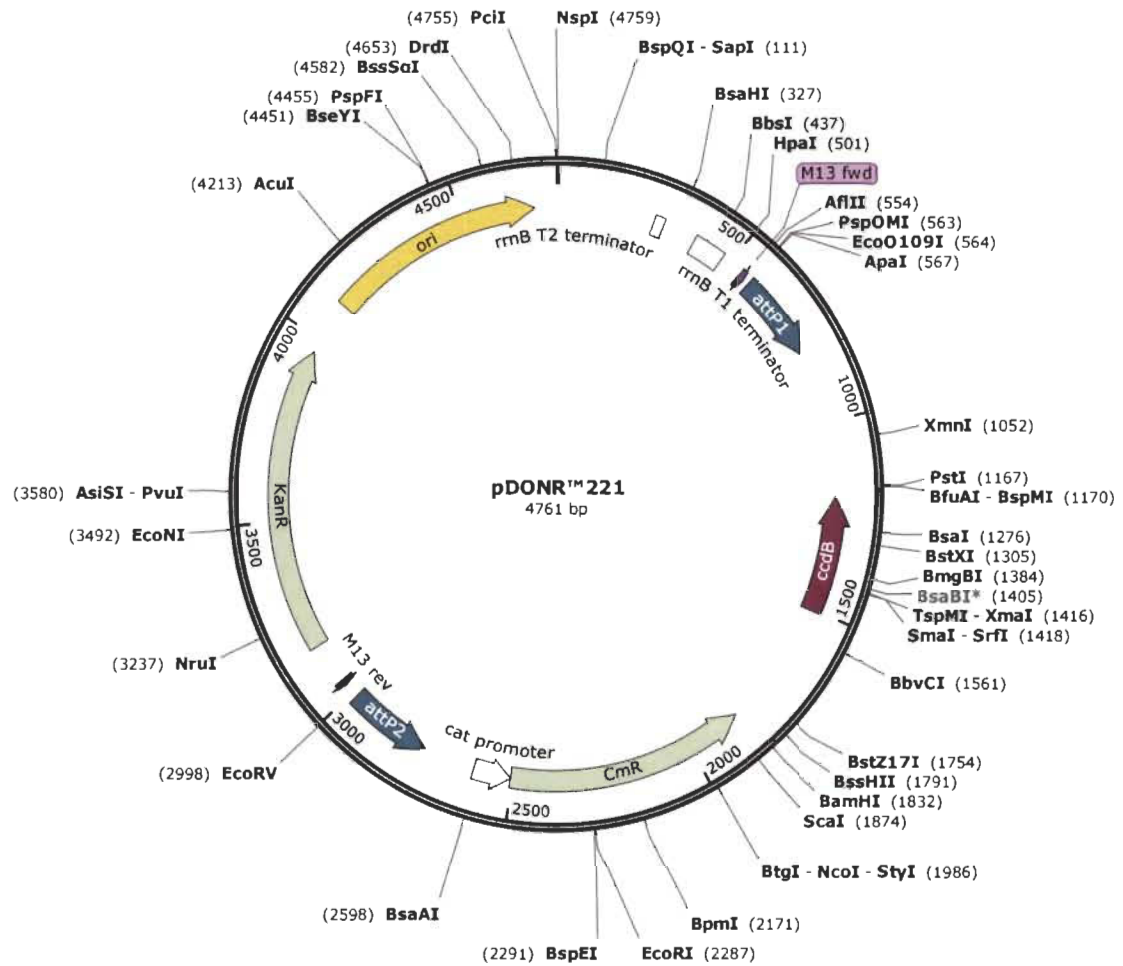
AT5G39820	-2.02715589	0.011244179	ANAC094	Putative NAC domain-containing protein 94 [Source:UniProtKB/Swiss-Prot;Acc:Q9FIW5]
AT2G47140	-2.02573214	0.002630032	SDR3B	Short-chain dehydrogenase reductase 3b [Source:UniProtKB/Swiss-Prot;Acc:Q94K41]
AT1G09080	-2.02557862	0.00780328	MED37B	Probable mediator of RNA polymerase II transcription subunit 37b [Source:UniProtKB/Swiss-Prot;Acc:Q8H1B3]
AT2G29110	-2.02503695	0.000280778	ATGLR2.8	Glutamate receptor [Source:UniProtKB/TrEMBL;Acc:A0A178VW76]
AT5G10670	-2.02420663	0.012483961	None	None
AT1G66960	-2.02375918	0.012821974	AT1G66960	Terpenoid cyclases family protein [Source:TAIR;Acc:AT1G66960]
AT5G57240	-2.02258485	0.000211836	ORP4C	ORP4C [Source:UniProtKB/TrEMBL;Acc:A0A384LHK8]
AT4G13580	-2.02258462	0.011615444	DIR18	Dirigent protein 18 [Source:UniProtKB/Swiss- Prot;Acc:Q9T0H8]

AT4G24150	-2.02254973	0.000401013	GRF8	Growth-regulating factor 8 [Source:UniProtKB/Swiss-Prot;Acc:Q9SU44]
AT1G08630	-2.02152364	0.008693502	THA1	Probable low-specificity L-threonine aldolase 1 [Source:UniProtKB/Swiss-Prot;Acc:Q8RXU4]
ATCG00830	-2.01909754	0.002020465	rpl2-A	50S ribosomal protein L2, chloroplastic [Source:UniProtKB/TrEMBL;Acc:A0A1B1W512]
AT1G67328	-2.01612344	0.013172945	AT1G67328	other RNA [Source:TAIR;Acc:AT1G67328]
AT5G24200	-2.01545931	0.005500583	AT5G24200	alpha/beta-Hydrolases superfamily protein [Source:TAIR;Acc:AT5G24200]
AT2G32190	-2.01291092	0.003049274	AT2G32190	Cysteine-rich/transmembrane domain A-like protein [Source:UniProtKB/TrEMBL;Acc:Q9SKY1]
AT4G16680	-2.01018685	0.000786029	AT4G16680	P-loop containing nucleoside triphosphate hydrolases superfamily protein [Source:TAIR;Acc:AT4G16680]
AT2G19660	-2.00939159	7.35E-05	AT2G19660	Cysteine/Histidine-rich C1 domain family protein [Source:TAIR;Acc:AT2G19660]

AT1G53090	-2.0090146	4.58E-07	SPA4	SPA4 [Source:UniProtKB/TrEMBL;Acc:A0A178WBA0]
AT3G42800	-2.00869498	2.98E-05	AT3G42800	Protein BIG GRAIN 1-like C [Source:UniProtKB/Swiss-Prot;Acc:Q9M2B3]
AT2G21320	-2.00831833	0.006288326	BBX18	B-box zinc finger protein 18 [Source:UniProtKB/Swiss-Prot;Acc:Q9SJU5]
AT2G07734	-2.00696803	0.003163213	AT2G07734	Alpha-L RNA-binding motif/Ribosomal protein S4 family protein [Source:TAIR;Acc:AT2G07734]
AT5G08790	-2.00687685	0.001323631	NAC081	Protein ATAF2 [Source:UniProtKB/Swiss-Prot;Acc:Q9C598]
AT2G27420	-2.00647567	0.014552908	AT2G27420	Cysteine proteinases superfamily protein [Source:UniProtKB/TrEMBL;Acc:Q9ZQH7]
AT1G30370	-2.00583191	0.004963239	AT1G30370	DLAH [Source:UniProtKB/TrEMBL;Acc:A0A178W2K8]
AT1G72240	-2.00188373	0.008358888	AT1G72240	Uncharacterized protein T9N14.5 [Source:UniProtKB/TrEMBL;Acc:Q9C7T1]
AT4G30290	-2.00097848	0.001290645	XTH19	Xyloglucan endotransglucosylase/hydrolase [Source:UniProtKB/TrEMBL;Acc:A0A178UU22]

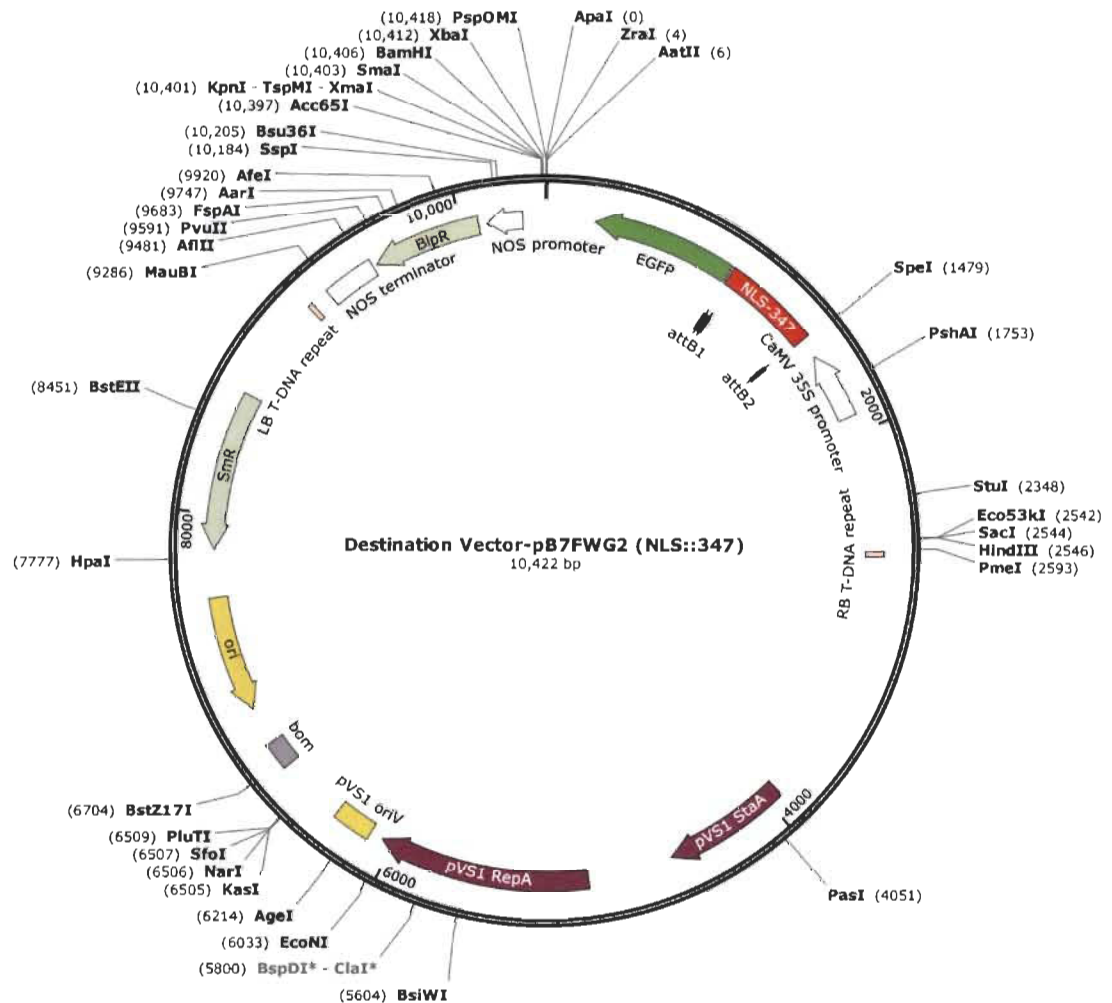


AT1G66540	-2.00024519	0.003172505	AT1G66540	At1g66540 [Source:UniProtKB/TrEMBL;Acc:A2RVN3]
AT4G16670	-2.00003247	0.000517208	AT4G16670	At4g16670 [Source:UniProtKB/TrEMBL;Acc:Q5HZ31]



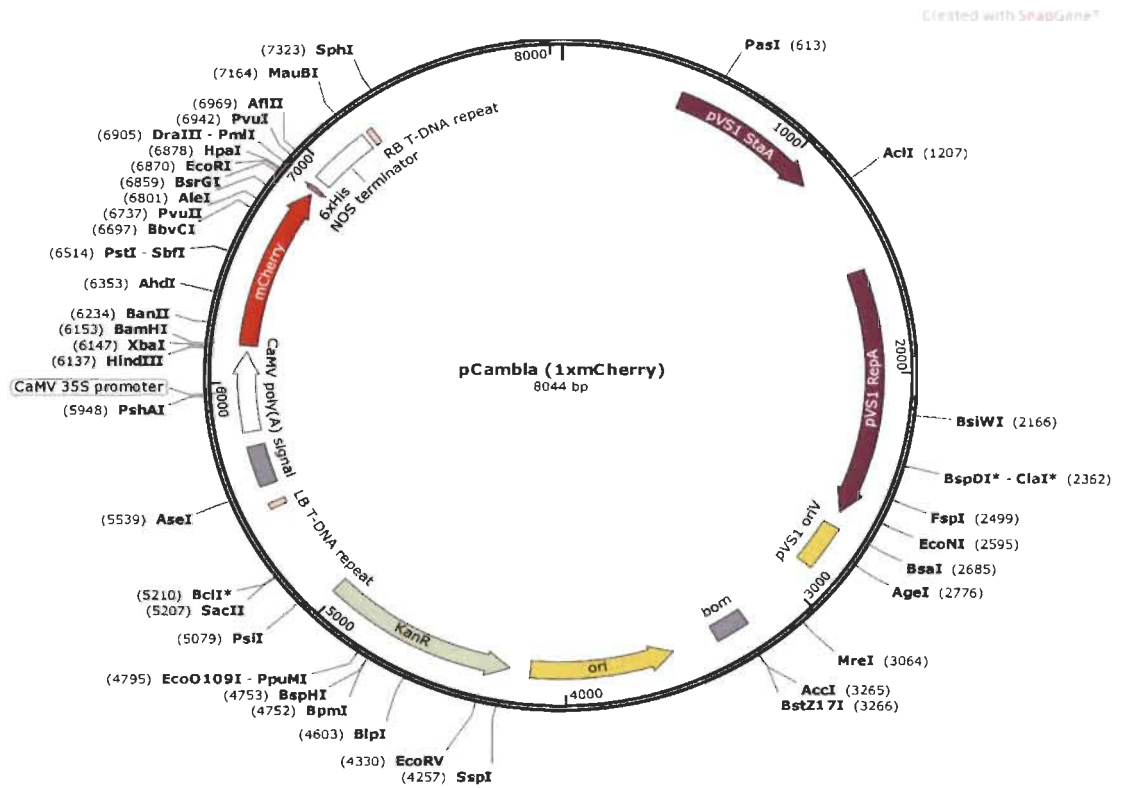
### Supplementary Figure 1. Gateway pDONR™221 vector.

Gateway donor vector with recombinational sites attP 1 and aatP2, and kanamycin resistance marker. pDONR T~21 has a pUC origin for high plasmid yields and universal M13 sequencing sites.



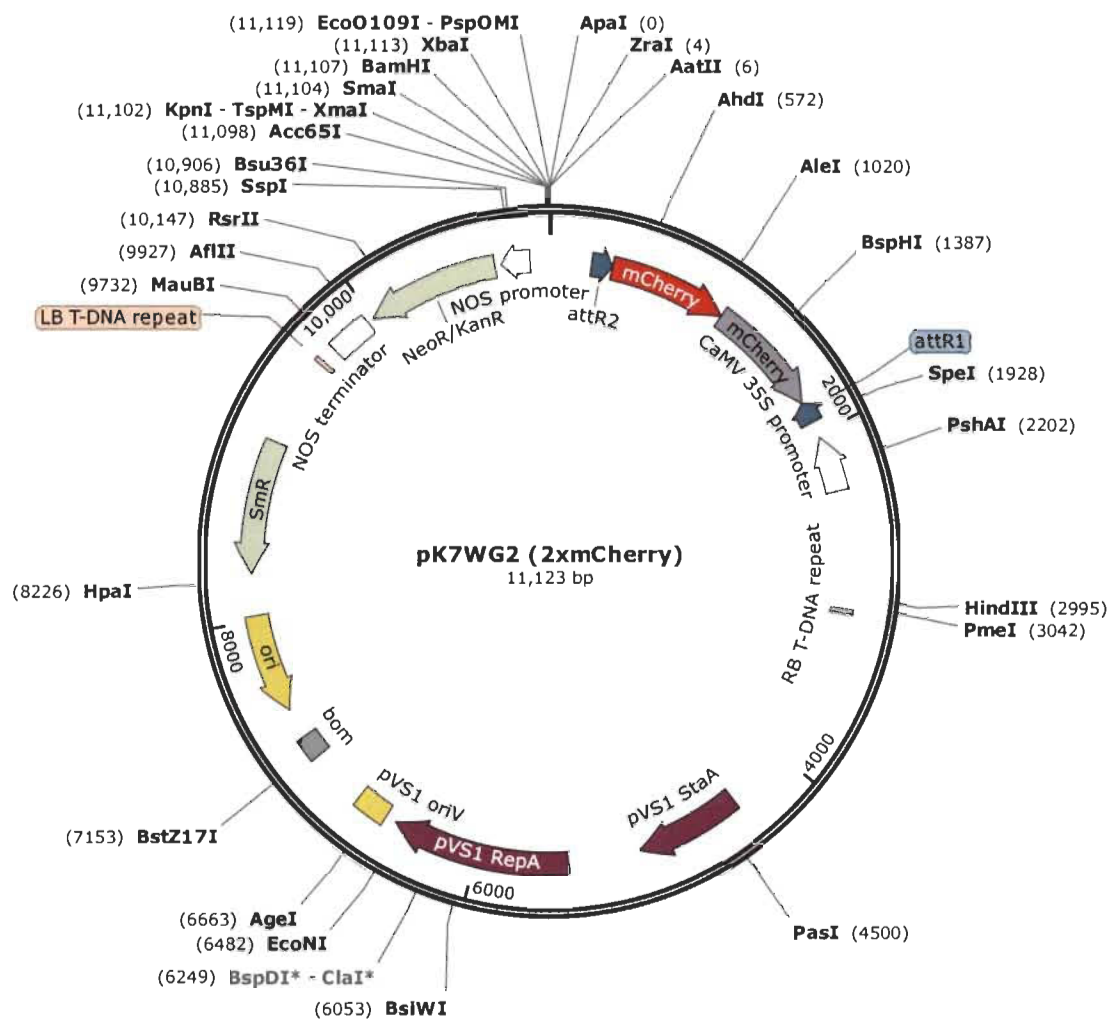
### Supplementary Figure 2. Gateway destination vector pB7FWG2,O.

Gateway destination vector with recombinational sites attR1 and attR2, and spectinomycin resistance marker. pB7FWG2,O has a 35S promoter bar gene for selection, and Egfp at the C-terminal fusion to the protein (N-terminal fusion to fluorescence tag).



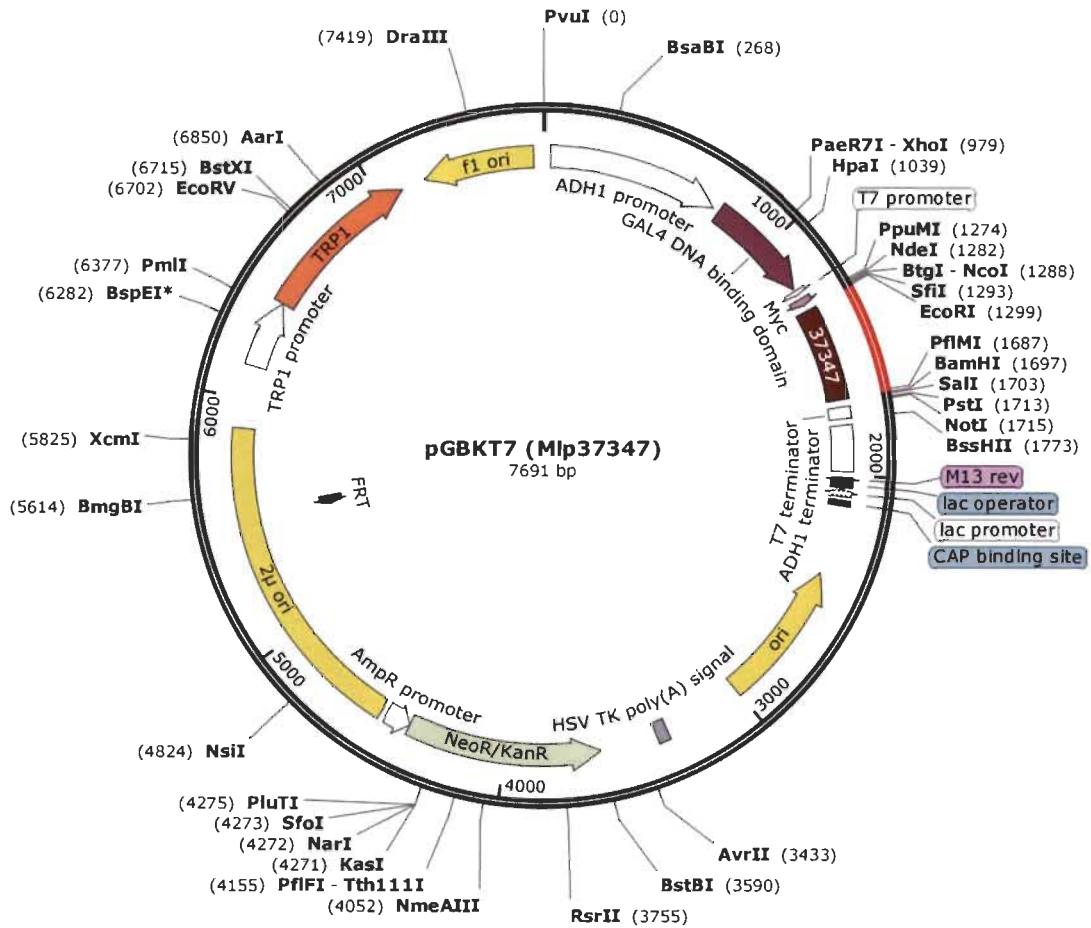
### Supplementary Figure 3. pCambia-1xmCherry construct vector map.

The pCambia-1xmCherry construct was modified from the original vector pCambia-1380. It has kanamycin resistance marker and 35S promoter bar gene for selection.

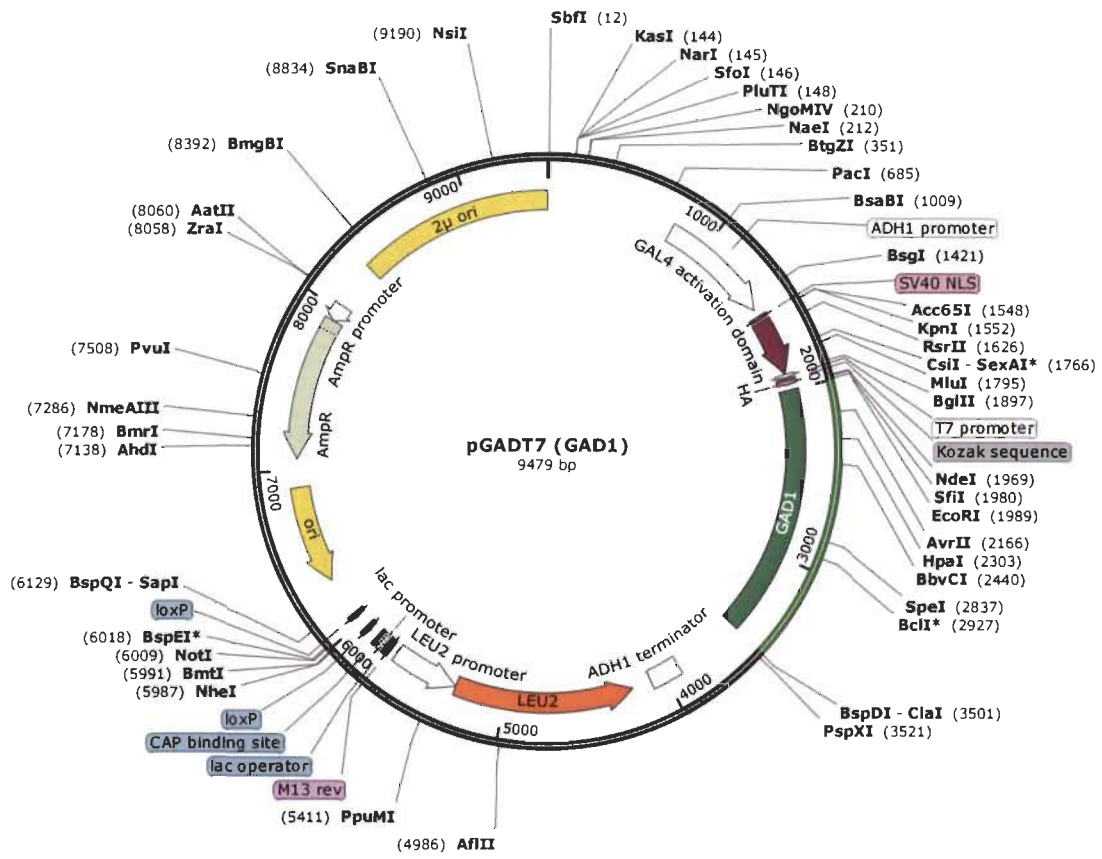


#### Supplementary Figure 4. Gateway destination vector pB7WG2.

Gateway destination vector with recombinational sites attR1 and attR2, and kanamycin resistance marker. pB7WG2 has a 35S promoter bar gene for selection.



Supplementary Figure 5. Yeast two-hybrid "bait" vector for expressing proteins fused to the GAL4 DNA-binding domain.



Supplementary Figure 6. Yeast two-hybrid "prey" vector for expressing proteins fused to the GAL4 activation domain.

## **ANNEX B**

### **VACUOLAR MEMBRANE STRUCTURES AND THEIR ROLES IN PLANT-PATHOGEN INTERACTIONS**

Mst Hur Madina, Md Saifur Rahman, Huanquan Zheng, and Hugo Germain

Annex B contains a published review article, containing about the role and targeting of vacuolar substructure in plant immunity and pathogenesis

I have equally participated in writing the review with the first author. I have written the part entitled Markers to study the vacuolar structures, the vacuole in plant-pathogen interaction, and carried out structural illustration.





## Vacuolar membrane structures and their roles in plant–pathogen interactions

Mst Hur Madina<sup>1</sup> · Md Saifur Rahman<sup>1</sup> · Huanquan Zheng<sup>2</sup> · Hugo Germain<sup>1</sup>

Received: 12 April 2019 / Accepted: 4 October 2019  
© Springer Nature B.V. 2019

**Key message** Short review focussing on the role and targeting of vacuolar substructure in plant immunity and pathogenesis.

**Abstract** Plants lack specialized immune cells, therefore each plant cell must defend itself against invading pathogens. A typical plant defense strategy is the hypersensitive response that results in host cell death at the site of infection, a process largely regulated by the vacuole. In plant cells, the vacuole is a vital organelle that plays a central role in numerous fundamental processes, such as development, reproduction, and cellular responses to biotic and abiotic stimuli. It shows divergent membranous structures that are continuously transforming. Recent technical advances in visualization and live-cell imaging have significantly altered our view of the vacuolar structures and their dynamics. Understanding the active nature of the vacuolar structures and the mechanisms of vacuole-mediated defense responses is of great importance in understanding plant–pathogen interactions. In this review, we present an overview of the current knowledge about the vacuole and its internal structures, as well as their role in plant–microbe interactions. There is so far limited information on the modulation of the vacuolar structures by pathogens, but recent research has identified the vacuole as a possible target of microbial interference.

**Keywords** Tonoplast · Vacuole · Bulb · Transvacuolar strand · Plant defense

### Introduction

#### The plant vacuole and its function in the cell

Unlike cells from other organisms, plant cells have a uniquely large and prominent organelle called the vacuole, occupying 90–95% of the cell's volume (Owens and Poole 1979). The vacuole has important physiological functions, one of the main being the preservation of turgor pressure against the cell wall, thus supporting the structural stability of the cell and of the surrounding tissue (Marty 1999). It also serves as a storage tank holding many different materials

needed by the cells, including but not limited to: sugars, metabolites, carbohydrates, lipids, amino acids, enzymes, proteins and anthocyanins (Marty 1999; Paris et al. 1996). In addition, the vacuole stores toxic ions and many other compounds that play a role in the defense against bacterial pathogens and herbivores (Martinoia et al. 2012; Van der Hooft and Jones 2004).

Depending on tissue and cell types, vacuoles are diverse in their morphologies and functions (Swanson et al. 1998). Two main types are found in plants, the protein storage vacuoles (PSV) and the lytic vacuoles (LV) and they are functionally distinct (Hoh et al. 1995; Paris et al. 1996; Robinson et al. 1995). The typical storage compartment PSVs are most abundant in seeds (Epimashko et al. 2004; Hoh et al. 1995; Otegui et al. 2005; Paris et al. 1996; Swanson et al. 1998) and are formed during seed development and maturation. They accumulate large amounts of storage proteins, which are synthesized in the endoplasmic reticulum (ER) and delivered into vacuoles via the prevacuolar complex (Sansebastiano et al. 2017), where they remain stored until they are mobilized during germination and seedling growth (Bewley and Black 1994). PSVs also store defense proteins for the response against microbial pathogens and

**Electronic supplementary material** The online version of this article (<https://doi.org/10.1007/s11103-019-00921-y>) contains supplementary material, which is available to authorized users.

✉ Hugo Germain  
hugo.germain@uqtr.ca

<sup>1</sup> Department of Chemistry, Biochemistry and Physics, Université du Québec à Trois-Rivières, 3351 boulevard des Forges, Trois-Rivières, QC G9A 5H7, Canada

<sup>2</sup> Department of Biology, McGill University, 1205 Dr. Penfield Avenue, Montreal, QC H3A 1B1, Canada

herbivores. After seed imbibition, PSVs are converted into lytic vacuoles (Bewley and Black 1994; Wang et al. 2007), which are the predominant compartments occurring in vegetative cells and are also called vegetative vacuoles. The identity of each vacuole is determined by its pH and by the presence of specific proteins known to be localized to PSVs or LVs, such as tonoplast intrinsic proteins (TIPs), which are integral membrane proteins found in specific vacuolar membranes (Jauh et al. 1999; Johnson et al. 1989). For example, the PSVs have a neutral pH and are defined by the presence of  $\alpha$ - and  $\delta$ -tonoplast intrinsic protein (TIP), whereas the LVs have an acidic pH and are marked by  $\gamma$ -TIP (Jiang et al. 2000; Jauh et al. 1999).

Vacuoles are increasingly recognized for their role in cellular signaling during growth (Zhang et al. 2014), the immune responses (Hatsugai and Hara-Nishimura 2010) and the regulation of cell death (CD) (Hara-Nishimura and Hatsugai 2011; Koyano et al. 2014). However, little is known about vacuolar structures and their roles in the defense response against pathogens. Several reviews have summarized the interactions between the plant vacuole and pathogenic microbes (Hara-Nishimura and Hatsugai 2011; Hatsugai et al. 2006). Here, the first section of this review focuses on the most up-to-date insights about the plant vacuolar structures and dynamics and vacuolar markers. The last section focuses on the role of the vacuole and vacuolar structures in plant-pathogen interactions.

### Vacuolar structures

Recent advances in the visualization of the vacuole together with developments in image analysis has revealed the highly organized and complex morphology of the vacuole as well as its dynamics. The plant vacuole is surrounded by a membrane barrier known as the tonoplast, which separates the vacuolar content from the cytoplasm (Fig. 1). The semi-permeable tonoplast maintains a balance of nutrients and ions inside and outside of the vacuole, thus keeping a suitable turgor pressure in the plant cell.

The tonoplast not only surrounds the typical large vacuole but also other transient and mobile structures such as transvacuolar strands (TVS) and bulbs, represented in Fig. 1 (Ruthardt et al. 2005; Uemura et al. 2002). TVSs are dynamic thin tubular structures that traverse the central vacuole, containing cytoplasm and even small organelles (Uemura et al. 2002). Moreover, TVSs provide a direct connection between the perinuclear cytoplasm and the cortical cytoplasm of the cell and as such they act as an important transport route for the distribution of the cytoplasmic content, including the smaller organelles (Grolig and Pierson 2000; Nebenführ et al. 1999). Indeed, it was observed that Golgi bodies (Nebenführ et al. 1999), mitochondria (Van Gestel et al. 2002), endosomes (Ovečka et al. 2005; Ruthardt

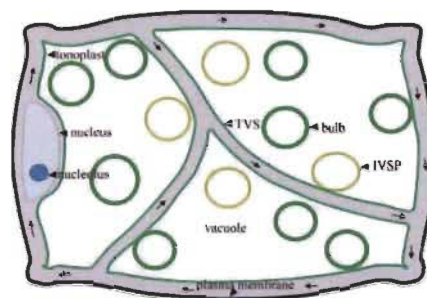


**Fig. 1** Schematic diagram presents the vacuole and vacuolar structures in plant cells. The vacuole structures tonoplast, TVS, bulb, IVSP, nucleus, nucleolus, and plasma membrane are shown with arrowheads and the cytosolic flow with arrows. TVS transvacuolar structures, IVSP intravacuolar spherical structures

et al. 2005), and amyloplasts (Saito et al. 2005) dynamically move through the TVSs. Additionally, they play a role in the positioning of the nucleus (Katsuta et al. 1990; Kumagai and Hasezawa 2001; Williamson 1993). The dynamics of the TVS depends on the actin cytoskeleton; consequently, the disruption of the actin filaments leads to the loss of the transvacuolar strands and inhibition of their movement (Kovar et al. 2000; Kutsuna et al. 2003; Tominaga et al. 2000).

On the other hand, the bulbs are highly dynamic spherical structures between 1 and 22  $\mu\text{m}$  of diameter located in the vacuolar lumen (Madina et al. 2018; Saito et al. 2002). 3-D reconstruction of electronic microscopic images indicates that the bulbs are formed of a double membrane and cytoplasmic material is detected between the two lipid bilayers (Saito et al. 2002). This double membrane of the bulbs is responsible for their brighter fluorescence signal compared to that of the tonoplast membrane (Saito et al. 2002). Similar to the dynamics of the TVSs, the movement of the bulbs is dependent on actin (Beebo et al. 2009; Uemura et al. 2002). However, whether bulbs are naturally occurring structures has recently been questioned by Segami et al. (2014), as they proposed that some bulbs are artifacts due to the dimerization of the GFP moiety of tagged tonoplastic proteins, while intravacuolar spherical structures (IVSP) form naturally. The IVSPs are different from bulbs in fluorescence intensity (two-folds the fluorescence intensity of the tonoplast vs. 3 or more folds for the bulbs) and thickness of the double membranes (Segami et al. 2014). These structures are also less abundant in cells and are believed to temporarily store membrane components, however, whether IVSPs are independent structures remains to be resolved (Segami et al. 2014). This model also needs to be further explored as GFP dimerization alone cannot explain the accumulation of bulbs in the YFP-2xFYVE *A. thaliana* line, as this marker binds to the membrane via a protein-lipid interaction and not a transmembrane domain



(Saito et al. 2011). Two functions have been proposed for bulbs; first they may be involved in tonoplasmic proteins degradation inside of the vacuole (Maftrejean et al. 2011; Saito et al. 2002). On the other hand, they may be useful for rapid cell expansion by serving as membrane reservoirs (Saito et al. 2002). Recently, Han et al. (2015) even proposed that bulbs may not have specific functions other than the transient accumulation of tonoplast and cytoskeletal proteins until the bulb membrane is reabsorbed back into the tonoplast. Thus, the definitive function and biogenesis mechanism of bulbs still need to be fully elucidated.

### Markers to study the vacuolar structures

The large central vacuole can be easily detected as a large transparent region in the plant cell as seen in light microscopy (Marty 1999), whereas the fine structure of the tonoplast and the intravacuolar compartments had mostly been studied by electron microscopy (Gaffal et al. 2007; Gao et al. 2015; Morita et al. 2002; Saito et al. 2002). The development of chemicals and fluorescent protein markers made possible the use of live-cell imaging to study the vacuole in a more detailed manner, which allows a greater understanding of its structure and dynamics under different growth conditions and various stress types (Reisen et al. 2005). Two different approaches for visualizing the plant vacuolar structures are presented here in below: chemical and protein markers. For selecting a particular technique, it is important to be aware of its advantages and limitations.

#### Chemical markers

To date, a number of fluorescent/chemical dyes have been identified for staining the tonoplast and vacuolar membranous structures (presented in Table 1). For example, the well-known amphiphilic styryl dyes, FM1-43 (*N*-(3-triethylammoniumpropyl)-4-(4-(dibutylamino)styryl) pyridinium dibromide) and FM4-64 (*N*-(3-triethylammoniumpropyl)-4-(4-diethylaminophenylhexatrienyl) pyridinium dibromide), are valuable and frequently used chemical dyes for vital staining of the tonoplast (i.e. staining in live cells) (Kim et al. 2001; Kutsuna and Hasezawa 2002; Kutsuna et al. 2003; Leshem et al. 2006; Okubo-Kurihara et al. 2008; Parton et al. 2001; Silady et al. 2008; Tanaka et al. 2007). The FM4-64 has also been reported for staining transvacuolar strands (Kutsuna and Hasezawa 2002; Kutsuna et al. 2003; Silady et al. 2008; Tanaka et al. 2007) and bulbs (Kim et al. 2001; Silady et al. 2008; Tanaka et al. 2007). The FM dyes initially stain the plasma membrane, then small cytoplasmic compartments, and finally reach the tonoplast in a process that is time, temperature, and energy-dependent. In general, to label the tonoplast with FM dyes, the cells are pulsed labeled for several

minutes and then chased for several hours in fresh medium. The optimal duration of the chase period depends on the trafficking activity of the cells. In the initial stage of the chase period, the dyes simultaneously label the tonoplast and the other endomembrane components, including the endosomal organelles and developing cell plates (Higaki et al. 2008; Kutsuna and Hasezawa 2002; Ovečka et al. 2005; Parton et al. 2001; Tanaka et al. 2007; Ueda et al. 2001; Vermeer et al. 2006), whereas a longer chase period is required to visualize only the tonoplast (Emans et al. 2002; Kutsuna and Hasezawa 2002; Ueda et al. 2001). In addition to the FM dyes, BCECF (2',7'-bis-(2-carboxyethyl)-5-(and-6)-carboxy-fluorescein) fluorescently labels the vacuolar lumen, the tonoplast, the transvacuolar strands, and the bulbs (Higaki et al. 2007; Kutsuna and Hasezawa 2002; Mitsuhashi et al. 2000; Swanson et al. 1998; Toyooka et al. 2006). Vital staining using dyes is rapid, simple to perform, and compatible with the concomitant visualization of fluorescently tagged protein markers. However, this method has several limitations, in either sensitivity or specificity, and vital dyes themselves can sometimes introduce artifacts that must be taken care of during sample preparation or live cells imaging (Melan 1999; Schnell et al. 2012).

#### Protein markers

In addition to chemical markers, many marker proteins tagged with fluorescent proteins are used to label the tonoplast and the vacuolar structures in living cells (Table 1). Most of those markers are integral membrane proteins, with the exception of YFP-2xFYVE which lacks a transmembrane domain and binds to phosphatidylinositol 3-phosphate (Saito et al. 2011). As YFP-2xFYVE labels bulbs more intensely than the tonoplast, it suggests that PI3P is more concentrated in the bulbs (Vermeer et al. 2006; Saito et al. 2011). However, not all tonoplast markers can also label bulbs, showing that bulb membranes are qualitatively different than tonoplast membranes (Saito et al. 2002). For example,  $\gamma$ -TIP-GFP was found to be concentrated in tonoplast and bulbs, whereas GFP-ATRAB7c, another tonoplast marker, did not give any fluorescent signal in bulbs from transgenic plants, although the presence of bulbs in these lines was confirmed by transmission electron microscopy (Saito et al. 2002). Some aquaporin isoforms also specifically label tonoplast or bulbs, for example TIP2;1-GFP exclusively localizes in the tonoplast but does not label the bulbs in salt-treated root cells, whereas TIP1;1 relocalized into intracellular spherical structures hypothesized to be tonoplast compartmentalization domains specialized for degradation of this isoform (Boursiac et al. 2005). In addition, two candidate effectors of pathogens have been observed to target the tonoplast and tonoplast-derived structures (TVSs and bulbs): HaRxLR17 from the oomycete *Hyaloperonospora arabidopsidis* (*Hpa*)

**Table 1** Chemical and protein markers for labeling tonoplast, TVS, and bulbs

Name of proteins	Tonoplast	TVS	Bulbs	References
<b>Protein markers</b>				
Nitrate transporter (chloride channel a; CLCa)	✓	X	X	(De Angeli et al. 2006)
gamma-TIPs	✓	X	X	(Okubo-Kurihara et al. 2008; Opalski et al. 2005)
	✓	X	✓	(Gattolin et al. 2009; Hunter et al. 2007)
	✓	✓	✓	(Beebo et al. 2009; Boursiac et al. 2005; Hawes et al. 2001; Hicks et al. 2004; Hunter et al. 2007; Saito 2003)
δ-TIP	✓	✓	✓	(Sheahan et al. 2007)
δ-TIP2;1	✓	X	X	(Boursiac et al. 2005; Jaquinod et al. 2007)
Small G protein (AtRab75c)	✓	✓	X	(Saito et al. 2002)
BobTIP26-1-GFP	✓	✓	✓	(Reisen et al. 2005)
Carbohydrate transporter	✓	X	X	(Endler et al. 2006; Jaquinod et al. 2007; Wormit et al. 2006)
Phosphate transporter homolog GFP	✓	X	✓	(Escobar et al. 2003)
Metal transporter	✓	X	X	(Jaquinod et al. 2007; Thomine et al. 2003)
Syntaxin (Vam3 or SYP22)	✓	X	✓	(Bottanelli et al. 2011; Foresti et al. 2006; Kusumi et al. 2005)
	✓	✓	✓	(Uemura et al. 2002)
Lipocalin	✓	X	X	(Jaquinod et al. 2007)
CCD1	✓	X	X	(Jaquinod et al. 2007)
Ca <sup>2+</sup> transporter	✓	X	X	(Kamiya et al. 2006; Peiter et al. 2005)
Zn <sup>2+</sup> transporter	✓	X	X	(Kobae et al. 2004)
Malate transporter	✓	X	X	(Kovermann et al. 2007)
Organic cation transporter	✓	X	X	(Küfner and Koch 2008)
Phospholipase-like protein	✓	X	X	(Morita et al. 2002)
AtREG2	✓	X	X	(Schaaf et al. 2006)
K <sup>+</sup> transporter	✓	X	✓	(Voelker et al. 2006)
Cytochrome P450	✓	X		(Xu et al. 2006)
Phosphatidylinositol 3-phosphate probe (2xFYVE)	✓	X	✓	(Vermeer et al. 2006)
GFP: EBD	✓	X	✓	(Kim et al. 2001)
YFP-AtRabG3c	✓	X	✓	(Bozkurt et al. 2015)
Tonoplast potassium channel 1 (TPK1)-GFP (AtTPK1-GFP)	✓	X	✓	(Mairejean et al. 2011)
DUF679 Membrane Protein 1 (DMP1)-enhanced GFP (DMP1-eGFP)	✓	✓	✓	(Kasaras et al. 2012)
Vacuolar H <sup>+</sup> -pyrophosphatase (VHP1)-GFP	✓	✓	✓	(Segami et al. 2014)
<b>Mutation of some genes</b>				
Vacuole defective gene ( <i>vac11</i> )	✓	✓	✓	(Hicks et al. 2004)
<i>rbb1</i>	✓	✓	✓	(Han et al. 2015)
<b>Pathogen's protein marker</b>				
Mlp124357	✓	✓	✓	(Madina et al. 2018)
HpaRxLR	✓	✓	✓	(Caillaud et al. 2012; Inada and Ueda 2014)
<b>Chemical markers</b>				
FM1-43	✓	X	X	(Kim et al. 2001; Kutsuna and Hasezawa 2002; Kutsuna et al. 2003; Leshem et al. 2006; Okubo-Kurihara et al. 2008; Parton et al. 2001; Silady et al. 2008; Tanaka et al. 2007)
FM4-64	✓	✓	✓	(Higaki et al. 2006; Kim et al. 2001; Kusumi et al. 2005; Kutsuna and Hasezawa 2002; Kutsuna et al. 2003; Leshem et al. 2006; Okubo-Kurihara et al. 2008; Parton et al. 2001; Silady et al. 2008; Tanaka et al. 2007)



Table 1 (continued)

Name of proteins	Tonoplast	TVS	Bulbs	References
BCECF (2',7'-bis-(2-carboxyethyl)-5-(and-6)-carboxy-fluorescein)	✓	✓	✓	(Higaki et al. 2007; Kutsuna and Hasezawa 2002; Mitsuhashi et al. 2000; Swanson et al. 1998; Toyooka et al. 2006)

✓ label, X not label

(Bozkurt et al. 2015; Caillaud et al. 2012) and Mlp124357 from the fungus *Melampsora larici-populina* (Mlp) (Madina et al. 2018), and they can be used to study those organelles. The GFP-tagged marker proteins allow the visualization of the vacuole and vacuolar structures without further experimental manipulations once the transgenic lines are constructed. Although this is a powerful technique, it is laborious, time-consuming, and often not practical for many laboratories (Melan 1999; Schnell et al. 2012).

### Protein distribution and motility of tonoplast and bulbs

#### Protein distribution

The complexity and dynamic changes in vacuolar lumen content raise the question of how cells regulate the movement of these materials between the cytosol and the vacuole. A controlled transport across the tonoplast is essential for appropriate plant responses to environmental conditions and for adequate intracellular signaling. The tonoplast contains numerous proteins that facilitate the transport of water, ions and metabolic products across the membrane (Martinoia et al. 2012; Zhang et al. 2014). In response to variation in the cytoplasmic environments, the activity of tonoplast enzymes, transporters, and channels is changed and thus they regulate the material exchange between the cytoplasm and the vacuolar lumen, maintaining cellular homeostasis. For example, H<sup>+</sup>-ATPase (V-ATPase), H<sup>+</sup>-pyrophosphatase (V-PPase), and water channels (aquaporins) have been characterized and their roles in the regulation of transport across the membrane have been discussed (Hedrich 2012; Martinoia et al. 2012; Neuhaus and Trentmann 2014).

On the other hand, the lipids of the tonoplast provide an essential molecular environment for the activity of the membrane proteins and serve as a barrier between the cytoplasm and the vacuolar lumen. Interestingly, lipids and proteins in the tonoplast are not always uniformly distributed and tend to be enriched in particular regions, termed membrane micro-domains, that depend on sphingolipids and sterols (Kusumi et al. 2005; Lillemeier et al. 2006; Minami et al. 2009). For example, the tonoplast of *Arabidopsis* suspension cultured cells contains micro-domains with higher ratios of the saturated phospholipids phosphatidylcholine (PC) and

phosphatidylethanolamine (PE) in which the vacuolar-type proton ATPase (V-ATPase) was more abundant in detergent-resistant microdomains and appeared to be unevenly distributed in the tonoplast, whereas the vacuolar-type proton pyrophosphatase (V-PPase) was distributed evenly (Yoshida et al. 2013). Another study showed a similar non-uniform distribution of the V-ATPase in the tonoplast of isolated maize root cells (Kluge et al. 2004) and detergent-resistant micro-domains containing a high percentage of sphingolipids, free sterols and saturated fatty acids were described in the tonoplast of sugar-beet roots (Ozolina et al. 2011). The causes of this precise distribution of lipids and proteins in the tonoplast membrane are not fully elucidated yet; however, the environmental conditions seem to act as important regulators. For example, under phosphate deficiency the *Arabidopsis* phospholipase D PLD $\zeta$ 2 adopts an uneven distribution in which the higher concentrations of PLD $\zeta$ 2 were preferentially positioned close to mitochondria and chloroplasts and thus facilitated transfer between them and the tonoplast (Yamaryo et al. 2008).

Recently, it was observed that an overexpression in *Arabidopsis* of tonoplast intrinsic protein 1;1 fused with GFP (AtTIP1;1-GFP) labels both the tonoplast and the bulbs of the central vacuole but that the distribution of the GFP fusion protein was uneven along the tonoplast (Beebo et al. 2009). We also observed an uneven distribution of a fluorescently tagged protein on the bulb membrane (Video S1). Our recent report showed that the candidate effector protein Mlp124357-eGFP localized in the tonoplast, the TVS, and the bulbs of the vacuolar lumen in *Arabidopsis* (Madina et al. 2018). With the help of high-resolution 3-D imaging, we observed two different distribution patterns on the bulb membranes for both Mlp124357-eGFP and the well-known tonoplast marker  $\gamma$ -TIP-YFP. This suggests the existence of two distinct bulb types in these cells, some with a regular marker protein distribution and some with exclusion spots.

#### Protein mobility

Previous description of bulbs and prevailing models indicate they are connected to the tonoplast (Saito et al. 2002). On the other hand, a report pointed out the qualitative differences in protein content between the bulb membranes and the tonoplast (Saito et al. 2011). To investigate the connection

between the two membranes, protein mobility between the tonoplast and the bulb membrane have recently been assessed using fluorescence recovery after photobleaching (FRAP) of young *Arabidopsis* leaf epidermal cells expressing Mlp124357-eGFP or  $\gamma$ -TIP-YFP. We observed the fluorescence of the bleached region of tonoplast recovered completely within 1 min, whereas the bleached area of the bulb membrane fluorescence did not recover (Madina et al. 2018). This observation can be explained by two mechanisms: (1) something restricts the movement of proteins from the tonoplast to the bulb membrane even though they are still attached or (2) the connection between the bulbs and the tonoplast is severed. Both explanations provide a new perception of the biology of tonoplast-derived substructures, but further investigation is required to validate the molecular mechanisms implicated. Furthermore, as the vacuole plays a crucial role in plant defense, the role of protein distribution and motility in tonoplast and bulbs should also be the focus of more research.

### The vacuole in plant-pathogen interaction

The immune system of plants lack antibodies or phagocytosis. As an alternative, they have evolved numerous layers of active defense responses against pathogens including the production of reactive oxygen species (ROS) (Alvarez et al. 1998; Zhang et al. 2003) and of many other defense compounds such as phytoalexins (Neuhaus et al. 1991). Attempted attacks by avirulent pathogens may result in cell death (CD) in the tissues, a reaction known as the hypersensitivity response (HR), which is effective in preventing the spread of pathogens (Mur et al. 2007). These defense responses largely depend on the plant's vacuole because it constitutes a reservoir for many secondary metabolites, hydrolytic enzymes and defense proteins (Marty 1999; Hara-Nishimura and Hatsugai 2011).

### Secondary metabolites

Plant vacuoles accumulate a variety of secondary metabolites including cyanogenic glycosides, benzoxazinoids, and phenolics, some of which are thought to function as direct defenses against pathogens by reducing their performance, survival, and reproduction (Shitan 2016; Steppuhn et al. 2004). For example, the well-known cyanogenic glycosides are stored in the plant vacuole as inactive precursors and are able to form toxic hydrocyanic acid (HCN) in response to tissue damage by different phytopathogens (Vetter 2000; Freeman and Beattie 2008). A recent study reported that mutation of the cyanogenic 4-hydroxyindole-3-carbonyl nitrile (4-OH-ICN) pathway increases susceptibility to the bacterial pathogen *Pseudomonas syringae* in *Arabidopsis*, suggesting a role in inducible pathogen defense (Rajniak

et al. 2015). Benzoxazinoids are among the most important plant defense compounds for grasses (Poaceae) and are also stored as inactive glucosides in the vacuole to avoid toxicity to the plant itself (Niemeyer 2009; Handrick et al. 2016; Zhou et al. 2018). While some benzoxazinoids are constitutively present, others are only synthesised following pathogen infection. Upon tissue damage, they undergo enzymatic and chemical degradation to become the active benzoxazinoid form (Niemeyer 2009). Benzoxazinoids have also been shown to act as defense signaling molecules and to induce callose deposition in response to the pathogenic fungal elicitor chitosan in maize (Ahmad et al. 2011). Another large group of secondary metabolites implicated in defense are the flavonoids, which are widely distributed in terrestrial plants and serve as defense compounds in the plant-microbe interaction (Harborne and Williams 2000; Taylor and Grotewold 2005; Grotewold 2006). For example, silencing of a G-type ABC transporter of *M. truncatula* (MtABCG10) results in a lower concentration of isoflavonoids in the roots which in turns results in increased growth of *Fusarium oxysporum*, indicating that flavonoids play an important role in the defense against root-infecting pathogens (Banasiak et al. 2013). Finally, the seed coat accumulates flavonoids to protect the embryo and the endosperm from external stresses such as UV radiation and pathogen infections (Lepiniec et al. 2006; Shimada et al. 2006, 2018).

### Hydrolytic enzymes

Like animal lysosome, plant vacuole contains hydrolytic enzymes (e.g. aspartate proteinases, cysteine proteinases, and nucleases) that play an important role in the crucial events of plant cell death to prevent the spread of biotrophic pathogens (Boller and Kende 1979; Wada 2013). As first reported by Jones almost two decades ago, the plant vacuole play an important role in the programmed cell death that occurs in response to biotrophic pathogens (Jones 2001). It was also reported that the vacuolar processing enzyme (VPE) is up-regulated during cell death associated with leaf senescence and lateral root formation in *Arabidopsis* (Hatsugai et al. 2004). The same group confirmed that during the defense response, plants use the vacuole content in both a destructive and a non-destructive way. The destructive pathway is effective against virus infection, during which the tonoplast collapses and releases vacuolar hydrolytic enzymes called vacuolar processing enzymes (VPE) to suppress virus proliferation in the host cytosol (Hatsugai et al. 2004). The non-destructive way is effective against extracellular bacterial infections and involves the fusion of the plasma membrane to the tonoplast, which allows the discharge of the vacuolar content, including the proteasome subunit PBA1, in the apoplast. This leads to a hypersensitive cell death which suppresses the bacterial proliferation (Hatsugai et al.



2009). Interestingly, although structurally unrelated to caspases, both the vacuolar processing enzyme and the proteasome subunit PBA1 exhibit a caspase-like activity (Hatsugai et al. 2009). As it has been observed that proteasome defects impair the vacuole membrane fusion and VPE deficiency prevents virally induced hypersensitive cell death (Hatsugai et al. 2004, 2009), the identification of PBA1 and VPE substrates would help to unravel the molecular mechanisms of tonoplast breakdown or fusion with the PM.

### Defense proteins

The defense proteins, including pathogenesis related proteins (PR proteins) (Neuhaus et al. 1991), myrosinases (Ueda et al. 2006), and lectins (Bowles et al. 1986), are located in the vacuole and act as an effective second line of defense when a pathogen causes tissue damage. For example, overexpression of the pathogen-inducible PR1 genes in tobacco enhances resistance to several fungi, including *Peronospora tabacina* and *Phytophthora parasitica f.sp. nicotianae*, and to the bacteria *Pseudomonas syringae pv. tabaci* (Broekaert et al. 2000). The association between PR-1 proteins and enhanced resistance against oomycetes has also been noted when PR1 expression was transiently silenced by double-stranded RNA interference in barley (Schultheiss et al. 2003). The myrosinases accumulate mainly in the vacuoles of idioblastic myrosin cells, a cell type specific to the abaxial side of the leaf known to accumulate myrosinases (Höglund et al. 1991, 1992; Thangstad et al. 1990, 1991). When plants experience tissue damage, the myrosinases are released from the collapsed vacuoles of the myrosin cells and start the hydrolysis of their glucosinolate substrates to produce isothiocyanates, which are toxic for bacteria. This chemical defense system is known as the myrosinase-glucosinolate system, which is also called the mustard oil bomb (Fuji et al. 2016; Grubb and Abel 2006; Halkier and Gershenzon 2006; Hopkins et al. 2009; Kissen et al. 2009; Rask et al. 2000; Wittstock and Halkier 2002). Moreover, overexpression of Ta-JA1, a jacalin-related lectin gene that resides in vacuole, has been found to increase resistance to bacteria, fungal, and viral pathogens in tobacco plant (Ma et al. 2010).

### Vacuole dynamics

The relationship between vacuole dynamics and cell death during the defense response has been discussed for over a decade (Jones 2001). For example, during cell death of the tracheary element in *Zinnia elegans*, disintegration of the tonoplast was observed (Obara et al. 2001). Recent studies have demonstrated that during cell death induced by a pathogenic signal such as the oomycete elicitor cryptogein from *Phytophthora cryptogea* or the bacteria *Erwinia carotovora*, the complex vacuole of BY-2 cells simplified and

then ruptured (Higaki et al. 2007; Hirakawa et al. 2015). This seem to be regulated by the vacuolar-localized protease called VPE (Higaki et al. 2011). The structural simplification of vacuoles is also observed in various processes involving program cell death, such as gibberellin-mediated cell death in central aleurone cells (Gao et al. 2015), embryogenesis of gymnosperms (Smertenko et al. 2003), and leaf formation in lace plants (Gunawardena 2007). However, it remains elusive whether simplification of the vacuole is a typical process in defense-related CD.

### Tonoplast, TVS, and bulbs in plant-pathogen interaction

Although the vacuole plays an important role in plant defense, little is known about the manipulation of plant vacuolar structures by pathogens. To date, only two effector proteins, one from *H. arabidopsidis* and the other from *M. larici-populina*, have been found to reside in the host tonoplast, TVS, and bulbs (Bozkurt et al. 2015; Caillaud et al. 2012; Madina et al. 2018). Such localization of effector proteins may indicate a pathogenic strategy to modulate the host vacuole and vacuolar structures to suppress the vacuole-mediated defense response. For example, dynamic changes of the vacuolar structures are observed during cryptogein-induced PCD in tobacco BY-2 cells (Higaki et al. 2007). As illustrated in Fig. 2, immediately after cryptogein-treatment, no prominent structural changes of the cells were observed, rather, a complex vacuole structures featuring many trans-vacuolar strands were seen and the nuclei localizes in the central region of the cell (Fig. 2a). However, after some time the TVSs are gradually decreased in number and complexity and bulb structures appeared (Fig. 2b). Subsequently, bulb structures disappeared resulting the simpler vacuolar structure before the cell death (Fig. 2c, d). The simple-shaped vacuole weakened the tonoplast, leading to its ruptures, which sequentially would be lethal for the cell since it would dilute and acidify the cytosol and release cellular reactive secondary metabolites and hydrolytic enzymes (Higaki et al. 2011). A similar kind of vacuolar simplification was observed in BY-2 cells treated with culture filtrates of *Erwinia carotovora*, a plant pathogenic bacterium (Hirakawa et al. 2015), but in that situation the lysis of the plasma membrane seemed to occur while the vacuole was still intact. It is believed that the simplification of the vacuole is crucial for the vacuolar breakdown, but how these phenomena are orchestrated remains to be elucidated.

### Conclusions and future perspectives

Although the role of the vacuole in plant-pathogen interactions has recently attracted much attention, our knowledge of the pathogen manipulation of host vacuolar membrane

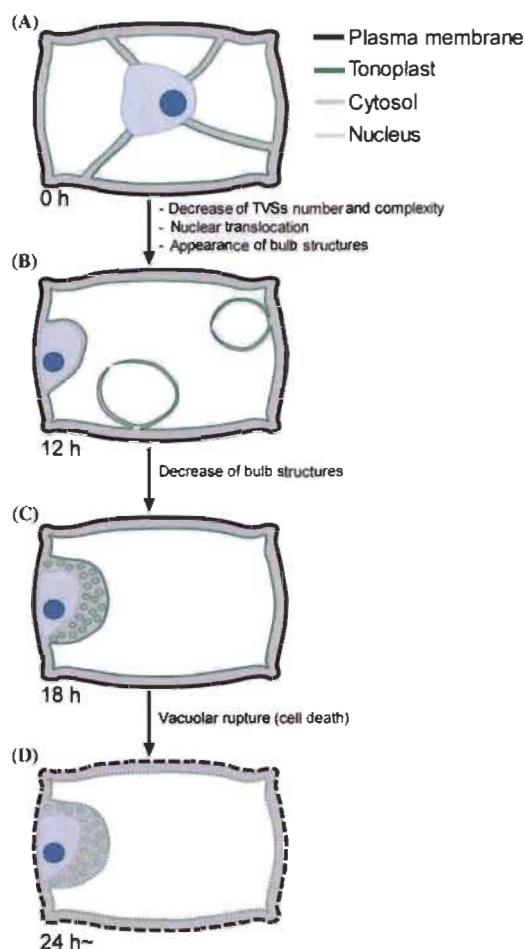


**Fig. 2** A schematic illustration of the reorganization of the vacuolar structures during pathogen-induced cell death in BY-2 cells. **a** After cryptogin treatment at 0 h, the vacuole contains many transvacuolar strands and the nucleus localizes at the central region of the cell. **b** After 12 h, the nucleus moves from the center to the periphery of the cell and bulb-like structures appear within the vacuole while transvacuolar strands are gradually disrupted. **c** After 18 h, the bulb-like structures disappear, and small spherical vacuoles appear. **d** After 24 h, the VM and PM lose their integrity. Dashed lines indicate broken membranes

structures and trafficking remains minimal. As we have reviewed here, plant vacuolar structures are highly organized and dynamic, and they are involved in many cellular processes including plant-pathogen interactions. However, further studies are necessary to characterize the biogenesis mechanisms of bulbs and transvacuolar strands and to elucidate which physiological roles they play in the environmental responses of plants. Live-cell imaging using chemical

dyes or fluorescently tagged proteins will undoubtedly serve as a critical technique to reveal the underlying mechanisms between vacuolar structural trafficking and plant-pathogen interactions and the use of plants defective in specific transport steps in vacuolar trafficking will help to elucidate the intracellular itinerary of still uncharacterized bulb membrane proteins.

**Acknowledgements** We are very thankful to Melodie B. Plourde for critical review of the manuscript.

**Author contributions** Conceptualization: MHM, HZ, HG. Data curation: MHM, MSR, HZ, HG. Funding acquisition: HG. Methodology: MHM, MSR, HG. Project administration: HZ, HG. Resources: HG. Software: MSR, HG. Supervision: HZ, HG. Validation: MHM, MSR, HZ, HG. Visualization: MHM, HG. Writing—original draft: MHM, MSR, HG. Writing—review & editing: HZ, HG.

**Funding** This work was supported by a NSERC Grant No. RGPIN/435870-2013 and Canada Research Chair number 950-231 790.

### Compliance with ethical standards

**Conflict of interest** All the authors declare that there are no conflicts of interest.

### References

- Ahmad et al (2011) Benzoxazinoid metabolites regulate innate immunity against aphids and fungi in maize. *Plant Physiol* 157:317–327
- Alvarez ME, Pennell RI, Meijer PJ, Ishikawa A, Dixon RA, Lamb C (1998) Reactive oxygen intermediates mediate a systemic signal network in the establishment of plant immunity. *Cell* 92:773–784
- Banasiak J, Biala W, Staszko A, Swarczewicz B, Kępczyńska E, Figlerowicz M, Jasiński M (2013) A *Medicago truncatula* ABC transporter belonging to subfamily G modulates the level of iso-flavonoids. *J Exp Bot* 64:1005–1015
- Beebo A et al (2009) Life with and without AtTIPI1; 1, an *Arabidopsis* aquaporin preferentially localized in the apposing tonoplasts of adjacent vacuoles. *Plant Mol Biol* 70:193–209
- Bewley JD, Black M (1994) Seeds: physiology of development and germination, 2nd edn. Plenum Press, New York
- Boller T, Kende H (1979) Hydrolytic enzymes in the central vacuole of plant cells. *Plant Physiol* 63:1123–1132
- Bottanelli F, Foresti O, Hanton S, Denecke J (2011) Vacuolar transport in tobacco leaf epidermis cells involves a single route for soluble cargo and multiple routes for membrane cargo. *Plant Cell* 23:3007–3025
- Boursiac Y, Chen S, Luu D-T, Sorieul M, Van den Dries N, Maurel C (2005) Early effects of salinity on water transport in *Arabidopsis* roots. Molecular and cellular features of aquaporin expression. *Plant Physiol* 139:790–805
- Bowles DJ, Marcus SE, Pappin D, Findlay J, Eliopoulos E, Maycox PR, Burgess J (1986) Posttranslational processing of concanavalin A precursors in jackbean cotyledons. *J Cell Biol* 102:1284–1297
- Bozkurt TO, Belhaj K, Dagdas YF, Chaparro-Garcia A, Wu CH, Cano LM, Kamoun S (2015) Rerouting of plant late endocytic trafficking toward a pathogen interface. *Traffic* 16:204–226
- Broekaert WF, Terras FRG, Cammue BPA (2000) Induced and pre-formed antimicrobial proteins. In: Slusarenko AJ, Fraser RSS,



- van Loon LC (eds) Mechanisms of resistance to plant diseases. Kluwer Academic Publishers, Dordrecht, pp 371–477
- Cuillaud MC, Piquerez SJ, Fahro G, Steinbrenner J, Ishaque N, Beynon J, Jones JD (2012) Subcellular localization of the Hpa RxLR effector repertoire identifies a tonoplast-associated protein HaRxLR17 that confers enhanced plant susceptibility. *Plant J* 69:252–265
- De Angeli A, Monachello D, Ephritikhine G, Frachisse J, Thomine S, Gambale F, Barbier-Brygoo H (2006) The nitrate/proton antiporter AtCLCa mediates nitrate accumulation in plant vacuoles. *Nature* 442:939
- Emans N, Zimmermann S, Fischer R (2002) Uptake of a fluorescent marker in plant cells is sensitive to brefeldin A and wortmannin. *Plant Cell* 14:71–86
- Endler A et al (2006) Identification of a vacuolar sucrose transporter in barley and *Arabidopsis* mesophyll cells by a tonoplast proteomic approach. *Plant Physiol* 141:196–207
- Epimashko S, Meckel T, Fischer-Schliebs E, Lüttge U, Thiel G (2004) Two functionally different vacuoles for static and dynamic purposes in one plant mesophyll leaf cell. *Plant J* 37:294–300
- Escobar NM, Haupt S, Thow G, Boevink P, Chapman S, Oparka K (2003) High-throughput viral expression of cDNA-green fluorescent protein fusions reveals novel subcellular addresses and identifies unique proteins that interact with plasmodesmata. *Plant Cell* 15:1507–1523
- Foresti O, Luis L, Denecke J (2006) Overexpression of the *Arabidopsis* syntaxin PEP12/SYP21 inhibits transport from the pre-vacuolar compartment to the lytic vacuole in vivo. *Plant Cell* 18:2275–2293
- Freeman BC, Beattie GA (2008) An overview of plant defenses against pathogens and herbivores. *Plant Health Instr* 149
- Fuji K, Shirakawa M, Shimono Y, Kunieda T, Fukao Y, Koumoto Y, Takahashi H, Hara-Nishimura I, Shimada T (2016) The adaptor complex AP-4 regulates vacuolar protein sorting at trans-Golgi network by interacting with VACUOLAR SORTING RECEPTOR 1. *Plant Physiol* 170:211–219
- Gaffal KP, Friedrichs GJ, El-Gammal S (2007) Ultrastructural evidence for a dual function of the phloem and programmed cell death in the floral nectary of *Digitalis purpurea*. *Ann Bot* 99:593–607
- Guo C, Zhao Q, Jiang L (2015) Vacuoles protect plants from high magnesium stress. *Proc Natl Acad Sci USA* 112:2931–2932
- Gattolin S, Sorieul M, Hunter PR, Khonsari RH, Frigerio L (2009) In vivo imaging of the tonoplast intrinsic protein family in *Arabidopsis* roots. *BMC Plant Biol* 9:133
- Grolig F, Pierson ES (2000) Cytoplasmic streaming: from flow to track. In: Actin: a dynamic framework for multiple plant cell functions, vol 89. Springer, New York, pp 165–190
- Grotewold E (2006) The genetics and biochemistry of floral pigments. *Ann Rev Plant Biol* 57:761–780
- Grubb CD, Abel S (2006) Glucosinolate metabolism and its control. *Trends Plant Sci* 11:89–100
- Gunawardena AH (2007) Programmed cell death and tissue remodeling in plants. *J Exp Bot* 59:445–451
- Halkier BA, Gershenzon J (2006) Biology and biochemistry of glucosinolates. *Ann Rev Plant Biol* 57:303–333
- Han SW, Alonso JM, Rojas-Pierce M (2015) REGULATOR OF BULB BIOGENESIS1 (RBB1) is involved in vacuole bulb formation in *Arabidopsis*. *PLoS ONE* 10:e0125621
- Handrick V et al (2016) Biosynthesis of 8-o-methylated benzoxazinoid defense compounds in maize. *Plant Cell* 28:1682–1700
- Hara-Nishimura I, Hatsugai N (2011) The role of vacuole in plant cell death. *Cell Death Differ* 18:1298–1304
- Harborne JB, Williams CA (2000) Advances in flavonoid research since 1992. *Phytochem* 55:481–504
- Hatsugai N, Hara-Nishimura I (2010) Two vacuole-mediated defense strategies in plants. *Plant Signal Behav* 5:1568–1570
- Hatsugai N et al (2004) A plant vacuolar protease, VPE, mediates virus-induced hypersensitive cell death. *Science* 305:855–858
- Hatsugai N, Kuroyanagi M, Nishimura M, Hara-Nishimura I (2006) A cellular suicide strategy of plants: vacuole-mediated cell death. *Apoptosis* 11:905–911
- Hatsugai N et al (2009) A novel membrane fusion-mediated plant immunity against bacterial pathogens. *Genes Dev* 23:2496–2506
- Hawes C, Saint-Jore CM, Brandizzi F, Zheng H, Andreeva AV, Boevink P (2001) Cytoplasmic illuminations: in planta targeting of fluorescent proteins to cellular organelles. *Protoplasma* 215:77–88
- Hedrich R (2012) Ion channels in plants. *Physiol Rev* 92:1777–1811
- Hicks GR, Rojo E, Hong S, Carter DG, Raikhel NV (2004) Germinating pollen has tubular vacuoles, displays highly dynamic vacuole biogenesis, and requires VACUOLESS1 for proper function. *Plant Physiol* 134:1227–1239
- Higaki T, Kutsuna N, Okubo E, Sano T, Hasezawa S (2006) Actin microfilaments regulate vacuolar structures and dynamics: dual observation of actin microfilaments and vacuolar membrane in living tobacco BY-2 cells. *Plant Cell Physiol* 47:839–852
- Higaki T et al (2007) Elicitor-induced cytoskeletal rearrangement relates to vacuolar dynamics and execution of cell death: in vivo imaging of hypersensitive cell death in tobacco BY-2 cells. *Plant Cell Physiol* 48:1414–1425
- Higaki T, Kutsuna N, Sano T, Hasezawa S (2008) Quantitative analysis of changes in actin microfilament contribution to cell plate development in plant cytokinesis. *BMC Plant Biol* 8:80
- Higaki T, Kuru T, Hasezawa S, Kuchitsu K (2011) Dynamic intracellular reorganization of cytoskeletons and the vacuole in defense responses and hypersensitive cell death in plants. *J Plant Res* 124:315–324
- Hirakawa Y, Nomura T, Hasezawa S, Higaki T (2015) Simplification of vacuole structure during plant cell death triggered by culture filtrates of *Erwinia carotovora*. *J Integr Plant Biol* 57:127–135
- Höglund A-S, Lenman M, Falk A, Rask L (1991) Distribution of myrosinase in rapeseed tissues. *Plant Physiol* 95:213–221
- Höglund A-S, Lenman M, Rask L (1992) Myrosinase is localized to the interior of myrosin grains and is not associated to the surrounding tonoplast membrane. *Plant Sci* 85:165–170
- Hoh B, Hinz G, Jeong B-K, Robinson DG (1995) Protein storage vacuoles form de novo during pea cotyledon development. *J Cell Sci* 108:299–310
- Hopkins RJ, van Dam NM, van Loon JJ (2009) Role of glucosinolates in insect-plant relationships and multitrophic interactions. *Ann Rev Entomol* 54:57–83
- Hunter PR, Craddock CP, Di Benedetto S, Roberts LM, Frigerio L (2007) Fluorescent reporter proteins for the tonoplast and the vacuolar lumen identify a single vacuolar compartment in *Arabidopsis* cells. *Plant Physiol* 145:1371–1382
- Inada N, Ueda T (2014) Membrane trafficking pathways and their roles in plant-microbe interactions. *Plant Cell Physiol* 55:672–686
- Jaquinod M, Villiers F, Kieffer-Jaquinod S, Hugouvioux V, Bruley C, Garin J, Bourguignon J (2007) A proteomics dissection of *Arabidopsis thaliana* vacuoles isolated from cell culture. *Mol Cell Proteomics* 6:394–412
- Jauh G-Y, Phillips TE, Rogers JC (1999) Tonoplast intrinsic protein isoforms as markers for vacuolar functions. *Plant Cell* 11:1867–1882
- Jiang L, Phillips TE, Rogers SW, Rogers JC (2000) Biogenesis of the protein storage vacuole crystalloid. *J Cell Biol* 150:755–769
- Johnson KD, Herman EM, Chrispeels MJ (1989) An abundant, highly conserved tonoplast protein in seeds. *Plant Physiol* 91:1006–1013
- Jones AM (2001) Programmed cell death in development and defense. *Plant Physiol* 125:94–97
- Kanaiya T, Akahori T, Ashikari M, Maeshima M (2006) Expression of the vacuolar Ca<sup>2+</sup>/H<sup>+</sup> exchanger, OsCAX1a, in rice: cell and

- age specificity of expression, and enhancement by  $\text{Ca}^{2+}$ . *Plant Cell Physiol* 47:96–106
- Kasaras A, Melzer M, Kunze R (2012) *Arabidopsis* senescence-associated protein DMP1 is involved in membrane remodeling of the ER and tonoplast. *BMC Plant Biol* 12:54
- Katsuta J, Hashiguchi Y, Shibaoka H (1990) The role of the cytoskeleton in positioning of the nucleus in premitotic tobacco BY-2 cells. *J Cell Sci* 95:413–422
- Kim DH et al (2001) Trafficking of phosphatidylinositol 3-phosphate from the trans-Golgi network to the lumen of the central vacuole in plant cells. *Plant Cell* 13:287–301
- Kissen R, Rossiter JT, Bones AM (2009) The ‘mustard oil bomb’: not so easy to assemble?! Localization, expression and distribution of the components of the myrosinase enzyme system. *Phytochem Rev* 8:69–86
- Kluge C et al (2004) Subcellular distribution of the V-ATPase complex in plant cells, and in vivo localisation of the 100 kDa subunit VHA-a within the complex. *BMC Cell Biol* 5:29
- Kobae Y, Uemura T, Sato MH, Ohnishi M, Mimura T, Nakagawa T, Maeshima M (2004) Zinc transporter of *Arabidopsis thaliana* AtMTP1 is localized to vacuolar membranes and implicated in zinc homeostasis. *Plant Cell Physiol* 45:1749–1758
- Kovar DR, Staiger CJ, Weaver EA, McCurdy DW (2000) AtFim1 is an actin filament crosslinking protein from *Arabidopsis thaliana*. *Plant J* 24:625–636
- Kovermann P et al (2007) The *Arabidopsis* vacuolar malate channel is a member of the ALMT family. *Plant J* 52:1169–1180
- Koyano T, Kurusu T, Hanamata S, Kuchitsu K (2014) Regulation of vacuole-mediated programmed cell death during innate immunity and reproductive development in plants. In: Sawada H, Inoue N, Iwano M (eds) Sexual reproduction in animals and plants. Springer, Tokyo, pp 431–440
- Küfner I, Koch W (2008) Stress regulated members of the plant organic cation transporter family are localized to the vacuolar membrane. *BMC Res Notes* 1:43
- Kumagai F, Hasezawa S (2001) Dynamic organization of microtubules and microfilaments during cell cycle progression in higher plant cells. *Plant Biol* 3:4–16
- Kusumi A et al (2005) Paradigm shift of the plasma membrane concept from the two-dimensional continuum fluid to the partitioned fluid: high-speed single-molecule tracking of membrane molecules. *Ann Rev Biophys Biomol Struct* 34:351–378
- Kutsuna N, Hasezawa S (2002) Dynamic organization of vacuolar and microtubule structures during cell cycle progression in synchronized tobacco BY-2 cells. *Plant Cell Physiol* 43:965–973
- Kutsuna N, Kumagai F, Sato MH, Hasezawa S (2003) Three-dimensional reconstruction of tubular structure of vacuolar membrane throughout mitosis in living tobacco cells. *Plant Cell Physiol* 44:1045–1054
- Lepiniec L, Debeaujon I, Routaboul J-M, Baudry A, Pourcel L, Nesi N, Caboche M (2006) Genetics and biochemistry of seed flavonoids. *Ann Rev Plant Biol* 57:405–430
- Leshem Y et al (2006) Suppression of *Arabidopsis* vesicle-SNARE expression inhibited fusion of  $\text{H}_2\text{O}_2$ -containing vesicles with tonoplast and increased salt tolerance. *Proc Natl Acad Sci USA* 103:18008–18013
- Lillemeier BF, Pfeiffer JR, Surviladze Z, Wilson BS, Davis MM (2006) Plasma membrane-associated proteins are clustered into islands attached to the cytoskeleton. *Proc Natl Acad Sci USA* 103:18992–18997
- Ma QH, Tian B, Li YL (2010) Overexpression of a wheat jasmonate-regulated lectin increases pathogen resistance. *Biochimie* 92:187–193
- Madina MH, Zheng H, Germain H (2018) New insight into bulb dynamics in the vacuolar lumen of *Arabidopsis* cells. *Botany* 96:511–520
- Maîtrejean M et al (2011) Assembly and sorting of the tonoplast potassium channel AtTPK1 and its turnover by internalization into the vacuole. *Plant Physiol* 156:1783–1796
- Martinoia E, Meyer S, De Angeli A, Nagy R (2012) Vacuolar transporters in their physiological context. *Plant Biol* 63:183–213
- Marty F (1999) Plant vacuoles. *Plant Cell* 11:587–599
- Melan MA (1999) Overview of cell fixatives and cell membrane permeants. *Methods Mol Biol* 115:45–55
- Minami A et al (2009) Alterations in detergent-resistant plasma membrane microdomains in *Arabidopsis thaliana* during cold acclimation. *Plant Cell Physiol* 50:341–359
- Mitsuhashi N, Shimada T, Mano S, Nishimura M, Hara-Nishimura I (2000) Characterization of organelles in the vacuolar-sorting pathway by visualization with GFP in tobacco BY-2 cells. *Plant Cell Physiol* 41:993–1001
- Morita MT, Kato T, Nagafusa K, Saito C, Ueda T, Nakano A, Tasaka M (2002) Involvement of the vacuoles of the endodermis in the early process of shoot gravitropism in *Arabidopsis*. *Plant Cell* 14:47–56
- Mur LA, Kenton P, Lloyd AJ, Ougham H, Prats E (2007) The hypersensitive response; the centenary is upon us but how much do we know? *J Exp Bot* 59:501–520
- Nebenführ A, Gallagher LA, Dunahay TG, Fröhlich JA, Mazurkiewicz AM, Meehl JB, Staehelin LA (1999) Stop-and-go movements of plant Golgi stacks are mediated by the acto-myosin system. *Plant Physiol* 121:1127–1141
- Neuhaus HE, Trentmann O (2014) Regulation of transport processes across the tonoplast. *Front Plant Sci* 5:460
- Neuhaus J-M, Sticher L, Meins F, Boller T (1991) A short C-terminal sequence is necessary and sufficient for the targeting of chitinases to the plant vacuole. *Proc Natl Acad Sci USA* 88:10362–10366
- Niemeyer HM (2009) Hydroxamic acids derived from 2-hydroxy-2H-1,4-benzoxazin-3(4H)-one: key defense chemicals of cereals. *J Agric Food Chem* 57:1677–1696
- Obara K, Kuriyama H, Fukuda H (2001) Direct evidence of active and rapid nuclear degradation triggered by vacuole rupture during programmed cell death in *Zinnia*. *Plant Physiol* 125:615–626
- Okubo-Kurihara E, Sano T, Higaki T, Kutsuna N, Hasezawa S (2008) Acceleration of vacuolar regeneration and cell growth by overexpression of an aquaporin NtTIP1;1 in tobacco BY-2 cells. *Plant Cell Physiol* 50:151–160
- Opalski KS, Schultheiss H, Kogel KH, Hüchelhofen R (2005) The receptor-like MLO protein and the RAC/ROP family G-protein RACB modulate actin reorganization in barley attacked by the biotrophic powdery mildew fungus *Blumeria graminis* f. sp. hordei. *Plant J* 41:291–303
- Otegui MS, Noh YS, Martínez DE, Vila PMG, Andrew SL, Amasino RM, Guiamet JJ (2005) Senescence-associated vacuoles with intense proteolytic activity develop in leaves of *Arabidopsis* and soybean. *Plant J* 41:831–844
- Ovečka M, Lang I, Baluška F, Ismail A, Illeš P, Lichtscheidel I (2005) Endocytosis and vesicle trafficking during tip growth of root hairs. *Protoplasma* 226:39–54
- Owens T, Poole RJ (1979) Regulation of cytoplasmic and vacuolar volumes by plant cells in suspension culture. *Plant Physiol* 64:900–904
- Ozolina N, Nesterkina I, Nurminsky V, Stepanov A, Kolesnikova E, Gurina V, Salyaev R (2011) Recognition of lipid-protein rafts in vacuolar membrane. *Biochem Biophys Mol Biol* 438:120–122
- Paris N, Stanley CM, Jones RL, Rogers JC (1996) Plant cells contain two functionally distinct vacuolar compartments. *Cell* 85:563–572
- Parton R, Fischer-Parton S, Watahiki M, Trewavas A (2001) Dynamics of the apical vesicle accumulation and the rate of growth are related in individual pollen tubes. *J Cell Sci* 114:2685–2695

- Peiter E, Maathuis FJ, Mills LN, Knight H, Pelloux J, Hetherington AM, Sanders D (2005) The vacuolar Ca<sup>2+</sup>-activated channel TPC1 regulates germination and stomatal movement. *Nature* 434:404
- Rajniak J, Barco B, Clay NK, Sattely ES (2015) A new cyanogenic metabolite in *Arabidopsis* required for inducible pathogen defence. *Nature* 525:376–379
- Rask L, Andréasson E, Ekblom B, Eriksson S, Pontoppidan B, Meijer J (2000) Myrosinase: gene family evolution and herbivore defense in Brassicaceae. *Plant Mol Biol* 42:93–114
- Reisen D, Marty F, Leborgne-Castel N (2005) New insights into the tonoplast architecture of plant vacuoles and vacuolar dynamics during osmotic stress. *BMC Plant Biol* 5:1
- Robinson DG, Hoh B, Hinz G, Jeong B-K (1995) One vacuole or two vacuoles: do protein storage vacuoles arise de novo during pea cotyledon development? *J Plant Physiol* 145:654–664
- Ruthardt N, Gulde N, Spiegel H, Fischer R, Emans N (2005) Four-dimensional imaging of transvacuolar strand dynamics in tobacco BY-2 cells. *Protoplasma* 225:205–215
- Saito C (2003) A “bulb” subregion in the vacuolar membrane. *Plant Morphol* 15:60–67
- Saito C et al (2002) A complex and mobile structure forms a distinct subregion within the continuous vacuolar membrane in young cotyledons of *Arabidopsis*. *Plant J* 29:245–255
- Saito C, Morita MT, Kato T, Tasaka M (2005) Amyloplasts and vacuolar membrane dynamics in the living graviperceptive cell of the *Arabidopsis* inflorescence stem. *Plant Cell* 17:548–558
- Saito C et al (2011) The occurrence of ‘bulbs’, a complex configuration of the vacuolar membrane, is affected by mutations of vacuolar SNARE and phospholipase in *Arabidopsis*. *Plant J* 68:64–73
- Sansebastiano GPD, Barozzi F, Piro G, Denecke J, Lousa CDM (2017) Trafficking routes to the plant vacuole: connecting alternative and classical pathways. *J Exp Bot* 69:79–90
- Schaaf G, Honsbein A, Meda AR, Kirchner S, Wipf D, Von Wirén N (2006) *AtIREG2* encodes a tonoplast transport protein involved in iron-dependent nickel detoxification in *Arabidopsis thaliana* roots. *J Biol Chem* 281:25532–25540
- Schnell U, Dijk F, Sjollem KA, Giepmans BN (2012) Immunolabeling artifacts and the need for live-cell imaging. *Nat Methods* 9:152–158
- Schultheiss H, Dechert C, Kiraly L, Fodor J, Michel K, Kogel KH, Hüchelhoven R (2003) Functional assessment of the pathogenesis-related protein PR-1b in barley. *Plant Sci* 165:1275–1280
- Segami S, Makino S, Miyake A, Asaoka M, Maeshima M (2014) Dynamics of vacuoles and H<sup>+</sup>-pyrophosphatase visualized by monomeric green fluorescent protein in *Arabidopsis*: artifactual bulbs and native intravacuolar spherical structures. *Plant Cell* 26:3416–3434
- Sheahan MB, Rose RJ, McCurdy DW (2007) Actin-filament-dependent remodeling of the vacuole in cultured mesophyll protoplasts. *Protoplasma* 230:141–152
- Shimada C, Lipka V, O’Connell R, Okuno T, Schulze-Lefert P, Takano Y (2006) Nonhost resistance in *Arabidopsis-Colletotrichum* interactions acts at the cell periphery and requires actin filament function. *Mol Plant-Microbe Interact* 19:270–279
- Shimada T, Takagi J, Ichino T, Shirakawa M, Hara-Nishimura I (2018) Plant vacuoles. *Ann Rev Plant Biol* 69:123–145
- Shitan N (2016) Secondary metabolites in plants: transport and self-tolerance mechanisms. *BioSci Biotechnol Biochem* 80:1283–1293
- Silady RA, Ehrhardt DW, Jackson K, Faulkner C, Oparka K, Somerville CR (2008) The GRV2/RME-8 protein of *Arabidopsis* functions in the late endocytic pathway and is required for vacuolar membrane flow. *Plant J* 53:29–41
- Smertenko AP, Bozhkov PV, Filonova LH, Arnold S, Hussey PJ (2003) Re-organisation of the cytoskeleton during developmental programmed cell death in *Picea abies* embryos. *Plant J* 33:813–824
- Steppuhn A, Gase K, Krock B, Halitschke R, Baldwin IT (2004) Nicotine’s defensive function in nature. *PLoS Biol* 2:e217
- Swanson SJ, Bethke PC, Jones RL (1998) Barley aleurone cells contain two types of vacuoles: characterization of lytic organelles by use of fluorescent probes. *Plant Cell* 10:685–698
- Tanaka Y, Kutsuna N, Kanazawa Y, Kondo N, Hasezawa S, Sano T (2007) Intra-vacuolar reserves of membranes during stomatal closure: the possible role of guard cell vacuoles estimated by 3-D reconstruction. *Plant Cell Physiol* 48:1159–1169
- Taylor LP, Grotewold E (2005) Flavonoids as developmental regulators. *Curr Opin Plant Biol* 8:317–323
- Thangstad O, Iversen T-H, Slupphaug G, Bones A (1990) Immunocytochemical localization of myrosinase in *Brassica napus* L. *Planta* 180:245–248
- Thangstad O, Evjen K, Bones A (1991) Immunogold-EM localization of myrosinase in *Brassicaceae*. *Protoplasma* 161:85–93
- Thomine S, Lelièvre F, Debarbieux E, Schroeder JI, Barbier-Brygoo H (2003) AtNRAMP3, a multispecific vacuolar metal transporter involved in plant responses to iron deficiency. *Plant J* 34:685–695
- Tominaga M, Yokota E, Vidali L, Sonobe S, Hepler PK, Shimmen T (2000) The role of plant villin in the organization of the actin cytoskeleton, cytoplasmic streaming and the architecture of the transvacuolar strand in root hair cells of *Hydrocharis*. *Planta* 210:836–843
- Toyooka K, Moriyasu Y, Goto Y, Takeuchi M, Fukuda H, Matsuoka K (2006) Protein aggregates are transported to vacuoles by macroautophagic mechanism in nutrient-starved plant cells. *Autophagy* 2:96–106
- Ueda T, Yamaguchi M, Uchimiya H, Nakano A (2001) Ara6, a plant-unique novel type Rab GTPase, functions in the endocytic pathway of *Arabidopsis thaliana*. *EMBO J* 20:4730–4741
- Ueda H et al (2006) AtVAM3 is required for normal specification of idioblasts, myrosin cells. *Plant Cell Physiol* 47:164–175
- Uemura T, Yoshimura SH, Takeyasu K, Sato MH (2002) Vacuolar membrane dynamics revealed by GFP-AtVam3 fusion protein. *Genes Cells* 7:743–753
- Van der Hoorn RA, Jones JD (2004) The plant proteolytic machinery and its role in defence. *Curr Opin Plant Biol* 7:400–407
- Van Gestel K, Köhler R, Verbelen JP (2002) Plant mitochondria move on F-actin, but their positioning in the cortical cytoplasm depends on both F-actin and microtubules. *J Exp Bot* 53:659–667
- Vermeer JE et al (2006) Visualization of PtdIns3P dynamics in living plant cells. *Plant J* 47:687–700
- Vetter J (2000) Plant cyanogenic glycosides. *Toxicol* 38:11–36
- Voelker C, Schmidt D, Mueller-Roeber B, Czempinski K (2006) Members of the *Arabidopsis* AtTPK/KCO family form homomeric vacuolar channels in planta. *Plant J* 48:296–306
- Wada Y (2013) Vacuoles in mammals: a subcellular structure indispensable for early embryogenesis. *Bioarchitecture* 3:13–19
- Wang J, Li Y, Lo SW, Hillmer S, Sun SS, Robinson DG, Jiang L (2007) Protein mobilization in germinating mung bean seeds involves vacuolar sorting receptors and multivesicular bodies. *Plant Physiol* 143:1628–1639
- Williamson RE (1993) Organelle movements. *Ann Rev Plant Biol* 44:181–202
- Wittstock U, Halkier BA (2002) Glucosinolate research in the *Arabidopsis* era. *Trends Plant Sci* 7:263–270
- Wormit A et al (2006) Molecular identification and physiological characterization of a novel monosaccharide transporter from *Arabidopsis* involved in vacuolar sugar transport. *Plant Cell* 18:3476–3490
- Xu Y, Ishida H, Reisen D, Hanson MR (2006) Upregulation of a tonoplast-localized cytochrome P450 during petal senescence in *Petunia inflata*. *BMC Plant Biol* 6:8

- Yamaryo Y, Dubots E, Albrieux C, Baldan B, Block MA (2008) Phosphate availability affects the tonoplast localization of PLD $\zeta$ 2, an *Arabidopsis thaliana* phospholipase D. FEBS Lett 582:685–690
- Yoshida K et al (2013) Studies on vacuolar membrane microdomains isolated from *Arabidopsis* suspension-cultured cells; local distribution of vacuolar membrane proteins. Plant Cell Physiol 54:1571–1584
- Zhang W, Wang C, Qin C, Wood T, Olafsdottir G, Welti R, Wang X (2003) The oleate-stimulated phospholipase D, PLD $\delta$ , and phosphatidic acid decrease H<sub>2</sub>O<sub>2</sub>-induced cell death in *Arabidopsis*. Plant Cell 15:2285–2295
- Zhang C, Hicks GR, Raikhel NV (2014) Plant vacuole morphology and vacuolar trafficking. Front Plant Sci 5:476
- Zhou S, Richter A, Jander G (2018) Beyond defense: multiple functions of benzoxazinoids in maize metabolism. Plant Cell Physiol 59(8):1528–1537

**Publisher's Note** Springer Nature remains neutral with regard to jurisdictional claims in published maps and institutional affiliations.

## ANNEX C

### **A POPLAR RUST EFFECTOR PROTEIN ASSOCIATES WITH PROTEIN DISULFIDE ISOMERASE AND ENHANCES PLANT SUSCEPTIBILITY**




Mst Hur Madina, Md Saifur Rahman, Xiaoqiang Huang, Yang Zhang,  
Huanquan Zheng and Hugo Germain

Annex C contains an original article, in the article we further exploited the *A. thaliana* experimental system, discovered that this tonoplast-localized effector Mlp124357 from *Melampsora larici-populina* (*Mlp*) affects plant susceptibility to pathogens and tried to elucidate the mechanisms through which it does so. I have participated in writing and carried out *in-silico* experiments and analysis.



Article

# A Poplar Rust Effector Protein Associates with Protein Disulfide Isomerase and Enhances Plant Susceptibility

Mst Hur Madina <sup>1</sup>, Md Saifur Rahman <sup>1</sup>, Xiaoqiang Huang <sup>2</sup> , Yang Zhang <sup>2</sup>,  
Huanquan Zheng <sup>3</sup>  and Hugo Germain <sup>1,\*</sup> 

<sup>1</sup> Department of Chemistry, Biochemistry and Physics, Université du Québec à Trois-Rivières, 3351 boulevard des Forges, Trois-Rivières, QC G9A 5H7, Canada;

mosammad.hur.madina@uqtr.ca (M.H.M.); md.saifur.rahman@uqtr.ca (M.S.R.)

<sup>2</sup> Department of Computational Medicine and Bioinformatics, University of Michigan, 100 Washtenaw Avenue, Ann Arbor, MI 48109, USA; xiaoqiah@umich.edu (X.H.); zhng@umich.edu (Y.Z.)

<sup>3</sup> Department of Biology, McGill University, 1205 Dr. Penfield Avenue, Montreal, QC H3A 1B1, Canada; hugo.zheng@mcgill.ca

\* Correspondence: hugo.germain@uqtr.ca

Received: 28 July 2020; Accepted: 7 September 2020; Published: 16 September 2020



**Abstract:** *Melanopsora larici-populina* (*Mlp*), the causal agent of *Populus* leaf rust, secretes an array of effectors into the host through the haustorium to gain nutrients and suppress immunity. The precise mechanisms by which these effectors promote virulence remain unclear. To address this question, we developed a transgenic *Arabidopsis* line expressing a candidate effector, Mlp124357. Constitutive expression of the effector increased plant susceptibility to pathogens. A GxxxG motif present in Mlp124357 is required for its subcellular localization at the vacuolar membrane of the plant cell, as replacement of the glycine residues with alanines led to the delocalization of Mlp124357 to the nucleus and cytoplasm. We used immunoprecipitation and mass spectrometry (MS) to identify Mlp124357 interaction partners. Only one of the putative interaction partners knock-out line caused delocalization of the effector, indicating that *Arabidopsis* protein disulfide isomerase-11 (AtPDI-11) is required for the effector localization. This interaction was further confirmed by a complementation test, a yeast-two hybrid assay and a molecular modeling experiment. Moreover, localization results and infection assays suggest that AtPDI-11 act as a helper for Mlp124357. In summary, our findings established that one of *Mlp* effectors resides at the vacuole surface and modulates plant susceptibility.

**Keywords:** fungal rust; effector; GxxxG motif; protein disulfide isomerase; helper protein; plant susceptibility

## 1. Introduction

During infection, plant pathogenic microbes deliver virulence proteins, known as effectors, into host cells to overcome plant immunity and promote parasitic colonization through the manipulation of cellular processes [1]. Once inside host tissues, effectors traffic to various cellular compartments where they interact with host proteins or nucleic acids and exert their virulence function [2–6]. To target these destinations, effectors possess domains or motifs in their sequence; for example, nucleus localized effectors can contain nuclear-localized signals (NLS) and some chloroplast localized effectors may carry a transit peptide [4,7,8]. Uncovering how effector proteins function inside the plant is key to understand pathogenicity mechanisms and to develop more resistant crops [9]. Because investigating pathogenesis on crop species can be challenging, alternative approaches using heterologous expression

in *Arabidopsis thaliana* and *Nicotiana benthamiana* are extensively used in the functional investigation of effector biology [3,5,10–12].

Host proteins that associate with effectors can be categorized as targets or helpers [13]. Target proteins are directly targeted and modulated by effectors to alter host cellular processes. For example, the bacterial effector HopZ1a interacts with positive regulators of immunity to inhibit their activity [14], whereas the *Pseudomonas syringae* T3E AvrB effector binds to the *Arabidopsis* mitogen-activated protein kinase 4 (MPK4), a suppressor of immunity, to induce plant susceptibility [15]. On the other hand, helper proteins may act as co-factors to enable the function, the maturation, or the trafficking of an effector. Less information is available about helpers than about targets so far, perhaps as mutation in helpers may not directly enhance susceptibility to pathogens. For instance, the effectors AvrRPM1 and AvrPto both require myristoylation for their activity, suggesting an interaction with a myristoyl transferase which would serve as a helper for their maturation [16,17]. A well-known helper is the importin- $\alpha$ , a protein whose function is to mediate nuclear entry of NLS-containing proteins; several transcription activator-like (TAL) effectors and Crinklers were shown to require importin- $\alpha$  for their proper nuclear accumulation [7,18,19]. Regardless of whether host proteins act as an effector's target or helper, they are considered as host susceptibility factors [13].

Rust fungi (Basidiomycetes, Pucciniales) are obligate biotrophic parasites, infect numerous plant families and are the largest group of fungal pathogens [20]. Several rust species are devastating plant pathogens affecting crops and thus food security [21]. *Melampsora larici-populina* (Mlp) causes rust disease on poplar leaves and lead to major yield losses in poplar plantations worldwide [22–24]. Although poplar is not a food crop, this pathosystem can be used to better understand other rust pathosystems. Genome and transcriptome analyses have revealed that *M. larici-populina* may have as much as 1184 small secreted proteins (SSPs) [25]. Among these SSPs, candidate secreted effector proteins (CSEPs) have been selected based on features such as expression in poplar leaves during infection and specificity to the Pucciniales order [26–28]. When expressed in *N. benthamiana* or *A. thaliana*, several CSEPs of Mlp have been shown to accumulate in diverse cell compartments of leaf tissues such as the nucleus, the nucleolus, chloroplasts, mitochondria, and plasmodesmata [5,11]. To date, a number of Mlp effectors have been identified as promoting plant susceptibility as determined by *in planta* assays [2,11].

We recently reported that the candidate effector Mlp124357 accumulates in tonoplasts, transvacuolar strands, and bulbs [29]. In this study, we further exploited the *A. thaliana* experimental system to discover that this tonoplast-localized effector affects plant susceptibility to pathogens and we tried to elucidate the mechanisms through which it does so. We used the combined methods of genetics, live-cell imaging, immunoprecipitation, and biochemical analysis to look for the interaction partners of Mlp124357 at the tonoplast. We show that the constitutive expression of this effector increases plant susceptibility to bacterial and oomycete pathogens. We demonstrate that a specific motif of Mlp124357 is necessary for its tonoplast localization and interaction. We also provide evidence through mass spectrometry, a genetic complementation test, a yeast-two hybrid assay (Y2H), and *in silico* modeling that Mlp124357 associates with a protein disulfide isomerase (PDI) which acts as a helper protein for this effector but not for other Mlp effectors having similar numbers of disulfide bridges.

## 2. Materials and Methods

### 2.1. Plants Material and Growth Conditions

*A. thaliana* and *N. benthamiana* plants were grown in soil (AgroMix), in a growth chamber after the seeds underwent a stratification period of 48 h at 4 °C. The plant growth chamber was maintained at 22 °C, 60% relative humidity, and with a 16 h/8 h light/dark cycle. *In vitro* culture of *Arabidopsis* was performed onto Petri dish containing 1/2 Murashige and Skoog medium (1/2 MS) and 0.7% agar. For the selection of the single-insertion homozygous transgenic plants, 15 mg/mL Basta or 50 mg/mL Kanamycin was used.

## 2.2. Cloning Procedures and Plasmid Constructs

The open reading frame (ORF) of Mlp124357 without the portion coding for its signal peptide was obtained from GenScript (Piscataway, NJ, USA). The *PDI-11* coding sequence was amplified from *Arabidopsis*. Amplicons were inserted into the pDONR221 vector (Invitrogen, part of Thermo Fisher Scientific, Waltham, MA, USA) by BP recombination reactions and then into the plant expression vectors pB7FWG2 or pK7WG2 by LR recombination reactions using Gateway technology [30]. All the constructs were sequenced before transformation in *Agrobacterium* C58C1.

## 2.3. Protein Expression in *N. benthamiana* and *A. thaliana*

For transient protein expression, constructs were introduced into *A. tumefaciens* strain C58C1 by electroporation and delivered into leaf cells of 4-week-old *N. benthamiana* using the agroinfiltration method previously described [31]. Briefly, recombinant bacterial strains were grown overnight in yeast extract peptone (YEP) medium with spectinomycin (50 mg/L) then harvested, and resuspended into an infiltration buffer (10 mM MgCl<sub>2</sub> and 150 μM acetosyringone) to obtain 0.5 unit of optical density at 600 nm. One hour after resuspension, leaves were infiltrated on their abaxial side. The agro-infected leaves were collected at 2-days post infiltration for confocal microscopy. Stable *A. thaliana* transgenics were developed by introducing the constructs into *A. thaliana* (Col-0) using the *A. tumefaciens*-mediated floral dip transformation (same strain as used for agroinfiltration) method as previously described [32]. Crossing between the transgenic line expressing the effector and the knockout lines was carried out by following the method as described by Madina et al. [29].

## 2.4. Pathogen Infections Assay

Bacterial infections were performed with 4-week-old *Arabidopsis* plants. *Pseudomonas syringae* pv. *tomato* (*Pst*) DC3000 was grown overnight at 28 °C and infiltrated with a needle-less syringe on the abaxial side of the leaves at 0.001 optical density at 600 nm as previously described by Germain et al. 2018 [11]. *Hyaloperonospora arabidopsidis* (*Hpa*) Noco2 infections were performed with 2-week-old *Arabidopsis* plants using the spray inoculation method described by Dong et al. [33], *eds1-2* allele was used as a control. Statistical significance was determined by Student's *t*-test ( $p < 0.05$ ) or one-way analysis of variance (ANOVA  $p < 0.05$ ) complemented with Tukey's HSD test [34].

## 2.5. Membrane Fractionation

The membrane fractionation experiment was carried out according to the method of Widell and Larsson et al. (1981) with the modification applied in Germain et al. (2013) [35,36]. Briefly, a two-phase separation method was used to separate membrane fraction of plant cells, and all preparation steps were maintained at 4 °C or on the ice. 3–5 g of fresh leaves from 3-weeks old Col-0-eGFP and Mlp124357-eGFP were homogenized with a knife blender in the homogenization buffer. The homogenized sample was filtered twice through four layers of cheesecloth and centrifuged at 10,000× *g* for 10 min. Then, the supernatant was transferred to an ultracentrifuge tube and centrifuged at 50,000× *g* for 1 h. The supernatant, containing soluble proteins was discarded and the membrane pellet was resuspended in IP lysate buffer (10 mM MgCl<sub>2</sub>, 50 mM Tris-HCl (pH 7.5), 100 mM NaCl, 0.1% Triton X-100, 1 mM PMSF, and 1X cOmplete protease inhibitor cocktail) [37]. Affinity chromatography of the protein complexes were performed with GFP beads following the protocol by Serino G and Deng XW (2007). Proteins were eluted from the beads by heating the samples at 95 °C for 10 min and analyzed by standard SDS-PAGE followed by Western blotting or mass spectrometry.

## 2.6. Sample Preparation for Mass Spectrometry

Protein digestion and mass spectrometry experiments were performed by the Proteomics Platform of the Centre hospitalier universitaire of the Quebec Research Center, Quebec, Canada. Gel bands of interest were reduced and alkylated then digested with trypsin into peptides prior to mass spectrometry



analysis. Peptide samples were injected and separated by LC-MS/MS on a 5600+ triple TOF mass spectrometer (Sciex, Framingham, MA, USA) coupled to an Eksport NanoLC425 (Sciex). Peptide separation took place on a self-packed picofrit column (New Objective) with repositil 3u, 120A C18, 15 cm × 0.075 mm internal diameter, (Dr Maisch). Peptides were eluted with a linear gradient from 5–35% solvent B (acetonitrile, 0.1% formic acid) in 35 min, at 300 nL/min. Mass spectra were acquired using a data-dependent acquisition mode using Analyst software version 1.7. Each full scan mass spectrum (400 to 1250 m/z) was followed by collision-induced dissociation of the twenty most intense ions. Dynamic exclusion was set for a period of 12 sec and a tolerance of 100 ppm.

MGF peak list files were created using Protein Pilot version 4.5 software (Sciex). MGF sample files were then analyzed using Mascot (Matrix Science, London, UK; version 2.4.1). Mascot was set up to search against a contaminant database, an *A. thaliana* Uniprot database (82,874 entries) assuming the digestion enzyme trypsin. Mascot analysis was conducted with a parent and fragment ion mass tolerance of 0.10 Da. Carbamidomethyl of cysteine was specified as a fixed modification while deamidation of asparagine and glutamine and oxidation of methionine were specified as variable modifications; 2 missed cleavages were allowed.

Scaffold (version Scaffold\_4.8.4, Proteome Software Inc., Portland, OR) was used to validate MS/MS based peptide and protein identifications. Peptide identifications were accepted if they could be established at greater than 5.0% probability to achieve an FDR less than 1.0% by the Scaffold Local FDR algorithm. Protein identifications were accepted if they could be established at greater than 96.0% probability to achieve an FDR less than 1.0% and contained at least 2 identified peptides. Protein probabilities were assigned by the Protein Prophet algorithm [38]. Proteins that contained similar peptides and could not be differentiated based on MS/MS analysis alone were grouped to satisfy the principles of parsimony. All the mass spectrometry results were deposited in the Mass Spectrometry Interactive Virtual Environment (MASSIVE) database and made publicly available using the PXD021290 data identifier.

### 2.7. Western Blot Analysis

The presence of Mlp124357-eGFP, eGFP, and AtPDI-11-eGFP were determined by SDS-PAGE and western blotting. Leaf tissue was harvested from 2–3 week-old stable transgenic plants and protein extracts were prepared as described [39]. The blot was probed with an  $\alpha$ -GFP-HRP antibody (1:500 dilution, Molecular Probes, Santa Cruz Biotechnology, Dallas, TX, USA). The bands were revealed with the Clarity™ western ECL substrate (Bio-Rad) according to the manufacturer's recommendations.

### 2.8. Confocal Microscopy

Small pieces of young leaves from *A. thaliana* or *N. benthamiana* were mounted in water between a slide and a coverslip and were immediately observed. Live-cell imaging was performed on Leica TCS SP8 confocal laser scanning microscope (Leica Microsystems) with a 40X/1.40 oil immersion objective. Images were taken at 1024 × 1024 pixels resolution using line-by-line sequential scanning (when appropriate). The excitation wavelength for eGFP was 488 nm and its emission was collected from 500 to 525 nm. Z-stacks of between 50 and 100 confocal images were acquired and used to generate three-dimensional (3-D) reconstructions using Leica TCS SP8 software (when required). The LAS AF Lite software (Version 3.3) and Adobe Photoshop CS6 were used for the post-acquisition images processing.

### 2.9. RNA Extraction and Transcriptome Analysis

RNA isolation was carried out as described previously [2]. Briefly, total RNA was extracted from 4-day-old *Arabidopsis* plants grown in Petri dishes and quantified before sending for sequencing. Ion Torrent Technology was used for library construction and sequencing (Université Laval, Quebec City, Canada). Transcriptomics data were processed as reported previously [2] and all transcriptomic data were submitted to Genbank under project ID PRJNA608508. Gene Ontology (GO) enrichment of both

up- and down-regulated genes (having Q-value  $\leq 0.05$  and a fold-change  $\geq 3$ ) were investigated using the Cytoscape software (version 3.1.1) with the plug-in ClueGO and CluePedia [40].

#### 2.10. Y2H Reporter Assays

Coding sequences of Mlp124357 and *AtPDI-11* without their signal peptide were cloned into pGBKT7 (binding domain) and pGADT7 (activation domain), respectively, by homologous recombination in yeast strain Y187 or Y2H gold. Bait protein-encoding vector pGBKT7 expressing Mlp124357 and the prey protein-encoding vector pGADT7 expressing *AtPDI-11* were transformed into the yeast strain Y2H gold according to the Clontech Y2H protocol. Transformants were plated along with a negative control onto yeast synthetic double dropout medium (DDO) lacking Leu and Trp and quadruple dropout selective medium (QDO) lacking Trp, Leu, His, and Ade (Takara, Mountain View, CA, USA) and incubated at 30 °C for 3 to 4 days. For photographing, series of dilution ( $10^{-0}$ ,  $10^{-1}$ ,  $10^{-2}$ ) were prepared for each transformant and 10  $\mu$ L were placed onto DDO and QDO medium and incubated at 30 °C for 3 to 4 days.

#### 2.11. Molecular Modeling of the Proteins

Three-dimensional structures of the Mlp124357 were produced through homology modeling using the online tool QUARK [41]. *AtPDI-11* and PtPDI structure homology-modeling was obtained from sequence alignment against the homology template of Protein disulfide-isomerase A3 (PDB: 6eny) using I-TASSER [42]. The binding efficiency of the effector to *AtPDI-11* or PtPDI was determined using four different protein-protein docking servers Cluspro, Grammx, Patchdock, and ZDock [43–46]. The generated protein-protein complexes were visualized and analyzed through PyMOL [47,48].

### 3. Results

#### 3.1. Selection and Phylogenetic Analysis of Mlp124357

The analysis of *M. larici-populina's* genome revealed more than one thousand potential small-secreted proteins [25]. To select candidate secreted effector proteins for functional investigation, we followed various criteria that were previously described [5,11]: these included that the sequences must be of small size, possess a signal peptide and conserved cysteines, and must not have conserved sequences outside the order Pucciniales; they must also be detected in infection structures. One of the small secreted peptides that met these criteria is Mlp124357. It belongs to the family CPG4890, which contains 10 members and appears to be under positive selective pressure [27]. Each member carries an N-terminal signal peptide region (amino acids 1–22 in the case of Mlp124357) and encodes a short peptide 80–98 amino acids long (molecular weights 9–10 kDa) (Figure 1A,B).

The sequence identity ranges from 40–60% between Mlp124357 and the other family members (Figure 1C). In addition, this peptide contains eight cysteine residues, and its expressed sequence tag (EST) has not been detected in spores but is abundant in infected poplar leaves, supporting infection specific expression. With the exception of the members of its close family, Mlp124357 shows little similarity to other proteins, whether in Pucciniales or any other genus, indicating that it is a fairly unique protein in all kingdoms. Hence, the infection specific expression of Mlp124357 and its uniqueness triggered us to investigate its localization and role *in planta* during infection.

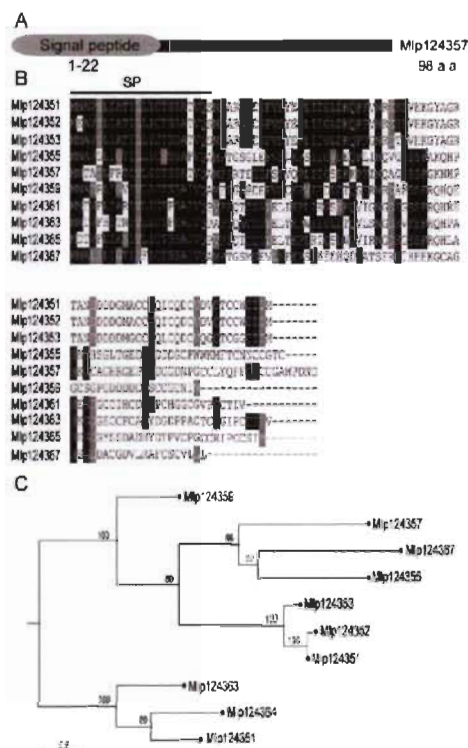


**Figure 1.** Selection and phylogenetic analysis of Mlp124357. (A) Schematic representation of protein topology of Mlp124357. N-terminus of Mlp124357 contains a secretory signal peptide (SP) (B) Multiple sequence alignment of the ten effector proteins that are the members of the *M. larici-populina* CPG4890 SSP family. Predicted signal peptides (SP) are marked with a line. Black boxes indicate conserved residues and grey boxes indicate similar residues. (C) Phylogenetic tree of the CPG4890 gene family, obtained with CLC workbench using the Kimura protein distance value and neighbor-joining tree method. Bootstrap values are indicated.

### 3.2. Mlp124357 Expression in Planta Affects the Plant Susceptibility to Bacterial and Oomycete Pathogens

To express Mlp124357 and determine its localization *in planta*, we cloned its coding sequence without the signal peptide tagged with enhanced Green Fluorescent Protein (eGFP) under the control of a CaMV35S promoter in a Gateway expression vector (Figure 2A). Then, we expressed the Mlp124357 fusion construct in wild-type *Arabidopsis* (Col-0) as a stable transgenic line and also developed a control line expressing eGFP under the control of the same promoter. Figure S1 shows that both proteins (eGFP and Mlp124357-eGFP) were expressed at the appropriate molecular weight. This result confirms that Mlp124357-eGFP is expressed *in planta*, is not further processed, and thus can be used for further investigations. The resulting transgenic plants are shown in Figure 2B. The plants expressing only eGFP are indistinguishable from the wild-type whereas the plants overexpressing Mlp124357-eGFP display narrower leaves, darker green leaves, chlorosis, and drying of the leaf tips (Figure 2B).

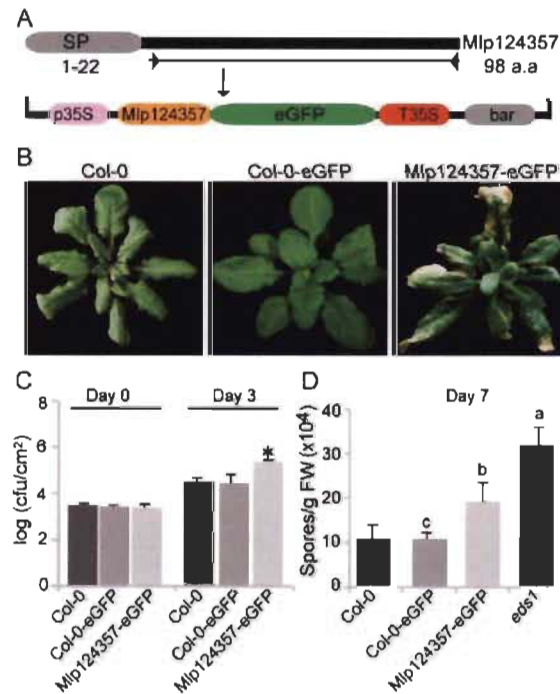


**Figure 2.** Mlp124357 expression *in planta* affects the plant susceptibility to bacterial and oomycete pathogens. (A) Schematic representation of the T-DNA construct used for *in planta* expression of the Mlp124357 mature coding sequence. (B) Morphology of wild-type (Col-0) expressing eGFP or Mlp124357-eGFP. Photographs were taken from 4-week-old soil-grown plants. (C) Growth of PstDC3000 bacteria in *Arabidopsis*. Leaves of each genotype were infiltrated with a PstDC3000 bacterial suspension (OD<sub>600</sub> = 0.001) and the bacterial growth was measured on day 0 and day 3 after infection. Statistical significance was evaluated using a Student's *t*-test ( $p < 0.05$ ); asterisk indicates a statistically significant difference between plants carrying effector and Col-0-GFP. Five replicates were used for each genotype; cfu, colony-forming unit. (D) Growth of *H. arabidopsidis* Noco2 in *Arabidopsis*. Each genotype was spray inoculated with *H. arabidopsidis* Noco2 spores (20,000 conidiospores/mL) and the number of conidiospores was quantified 7 days after inoculation. Statistical significance was evaluated using ANOVA ( $p < 0.05$ ) with Tukey's test. Letters denote a significant difference between Col-0-eGFP, Mlp124357-eGFP, and *eds1*. FW, fresh weight. Both bacterial and oomycete infection experiments were repeated at least three times and representative data are shown.

To evaluate if Mlp124357 could interfere with the plant susceptibility to pathogens, we subjected control plants and plants expressing Mlp124357 to bacterial and oomycete pathogens. The plants expressing Mlp124357 harbored nearly 10-fold more *Pseudomonas syringae* pv. *tomato* DC3000 bacteria after three days than control plants, indicating that they are hypersusceptible to this bacterial hemibiotrophic pathogen (Figure 2C). As rusts cannot infect *A. thaliana*, we used *H. arabidopsidis* for our infection assay. Although *H. arabidopsidis* is not a rust (it is an oomycete), it is also an obligate biotrophic pathogen that infects plants by making haustoria. Seven days after inoculation, we quantified the number of spores and detected a significant increase in the susceptibility of Mlp124357-eGFP transgenic plants compared to Col-0 ( $p < 0.05$ ) (Figure 2D), but not as pronounced as the one observed in the hypersusceptible mutant line *eds1*, indicating that the effector does not make the plant as susceptible as the *eds1-2* mutation.



### 3.3. Mlp124357 Possesses a GxxxG Motif that Is Required for the Interaction with Tonoplasts

We have previously reported that Mlp124357 targets the tonoplasts *in planta* [29]. However, Mlp124357 does not possess any transmembrane domain. Thus, we rationalized that Mlp124357 may interact with an integral tonoplast protein. We investigated the primary sequence of Mlp124357 and discovered a GxxxG motif (Figure 3A), which is known for mediating interactions with membrane proteins [49,50]. The secondary structure of the Mlp124357 sequence was modeled as an alpha-helical wheel projection using helix prediction software (<http://kael.net/helical.htm>). The two glycines of the GxxxG motif at positions 76 and 80 were found on the same side of the  $\alpha$ -helix (Figure 3B, pink box). This amino acid orientation of the GxxxG motif can be involved in protein interactions between membrane proteins [51].

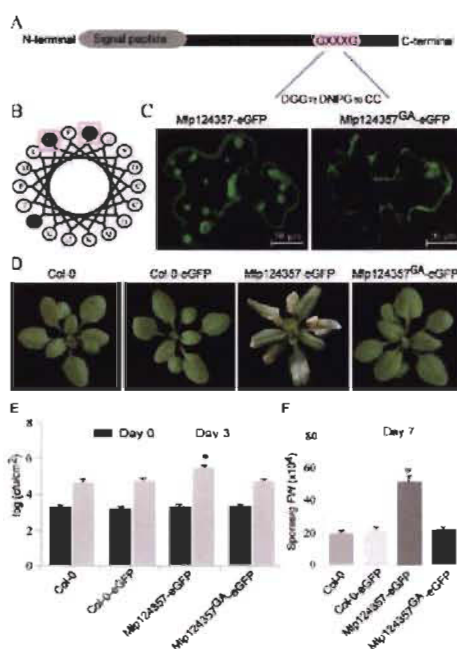


**Figure 3.** Mlp124357 possesses a GxxxG motif that is required for the interaction with tonoplasts. (A) Schematic representation of the GxxxG motif in the C-terminus region of Mlp124357. (B) A predicted helical wheel projection of Mlp124357. The glycine residues at positions 76 and 80 are indicated by square boxes. (C) Fluorescence imaging of *N. benthamiana* cells expressing eGFP fusions of Mlp124357 and Mlp124357<sup>GA</sup> mutant at 2 dpi using confocal microscopy of epidermal cells. (D) Morphology of each genotype. Photographs are from 4-week-old soil-grown plants. (E) Leaves of each genotype were infiltrated with a PstDC3000 bacterial suspension at OD 600 = 0.001 and bacterial growth was quantified in colony-forming units (cfu) on day 0 and day 3 after infection. One-way ANOVA ( $p < 0.05$ ) with Tukey's test was performed. The asterisk indicates a statistically significant difference between Col-0-eGFP, Mlp124357-eGFP, and Mlp124357<sup>GA</sup>-eGFP. Five replicates were used for each genotype. (F) Each genotype was spray inoculated with *H. arabidopsidis* Noco2 spores (20,000 conidiospores/mL) and the number of conidiospores was quantified 7 days after inoculation. Statistical significance was evaluated using one-way ANOVA with Tukey's test (significance set at  $p < 0.05$ ). The asterisk denotes a significant difference between Col-0-eGFP, Mlp124357-eGFP, and Mlp124357<sup>GA</sup>-eGFP. FW, fresh weight. Both bacterial and oomycete infection experiments were repeated at least three times and representative data are shown.

To investigate whether the two glycines are implicated in Mlp124357 localization, we carried out site-directed mutagenesis to substitute them into alanines (Ala). We generated a mutant construct Mlp124357<sup>G76A-G80A</sup> fused in C-terminal to eGFP, which is hereafter referred to as Mlp124357<sup>GA</sup>. The fusion protein was transiently expressed in *N. benthamiana* leaves and its subcellular localization was assessed by confocal laser microscopy. The expression of wild type Mlp124357-eGFP was still detected in tonoplasts and bulbs of epithelial cells (Figure 3C). However, the replacement of the glycine residues with alanines led to the delocalization of the effector (Figure 3C).

Subsequently, to test whether the delocalization of Mlp124357 affects the activity of the effector, we developed a stable *Arabidopsis* transgenic line (Figure 3D) with the glycine mutant construct. The glycine mutant line no longer displayed the chlorotic phenotype on the leaves; rather, it was indistinguishable from WT plants (Figure 3D). We then confirmed that Mlp124357<sup>GA</sup> localization in *A. thaliana* correlated with what was observed in *N. benthamiana*, which is that Mlp124357-eGFP accumulates in the tonoplast, transvacuolar strands, and bulbs while Mlp124357<sup>GA</sup> accumulates in the nucleus and cytoplasm (Figure S2). Further, these transgenic lines were used to perform infection assays to evaluate their susceptibility to pathogens. The plants expressing Mlp124357<sup>GA</sup> showed a level of bacterial growth that was similar to control plants Col-0 and Col-0-eGFP (Figure 3E). Similarly, inoculation experiment with *H. arabidopsidis* spores demonstrated wild-type like susceptibility of Mlp124357<sup>GA</sup>-eGFP compared to Mlp124357-eGFP ( $p < 0.0001$ ) (Figure 3F). From these experiments, we conclude that the GxxG motif is required for the localization and the function of the Mlp124357 effector.

### 3.4. Protein Disulfide Isomerase 11 as a Potential Plant Interactor of Mlp124357

Since the Mlp124357 peptidic sequence lacks a transmembrane domain and that no post-translational modification (myristoylation, acetylation, or mannosylation) could be predicted, we rationalized that the small secreted peptide may interact with a plant protein to achieve its tonoplastic localization. To identify putative interaction partners of Mlp124357 in membranes, we first assessed if it could be isolated from membrane enriched fractions. It appears that Mlp124357's association with the membranes is not very strong as it could also be detected in the supernatant of the membrane fraction (Figure S3). However, since Mlp124357 was mostly retained in membranes, we immunoprecipitated it from the membrane fraction using anti-GFP beads and subjected SDS-PAGE gel bands to mass spectrometry to identify potential plant protein interactors. From the MS analysis, 40 *A. thaliana* proteins were identified as potential interactors of the Mlp124357 effector (Table S1). However, since Mlp124357 accumulates in the tonoplasts, we only selected five proteins predicted to be tonoplastic for further investigation (Figure 4A).

To verify the potential interacting protein partners, we crossed knockout (KO) lines of four of those five tonoplast proteins (line SALK-200520 could not be made homozygous) with the Mlp124357-eGFP transgenic line and then assessed Mlp124357-eGFP localization using confocal microscopy (Figure 4A). We hypothesized that if one of those proteins was an interactor serving as an anchor protein to Mlp124357 at the tonoplasts, the effector would change localization in the knockout line. Interestingly, the absence of one tonoplast protein named protein disulfide isomerase 11 (*PDI-11*; gene ID: AT2G47470) led to the delocalization of Mlp124357-eGFP (Figure 4B and Figure S4). We confirmed that the delocalization was caused by the absence of PDI-11 by complementing the knockout line with the wild-type *Arabidopsis PDI-11* sequence, which restored Mlp124357-eGFP's localization. As *Mlp*'s host is poplar, we also assessed by genetic complementation if the effector could interact with *Populus trichocarpa* PDI (AtPDI-11 and PtPDI share about 87% sequence identity) (Figure S5). We observed that both *Arabidopsis PDI-11* and poplar PDI could restore the tonoplastic localization of Mlp124357-eGFP in the *pdi-11* KO background (Figure 4B panels IV and V). In addition, to verify the cellular localization of AtPDI-11 or PtPDI, both were cloned in fusion with eGFP (AtPDI-11-eGFP or PtPDI-eGFP), transiently overexpressed in *N. benthamiana* leaf cells by *Agro*-infiltration and observed by confocal microscopy. The eGFP signal suggested a localization in both the tonoplasts and ER structures

(Figure S6). Overall, these results suggest that PDI is required for the localization of Mlp124357 at the tonoplast. We also assessed whether AtPDI-11 or PtPDI were in frame with the eGFP using immunoblot and found that both proteins are at the expected molecular weight (Figure S1).

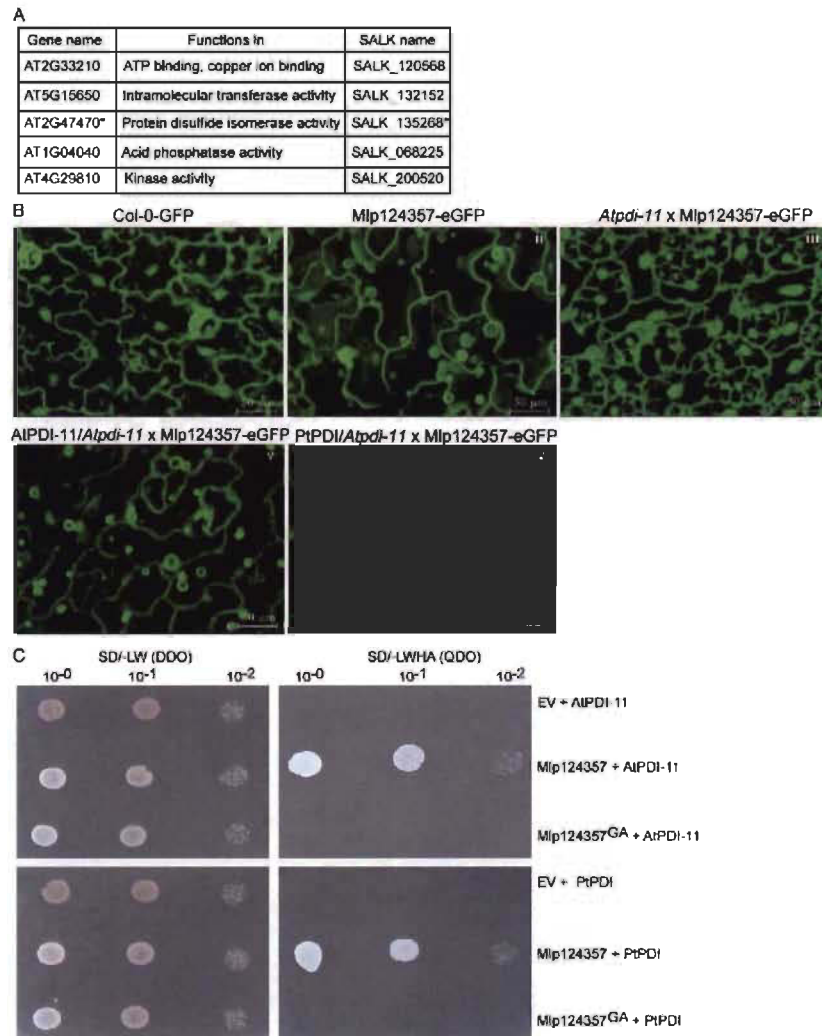


**Figure 4.** Protein Disulfide Isomerase 11 as a potential plant interactor of Mlp124357. (A) The five tonoplast-localized proteins selected from the IP/MS list. (B) Interaction between Mlp124357 and AtPDI-11 or PtPDI was detected by a genetic analysis/complementation test. Live-cell imaging of leaf epidermal cells of each genotype. (C) Interaction between Mlp124357 and AtPDI-11 or PtPDI was evaluated by Y2H. The plates were photographed 2 days after inoculation.

Further confirmation of the interaction between Mlp124357 and AtPDI-11 or PtPDI was carried out using a Y2H assay. All construct combinations could grow on the double dropout media, indicating that the yeast had received both plasmids in all cases (Figure 4C left panel). Independent co-transformation

experiments showed that yeast co-expressing a bait-Mlp124357 construct with a prey-AtPDI-11 or a prey PtPDI construct was able to grow on quadruple dropout medium (Figure 4C), whereas the bait-Mlp124357<sup>G1A</sup> construct did not grow (Figure 4C) when coexpressed with *Arabidopsis* or poplar PDI. The quadruple dropout media will enable the growth of the yeast only if there is a protein-protein interaction between the activation and binding domain of the GAL4 transcription factor. The immunoprecipitation, the complementation, and the Y2H results provide evidence that Mlp124357 associates with protein disulfide isomerase 11, which is required for the localization of the effector *in planta*.

### 3.5. Molecular Modeling also Supports the Association of AtPDI-11 and Mlp124357 Effector

To further assess the interaction between PDI and the effector, we sought to use protein structures modeling. The three-dimensional (3D) structure of Mlp124357 was built through the ab initio protein structure prediction software QUARK [41] (Figure 5A) because, as we mentioned earlier, Mlp124357 is a unique effector and no good template can be identified through template-based structure modeling, i.e., I-TASSER [52]. However, the 3D structure models of both AtPDI-11 and PtPDI were constructed using I-TASSER, with estimated template modeling scores (TM-score) of 0.6 and 0.7, respectively (Figure 5B).

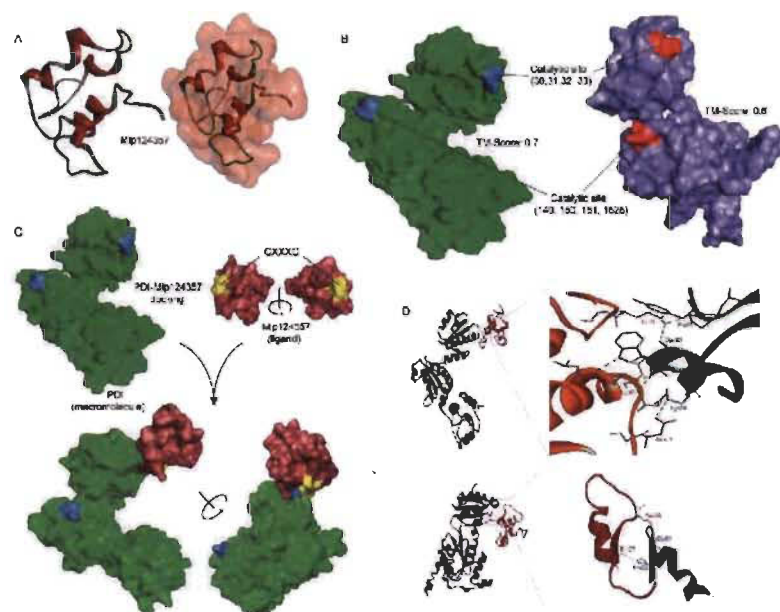


**Figure 5.** Molecular modeling also supports the association of AtPDI-11 and Mlp124357 effector. (A) Ab initio structure of Mlp124357. (B) Predicted structure and catalytic sites of PtPDI (left-green) and AtPDI-11 (right-blue). TM-scores have values between 0 and 1, where 1 indicates a perfect match between two structures. (C) Functional approach of docking between Mlp124357 and PtPDI. (D) The orientation and interactions of PtPDI-Mlp124357 (upper panel) and AtPDI-Mlp124357 (lower panel) complexes.

Protein-protein docking was performed between Mlp124357 and AtPDI-11 or PtPDI using different methods (e.g., Z-DOCK, ClusPro, PatchDock [43–45]). The top-ranked docking results from different servers showed similar binding poses of Mlp124357 bound to AtPDI-11 or PtPDI



(Figure 5C; a representative pose from Z-DOCK). Common catalytic residues (CYS<sub>30/149</sub>, GLY<sub>31/150</sub>, HIS<sub>32/151</sub>, and CYS<sub>33/152</sub>) are found in both AtPDI-11 and PtPDI (Figure 5B) and they are involved in well-established hydrogen bonding networks with Mlp124357 (Figure 5D). Hence the molecular modeling seems to support the robust experimental data obtained so far and gives some insights on how the effector protein Mlp124357 interacts with its binding partner (e.g., AtPDI-11 and PtPDI).

In addition, to assess if the previously observed delocalization and phenotype suppression observed with the Mlp124357<sup>GA</sup> mutant is caused by impaired protein folding, generating a misfolded non-functional protein, we subjected the Mlp124357<sup>GA</sup> mutant to the same modeling (Figure S7). The results indicate that the change of GXXXG to AXXXA causes a similar albeit different folding of Mlp124357 (RMSD: 7.23, TM: 0.3) which is sufficient to disrupt the binding affinity to the PDI catalytic site.

### 3.6. The Mlp124357-PDI Association Takes Place in an Effector-Specific Manner

As protein disulfide isomerases catalyze the formation of a disulfide bond between cysteine residues within proteins and as most effector proteins contain several cysteine residues (normally 5–8), we considered that the interaction with PDI-11 could be a general interaction between all (or many) effectors and PDI-11. To determine whether the interaction between Mlp124357 and AtPDI-11 was specific or general, we use the yeast two-hybrid system to assess the interaction between AtPDI-11 prey and eight *Mlp*-effectors also having several predicted disulfide intramolecular bridges (Mlp1104486, Mlp51108708, Mlp772983, Mlp3351690, Mlp1123281, Mlp752166, Mlp3353845 and Mlp151107359). The yeasts co-expressing the effectors with AtPDI-11 did not grow on quadruple dropout medium, like the negative control (Figure 6). This result suggests that the interaction between PDI-11 and Mlp124357 is specific and that PDI-11 does not serve as a general effector maturation interactor.

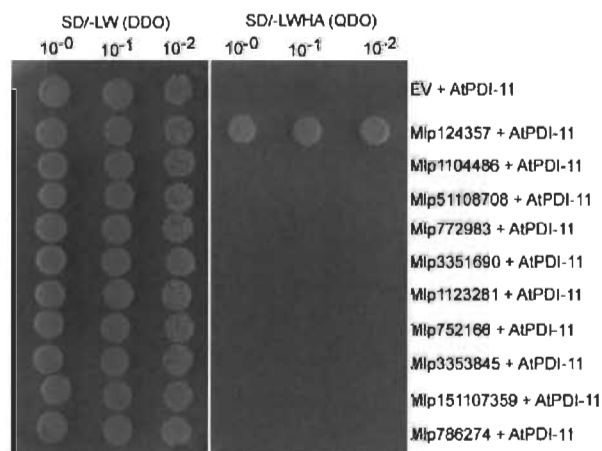


**Figure 6.** The Mlp124357-PDI association takes place in an effector-specific manner. Co-expression of a prey construct containing AtPDI-11, with Mlp124357, Mlp1104486, Mlp51108708, Mlp772983, Mlp3351690, Mlp1123281, Mlp752166, Mlp3353845, Mlp151107359, or Mlp786274 as baits in yeast to test interaction between PDI and effectors containing multiple cysteines. Yeast co-expressing the indicated combination of bait and prey were spotted on the synthetic double dropout medium lacking leucine and tryptophan (SD/-LW (DDO)) to show the expression of both constructs and quadruple dropout medium lacking leucine, tryptophan, histidine, and adenine (SD/-LWHA (QDO)) to reveal an interaction. Only yeast co-expressing AtPDI-11 and Mlp124357 grew on SD/-LWHA plates. The plates were photographed 2 days after inoculation.

### 3.7. Protein Disulfide-Isomerase 11 Acts as a Helper of Mlp124357

To assess whether AtPDI-11 is a target or a helper of Mlp124357, we conducted infection assays with two different pathogens (*Pst*DC3000 and *H. arabidopsidis*) on plants expressing PDI-11 or not. It should be noted that the leaf phenotypes of *Atpdi-11* and AtPDI-11/*Atpdi-11* were similar to control plants Col-0 or Col-0-eGFP, but in the presence of the Mlp124357 effector, the *Atpdi-11*, AtPDI-11/*Atpdi-11*, and PDI11/*Atpdi-11* lines exhibited chlorotic symptoms on their leaves (Figure 7A). This result suggests that, although the effector is mislocalized in the *pdi-11* line, it seems to retain its phenotype-altering activity.

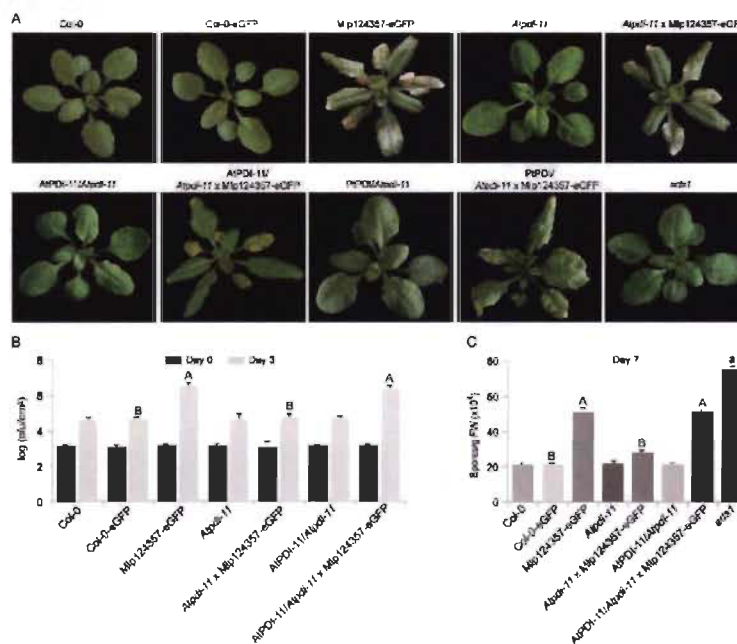


**Figure 7.** PDI-11 is not involved in plant immunity. (A) Morphology of each genotype that were used for the infection assays. Photographs were taken from 4-week-old soil-grown plants. (B) Growth of *Pst*DC3000 bacteria in *Arabidopsis*. One-way ANOVA ( $p < 0.05$ ) with Tukey's test was performed to compare genotypes with GFP or without GFP. There was no difference between genotype without GFP. Different letters indicate statistically significant difference between Col-0-eGFP, Mlp124357-eGFP, Atpdi-11 x Mlp124357-eGFP, and AtPDI-11/Atpdi-11 x Mlp124357-eGFP. For each genotype five replicates were used; cfu, colony-forming unit. (C) Growth of *H. arabidopsidis* Noco2 oomycete in *Arabidopsis*. For genotypes without eGFP (Col-0, Atpdi-11, AtPDI-11/Atpdi-11, and *eds1*), significance was evaluated using ANOVA ( $p < 0.05$ ) with Tukey's. For genotypes with eGFP (Col-0-eGFP, Mlp124357-eGFP, Atpdi-11 x Mlp124357-eGFP and AtPDI-11/Atpdi-11 x Mlp124357-eGFP) significance was evaluated using ANOVA ( $p < 0.05$ , different capital letters denote significant difference) with Tukey's test. FW, fresh weight. Both bacterial and oomycete infection experiments were repeated at least three times and representative data are shown.

Compared to the control wild-type Col-0 or Col-0-eGFP, the *Atpdi-11* and AtPDI-11/*Atpdi-11* lines showed similar pathogen growth (Figure 7B,C). This result suggests that PDI-11 does not contribute significantly to the plant immunity and that Mlp124357 is unlikely to target it to increase the pathogen virulence. As shown previously, Mlp124357 promoted bacterial and oomycete growth, but interestingly

it was unable to do so in the absence of AtPDI-11. As such, AtPDI-11 appears to be required for the localization and the virulence activity of Mlp124357, although the effector's capacity to affect the global plant phenotype appears to be uncoupled from its virulence activity. Moreover, both *P. syringae* and *H. arabidopsidis* are pathogens that translocate effectors into *Arabidopsis*. The fact that their virulence in a *pdi-11* KO line is similar to the control (Col-0 or Col-0-eGFP) further supports that AtPDI-11 is not required for the maturation of other effectors than Mlp124357, as if *H. arabidopsidis* or *P. syringae* effectors would require AtPDI-11 for their maturation, a decrease in pathogen growth would be observed in the KO line, which is not the case.

### 3.8. Transcriptome Analysis of the *Arabidopsis* Transgenics Line Expressing Mlp124357

To identify host molecular pathways altered by Mlp124357, we performed a genome-wide gene expression analysis using RNA-seq of 4-day-old *A. thaliana* Mlp124357 stable transgenic line and control plants expressing eGFP. In the Mlp124357 transgenic line, 268 and 353 genes were up- and down-regulated by 2-fold change or greater, respectively, in comparison with control plants (Table S2). Next, we performed GO term enrichment analysis of genes that were 3-fold change up- and down-regulated in plants expressing Mlp124357 to determine the relevant biological processes altered by Mlp124357. Four functional groups of significantly enriched GO terms were noted: cellular response to iron ion starvation, indole-containing compound biosynthetic process, organ senescence, and small molecule catabolic process (Figure 8).

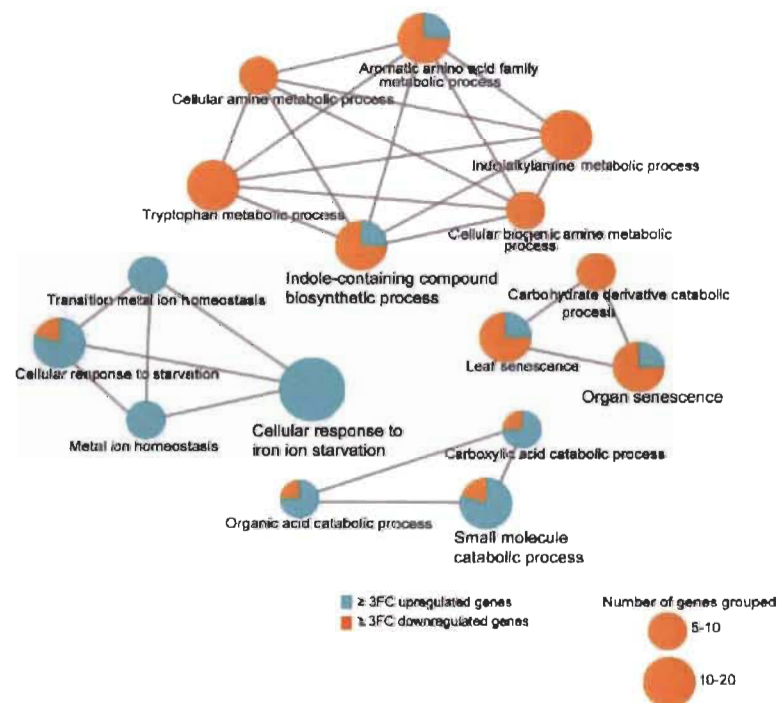


**Figure 8.** Transcriptome analysis of the *Arabidopsis* transgenic line expressing Mlp124357. Expression of Mlp124357 in *Arabidopsis* deregulates groups of genes associated with senescence, Fe homeostasis, and fungus defense. GO term enrichment analysis was performed with both up and down-regulated genes filtered by Q-value  $\leq 0.05$  and fold-change  $\geq 3$  using the Cytoscape software (version 3.1.1). ClueGO plug-in of Cytoscape was used to visualize enriched functions for both up- and down-regulated genes.

Remarkably, multiple defense-related genes such as YLS9, CHI, CYP79B2, BGLU21 were down-regulated in the Mlp124357-eGFP transgenic line compared to the eGFP transgenic plants. Several genes coding for BHLH transcription factors, for example, BHLH038, BHLH039, and BHLH040, which are involved in the plant Fe deficiency response, as well as GLK2, which is involved in plant susceptibility to fungus, were up-regulated in the Mlp124357-eGFP transgenic line (Figure 8). These results support our observations of leaf chlorosis (Figure 2C) and plant susceptibility to pathogens (Figure 3D,E).

#### 4. Discussion

Effectors play a key role in plant-microbe interactions [53] and many of them are shown to act as virulence factors that are capable to suppress plant defense responses and enhance pathogenesis [54]. However, little is known about the effector functions of *Melampsora larici-populina*, a devastating pathogen of poplars worldwide. In this study, we used *A. thaliana* and *N. benthamiana* as heterologous systems and a poplar leaf rust effector, Mlp124357, as a probe to understand the potential function of this *Mlp* effector in plants. We identified PDI-11 as a putative helper of Mlp124357, defined their specific physical interaction both in yeast and *in planta*, and showed that this interaction between Mlp124357 and PDI-11 is required for the increased plant susceptibility to pathogens. Specifically, we identified a GxxxG motif in Mlp124357 that mediates its interaction with PDI-11. Normally, Mlp124357 accumulates in the tonoplasts, bulbs, and transvacuolar strands; however, when the two glycines of the GxxxG motif were replaced by alanines, the Mlp124357<sup>GA</sup> mutant lost its *in planta* tonoplastic localization and was no longer able to enhance pathogen growth. To our knowledge, a connection between rust pathogens and the tonoplasts has not previously been established.

When *Arabidopsis* was exposed to pathogens with different lifestyles (e.g., bacteria and oomycetes), we observed that Mlp124357 enhanced pathogen growth. Both *Hpa* and *Mlp* are obligate biotrophic filamentous pathogens of dicot plants and possess a similar infection strategy in leaf tissues. However, Mlp124357 also increased the growth of a bacterial pathogen (*Pst*). Therefore, we conclude that Mlp124357 alters a host mechanism that is active against both bacteria and biotrophic filamentous pathogens.

The morphology of plants expressing Mlp124357 is altered, e.g., the plants show narrower leaves, chlorosis, and yellowing of the leaf tips (Figures 2 and 7). Expression of bacterial as well as filamentous pathogen effectors can affect the host immune response and induce a variety of phenotypes in plants, including chlorosis [55,56]. For instance, fungal effectors SnTox [57,58] and FvTox1 [59] as well as bacterial effectors AvrB [60] and HOPQ-1 [61] induce chlorosis symptoms in plants. A chlorotic phenotype has previously been reported to correlate with plant susceptibility [62], thus induction of both chlorosis and plant susceptibility by Mlp124357 can reflect a genuine effector activity. However, when we mutated the glycine residues of the GxxxG motif of Mlp124357 and expressed it in *Arabidopsis*, we could no longer observe leaf chlorosis, suggesting that adequate protein localization is required for the chlorosis-inducing activity of the effector. In addition, the *in silico* folding of the effector suggests that the AxxxA mutant adopts a very similar folding to the wild-type effector, suggesting that, although it no longer interacts with PDI-11, the protein would still be stable. On the other hand, Mlp124357 was still capable of inducing chlorosis in *pdi-11* KO plants, but was unable to induce plant susceptibility in these plants, suggesting that virulence and chlorosis can be uncoupled. One possible explanation is that the interaction with PDI-11 is required for a subsequent interaction with an unidentified virulence target involved in conferring susceptibility to pathogens, but that the effector also has a second target which can be reached independently of the interaction with PDI-11.

Recently, we reported that Mlp124357 localizes to tonoplasts, bulbs, and transvacuolar strands [29]. However, how the *Mlp* pathogen benefits from manipulating the host tonoplasts and vacuolar substructures is unclear [63]. An effector of *Hpa*, HaRxL17, was also reported to localize to tonoplasts and to enhance plant susceptibility [3]. Therefore, pathogen effectors may target the tonoplasts to modulate/suppress vacuole-mediated defense responses. Further mechanistic investigations



of the pathogen effector/tonoplasts interplay should shed light on the biological significance of this phenomenon.

We identified Protein Disulfide Isomerase-11, a member of the Protein Disulfide Isomerase (PDI) gene family, as a plant interactor of Mlp124357 in *Arabidopsis*. The major function of PDIs in plants is to facilitate the formation of disulfide bonds by induction, oxidization, and isomerization; all of which are essential for the proper folding and maturation of proteins. For example, HSP70, HSP90, and DNAJ-like proteins have been shown to perform similar functions as chaperones in plant-pathogen interaction [64]. Like other effectors, cysteine-rich Mlp124357 is expected to translocate as an unfolded protein to the plant cell, thus, we speculated that a PDI could be recruited by Mlp to act as a cellular chaperone during infection. The identification of AtPDI-11 or PtPDI as mediators of Mlp virulence activity suggests that other members of the PDI gene family might play a similar role in other plant-rust interactions; however, our evidence suggests that PDI-11 is not a generic interactor for all Mlp effectors since it did not interact with any of the other effectors tested. Additionally, the *pdi-11* line did not exhibit a pathogen resistance phenotype, which would have been the case if the assayed pathogens' effectors would not have been able to mature as a result of the absence of a universal maturation PDI protein.

Variation has been reported in the subcellular localization of PDIs in *Arabidopsis* [65]. *A. thaliana* encodes 12 PDIs, which are classified in three subfamilies, PDI-11 is the only member of the PDI-D subfamily and it is also the only *Arabidopsis* PDI lacking an ER retention signal [65]. Most PDIs were shown to localize to the ER lumen [66–68], while several PDI isoforms have been localized to other cellular organelles such as Golgi, chloroplasts, nucleus, and tonoplasts [66–68]. Moreover, functional human PDIs are also demonstrated to accumulate at the cell surface, the extracellular space, the cytosol, and the nucleus [69]. Our result indicates that AtPDI-11 accumulates both at the ER and tonoplasts and interacts with Mlp124357. However, in the *pdi-11* knockout line which expressed Mlp124357, we observed that Mlp124357 was delocalized to the cytosol and nucleus. This result strongly suggests that the interaction between the two proteins occurs on the cytosolic side of the tonoplasts rather than on the luminal side of the tonoplasts.

Some host proteins that are targeted by pathogen effectors can be “helpers” who enable effector functions, while others are “targets” [70]. Previous studies demonstrated that the folding of a pathogen's effector facilitated by host protein might be important to modulate this effector's functions in host cells during pathogenesis. For instance, cyclophilin ROC1 (*Arabidopsis*) and GmCYP1 (soybean) are required to activate the bacterial effector AvrRpt2 [71,72] and the fungal effector Avr3b [73], respectively. Our study demonstrated that PDI absence by itself does not affect plant susceptibility, suggesting that PDI is not directly involved in immunity but may be responsible for the activation of the *Melampsora larici-populina* effector Mlp124357. In other words, AtPDI-11 is likely the host helper recruited by Mlp124357 to enhance plant susceptibility. These results suggest that recruitments of host factors as “helper” is a common pathogenesis mechanism shared by pathogens.

The molecular interaction of poplar with the economically important pathogen *Melampsora larici-populina* remains largely unknown. This work can essentially increase our knowledge of the poplar-*Melampsora larici-populina* pathosystem as well as highlight the importance of helper proteins as susceptibility factors. Future work will be directed toward understanding whether Mlp124357 has other target proteins in plant cells and uncovering the specific mechanism by which Mlp124357 affects plant defense, which could help plan control strategies of rust pathogens.

**Supplementary Materials:** The following are available online at <http://www.mdpi.com/2079-7737/9/9/294/s1>, Figure S1: Immunodetection of eGFP protein in wild-type (Col-0) and stable transgenic seedlings expressing eGFP, Mlp124357-eGFP, Mlp124357GA-eGFP, AtPDI-11-eGFP or PtPDI-eGFP from 14-days-old plantlets, Figure S2: Mlp124357GA loses tonoplast localization in stable *Arabidopsis* transgenic line. Live-cell imaging of leaf epidermal cells of seven-day-old stable *Arabidopsis* eGFP, Mlp124357-eGFP or Mlp124357<sup>GA</sup>-eGFP transgenic lines, Figure S3: Distribution of Mlp124357-eGFP proteins in subcellular fractions. Cellular membrane fractions were obtained from fresh leaves of 3-week-old Col-0-eGFP and Mlp124357-eGFP plants by differential centrifugation and Mlp124357 was detected by Western hybridization with an antibody recognizing eGFP, Figure S4: Localization of Mlp124357

in tonoplast, bulbs, and TVSSs does not change in the absence of AT2G33210, AT5G15650, and AT1G04040 genes in *Arabidopsis*. Live-cell imaging of leaf epidermal cells of the crossed lines between Mlp124357-eGFP with the indicated genes knock-out lines; SALK-120568, SALK-132152, or SALK-068225, Figure S5: Multiple sequence alignment of PDIs. The amino acid sequence of AtPDI-11, PtPDI, and MlpPDI was compared. Identical/highly conserved residues (\*); semi-conserved residues (:) and conserved residues (.) are marked. The AtPDI-11 shows 87% and 30% of sequence identity with PtPDI and MlpPDI, respectively, Figure S6: Sub-cellular localization of AtPDI-11 or PtPDI in *N. benthamiana* epidermal cells. Laser-scanning confocal microscopy shows that AtPDI-11-eGFP (A,B) and PtPDI-eGFP (C,D) accumulate both in the tonoplast and endoplasmic reticulum (ER), Figure S7: Heatmap of differentially expressed genes in Col-0-eGFP and Mlp124357-eGFP based on transcriptome analysis. Table S1: List of putative interactor proteins of Mlp124357 from IP/MS, Table S2: List of up- and down-regulated genes from transcriptome analysis.

**Author Contributions:** Conceptualization, M.H.M. and H.G.; methodology, M.H.M. and H.G.; investigation, M.H.M. and H.G.; in silico docking study, M.H.M., M.S.R., X.H., and Y.Z.; writing—original draft, M.H.H.; writing—review and editing, M.H.M., M.S.R., H.Z., and H.G.; supervision, H.Z. and H.G. All authors have read and agreed to the published version of the manuscript.

**Funding:** This research was funded by a Tier-II Canada Research Chair to HG and two Fonds de Recherche Nature et Technologies scholarships to MHM and MSR.

**Acknowledgments:** We are thankful to Melodie B. Plourde for critical comments on the manuscript. The laboratory of Xin Li graciously provided the *adi-2* line. Karen Cristine Gonçalves dos Santos performed the heat map and new statistics requested in the review process.

**Conflicts of Interest:** The funders had no role in the design of the study; in the collection, analyses, or interpretation of data; in the writing of the manuscript, or in the decision to publish the results.

## References

1. Dodds, P.N.; Rathjen, J.P. Plant immunity: Towards an integrated view of plant–pathogen interactions. *Nat. Rev. Genet.* **2010**, *11*, 539. [[CrossRef](#)] [[PubMed](#)]
2. Ahmed, M.B.; dos Santos, K.C.G.; Sanchez, I.B.; Petre, B.; Lorrain, C.; Plourde, M.B.; Duplessis, S.; Desgagné-Penix, I.; Germain, H. A rust fungal effector binds plant DNA and modulates transcription. *Sci. Rep.* **2018**, *8*, 14718. [[CrossRef](#)] [[PubMed](#)]
3. Caillaud, M.C.; Piquerez, S.J.; Fabro, G.; Steinbrenner, J.; Ishaque, N.; Beynon, J.; Jones, J.D. Subcellular localization of the Hpa RxLR effector repertoire identifies a tonoplast-associated protein HaRxLR17 that confers enhanced plant susceptibility. *Plant J.* **2012**, *69*, 252–265. [[CrossRef](#)] [[PubMed](#)]
4. Petre, B.; Lorrain, C.; Saunders, D.G.; Win, J.; Sklenar, J.; Duplessis, S.; Kamoun, S. Rust fungal effectors mimic host transit peptides to translocate into chloroplasts. *Cell. Microbiol.* **2016**, *18*, 453–465. [[CrossRef](#)]
5. Petre, B.; Saunders, D.G.; Sklenar, J.; Lorrain, C.; Win, J.; Duplessis, S.; Kamoun, S. Candidate effector proteins of the rust pathogen *Melampsora larici-populina* target diverse plant cell compartments. *Mol. Plant-Microbe Interact.* **2015**, *28*, 689–700. [[CrossRef](#)]
6. Vargas, W.A.; Sanz-Martín, J.M.; Rech, G.E.; Armijos-Jaramillo, V.D.; Rivera, L.P.; Echeverria, M.M.; Diaz-Minguez, J.M.; Thon, M.R.; Sukno, S.A. A fungal effector with host nuclear localization and DNA-binding properties is required for maize anthracnose development. *Mol. Plant-Microbe Interact.* **2016**, *29*, 83–95. [[CrossRef](#)]
7. Schornack, S.; van Damme, M.; Bozkurt, T.O.; Cano, L.M.; Smoker, M.; Thines, M.; Gaulin, E.; Kamoun, S.; Huitema, E. Ancient class of translocated oomycete effectors targets the host nucleus. *Proc. Natl. Acad. Sci. USA* **2010**, *107*, 17421–17426. [[CrossRef](#)]
8. Wirthmueller, L.; Roth, C.; Fabro, G.; Caillaud, M.C.; Rallapalli, G.; Asai, S.; Sklenar, J.; Jones, A.M.; Wiermer, M.; Jones, J.D. Probing formation of cargo/importin- $\alpha$  transport complexes in plant cells using a pathogen effector. *Plant J.* **2015**, *81*, 40–52. [[CrossRef](#)]
9. Dangl, J.L.; Horvath, D.M.; Staskawicz, B.J. Pivoting the plant immune system from dissection to deployment. *Science* **2013**, *341*, 746–751. [[CrossRef](#)]
10. Bombarely, A.; Rosli, H.G.; Vrebalov, J.; Moffett, P.; Mueller, L.A.; Martin, G.B. A draft genome sequence of *Nicotiana benthamiana* to enhance molecular plant-microbe biology research. *Mol. Plant-Microbe Interact.* **2012**, *25*, 1523–1530. [[CrossRef](#)]

11. Germain, H.; Joly, D.L.; Mireault, C.; Plourde, M.B.; Letanneur, C.; Stewart, D.; Morency, M.J.; Petre, B.; Duplessis, S.; Séguin, A. Infection assays in *Arabidopsis* reveal candidate effectors from the poplar rust fungus that promote susceptibility to bacteria and oomycete pathogens. *Mol. Plant Pathol.* **2018**, *19*, 191–200. [[CrossRef](#)]
12. Goodin, M.M.; Zaitlin, D.; Naidu, R.A.; Lommel, S.A. *Nicotiana benthamiana*: Its history and future as a model for plant–pathogen interactions. *Mol. Plant-Microbe Interact.* **2008**, *21*, 1015–1026. [[CrossRef](#)] [[PubMed](#)]
13. Win, J.; Chaparro-García, A.; Belhaj, K.; Saunders, D.; Yoshida, K.; Dong, S.; Schornack, S.; Zipfel, C.; Robatzek, S.; Hogenhout, S. Effector biology of plant-associated organisms: Concepts and perspectives. *Proc. Cold Spring Harb. Symp. Quant. Biol.* **2012**, *77*, 235–247. [[CrossRef](#)] [[PubMed](#)]
14. Macho, A.P.; Guevara, C.M.; Tornero, P.; Ruiz-Albert, J.; Beuzon, C.R. The *Pseudomonas syringae* effector protein HopZ1a suppresses effector-triggered immunity. *New Phytol.* **2010**, *187*, 1018–1033. [[CrossRef](#)] [[PubMed](#)]
15. Cui, H.; Wang, Y.; Xue, L.; Chu, J.; Yan, C.; Fu, J.; Chen, M.; Innes, R.W.; Zhou, J.-M. *Pseudomonas syringae* effector protein AvrB perturbs *Arabidopsis* hormone signaling by activating MAP kinase 4. *Cell Host Microbe* **2010**, *7*, 164–175. [[CrossRef](#)]
16. Anderson, J.C.; Pascuzzi, P.E.; Xiao, F.; Sessa, G.; Martin, G.B. Host-mediated phosphorylation of type III effector AvrPto promotes *Pseudomonas* virulence and avirulence in tomato. *Plant Cell* **2006**, *18*, 502–514. [[CrossRef](#)]
17. Nimchuk, Z.; Marois, E.; Kjemtrup, S.; Leister, R.T.; Katagiri, F.; Dangl, J.L. Eukaryotic fatty acylation drives plasma membrane targeting and enhances function of several type III effector proteins from *Pseudomonas syringae*. *Cell* **2000**, *101*, 353–363. [[CrossRef](#)]
18. Bai, X.; Correa, V.R.; Toruño, T.Y.; Ammar, E.-D.; Kamoun, S.; Hogenhout, S.A. AY-WB phytoplasma secretes a protein that targets plant cell nuclei. *Mol. Plant-Microbe Interact.* **2009**, *22*, 18–30. [[CrossRef](#)]
19. Szurek, B.; Marois, E.; Bonas, U.; Van den Ackerveken, G. Eukaryotic features of the *Xanthomonas* type III effector AvrBs3: Protein domains involved in transcriptional activation and the interaction with nuclear import receptors from pepper. *Plant J.* **2001**, *26*, 523–534. [[CrossRef](#)]
20. Duplessis, S.; Joly, D.L.; Dodds, P.N. Rust effectors. In *Effectors in Plant-Microbe Interactions*; John Wiley & Sons: Hoboken, NJ, USA, 2012; pp. 155–193.
21. Pernisi, E. Armed and dangerous. *Science* **2010**, *327*, 804–805.
22. Duplessis, S.; Major, I.; Martin, F.; Séguin, A. Poplar and pathogen interactions: Insights from *Populus* genome-wide analyses of resistance and defense gene families and gene expression profiling. *Crit. Rev. Plant Sci.* **2009**, *28*, 309–334. [[CrossRef](#)]
23. Hacquard, S.; Petre, B.; Frey, P.; Hecker, A.; Rouhier, N.; Duplessis, S. The poplar–poplar rust interaction: Insights from genomics and transcriptomics. *J. Pathog.* **2011**, *2011*. [[CrossRef](#)] [[PubMed](#)]
24. Major, I.T.; Nicole, M.-C.; Duplessis, S.; Séguin, A. Photosynthetic and respiratory changes in leaves of poplar elicited by rust infection. *Photosynth. Res.* **2010**, *104*, 41–48. [[CrossRef](#)]
25. Duplessis, S.; Cuomo, C.A.; Lin, Y.-C.; Aerts, A.; Tisserant, E.; Veneault-Fourrey, C.; Joly, D.L.; Hacquard, S.; Amselem, J.; Cantarel, B.L. Obligate biotrophy features unraveled by the genomic analysis of rust fungi. *Proc. Natl. Acad. Sci. USA* **2011**, *108*, 9166–9171. [[CrossRef](#)] [[PubMed](#)]
26. Hacquard, S.; Delaruelle, C.; Legu e, V.; Tisserant, E.; Kohler, A.; Frey, P.; Martin, F.; Duplessis, S. Laser capture microdissection of uredinia formed by *Melampsora larici-populina* revealed a transcriptional switch between biotrophy and sporulation. *Mol. Plant-Microbe Interact.* **2010**, *23*, 1275–1286. [[CrossRef](#)]
27. Hacquard, S.; Joly, D.L.; Lin, Y.-C.; Tisserant, E.; Feau, N.; Delaruelle, C.; Legu e, V.; Kohler, A.; Tanguay, P.; Petre, B. A comprehensive analysis of genes encoding small secreted proteins identifies candidate effectors in *Melampsora larici-populina* (poplar leaf rust). *Mol. Plant-Microbe Interact.* **2012**, *25*, 279–293. [[CrossRef](#)]
28. Saunders, D.G.; Win, J.; Cano, L.M.; Szabo, L.J.; Kamoun, S.; Raffaele, S. Using hierarchical clustering of secreted protein families to classify and rank candidate effectors of rust fungi. *PLoS ONE* **2012**, *7*, e29847. [[CrossRef](#)]
29. Madina, M.H.; Zheng, H.; Germain, H. New insight into bulb dynamics in the vacuolar lumen of *Arabidopsis* cells. *Botany* **2018**, *96*, 511–520. [[CrossRef](#)]
30. Karimi, M.; Inz e, D.; Depicker, A. GATEWAY™ vectors for *Agrobacterium*-mediated plant transformation. *Trends Plant Sci.* **2002**, *7*, 193–195. [[CrossRef](#)]



31. Sparkes, I.A.; Runions, J.; Kearns, A.; Hawes, C. Rapid, transient expression of fluorescent fusion proteins in tobacco plants and generation of stably transformed plants. *Nat. Protoc.* **2006**, *1*, 2019. [CrossRef]
32. Mireault, C.; Paris, L.-E.; Germain, H. Enhancement of the Arabidopsis floral dip method with XIAMETER OFX-0309 as alternative to Silwet L-77 surfactant. *Botany* **2014**, *92*, 523–525. [CrossRef]
33. Dong, O.X.; Metegnier, L.V.; Plourde, M.B.; Ahmed, B.; Wang, M.; Jensen, C.; Jin, H.; Moffett, P.; Germain, H. Arabidopsis TAF15b Localizes to RNA Processing Bodies and Contributes to sncl-Mediated Autoimmunity. *Mol. Plant Microbe Interact.* **2016**, *29*, 247–257. [CrossRef] [PubMed]
34. Hammer, O.; Harper, D.A.T.; Ryan, P.D. PAST: Paleontological statistics software package for education and data analysis. *Paleontol. Electron.* **2001**, *4*, 9.
35. Germain, H.; Gray-Mitsumune, M.; Houde, J.; Benhamman, R.; Sawasaki, T.; Endo, Y.; Matton, D.P. The Solanum chacoense ovary receptor kinase 11 (ScORK11) undergoes tissue-dependent transcriptional, translational and post-translational regulation. *Plant Physiol. Biochem.* **2013**, *70*, 261–268. [CrossRef]
36. Widell, S.; Larsson, C. Separation of presumptive plasma membranes from mitochondria by partition in an aqueous polymer two-phase system. *Physiol. Plant.* **1981**, *51*, 368–374. [CrossRef]
37. Serino, G.; Deng, X.W. Protein coimmunoprecipitation in Arabidopsis. *CSH Prot.* **2007**, *2007*, pdb prot 4683. [CrossRef]
38. Nesvizhskii, A.I.; Keller, A.; Kolker, E.; Aebersold, R. A statistical model for identifying proteins by tandem mass spectrometry. *Anal. Chem.* **2003**, *75*, 4646–4658. [CrossRef]
39. Germain, H.; Gray-Mitsumune, M.; Lafleur, E.; Matton, D.P. ScORK17, a transmembrane receptor-like kinase predominantly expressed in ovules is involved in seed development. *Planta* **2008**, *228*, 851–862. [CrossRef]
40. Bindea, G.; Galon, J.; Mlecnik, B. CluePedia Cytoscape plugin: Pathway insights using integrated experimental and in silico data. *Bioinformatics* **2013**, *29*, 661–663. [CrossRef]
41. Xu, D.; Zhang, Y. Ab initio protein structure assembly using continuous structure fragments and optimized knowledge-based force field. *Proteins Struct. Funct. Bioinform.* **2012**, *80*, 1715–1735. [CrossRef]
42. Yang, J.; Yan, R.; Roy, A.; Xu, D.; Poisson, J.; Zhang, Y. The I-TASSER Suite: Protein structure and function prediction. *Nat. Methods* **2015**, *12*, 7. [CrossRef] [PubMed]
43. Kozakov, D.; Hall, D.R.; Xia, B.; Porter, K.A.; Padhorna, D.; Yueh, C.; Beglov, D.; Vajda, S. The ClusPro web server for protein–protein docking. *Nat. Protoc.* **2017**, *12*, 255. [CrossRef] [PubMed]
44. Pierce, B.G.; Hourai, Y.; Weng, Z. Accelerating protein docking in ZDOCK using an advanced 3D convolution library. *PLoS ONE* **2011**, *6*, e24657. [CrossRef]
45. Schneidman-Duhovny, D.; Inbar, Y.; Nussinov, R.; Wolfson, H.J. PatchDock and SymmDock: Servers for rigid and symmetric docking. *Nucleic Acids Res.* **2005**, *33*, W363–W367. [CrossRef]
46. Tovchigrechko, A.; Vakser, I.A. GRAMM-X public web server for protein–protein docking. *Nucleic Acids Res.* **2006**, *34*, W310–W314. [CrossRef]
47. DeLano, W.L. The PyMOL Molecular Graphics System. 2002. Available online: <http://www.pymol.org> (accessed on 7 September 2020).
48. Yuan, S.; Chan, H.S.; Hu, Z. Using PyMOL as a platform for computational drug design. *Wiley Interdiscip. Rev. Comput. Mol. Sci.* **2017**, *7*, e1298. [CrossRef]
49. Bronnimann, M.P.; Chapman, J.A.; Park, C.K.; Campos, S.K. A transmembrane domain and GxxxG motifs within L2 are essential for papillomavirus infection. *J. Virol.* **2013**, *87*, 464–473. [CrossRef]
50. Cabanillas, D.G.; Jiang, J.; Movahed, N.; Germain, H.; Yamaji, Y.; Zheng, H.; Laliberte, J.-F. Turnip mosaic virus uses the SNARE protein VTI11 in an unconventional route for replication vesicle trafficking. *Plant Cell* **2018**, *30*, 2594–2615. [CrossRef]
51. Teese, M.G.; Langosch, D. Role of GxxxG motifs in transmembrane domain interactions. *Biochemistry* **2015**, *54*, 5125–5135. [CrossRef]
52. Yang, J.; Zhang, Y. Protein Structure and Function Prediction Using I-TASSER. *Curr. Protoc. Bioinform.* **2015**, *52*, 5–8. [CrossRef] [PubMed]
53. Jones, J.D.; Dangl, J.L. The plant immune system. *Nature* **2006**, *444*, 323. [CrossRef] [PubMed]
54. Speth, E.B.; Lee, Y.N.; He, S.Y. Pathogen virulence factors as molecular probes of basic plant cellular functions. *Curr. Opin. Plant Biol.* **2007**, *10*, 580–586. [CrossRef] [PubMed]
55. Cunnac, S.; Lindeberg, M.; Collmer, A. Pseudomonas syringae type III secretion system effectors: Repertoires in search of functions. *Curr. Opin. Microbiol.* **2009**, *12*, 53–60. [CrossRef] [PubMed]



56. Torto, T.A.; Li, S.; Styer, A.; Huitema, E.; Testa, A.; Gow, N.A.; Van West, P.; Kamoun, S. EST mining and functional expression assays identify extracellular effector proteins from the plant pathogen *Phytophthora*. *Genome Res.* **2003**, *13*, 1675–1685. [CrossRef] [PubMed]
57. Faris, J.D.; Zhang, Z.; Lu, H.; Lu, S.; Reddy, L.; Cloutier, S.; Fellers, J.P.; Meinhardt, S.W.; Rasmussen, J.B.; Xu, S.S. A unique wheat disease resistance-like gene governs effector-triggered susceptibility to necrotrophic pathogens. *Proc. Natl. Acad. Sci. USA* **2010**, *107*, 13544–13549. [CrossRef] [PubMed]
58. Liu, Z.; Zhang, Z.; Faris, J.D.; Oliver, R.P.; Syme, R.; McDonald, M.C.; McDonald, B.A.; Solomon, P.S.; Lu, S.; Shelver, W.L. The cysteine rich necrotrophic effector SnTox1 produced by *Stagonospora nodorum* triggers susceptibility of wheat lines harboring Snn1. *PLoS Pathog.* **2012**, *8*, e1002467. [CrossRef]
59. Brar, H.K.; Swaminathan, S.; Bhattacharyya, M.K. The *Fusarium virguliforme* toxin FvTox1 causes foliar sudden death syndrome-like symptoms in soybean. *Mol. Plant-Microbe Interact.* **2011**, *24*, 1179–1188. [CrossRef]
60. Shang, Y.; Li, X.; Cui, H.; He, P.; Thilmony, R.; Chintamanani, S.; Zwiesler-Vollick, J.; Gopalan, S.; Tang, X.; Zhou, J.-M. RAR1, a central player in plant immunity, is targeted by *Pseudomonas syringae* effector AvrB. *Proc. Natl. Acad. Sci. USA* **2006**, *103*, 19200–19205. [CrossRef]
61. Kanneganti, T.-D.; Huitema, E.; Cakir, C.; Kamoun, S. Synergistic interactions of the plant cell death pathways induced by *Phytophthora infestans* Nep1-like protein PiNPP1.1 and INF1 elicitor. *Mol. Plant-Microbe Interact.* **2006**, *19*, 854–863. [CrossRef]
62. Chang, H.-X.; Domier, L.L.; Radwan, O.; Yendrek, C.R.; Hudson, M.E.; Hartman, G.L. Identification of multiple phytotoxins produced by *Fusarium virguliforme* including a phytotoxic effector (FvNIS1) associated with sudden death syndrome foliar symptoms. *Mol. Plant-Microbe Interact.* **2016**, *29*, 96–108. [CrossRef]
63. Madina, M.H.; Rahman, M.S.; Zheng, H.; Germain, H. Vacuolar membrane structures and their roles in plant-pathogen interactions. *Plant Mol. Biol.* **2019**, *101*, 343–354. [CrossRef] [PubMed]
64. Verchot, J. Cellular chaperones and folding enzymes are vital contributors to membrane bound replication and movement complexes during plant RNA virus infection. *Front. Plant Sci.* **2012**, *3*, 275. [CrossRef] [PubMed]
65. Yuen, C.; Matsumoto, K.; Christopher, D. Variation in the subcellular localization and protein folding activity among *Arabidopsis thaliana* homologs of protein disulfide isomerase. *Biomolecules* **2013**, *3*, 848–869. [CrossRef] [PubMed]
66. Cho, E.J.; Yuen, C.Y.; Kang, B.-H.; Ondzighi, C.A.; Staehelin, L.A.; Christopher, D.A. Protein disulfide isomerase-2 of *Arabidopsis* mediates protein folding and localizes to both the secretory pathway and nucleus, where it interacts with maternal effect embryo arrest factor. *Mol. Cells* **2011**, *32*, 459–475. [CrossRef]
67. Ondzighi, C.A.; Christopher, D.A.; Cho, E.J.; Chang, S.-C.; Staehelin, L.A. *Arabidopsis* protein disulfide isomerase-5 inhibits cysteine proteases during trafficking to vacuoles before programmed cell death of the endothelium in developing seeds. *Plant Cell* **2008**, *20*, 2205–2220. [CrossRef]
68. Wittenberg, G.; Levitan, A.; Klein, T.; Dangoor, I.; Keren, N.; Danon, A. Knockdown of the *Arabidopsis thaliana* chloroplast protein disulfide isomerase 6 results in reduced levels of photoinhibition and increased D1 synthesis in high light. *Plant J.* **2014**, *78*, 1003–1013. [CrossRef]
69. Turano, C.; Coppari, S.; Altieri, F.; Ferraro, A. Proteins of the PDI family: Unpredicted non-ER locations and functions. *J. Cell Physiol.* **2002**, *193*, 154–163. [CrossRef]
70. Rovenich, H.; Boshoven, J.C.; Thomma, B.P. Filamentous pathogen effector functions: Of pathogens, hosts and microbiomes. *Curr. Opin. Plant Biol.* **2014**, *20*, 96–103. [CrossRef]
71. Coaker, G.; Falick, A.; Staskawicz, B. Activation of a phytopathogenic bacterial effector protein by a eukaryotic cyclophilin. *Science* **2005**, *308*, 548–550. [CrossRef]
72. Coaker, G.; Zhu, G.; Ding, Z.; Van Doren, S.R.; Staskawicz, B. Eukaryotic cyclophilin as a molecular switch for effector activation. *Mol. Microbiol.* **2006**, *61*, 1485–1496. [CrossRef]
73. Kong, G.; Zhao, Y.; Jing, M.; Huang, J.; Yang, J.; Xia, Y.; Kong, L.; Ye, W.; Xiong, Q.; Qiao, Y. The activation of *Phytophthora* effector Avr3b by plant cyclophilin is required for the nudix hydrolase activity of Avr3b. *PLoS Pathog.* **2015**, *11*, e1005139. [CrossRef] [PubMed]

